Consortium for Risk Evaluation with Stakeholder Participation III

Consortium Universities: **Vanderbilt University**, Howard University, Oregon State University,

Robert Wood Johnson Medical School, Rutgers University, University of Arizona, University of Pittsburgh

Leaching Results and Interpretation of Constituent Release from Representative Low-Activity Waste Treated with Reducing Grout

Andrew C. Garrabrants, Ph.D.

Rossane C. DeLapp

David S. Kosson, Ph.D.

December 2007

CRESP III

Vanderbilt University

Department of Civil & Environmental Engineering

VU Station B#351831

Nashville, TN 37235-1831

ACKNOWLEDGEMENT

This the data presented in this report is based on work supported by the U.S. Department of Energy, under Cooperative Agreement Number DE-FC01-06EW07053 entitled 'The Consortium for Risk Evaluation with Stakeholder Participation III' awarded to Vanderbilt University. The opinions, findings, conclusions, or recommendations expressed herein are those of the author(s) and do not necessarily represent the views of the Department of Energy or Vanderbilt University.

EXECUTIVE SUMMARY

Remediation of tank wastes stored at U.S. Department of Energy (USDOE) sites in Aiken, SC and Richland, WA will require management of secondary wastes of high-temperature treatment processes (e.g., vitrification, steam reformation) prior to on-site storage in shallow burial facilities. The composition and concentration of constituents of potential concern (COPCs) in the secondary wastes will vary depending on the source stream, efficiency of the high temperature treatment process, and other down-stream treatment steps (e.g. effluent treatment processes); however, secondary wastes requiring treatment may be assumed to be low activity liquid wastes with high ionic strengths. One common treatment methodology for treatment of low-activity wastes is solidification/stabilization (S/S) with a reducing grout or other cementitious matrix where the alkalinity and reducing capacity of the S/S material is thought to provide adequate retention of constituents of potential concern for long-term waste disposal. However, current waste performance criteria and release evaluation for stabilization of low-activity waste materials is based on leaching protocols that do not provide the clarity required to characterize the mechanisms that control constituent release.

Current regulatory leaching tests (e.g., the USEPA Toxicity Characteristic Leaching Procedure) and evaluations used in the USDOE performance assessment process may (i) be widely considered inappropriate for cement-based S/S materials or (ii) limit applicability through simulation of specific site or scenario conditions (e.g., use of simulated Hanford groundwater). These testing approaches cannot be used to adequately support waste management decisions based on mechanistic understanding of material durability and constituent release. One objective of on-going research is to provide the USDOE with a generalized methodology for characterization of waste materials and waste containment materials that focuses on determining the fundamental leaching parameters of the solid material under a broad range of test conditions. These fundamental parameters may then be applied using simulation models to a selection of release scenarios and conditions in order to evaluate treatment effectiveness, alternative treatment options and long-term material performance.

This report provides a preliminary assessment of leaching data from environmental evaluation of three solid materials treated by S/S. The materials were created by adding soluble metal salts to a "dry blend" S/S recipe consisting of Portland cement, fly ash, and blast furnace slag that is representative of the low-activity waste treatments used or under consideration at USDOE facilities. The three subject materials (i.e., a matrix blank, a secondary waste, and an enhanced academic matrix) differ in the levels of potentially hazardous constituents and the composition of the water used to hydrate the "dry blend" (e.g., deionized water or salt composition projected to come from the Hanford Effluent Treatment Facility).

Leach testing consisted of equilibrium-based leaching as a function of eluate pH on crushed S/S material and mass transfer-based testing of monolithic specimens. All tests were conducted in both deionized water (the standard eluant for waste characterization) and simulated Hanford groundwater (the eluant used for Hanford Site evaluations). Eluates were analyzed for a full range of constituents included bulk mineral species (e.g., Al, Ca, Mg, Fe, Si), species found in Hanford groundwater (e.g., Na, K, Cl, SO_4, inorganic and organic carbon) and species of potential concern (or surrogates) for DOE operations (e.g. I, Re, As, Sb, Cs, Se, Sr, Ba, V, Cd, Pb, and Cu).

The results of leaching tests were used to compare the release between solid materials and testing methodologies (i.e., deionized water and simulated Hanford groundwater). The comparisons show that some constituents (e.g., Pb, Cd, Cu) may be considered "well-retained" in the reducing grout, while others are more readily released (e.g., Sb, As, Ba). In addition, the release of some constituents (e.g., I, Re, Se) was seen to be sensitive to the degree of loading into the solid matrix. The groundwater simulant was found to have little or no effect on the mineralogy controlling release as illustrated by the solubility and release of constituents as a function of eluant pH. However, after three months of continuous mass transfer tank leaching, the mean interval fluxes for several species (e.g., As, Sb, Ba, Pb, Se) were lower by 1-2 orders of magnitude for samples testing in simulated groundwater than in comparative tests conducted in deionized water.

This report shows that interpretation of leaching data collected for the purpose of material characterization should be based on leaching tests conducted in deionized water rather than

tests conducted in groundwater simulants. The scatter in the groundwater data apparently stems from in-flux of eluant constituents (e.g., Ca and Mg) and resultant boundary layer (e.g., precipitation) in the solid material. While the formation of a boundary layer is beneficial to minimize mass transfer from monolithic materials and perhaps should be promoted in disposal scenarios, the mechanisms of constituent release cannot be easily evaluated during material characterization. On-going release simulation using coupled geochemical and mass transfer modeling is expected to provide the ability to describe scenario-specific release as simulated by testing in simulated Hanford groundwater.

LIST OF ACRONYMS

AM	Academic Matrix
ANSI/ANS	American National Standards Institute/American Nuclear Society
CCV	Continuing Calibration Verification
COPC	Constituent of Potential Concern
CRESP	Consortium for Risk Evaluation with Stakeholder Participation
DOE-EM	Department of Energy – Environmental Management
DI	Deionized
DIC	Dissolved Inorganic Carbon
DOC	Dissolved Organic Carbon
ETF	Effluent Treatment Facility
HDPE	High-Density Polyethylene
IC	Ion Chromatography
ICP-MS	Inductively-Coupled Plasma – Mass Spectrometry
ICV	Initial Calibration Verification
LAW	Low-Activity Waste
LDPE	Low-Density Polyethylene
LS	Liquid-Solid Ratio
LSP	Liquid-Solid Partitioning
MB	Matrix Blank
PNNL	Pacific Northwest National Laboratory
SHG	Simulated Hanford Groundwater
SRS	Savannah River Site
S/S	Solidification/Stabilization
SW	Solidified Waste
TC	Total Carbon
TCLP	Toxicity Characteristic Leaching Procedure
USEPA	United States Environmental Protection Agency
USDOE	United States Department of Energy

TABLE OF CONTENTS

TABLE OF CONTENTS (Cont'd.)

LIST OF FIGURES

LIST OF FIGURES (Cont'd.)

LIST OF TABLES

INTRODUCTION

Low-activity wastes at US Department of Energy (USDOE) facilities in Aiken, SC and Richland, WA are slated for on-site disposal in near-surface landfills or vaults following treatment by one of several treatment methods which are designed to chemically fix and physically retain potentially hazardous constituents. One commonly used treatment approach for inorganic contaminants and radionuclides is stabilization/solidification (S/S) with cementitious materials, such as Portland cement and reducing grouts. Constituents of potential concern (COPCs) may be chemically stabilized through precipitation in the pore solution or adsorption/incorporation with mineral phases or physically retained in tortuous pore structure. For most S/S materials, water contact with the waste is minimized by the formation of a relatively impermeable matrix.

Current plans at the Savannah River Site (SRS) involve solidification of low-activity wastes with reducing grout (saltstone) followed by disposal in concrete vaults in the Saltstone Disposal Facility. The Hanford Site remediation will require treatment of secondary wastes from vitrification of high-level waste and other high-temperature treatments (i.e., bulk vitrification and steam reformation) prior to on-site storage in the Integrated Disposal Facility. Other pertinent low-activity waste forms and disposal scenarios involving the use of grouts and cements either exist or are under consideration across the USDOE complex. Details of these disposal facilities and acceptable waste treatments are based on potential release estimates from performance assessments which are assumed to account for long-term release from these matrices and facilities over extended assessment intervals (e.g., thousands of years). However, many of the tests used to estimate COPC release are either inappropriate for cementitious materials (USEPA, 1991; USEPA 1999) or lack the mechanistic clarity needed to predict long-term release under temporally variable conditions.

The goal of current CRESP research is to demonstrate advanced leaching assessment methodologies which provide more accurate estimates of long-term waste form performance with consideration of matrix geochemistry and aging. The developed approaches will provide DOE-EM with a uniform, comprehensive assessment scheme for evaluating the leaching behavior of treated waste packages and containment materials. This report presents material characterization data and preliminary interpretation of leaching from matrices representative of low-activity wastes treated with reducing grout.

EXPERIMENTAL DESIGN

Leaching Assessments

Waste acceptability criteria for stabilized secondary LAW are partially based on the concentrations of toxicity characteristic pollutants in the extracts of TCLP (USEPA, 1980) and the leachability indices of radionuclides calculated from the ANS-16.1 tank leach test (ANSI/ANS, 1986). While this approach offers a relatively simple methodology for waste classification and comparisons of observed contaminant retention; however, little mechanistic understanding of the mechanisms of release is offered. Furthermore, the predictive capabilities of this approach are suspect and results cannot be extended to other release scenarios other than those simulated by the test conditions.

This study presents leaching characterization data from two types of leaching protocols: equilibrium-base leaching tests and mass-transfer based leaching tests. The goal of leaching characterization is to determine the intrinsic leaching parameters that can be used, in conjunction with geochemical and mass transport modeling, to describe release of COPCs from the waste matrix. Leaching characterization provides the basis for a "geochemical fingerprint" that may be applied to any number of likely release scenarios through the selection of appropriate mass transport models and field conditions. This alternate methodology offers considerable flexibility for evaluation of release scenarios and treatment options.

Eluant Composition

In order to provide harmonization between approaches and facilitate the resolution of release mechanisms, leaching characterization protocols in Europe use inert eluants like deionized (DI) water. However, the common approach in the United States is the employ pre-defined or site-specific solutions in simulation-based leaching tests which to produce a solution for chemical analysis that is considered "representative" of release in the simulated release scenario. For example, tank leaching tests conducted at Pacific Northwest National Laboratory (PNNL) for Hanford Site waste characterizations commonly utilize either groundwater drawn from wells on the site or a synthetic representation referred to as Simulated Hanford Groundwater (SHG). Well-drawn groundwater is highly concentrated with bicarbonate salts of mono- and divalent cations. Table 1 shows the composition of the SHG eluant.

Table 1: Composition of SHG Eluant (J. Serne, personal communication, 2004)

Component	Concentration [mM]
$NaHCO_3$	1.043
$KHCO_3$	0.194
$Mg(HCO_3)_2$	0.617
$Ca(HCO_3)_2$	0.184
$CaCl_2$	0.338
$CaSO_4$	1.20

The experiments presented in this document were conducted using two eluant compositions (DI water and SHG) in order to illustrate the effects of leaching solutions on chemical and physical retention mechanisms.

Constituents of Potential Concern

The COPCs for any leaching characterization study should include regulated or suspect trace constituents as well as major constituents comprising the bulk of the matrix. A wide spectrum of COPCs is important for development of a geochemical fingerprint that represents the leaching characteristics of the solid material. Assessment of the release of major constituents provides insight into release mechanisms and gives indications of the potential for degradation of the matrix over long assessment intervals. Specific to treatment of secondary wastes at Hanford with reducing grout mixtures, the trace COPCs are ^{129}I and ^{99}Tc; however, other radionuclides (e.g., isotopes of Cs and Sr) and some RCRA elements (e.g., Ba, Cr, As) may be of potential concern since similar S/S treatment recipes are common throughout the DOE complex.

MATERIALS AND METHODS

Model solidified materials were created by mixing reducing grout components and metal salts with a wastewater composition representative of secondary waste streams processes through the Hanford Effluent Treatment Facility (ETF). After curing, these solidified materials were subject to equilibrium- and mass transport-based leaching tests.

Wastewater Composition

A wastewater stimulant was selected from a range of compositions which might be representative of secondary waste processed through ETF at Hanford as a result of vitrification activities (Mahoney & Russell, 2004). Geochemical modeling using Visual MINTEQ v2.40 (Gustafsson, 2006) as well as previous practical experience (B. Clark, personal communication, 14 May 2004) indicated that the maximum sodium loading which would result in no salt precipitation was approximately 2.6 M. In this study, the salt solution shown in Table 2 was used to represent the wastewater composition at a sodium loading of 2.6 M. Dilution of the wastewater stream was considered expected in light of other effluents from facilities that contribute to ETF processing.

Table 2: Wastewater Composition for 2.6 M Sodium Load.

Wastewater Component	[mol/L]	[g/L]	[%]
DI Water	50.58	911.48	81.0
NH_4OH (50% solution)	1.49	52.24	4.6
NaOH	0.12	4.79	0.4
$NaCH_3COOH$	0.11	9.24	0.8
$NaNO_3$	0.02	1.95	0.2
$Na_2CO_3 \cdot H_2O$	1.18	145.89	13.0
NaI	1.83 E-5	0.0027	2.4 E-4
$KReO_4$	1.41 E-5	0.0041	3.6 E-4
Total	-	1125.6	100.0

S/S Treatment Matrices

Three solidified materials were made by mixing the wastewater composition show in Table 2 with a dry blend of fly ash, steel slag and Portland cement. The proportions of dry blend components are shown in Table 3. This recipe is representative of the “cast stone” formulation at the Hanford Site and similar to the “saltstone” formulation at the SRS.

Table 3: Dry Blend Composition (B. Clark, personal communication, 14 May 2004)

Component	Composition
Fly Ash	46%
Steel Slag	46%
Portland Cement	8%

Stabilized/Solidified Matrices

Three solidified matrices were created: (i) a matrix blank (MB) made by hydrating the dry blend components with DI water, (ii) a representative solidified secondary waste (SW) made by hydrating the dry blend components with simulated wastewater from the ETF, (iii) an enhanced academic matrix (AM) made by mixing metal salts in with the dry blend components prior to hydration with ETF wastewater simulant. Table 4 shows the composition of each matrix.

Table 4: Composition of Solidified Materials.

	Matrix Blank (MB)	Secondary Waste (SW)	Academic Matrix (AM)
Dry Blend	71.4%	71.4%	69.7%
Metal Salts	-	-	2.4%
DI Water	28.6%	-	-
Wastewater	-	28.6%	27.9%
Total	**100.0%**	**100.0%**	**100.0%**

Contaminants were added to the enhanced AM in relatively soluble forms as (i) sodium salts of arsenic and iodine, (ii) potassium salts of selenium and rhenium, (iii) nitrate salts of silver, barium, cadmium, copper, lead and zinc, (iv) antimony oxide, and (v) cesium chloride.

Water to dry blend ratio of 0.4, consistent with previous research on similar materials (Mattigod etal, 2001), was determined experimentally to result in no bleed water formation after 1-day curing in a sealed container. For AM, the water to dry blend ratio was maintained and metal salts added to the solid materials. Thus, there is an apparent dilution of the recipe due to the addition of soluble metal salts.

Treatment Procedure and Curing

Mixing of S/S treated materials was conducted in a 30-L stainless steel bowl using a Univex SRM-30 planetary mixer (Univex Corp., Salem, NH). The first step in the treatment procedure was to thoroughly mix dry materials (i.e., dry blend components and metal salts where appropriate) for a minimum of 5 minutes. When dry materials were visually well-mixed, liquid was added at a rate of approximately 1 L/min up to the water to dry blend ratio of 0.4 L/kg. Finally, the slurry was allowed to mix for an additional 2 min to ensure complete blending.

S/S treated material was scooped from the mixing bowl into 2"ϕ x 4" deep cylindrical LDPE cement molds (M.A. Industries Inc., Peachtree City, GA). Each mold was filled in roughly three layers interspersed with 30 seconds of vibration on a mini vortex mixer (VWR Scientific model 945300) to minimize air voids. Filled molds were closed with air-tight LDPE snap-on caps and sealed with paraffin wax film. Samples were cured in sealed containers for a minimum of 30 days and stored under these conditions until just before they were used for testing.

Sample Preparation for Leaching Tests

Samples used in monolithic leach testing (i.e., MT01 protocol) were cut within the plastic mold to depth of 5 cm using a tile saw (see Appendix C, Figure C1). The portion of the sample not used for monolithic leach testing was particle-size reduced for equilibrium testing. Gross particle-size reduction was accomplished by placing cylindrical samples into a double layer of plastic freezer bags and crushing the sample to ~5 mm with a rock hammer. A parallel ceramic plate mill was used to further process the material to a particle size of <2 mm.

Leaching Tests

Three leaching tests were performed on each model system: 1) an equilibrium test with final leachate pH as the independent variable, 2) an equilibrium test with liquid-to-solid ratio as the independent variable, and 3) a mass transport test using leaching time as the independent variable. As opposed to leaching tests designed to produce a leachate representative of a particular release scenario, each of these leaching tests is designed to isolate and determine one or more fundamental leaching parameters which are characteristic of the solid material. This scope of report is limited to the equilibrium test as a function of pH and the mass transfer test.

SR02 - Solubility and Release as a Function of pH (Kosson et al, 2002)

The SR02 protocol is a parallel batch equilibrium test that results in extractions over a range in final eluate pH (2< pH <12) using 11 parallel batch extractions with different acid and base additions. The solid material is particle-size reduced in order to facilitate equilibrium between solid and aqueous phases. This method provides a pH titration curve for the material, and solid-liquid equilibrium as a function of pH.

Subsamples of test material equal to a minimum dry equivalent mass (e.g., 20 g dry equivalent) were placed into each of eleven high-density polyethylene (HDPE) bottles. An aliquot of nitric acid or NaOH was added to each deionized (DI) water eluant in order to raise or lower the final pH, respectively. The extract bottles were sealed with leak-proof lids and tumbled in an end-over-end fashion at a room temperature (20 ± 2°C) for a contact time sufficient to establish equilibrium between solid and aqueous phases. For the current project, samples were particle-size reduced to <2 mm requiring a contact time of 48-hours. After the specified contact time, the eluates were clarified by allowing the extraction bottles to stand for 15 minutes. A minimum volume of clarified supernatant from each extraction bottle was decanted in order to measure and record the solution pH and conductivity. Eluates were then separated from the solid material by vacuum filtration through 0.45-μm pore size polypropylene filtration membranes. For each eluate, analytical samples were collected for i) elemental analysis (preserved with Optima grade nitric acid, 1% final concentration) and ii) total carbon and anion analysis. All samples were refrigerated at 4 ^{o}C for storage prior to analysis.

The outcomes of the SR02 protocol are (i) a titration curve of the solid material as a function of the amount of acid added to each batch extraction and (ii) constituent liquid-solid partitioning (LSP) curve as a function of final eluate pH.

SR03 – Solubility and Release as a Function of LS Ratio (Kosson et al, 2002)

The SR03 protocol is a batch equilibrium test that results in eluates over a range LS ratio from 10 to 0.5 mL/g-dry using five parallel batch extractions in DI water. No acid or base is added to the extractions. The solid material is particle-size reduced in order to facilitate equilibrium between solid and aqueous phases. This method provides data on the effect of ionic strength on equilibrium concentrations and an estimate of the composition of COPCs in the matrix pore solution.

Subsamples of test material equal to dry equivalent masses of 20, 40, 100, 200, and 400 g-dry were placed into five high-density polyethylene (HDPE) bottles. A 200-mL aliquot of DI water was added to each bottle resulting in LS ratios of 10, 5, 2, 1, and 0.5 mL/g-dry, respectively. The extract bottles were sealed with leak-proof lids and tumbled in an end-over-end fashion at a room temperature (20 ± 2°C) for a contact time sufficient to establish equilibrium between solid and aqueous phases. For the current project, samples were particle-size reduced to <2 mm requiring a contact time of 48-hours. After the specified contact time, the eluates were clarified by allowing the extraction bottles to stand for 15 minutes. A minimum volume of clarified supernatant from each extraction bottle was decanted in order to measure and record the solution pH and conductivity. Eluates were then separated from the solid material by vacuum filtration through 0.45-μm pore size polypropylene filtration membranes. For each eluate, analytical samples were collected for i) elemental analysis (preserved with Optima grade nitric acid, 1% final concentration) and ii) total carbon and anion analysis. All samples were refrigerated at 4 ^{o}C for storage prior to analysis.

The outcomes of the SR02 protocol are (i) a graph of the effect of LS ratio on equilibrium concentrations and (ii) a methodology for estimating the composition of matrix pore water at very low LS ratio.

MT01 – Mass Transfer in Monolithic Materials (Kosson etal, 2002)

This mass-transport based protocol consists of semi-dynamic tank leaching of continuously water-saturated monolithic samples. The test procedure is similar to commonly used leaching tests such as ANS 16.1; however, interpretation of leaching data from the test is different.

A monolithic sample is contacted with a volume of leaching solution at a ratio of 10 mL/cm^2 of exposed surface area. No or very little agitation is provided. The test is conducted at room temperature (20±2°C) in air-tight vessels with minimal headspace in order to minimize carbonation of alkaline solutions (see Appendix C, Figure C2). A schedule of periodic leaching solution renewals, at pre-determined cumulative times of 2, 5 and 8 hours, 1, 2, 4, and 8 days, results in seven leachates with leaching intervals of 2, 3, 3, 16 hours, 1, 2, and 4 days. This baseline schedule can be extended with additional intervals at cumulative leaching times of 14, 21, 30, 60 and 90 days for a total of twelve leaching fractions. A picture sequence of the leaching solution renewal procedures is shown in Figure C3 of Appendix C.

For each time interval, leachant pH and conductivity are measured prior to preparation of an analytical sample by vacuum filtration through a 0.45-µm pore size polypropylene filtration membrane. For each eluate, analytical samples were collected for i) elemental analysis (preserved with Optima grade nitric acid, 1% final concentration) and ii) total carbon and anion analysis. All samples were refrigerated at 4 ^{o}C for storage prior to analysis.

The outcomes of the MT01 protocol are the cumulative release and flux of COPCs as a function of leaching time. This data can be used to estimate mass transfer coefficients of COPCs through the granular material which can be used as input to predictive mass transport release.

Analytical Methods

Standard methods (i.e., USEPA guideline SW-846) and QA/QC measures were applied for all analyses. Aqueous concentrations of most major and trace elements were determined using inductively coupled plasma-mass spectrometry (ICP-MS). Ion chromatography (IC), using conductivity and ampometry detectors, was used to determine the aqueous concentrations of anions. Total carbon (TC) analysis via combustion catalytic oxidation was used to determine dissolved inorganic carbon (DIC) and dissolved organic carbon (DOC) as non-purgable organic carbon. Table 5 shows the full suite of analytes measured during material characterization.

Table 5: Measured Parameters, Methods and Chemical Analytes for Material Characterization.

Measurement	**Method**	**Analytes**
pH	Probe	
Conductivity	Probe	
Major and Trace Elements	ICP-MS	Al, Sb, As, Ba, Be, B, Cd, Ca, Cs, Cr, Co, Cu, Fe, Pb, Mg, Mn, Mo, Ni, K, Re, Se, Si, Ag, Na, Sr, Sn, Tl, Th, Ti, U, V, Zn
Anions	IC	Br, Cl, F, I, NO_3, NO_2, PO_4, SO_4
Carbon	TC	DOC, DIC

Quality Control

Protocol QA/QC primarily involved the use of method blanks to determine potentials for interfering releases from leaching solutions or equipment. In general, method blanks were extraction replicates for which no solid phase was included. However, for equilibrium testing as

a function of pH (SR02), three types of method blanks were used to represent (i) the deionized water used in the extract, (ii) the most concentrated nitric acid addition, and (iii) the most concentrated sodium hydroxide addition. Method blanks were carried through the entire protocol, including tumbling and filtration

Analytical QA/QC incorporated the use of blanks and spiked samples. All analyses were calibrated to a multipoint calibration curve using at least 4 standard concentrations and verified by initial calibration verification (ICV) standard obtained from a different source. In addition, instrument blanks and continuing calibration verification (CCV) standards were analyzed after every 10 analytical samples with the requirement that the concentration be within 10 percent of the expected value. CCV standards and instrument blanks also were run at the end of each batch of samples. For both ICP-MS, each sample was analyzed along with a matrix spike (an aliquot of the sample plus a known spike concentration of the element of interest) with the allowable spike "recovery" limit within 80-120% of the expected value.

RESULTS AND DISCUSSION

Leaching test results for the SR02 and MT01 protocols are discussed in terms of data consistency as well as the effects of matrix loading and eluant composition in this section. A full presentation of leaching test results for the three subject materials tested in DI water and simulated Hanford groundwater is presented in the Appendices A and B, respectively. Project pictures of samples and procedures are presented in Appendix C.

Data Set Presentation and Consistency

A comprehensive set of equilibrium and mass transport data for a constituent can be shown in one figure using four scatter plots: a) comparison of equilibrium-based concentrations for tank leach eluant concentrations, b) eluant pH evolved during the tank leach test, c) mean constituent flux plotted as a function of mean leaching interval, and d) cumulative release. Since all concentration values must be detectable and quantifiable, MDL and ML lines are typically plotted on these graphs. Concentration values are reported as ½ of the MDL value when found to be below MDL (e.g., commonly considered "non-detection" values). For flux and cumulative release, the concentrations at the ML and MDL are carried through calculation and the flux resulting from ML and MDL concentrations are plotted on the graph. This methodology of data

representation can be used to show that a set of equilibrium and mass transfer test data displays adequate analytical quality control and is consistent between equilibrium and mass transfer leaching tests.

An example of the typical presentation of equilibrium and mass transfer test data is shown in Figure 1 for constituent iodide leaching from the AM material. In Figure 1a, the SR02 data in the alkaline pH range, where the iodide ion (I^-) was detectable, indicate that the release of iodide is not a strong function of eluate pH and behaves as a "highly soluble" species in the AM material with concentrations well above the quantifiable and detection limits. For eluate pH below 7, the iodide ion is not detectable and, consequently, set to ½ the MDL concentration for reporting.

Since the duration of test intervals for the tank leaching tests is designed to maintain a driving force for mass transport between the solid material and the leaching solution, COPC concentrations in mass transport-based test eluants should not be higher than the equilibrium concentration at the pH of the tank leach test eluant. For the iodide data shown in Figure 1a, mass transfer eluate did not reach equilibrium and the mass driving force was maintained. Tank leach eluant concentrations above the equilibrium concentration at a particular pH indicates that the driving force for mass transport was significantly reduced in those leaching test intervals.

The results of mass transfer testing are shown in terms of mean interval flux and cumulative release in Figure 1c and d, respectively. The dashed line indicates the model where release varies with the square root of time and no matrix alterations are assumed (e.g., simple diffusion model). Due to the limiting assumptions of this model, predicted release is at least an order of magnitude overly-conservative after approximately one year of continuous tank leaching for most COPCs in this study. Realistic mass release predictions can only be accomplished using mass transport models that consider (i) matrix mineralogy with respect to the speciation of COPCs, (ii) physical retention in the solid matrix, and (iii) alterations in geochemistry and physical properties due to interaction with the surrounding environment (e.g. wetting-drying cycles, carbonation, oxidation, etc).

The iodide flux shown in Figure 1c indicates minor variations in the release of iodide that are not reflected in the cumulative mass release in Figure 1d because of the summing of interval mass releases and the logarithmic scale. The interpretation of the cumulative release curve can be

significantly altered by a minor fluctuation in the interval release (e.g., wash-off at early leaching intervals). Such fluctuations are shown in the mean flux plot, but typically do not influence interpretation. Therefore, the flux curve should be used to represent and interpret mass transfer release.

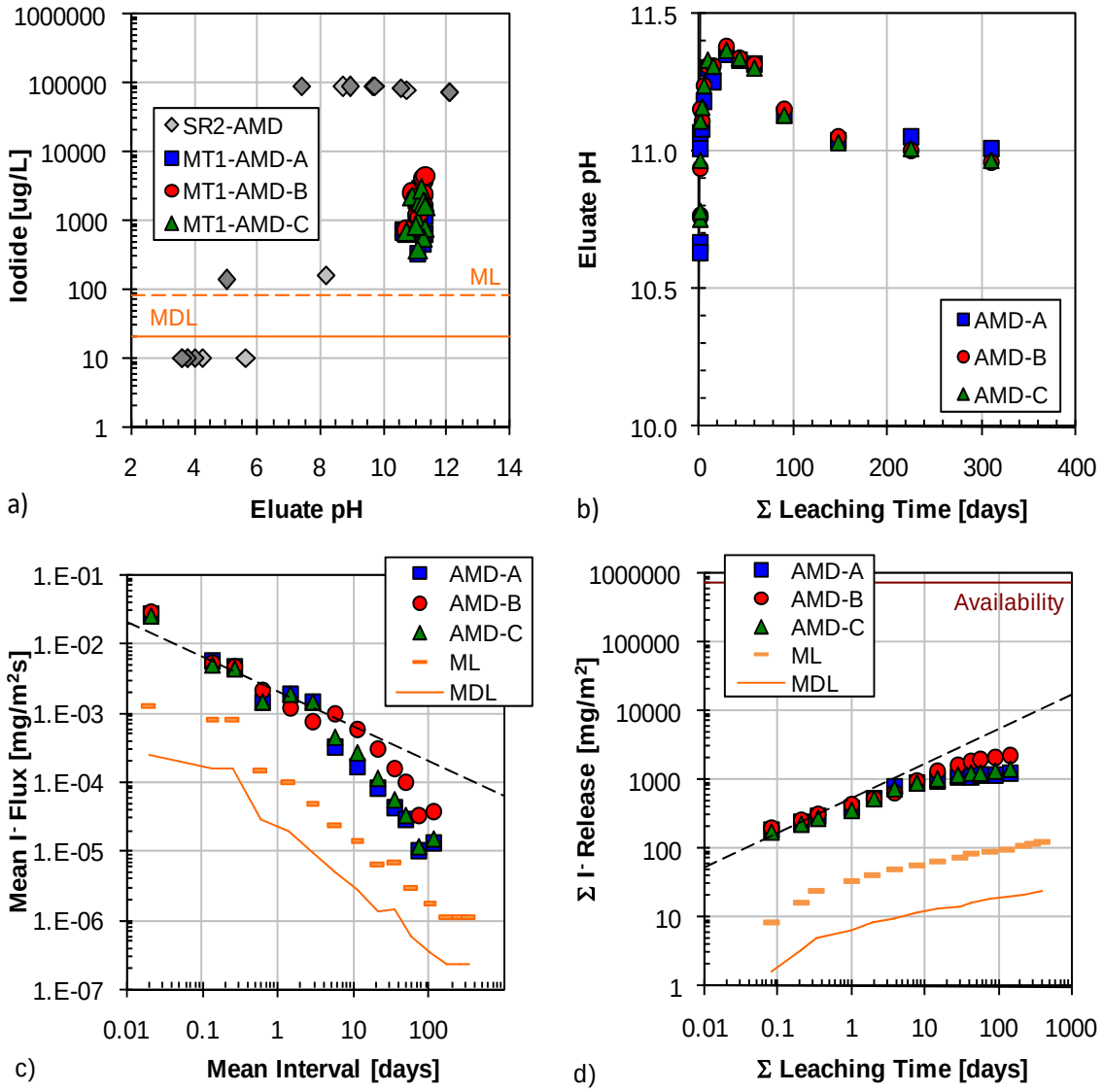

Figure 1: SR02 and MT01 test results for iodide leaching from the AM material.

Data Consistency in Similar Matrices

Data test for select constituents in similar matrices should be consistent. Each of the three matrices discussed in this report are based on the same combination of dry blend components (i.e., Portland cement, fly ash and steel slag). Leaching behavior (i.e., equilibrium and mass transport release) of common constituents inherent to the dry blend components is expected to be similar. This consistency can be demonstrated through plots of equilibrium-based concentration and mass transport-based mean flux for similar matrices on the same axes (see Figure 2).

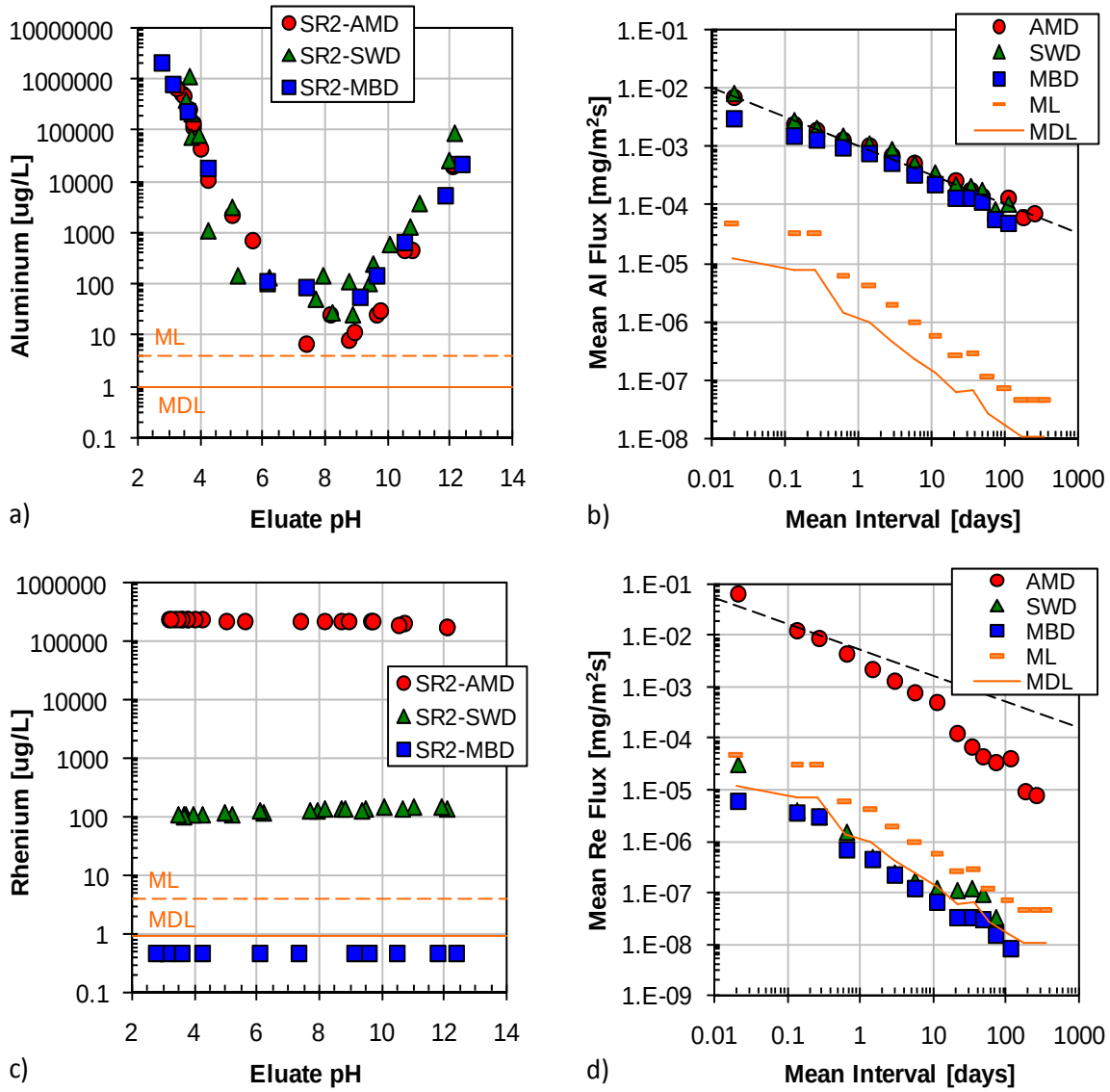

Figure 2: Data consistency check between similar matrices: a) aluminum LSP curve from SR02 test, b) aluminum flux from MT01 test, c) rhenium LSP curve from SR02 test, and d) rhenium flux from MT01 test.

The mass transport leaching behavior of aluminum is consistent for all three matrices (Figure 2a and b) as aluminum is a constituent inherent to the hydration mineralogy of the dry blend. However, the fact that rhenium release is not consistent between matrices (Figure 2c and d) is indicative of levels at which rhenium was spiked into these matrices. The LSP curves support that rhenium was spiked into AM at high level, SW at low level, and not at all into MB. Note that a significant increase in the rhenium LSP curve between MB and SW does not result in a detectable mass transport release. This may be attributed to the physical retention of the monolithic matrix.

Leaching Test Results

This document presents a large set of detailed leaching characterization data for three matrices, tested using two different eluants for eluate pH and 26 COPCs. In order to facilitate discussion of the leaching data, 24 of the 26 analytical parameters are grouped for presentation as shown in Table 6.

Table 6: COPC Groupings for Discussion of Leaching Test Results

Group 1 **Bulk Mineralogy**	**Group 2** **Salts & Carbon**	**Group 3** **AM & SW Spike**	**Group 4** **Other COPCs**
pH (OH^-)	Na [a]	I	Sr
Al	K [a]	Re	Ba
Ca [a]	Cl [a]	As [b]	V
Mg [a]	SO_4 [a]	Sb [b]	Pb [b]
Fe	DIC (CO_3 [a])	Cs [b]	Cd [b]
Si	DOC	Se [b]	Cu [b]

[a] COPC included in SHG recipe.
[b] COPC spiked into AM material only.

Constituents that make up the bulk mineralogy of cement-based materials are included in Group 1. Highly soluble constituents, dissolved inorganic carbon (DIC) and dissolved organic carbon (DOC) are presented as Group 2. Groups 3 and 4 contain constituents that were loaded into the

AM and SW materials (e.g., I, Re, As, Sb, Cs, Se, Cd, Pb, and Cu) or are trace constituents inherent to the dry blend materials (e.g., Sr, Ba, V).

The Comparison of Similar Matrices: Equilibrium-based Tests

The similarity of the LSP curves derived from the SR02 equilibrium-based leaching test for Group 1 constituents (Figure 3) indicate the basic mineralogy of the three subject materials is the same. The only mechanistic difference in the LSP curves for these primary matrix mineralogy constituents is seen in Figure 3f where the LSP curve for Si in the AM material deviates from those of the SW and MB materials.

Figure 4 shows that the LSP curves for Na, K, Cl, SO_4 and DOC in the Group 2 constituents are weak functions of eluate pH. This data indicates that these highly soluble constituents have low chemical retention in the matrix. The level of LSP curves for these constituents reflects the hydration of dry blend components with ETF wastewater (AM and SW) rather than DI water (MB).

Group 3 constituents were spiked into AM and SW (I and Re only) and not spiked into MB. While there are minor variations in the LSP curves for these constituents (Figure 5), the LSP levels are consistent with the relative levels of loading into the respective materials. For example, all levels of the LSP curve are highest for the AM material. In addition, the only significant difference between SW and MB materials is shown for I and Re which were included in SW at modest levels in the ETF wastewater. The solubility and release behavior of I and Re appear to be weak functions of eluate pH. Several constituents in this group (i.e., Sb, Cs, and Se) show flat LSP curves at high loading while pH-dependent LSP curves at lower loading. This may indicate a change of speciation or sorption mechanisms as loading levels change.

The LSP curves for Group 4 constituents are shown in Figure 6. From this group, Sr, Ba, and V were inherent to the dry blend materials and the respective LSP curves shown only minor differences in solubility and release behavior. The remainder of the group, Cd, Pb, and Cu were spiked into the AM material only; however, this is only evident in the LSP curves for Cd and Pb. Copper behaves in a very similar manner in all three subject materials.

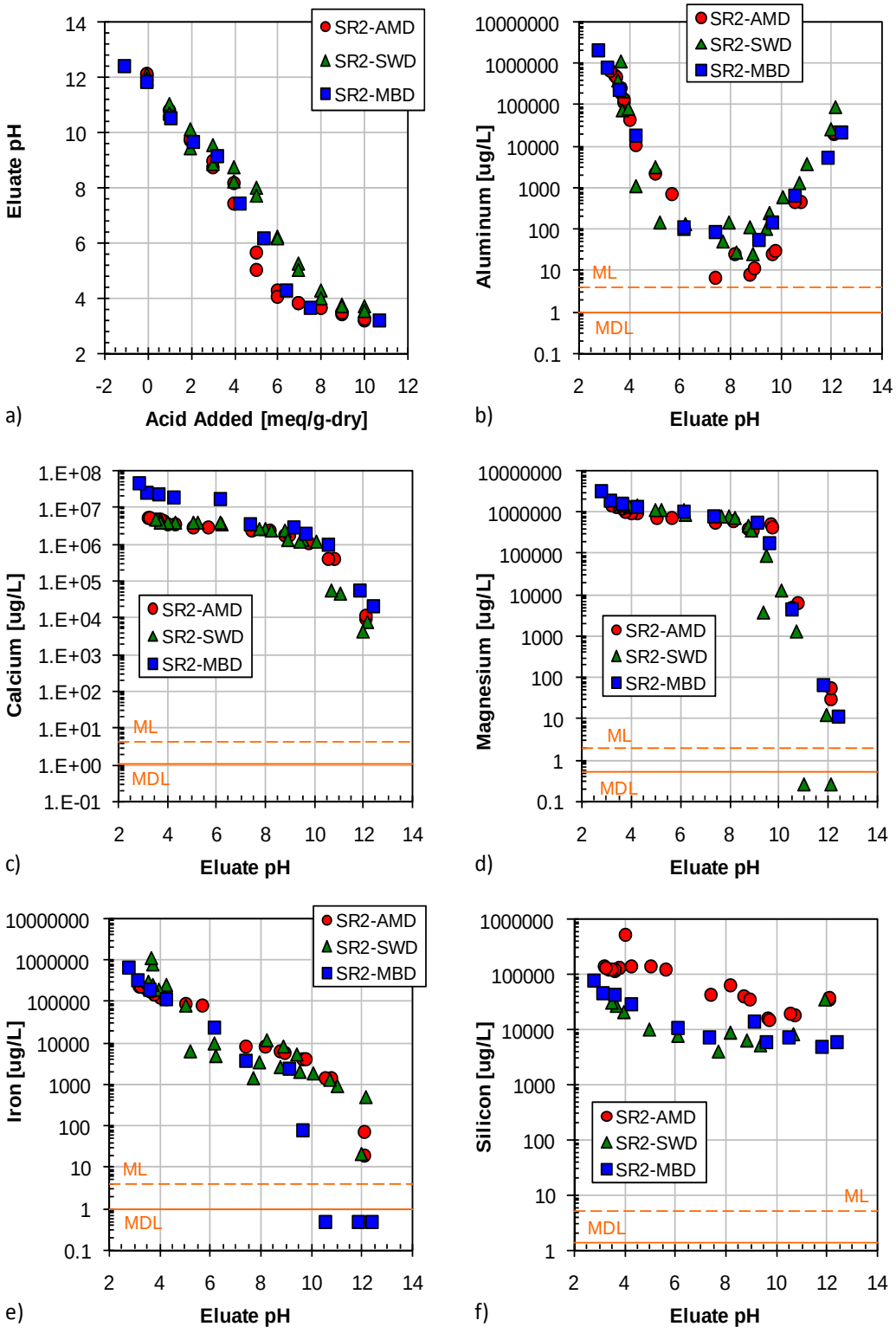

Figure 3: Comparison of LSP curves of Group 1 constituents from SR02 leaching test conducted with deionized water.

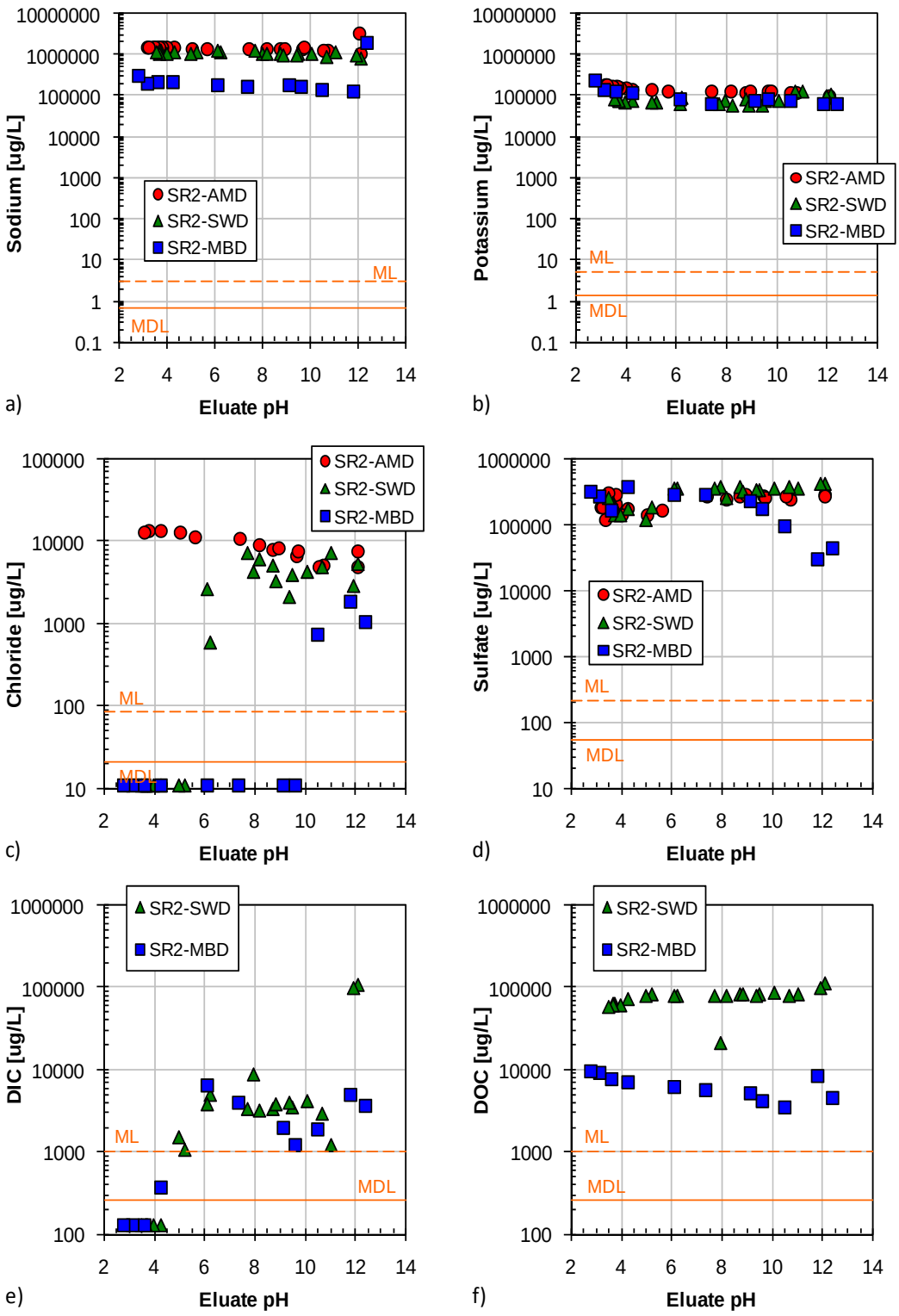

Figure 4: Comparison of LSP curves of Group 2 constituents from SR02 leaching test conducted with deionized water (DIC/DOC not analyzed for AM materials).

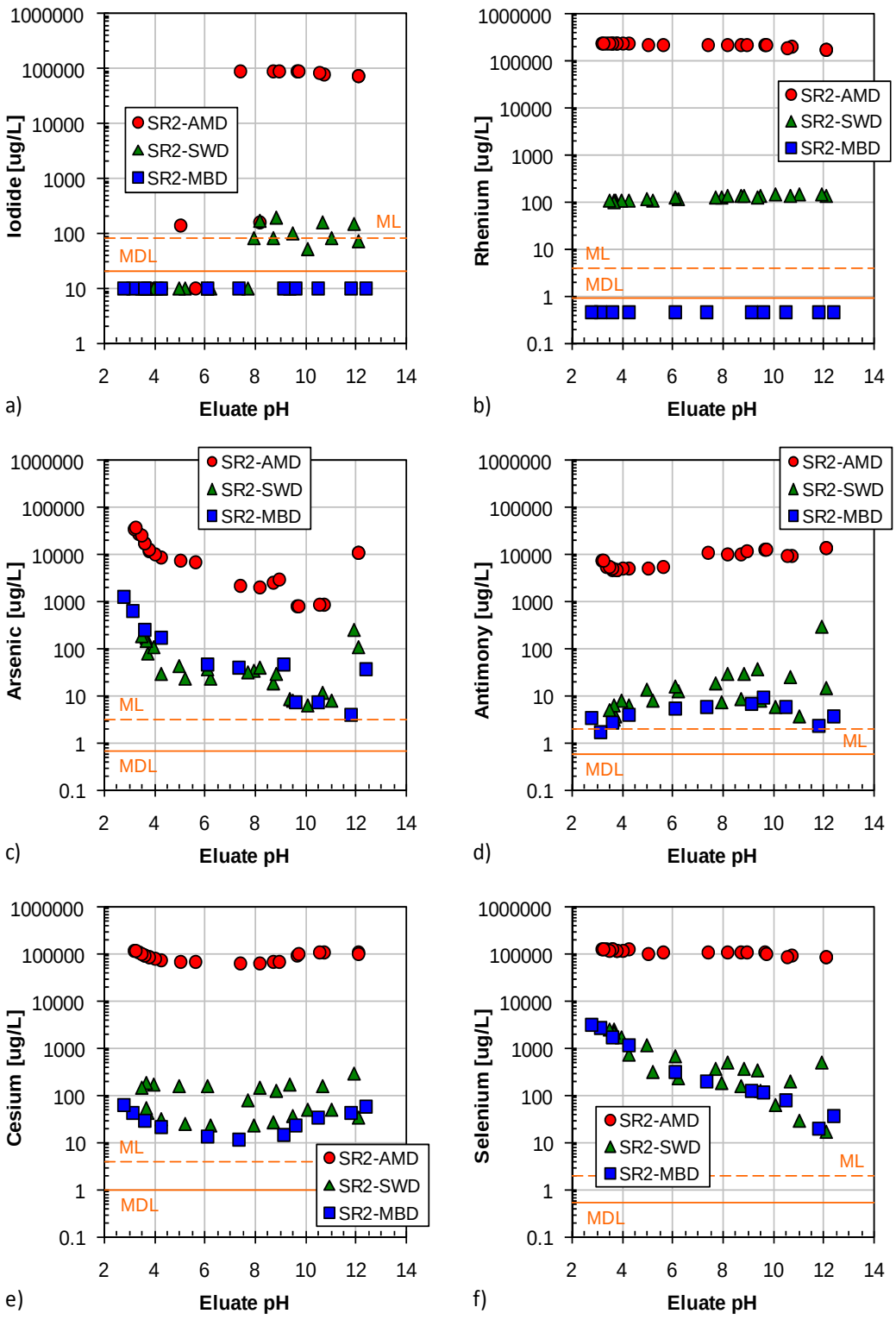

Figure 5: Comparison of LSP curves of Group 3 constituents from SR02 leaching test conducted with deionized water.

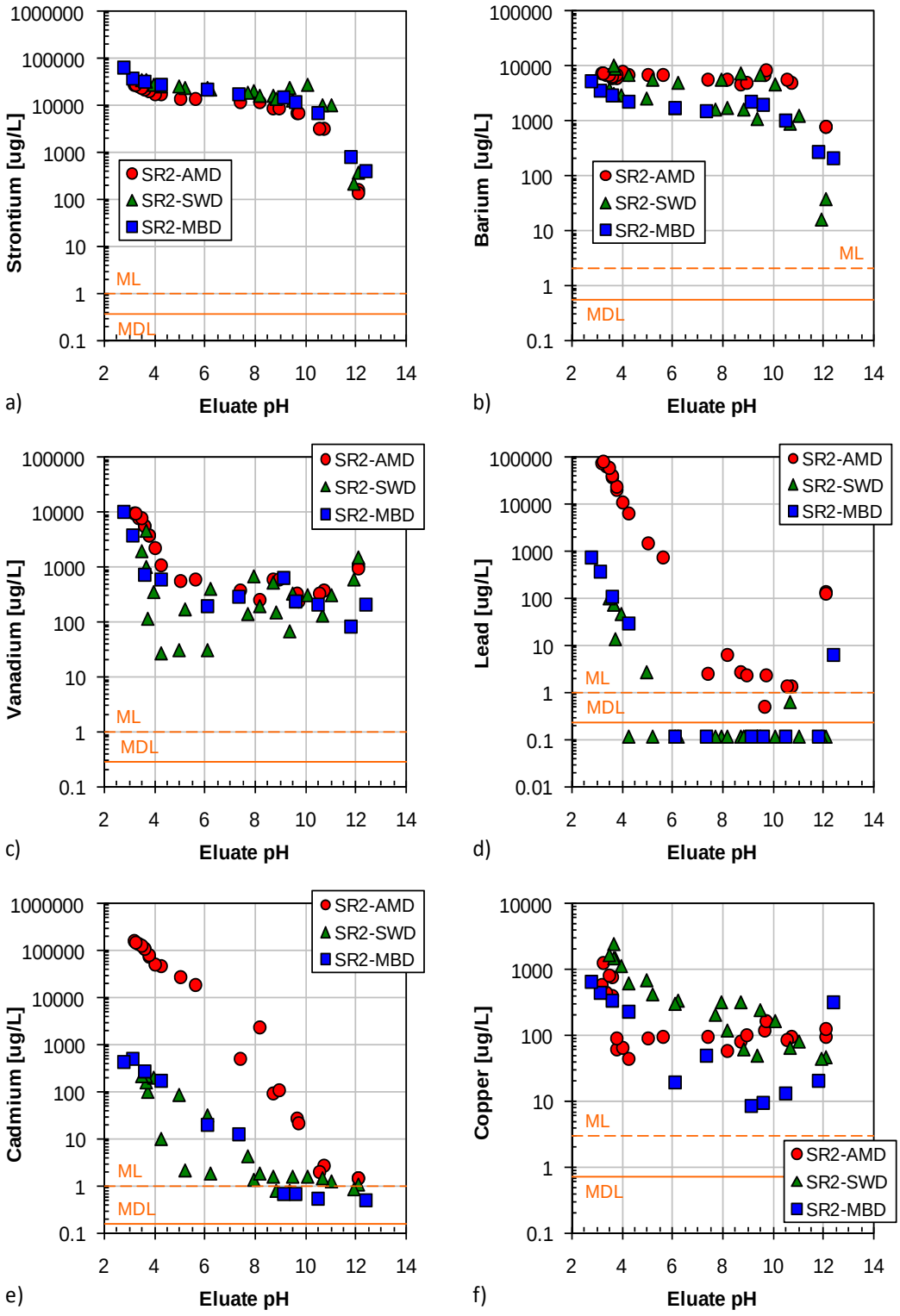

Figure 6: Comparison of LSP curves of Group 4 constituents from SR02 leaching test conducted with deionized water.

The Comparison of Similar Matrices: Mass Transfer-based Tests

Comparison of mass transfer test data between subject materials for the four constituents Groups 1-4 are shown in Figures 7-10 respectively.

Figure 7 shows that there are minor differences in the interval flux curves for the Group 1 constituents. For some constituents (e.g., Al, Mg), this is likely a consequence of the shift in pH (see Figure 7a) due to the addition of ETF wastewater to the SW and AM materials. The variation in Fe flux is likely due to the reduction capacity of the solid materials and the fact that Fe is sensitive to changes in redox; however, neither the reduction capacity of the solid materials nor the redox potentials of eluant were measured.

In general, the flux of Group 2 constituents is consistent with presence of these constituents in the ETF wastewater added to SW and AM materials (see Figure 8). For example, sodium flux is significantly higher in the SW and AM materials due to the 2.6M Na in the ETF wastewater. Added sodium, spiked into the AM material as sodium arsenate and sodium iodide, results in a high flux in the AM material over that of the SW matrix. A similar trend is shown in Figure 8b where potassium was spiked into AM as potassium rheniate and potassium selenate.

Figure 9 shows the release flux for Group 3 constituents. For many of the COPCs in this group, the fact that these constituents were only spiked into the AM material is obvious in that only the AM flux is above QA/QC limits. An interesting observation is that the low-level spiking of iodide and rhenium into SW matrix was not detected as an increase in mass flux over the matrix blank. However, when the level of iodide and rhenium loading was increased, these constituents were readily released from the solid material.

The mass transfer flux of Group 4 constituents is shown in Figure 10. Of these constituents, Ba, Sr, and V were inherent in the dry blend, while Pb, Cd, and Cu were spiked into the AM material only. Of the dry blend constituents, Ba flux displays a higher degree of variability than do Sr and V, which may be evidence of some mixing problem during treatment or of inherent heterogeneity in the dry blend components. For the spiked constituents, all may be considered "well-retained" in the AM matrix with only the Pb showing flux values above quantifiable levels.

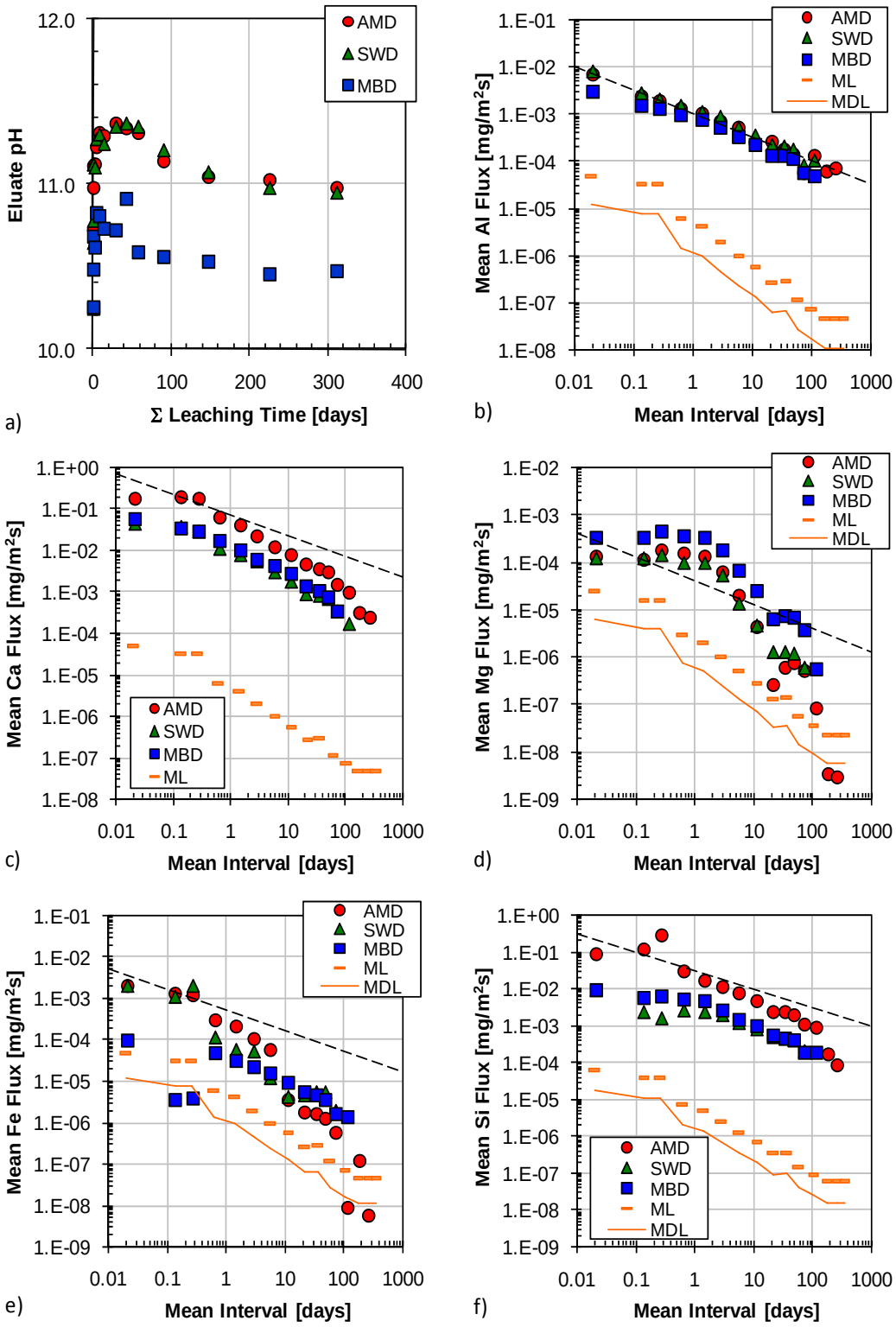

Figure 7: Comparison of mass transport flux of Group 1 constituents from MT01 leaching test conducted with deionized water.

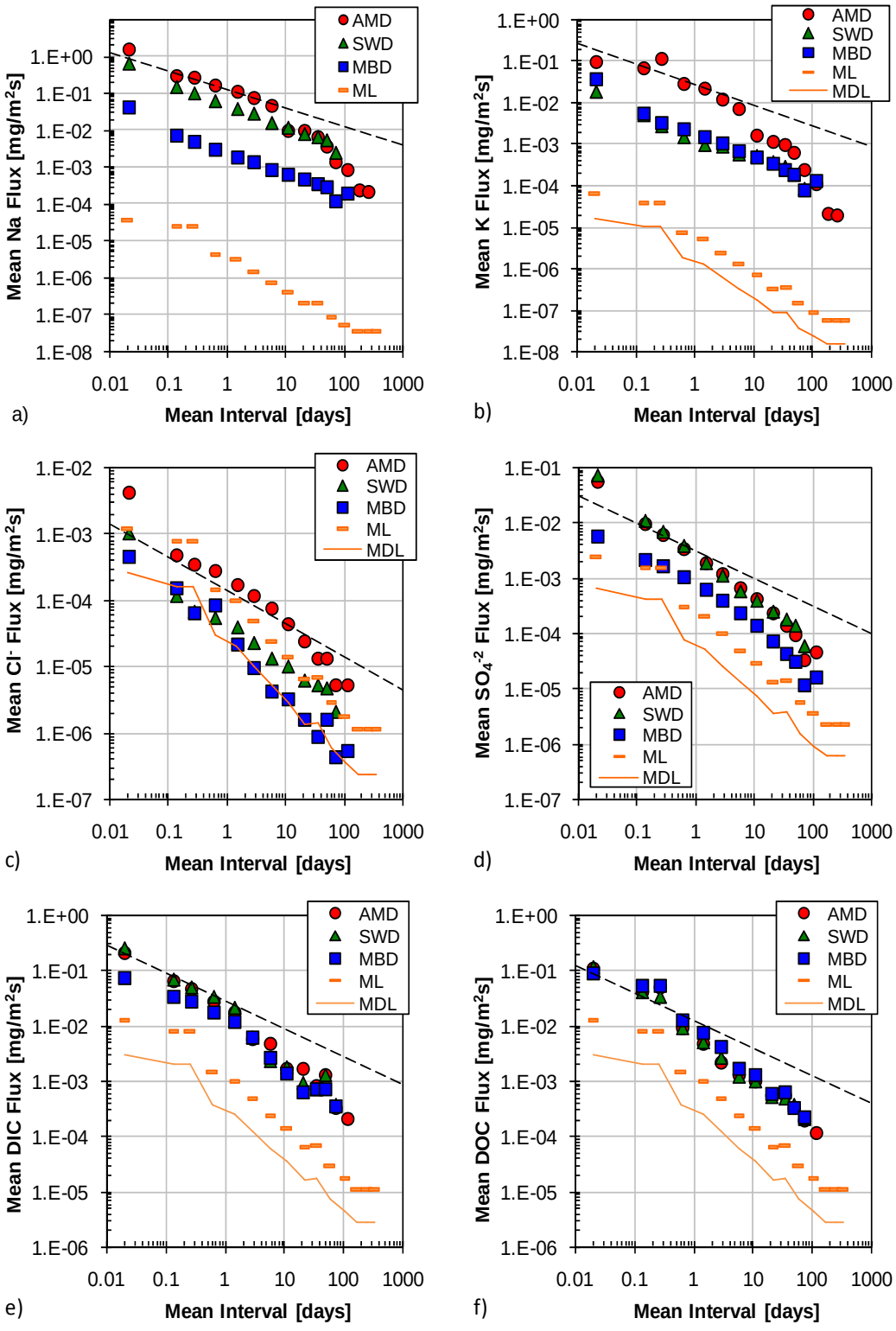

Figure 8: Comparison of mass transport flux of Group 2 constituents from MT01 leaching test conducted with deionized water.

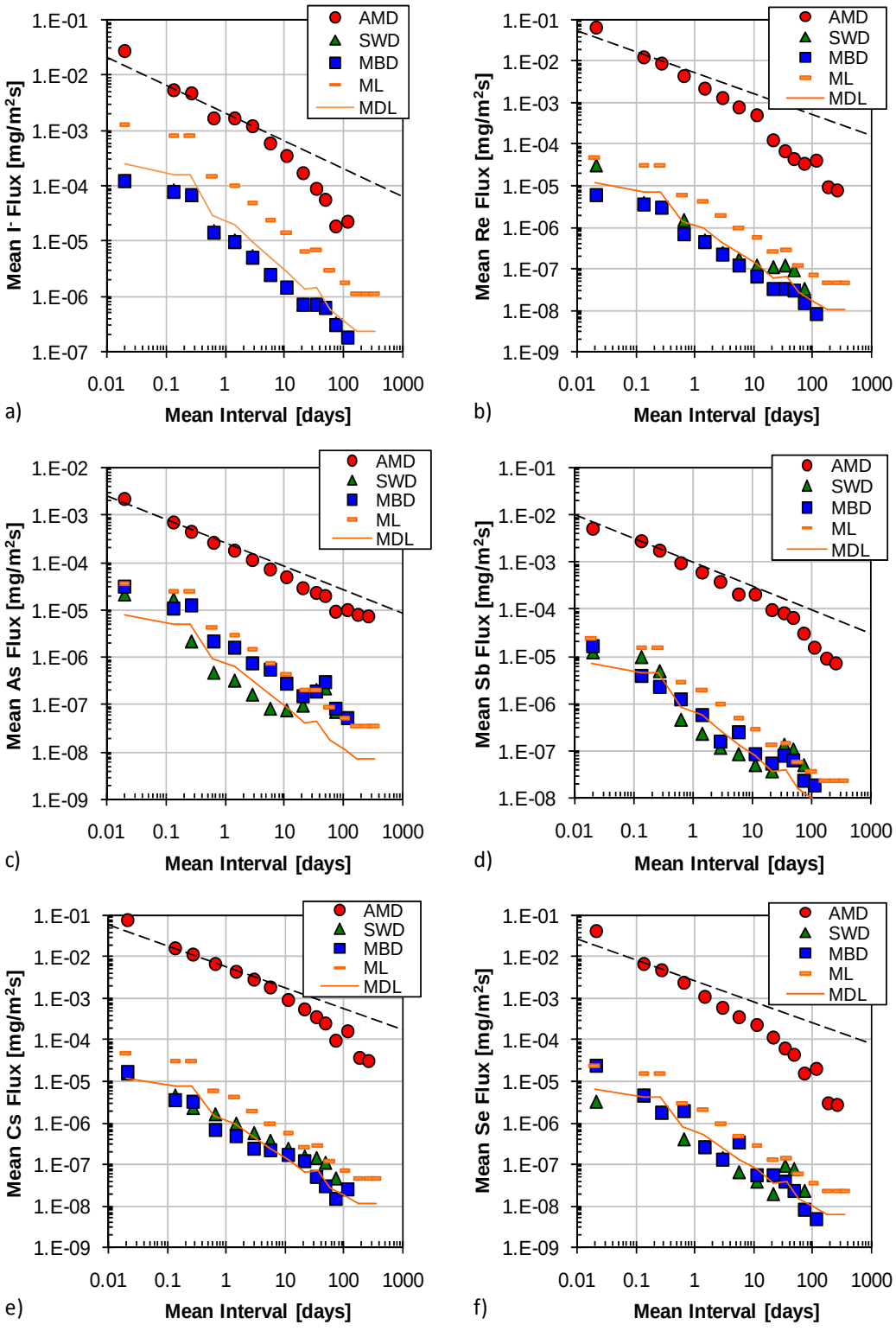

Figure 9: Comparison of mass transport flux of Group 3 constituents from MT01 leaching test conducted with deionized water.

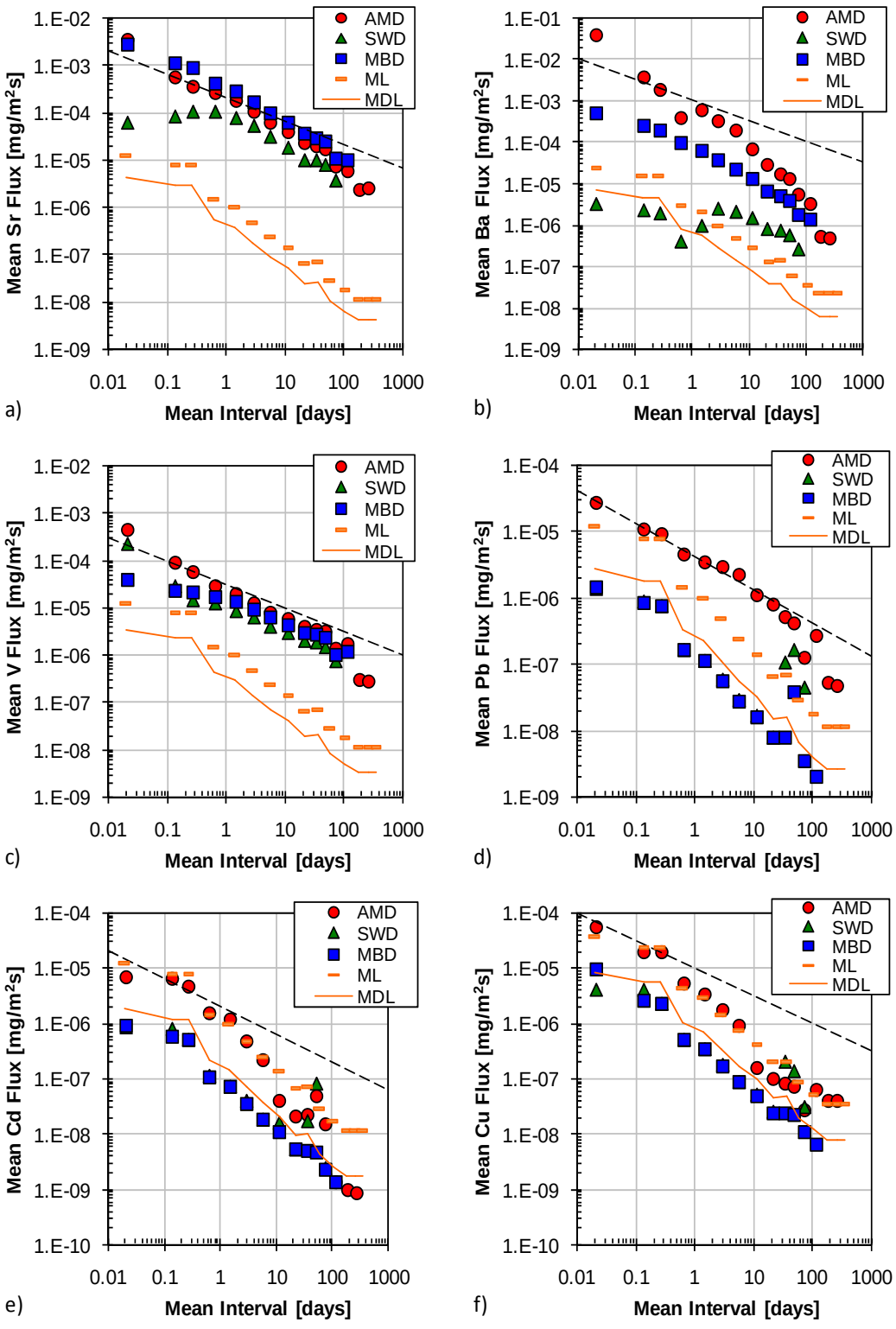

Figure 10: Comparison of mass transport flux of Group 4 constituents from MT01 leaching test conducted with deionized water.

The Effect of Eluant Composition: Equilibrium-based Tests

Comparison of LSP curves can be used to illustrate the effect of conducting equilibrium-based leaching tests in SHG rather than DI water. Figures 11-14 show the LSP curve data for SW and AM materials from the SR02 protocol with these eluants.

Figure 11a shows that there is a minor increase in the eluate pH for the SW material when the test is run with SHG. For the remaining Group 1 constituents, there is no obvious effect of eluant composition on the LSP curves, despite the fact that SHG contains high concentrations of Ca and Mg. This observation is consistent with the assumption that SHG is a saturated solution in terms of these two components. Thus, the solubility of these constituents would be controlled by the most soluble mineral form, calcium and magnesium hydroxides.

For Group 2 constituents, only chloride concentrations show a significant increase when the SR02 test is conducted with SHG. The levels of Na, K, and SO_4 are only slightly elevated over that LSP curve in DI water. Since the SW and AM materials contain high amounts of Na, K and SO_4, the LSP curves are not significantly affected by addition of $NaHCO_3$, $KHCO_3$, and $CaSO_4$ through the SHG.

The LSP curves for Group 3 and 4 constituents (Figure 13 and 14) show no effect of conducting equilibrium tests in SHG compared to SR02 test conducted in DI water.

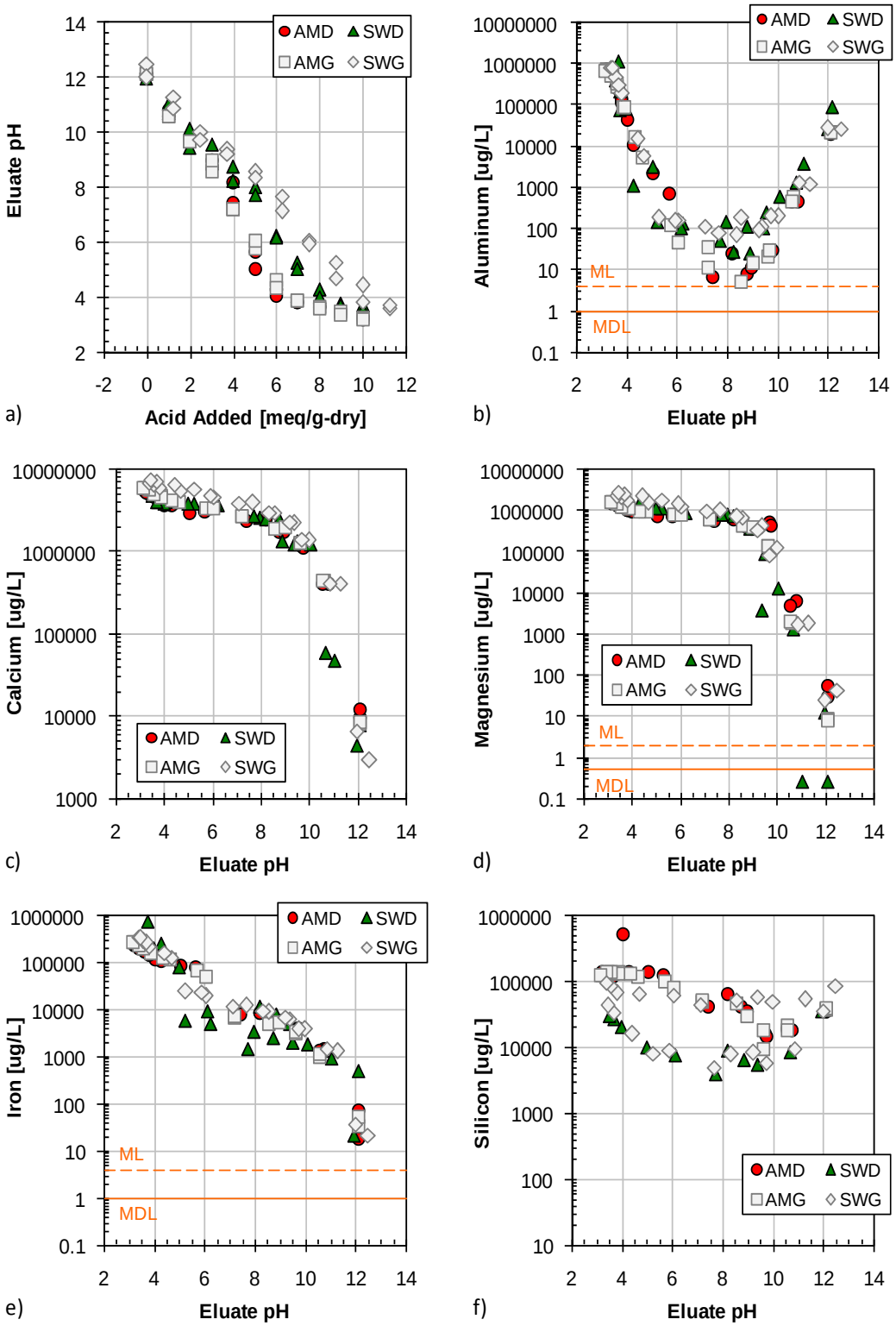

Figure 11: Comparison of LSP curves of Group 1 constituents from SR02 leaching test conducted with deionized water (AMD, SWD) and simulated Hanford groundwater (AMG, SWG).

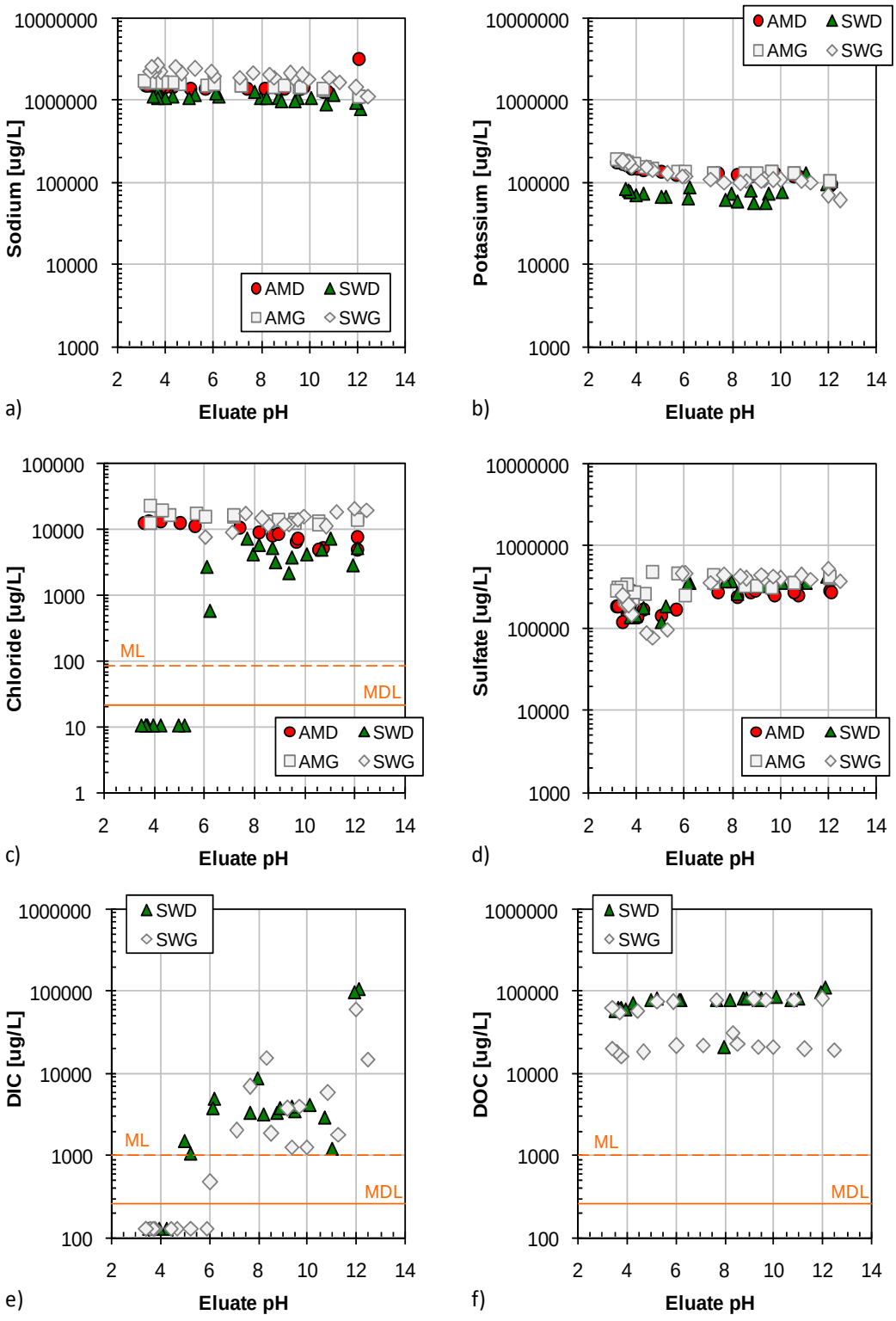

Figure 12: Comparison of LSP curves of Group 2 constituents from SR02 leaching test conducted with deionized water (AMD, SWD) and simulated Hanford groundwater (AMG, SWG).

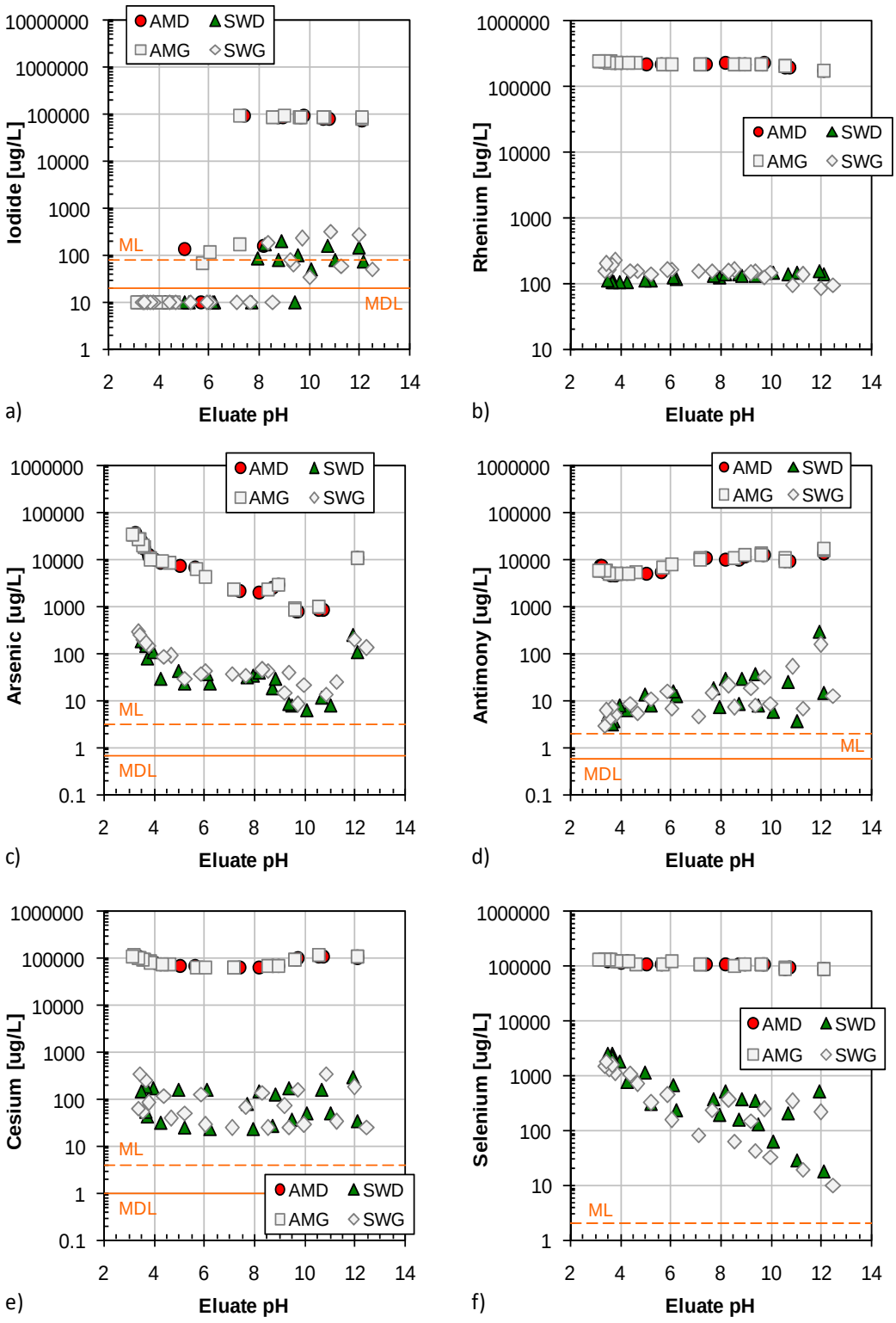

Figure 13: Comparison of LSP curves of Group 3 constituents from SR02 leaching test conducted with deionized water (AMD, SWD) and simulated Hanford groundwater (AMG, SWG).

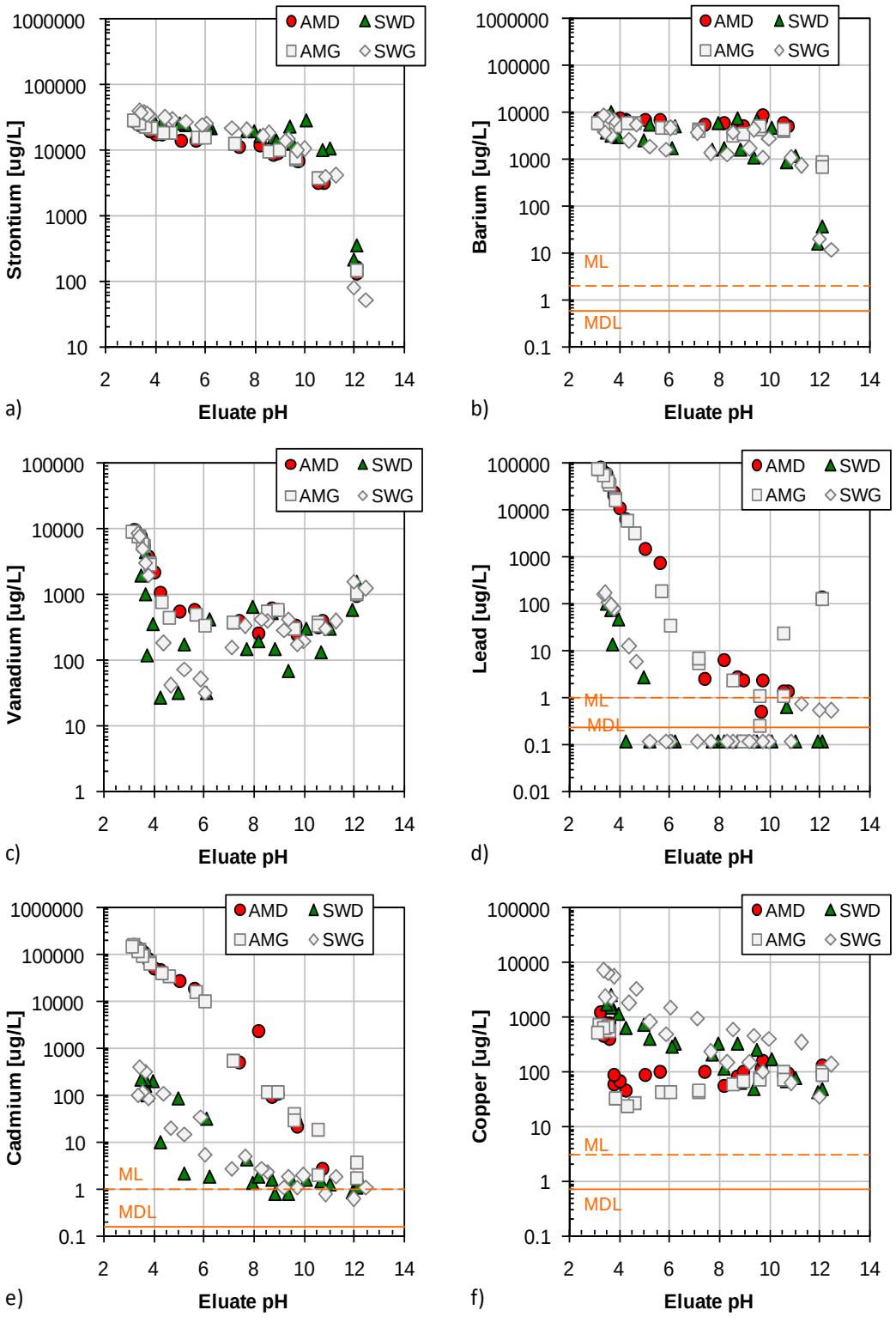

Figure 14: Comparison of LSP curves of Group 4 constituents from SR02 leaching test conducted with deionized water (AMD, SWD) and simulated Hanford groundwater (AMG, SWG).

The Effect of Eluant Composition: Mass Transfer-based Tests

The mass transfer test data for SW and AM materials in both DI water and SHG are show in Figures 15-18. During mass transfer testing in SHG, a precipitate formation was observed as a precipitate after approximately one day of continuous leaching (see Figures C4-C6, Appendix C). The mass flux plots for several constituent (e.g., Al, Ca, Fe, Si, I, Re, Sb, As, Cs, Se, Ba, V, and Pb) show a decrease in the mean interval flux at a leaching time corresponding to the appearance of the precipitate.

Figure 15 shows the effect of leaching in SHG on the mass release of Group 1 constituents. The evolution of eluate pH in SHG mass transfer test was erratic and 2-3 pH units below that of the DI water tests (Figure 15a). Overall, the mass release under SHG was less than that in DI water for bulk mineral constituents. The increased flux of Mg for tests conducted in SHG as shown in Figure 15d is due to the inclusion of Mg in SHG rather than from release from the solid material. The same can be said for Ca; however, in this case, the overall level of flux is lower in the SHG eluate potentially indicating movement of Ca into the solid matrix. Analysis of leachate blanks and evaluation of leaching in terms of actual flux from the matrix is on-going.

Except for organic carbon species, all Group 2 COPCs included in the SHG recipe and the mass transport flux for these constituents reflects higher eluate concentrations (Figure 16 a through e). The effect is much less significant for Na, K, and DIC (CO_3) than it is for Cl and SO_4. DOC flux from the both materials during leaching SHG is similar up to approximately 5 days of continuous leaching and is likely affected by the physical retention caused by the precipitation at the surface.

The mass transfer flux for constituents in Groups 3 and 4 are shown in Figures 17 and 18, respectively. For all constituents with flux values in the quantifiable range, mean interval flux when leaching is conducted in SHG is 1-2 orders of magnitude lower than the same in DI water. In some cases (e.g.,), the initial flux in SHG is higher than in DI water and decreases significantly after approximately one day of continuous leaching. It is unclear at this point whether the decrease is purely physical retention due to boundary layer formation or if there is a chemical interaction with the precipitate at the material interface.

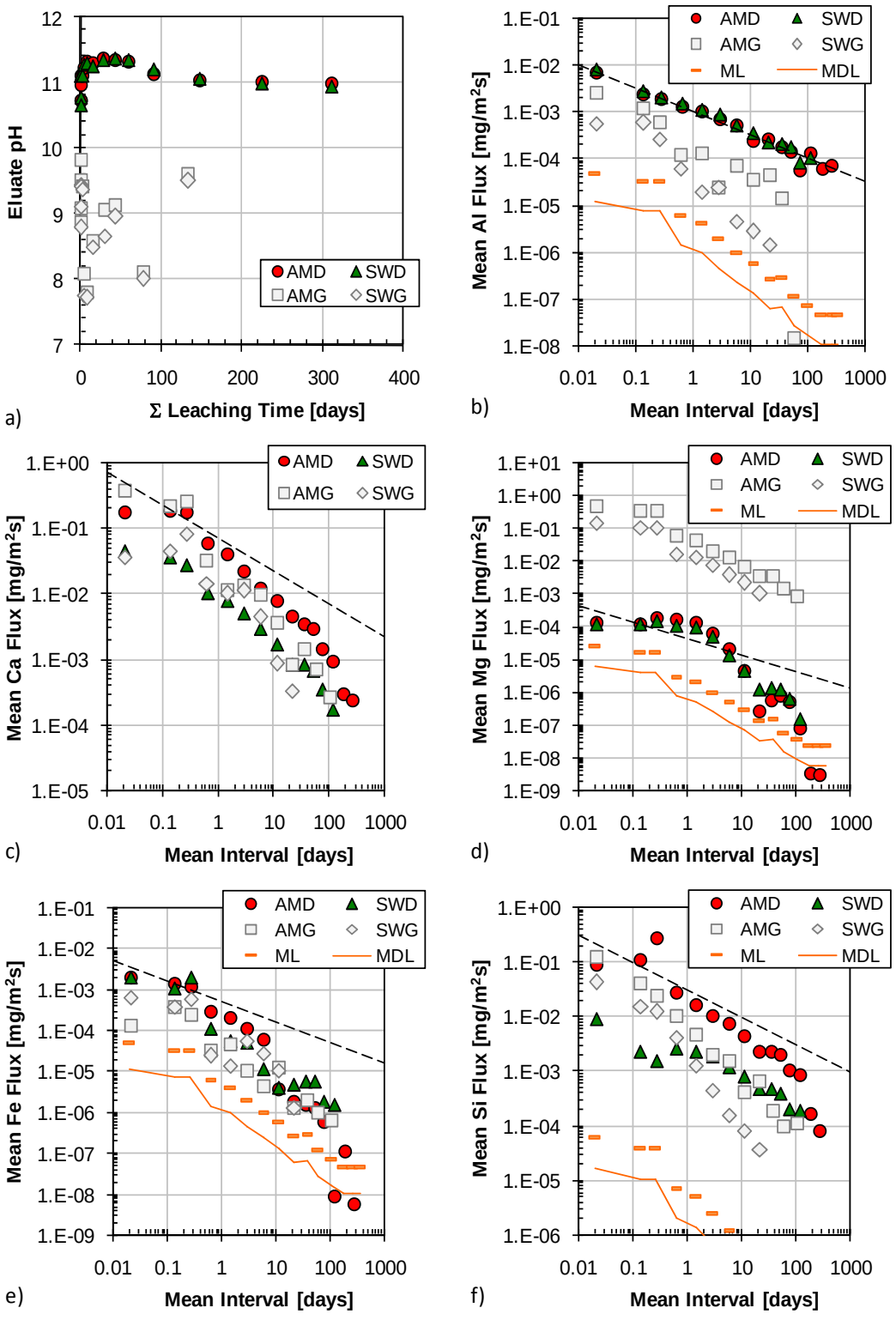

Figure 15: Comparison of mass transfer flux of Group 1 constituents from SR02 leaching test conducted with deionized water (AMD, SWD) and simulated Hanford groundwater (AMG, SWG).

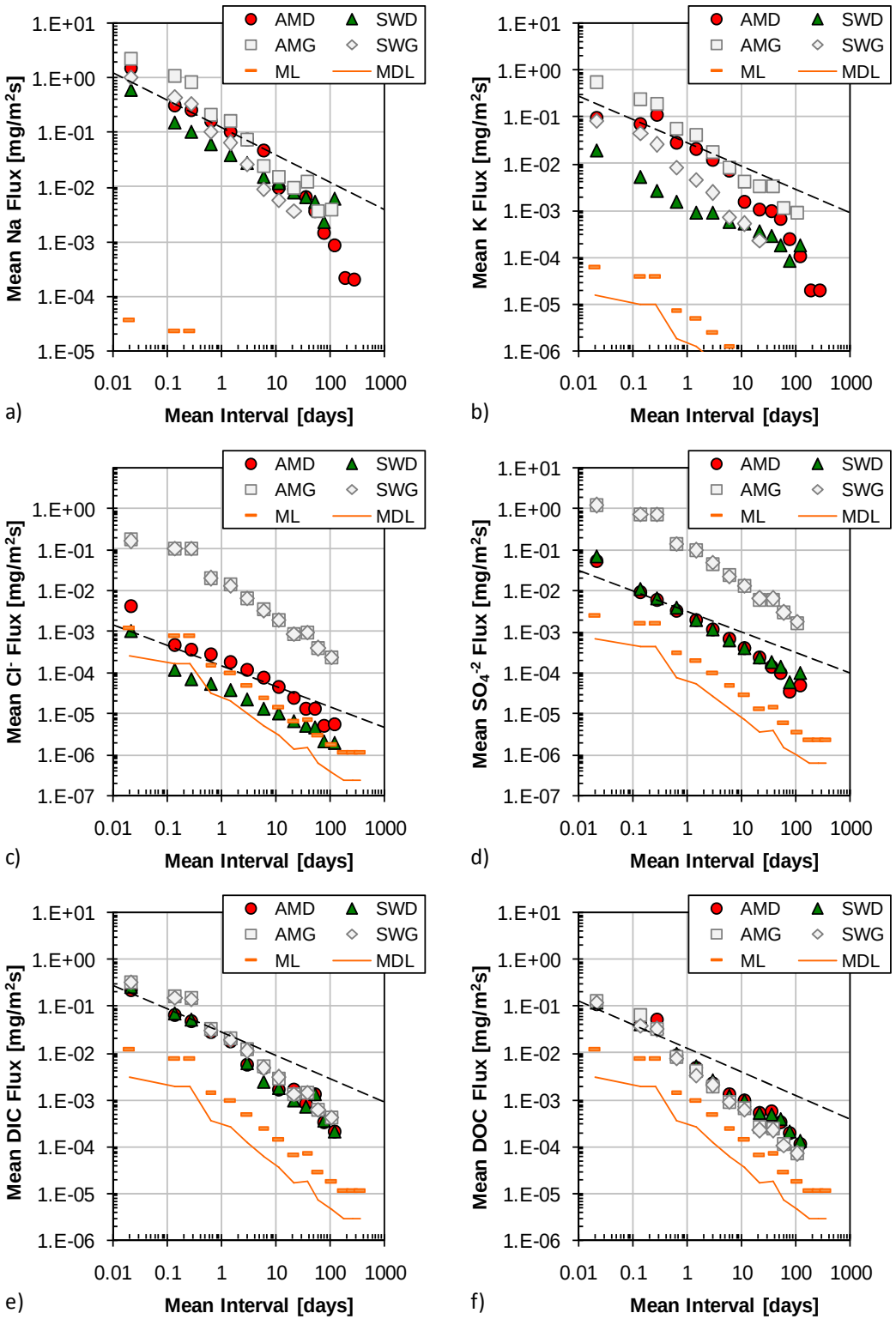

Figure 16: Comparison of mass transfer flux of Group 2 constituents from SR02 leaching test conducted with deionized water (AMD, SWD) and simulated Hanford groundwater (AMG, SWG).

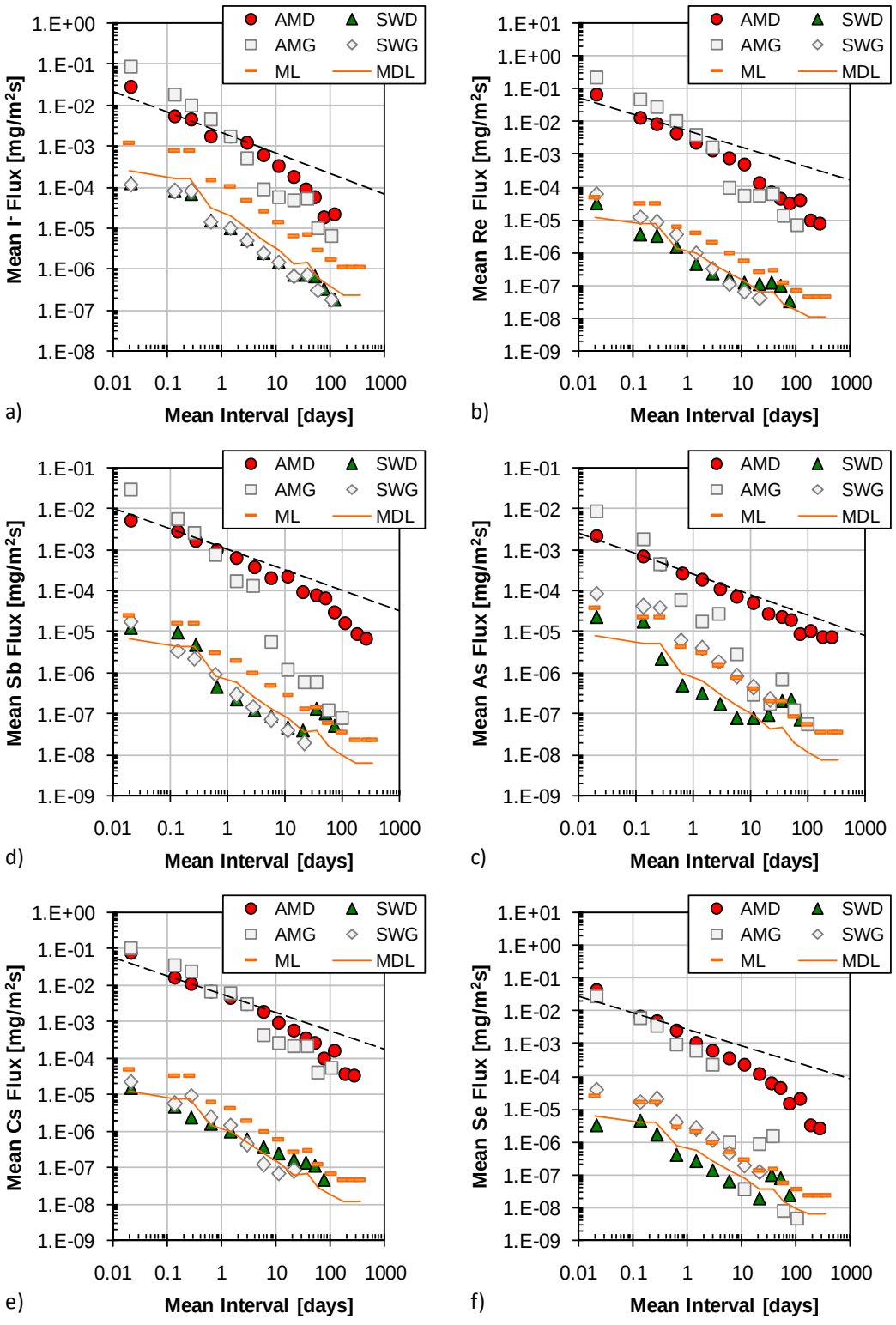

Figure 17: Comparison of mass transfer flux of Group 3 constituents from SR02 leaching test conducted with deionized water (AMD, SWD) and simulated Hanford groundwater (AMG, SWG).

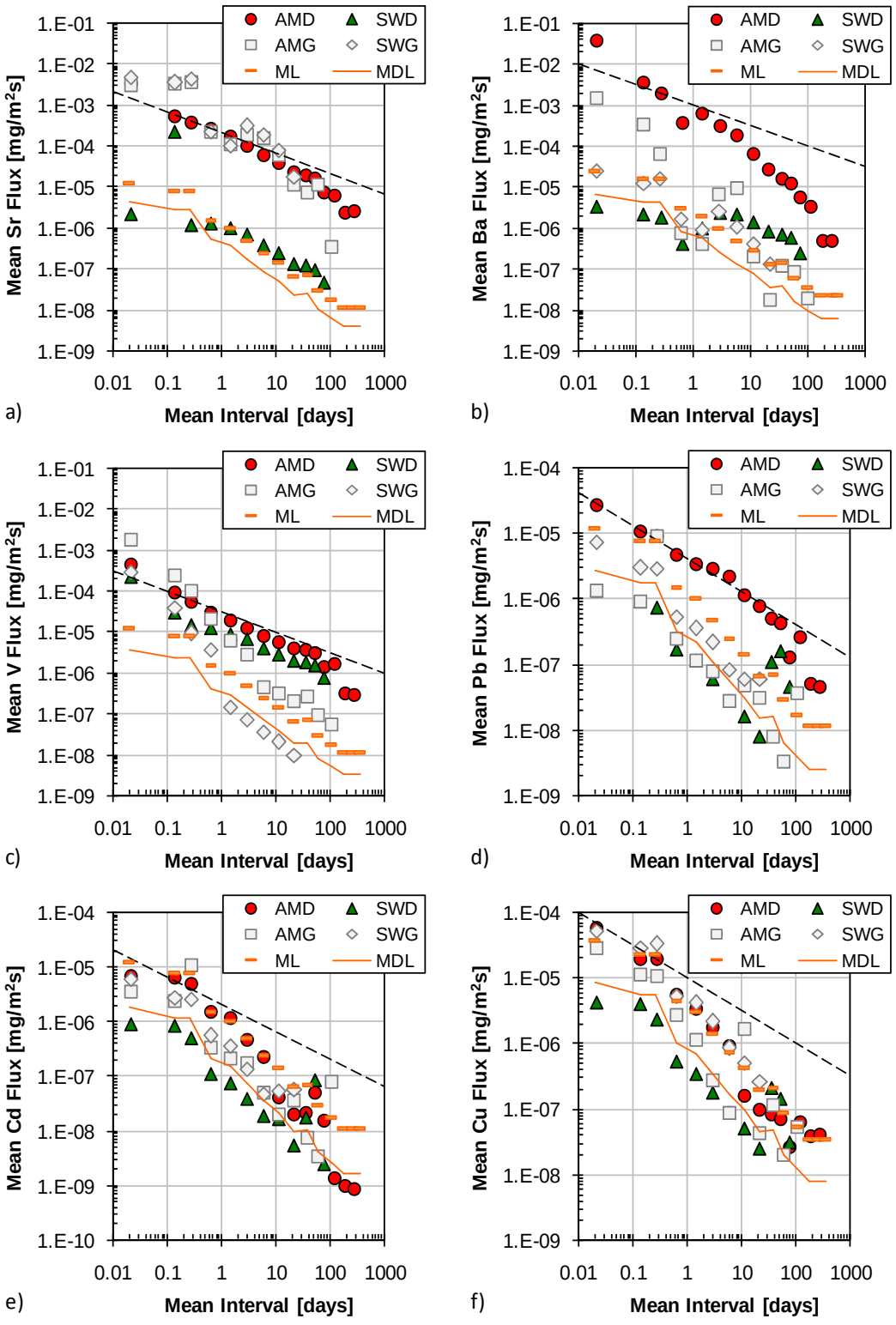

Figure 18: Comparison of mass transfer flux of Group 4 constituents from SR02 leaching test conducted with deionized water (AMD, SWD) and simulated Hanford groundwater (AMG, SWG).

GEOCHEMICAL REACTION AND TRANSPORT MODELING

A preliminary report on the geochemical speciation representing the equilibrium leaching data presented in this report has recently been completed (van der Sloot, etal, 2007) using the database/expert system, LeachXS, with an embedded geochemical reaction and transport model, ORCHESTRA (Meeussen, 2003). Within the LeachXS/ORCHESTRA environment, a characteristic mineral set describing the COPC release for pH and LS dependence leaching tests is formulated that can then be used as a "geochemical fingerprint" to simulate mass-transport controlled release from monolithic materials under site- or scenario-specific release conditions.

Currently, the "geochemical fingerprint" is being used to simulate the release of COPCs under defined mass-transfer controlled scenarios. Within the LeachXS/ORCHESTRA suite, this modeling approach makes use of a full mechanistic description of release processes, taking into account precipitation of minerals (selected from a standard thermodynamic database), sorption of substances onto Fe-oxides and Al oxides, interaction with dissolved and particulate organic matter, and, where relevant, incorporation of elements in solid solutions (e.g. ettringite). Using the geochemical modeling approach and material characteristics stored in the LeachXS database, geochemical interaction and boundary layer formation at the interface between the subject materials and the contacting liquid phase (e.g., DI water or SHG) can be investigated.

PRELIMINARY CONCLUSIONS

The following preliminary conclusions are based on the data set provided in this data report. Investigation into retention mechanisms and modeling of mass transport in deionized water and simulated Hanford groundwater is on-going.

- The LSP curves provided by SR02 equilibrium testing in deionized water reflect the speciation of constituents in the solid matrix. For several constituents (e.g., I, Re, As, Sb, Cs, Se, Pb, and Cd), the level of the LSP curves also indicate the degree to which the constituent was loaded into the subject materials.
- For all constituents tested, simulated Hanford groundwater has little to no effect on the LSP curves. Therefore, interaction with simulated Hanford groundwater does not appear to

change the speciation of COPCs or the bulk mineralogy of the solid material to a high degree.

- The solid matrix appears to retain Cd and Cu to a significant degree in all subject matrices as indicated by mass transfer flux values at or below method limits for these constituents.
- Iodide and rhenium are only weak functions of eluate pH and readily release from the solid material when spiked into the matrix at high loadings. However, these constituents appear to be retained to a significant degree at the lower loadings recommended for 2.6M effluent from the Hanford Effluent Treatment Plant.
- Boundary layer formation caused by interaction between simulated Hanford groundwater and the reducing grout matrices leads to a decrease in the mass transport release in tank leach tests for several constituents including: Al, Ca, Fe, Si, I, Re, Sb, As, Cs, Se, Ba, V, and Pb. The mechanism for increased retention (e.g. physical or chemical effects) is being investigated through coupled geochemical and mass-transport modeling.
- Data scatter, in mass-transfer tests conducted using simulated Hanford groundwater, was significant enough both between replicates of the same material and between similar material types to make interpretation of mass flux difficult. Therefore, it is recommended that mass transport testing be conducted with deionized water.
- Prediction of mass transfer-based release should consider the chemical and physical retention in the matrix obtained from deionized water leaching tests and interactions with the leaching environment through coupled mass transport and geochemical modeling.

REFERENCES

American National Standards Institute/American Nuclear Society (1986). *Measurement of the leachability of solidified low-level radioactive wastes by a short term test procedure*. ANSI/ANS-16.1, La Grange Park, IL.

Gustafsson, J.P., Visual MINTEQ (Version 2.40) [Software]. Available from KTH (Royal Institute of Technology): http://www.lwr.kth.se/english/oursoftware/vminteq/.

Kosson, D.S., van der Sloot, H.A., Sanchez, F. & Garrabrants, A.C. (2002). An integrated framework for evaluating leaching in waste management and utilization of secondary materials. *Environmental Engineering Science*, 19(3), 159-203.

Mahoney, L.A. & Russell, R.L. (2004). Vitrification offgas caustic scrubber secondary waste stimulant formulation. Pacific Northwest National Laboratory, PNNL-14582 r1.

Mattigod, S.V., Whyatt, G.A., Serne, R.J., Martin, P.F., Schwab, K.E. & Wood, M.I. (2001). Diffusion and leaching of selected radionuclides (iodine-129, technetium-99 and uranium) through category 3 waste encasement concrete and soil fill material. PNNL-13639.

Meeussen, J.C.L. (2003). ORCHESTRA: An object-oriented framework for implementing chemical equilibrium models. *Environmental Science and Technology* 3*(37)*, 1175-1182.

van der Sloot, H.A.; van Zomeren, A; Seignette, P.J.A.B.; Meeussen, J.C.L. (2007). Geochemical speciation modelling of simulated low radioactivity waste forms by treatment with a reducing grout. Consortium for Risk Evaluation with Stakeholder Participation.

USEPA. 1980, as revised. *Test Methods for Evaluating Solid Waste, Physical/Chemical Methods*. SW-846, Office of Solid Waste and Emergency Response, Washington, D.C.

USEPA. (1991). *Leachability Phenomena* (EPA Publication No. EPA-SAB-EEC-92-003). Washington, DC. USEPA Science Advisory Board.

USEPA. (1999). *Waste Leachability: The Need for Review of Current Agency Procedures* (EPA Publication No. EPA-SAB-EEC-COM-99-002). Washington, DC. USEPA Science Advisory Board.

APPENDIX A: DEIONIZED WATER LEACH TEST RESULTS

Academic Matrix in DI Water (AMD Material)

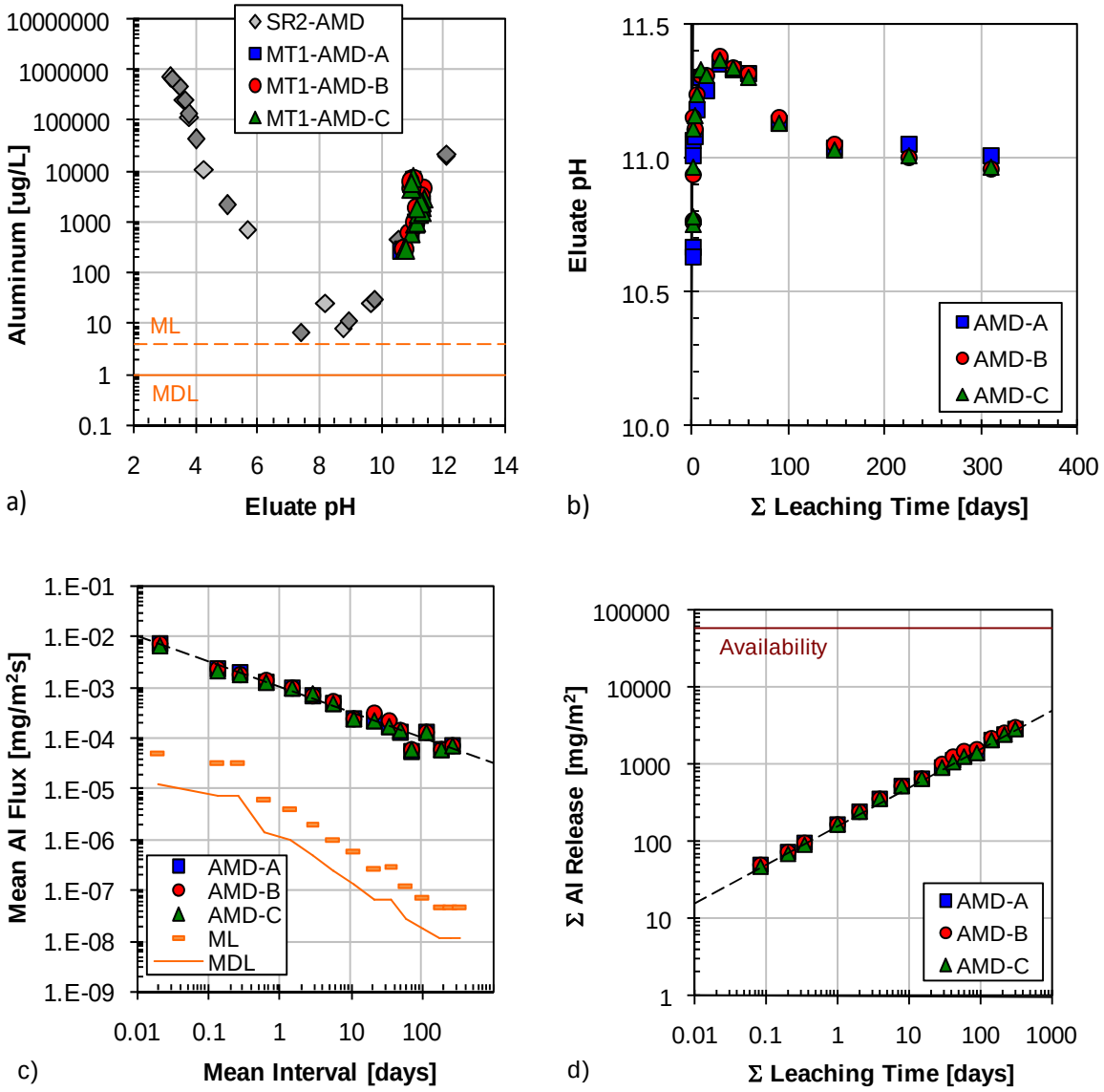

Figure A-1. Aluminum leaching test results from AMD: a) comparison of tank leach test eluants to saturation values (SR02 data) and QA/QC parameters, b) pH evolution in tank leach eluants, c) interval flux from tank leach test in comparison to flux values at the method limit ($t^{-1/2}$ model shown as dashed line), and d) cumulative mass release ($t^{1/2}$ model shown as dashed line).

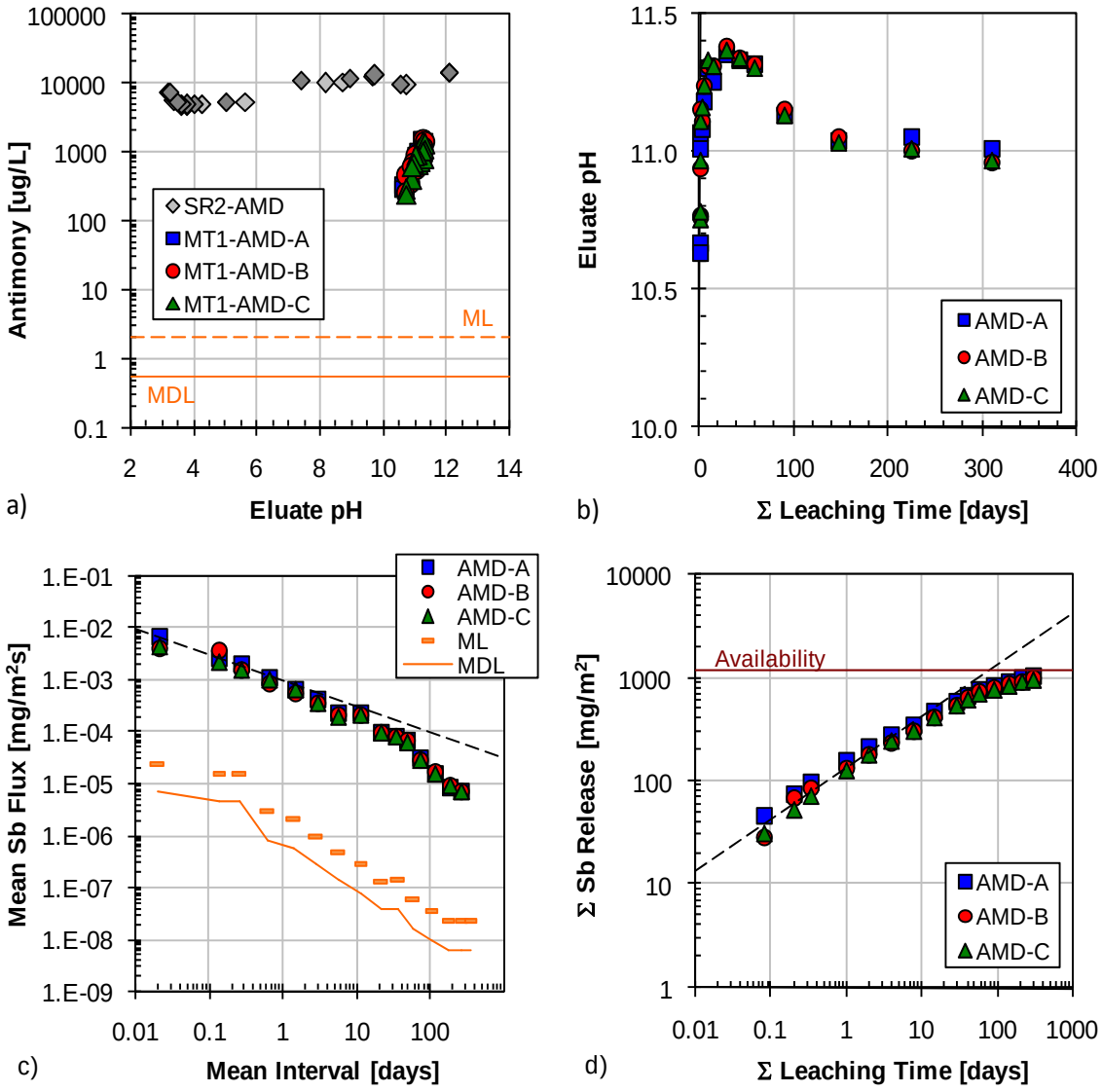

Figure A-2. Antimony leaching test results from AMD: a) comparison of tank leach test eluants to saturation values (SR02 data) and QA/QC parameters, b) pH evolution in tank leach eluants, c) interval flux from tank leach test in comparison to flux values at the method limit ($t^{-1/2}$ model shown as dashed line), and d) cumulative mass release ($t^{1/2}$ model shown as dashed line).

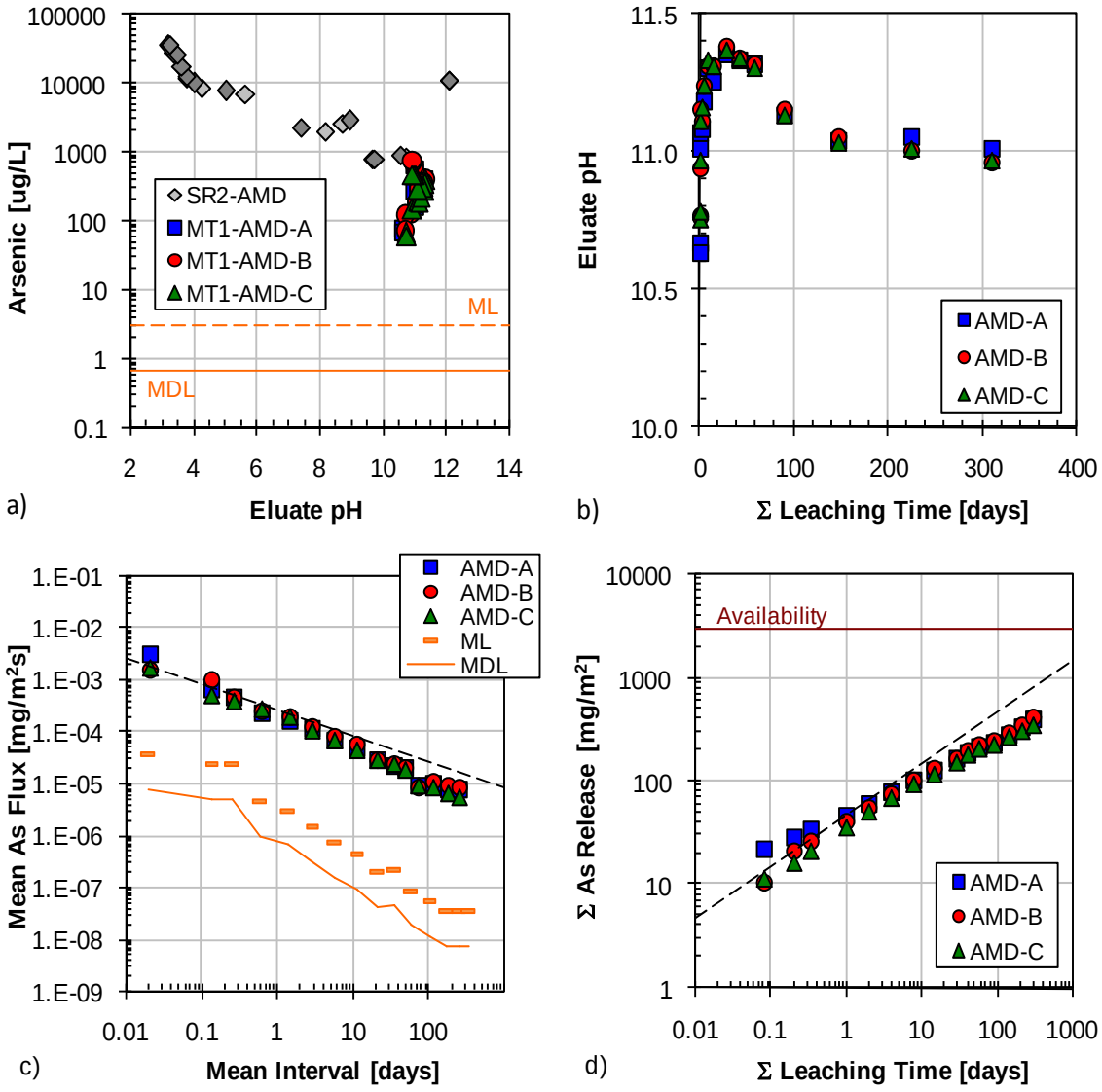

Figure A-3. Arsenic leaching test results from AMD: a) comparison of tank leach test eluants to saturation values (SR02 data) and QA/QC parameters, b) pH evolution in tank leach eluants, c) interval flux from tank leach test in comparison to flux values at the method limit ($t^{-1/2}$ model shown as dashed line), and d) cumulative mass release ($t^{1/2}$ model shown as dashed line).

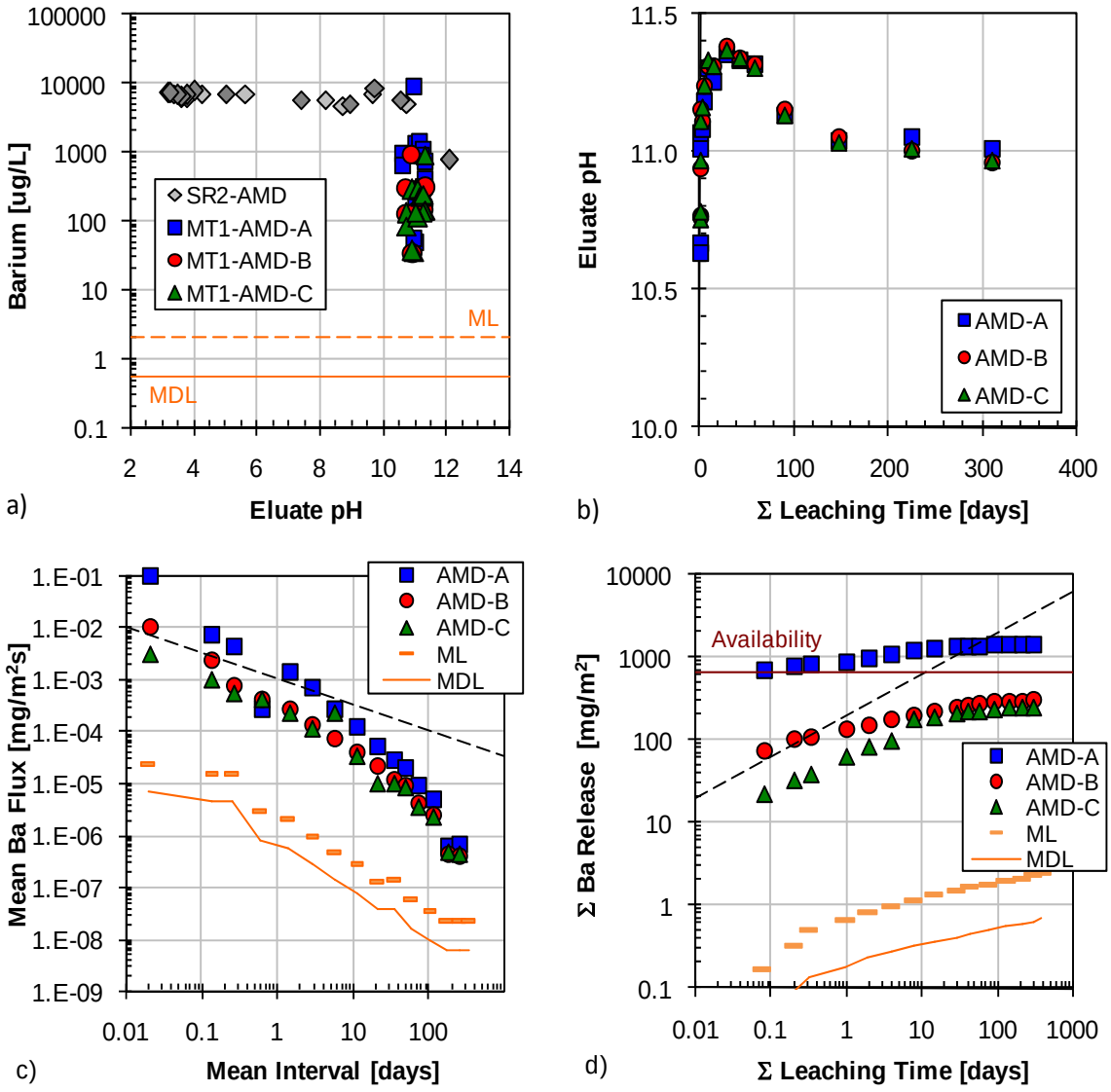

Figure A-4. Barium leaching test results from AMD: a) comparison of tank leach test eluants to saturation values (SR02 data) and QA/QC parameters, b) pH evolution in tank leach eluants, c) interval flux from tank leach test in comparison to flux values at the method limit ($t^{-1/2}$ model shown as dashed line), and d) cumulative mass release ($t^{1/2}$ model shown as dashed line).

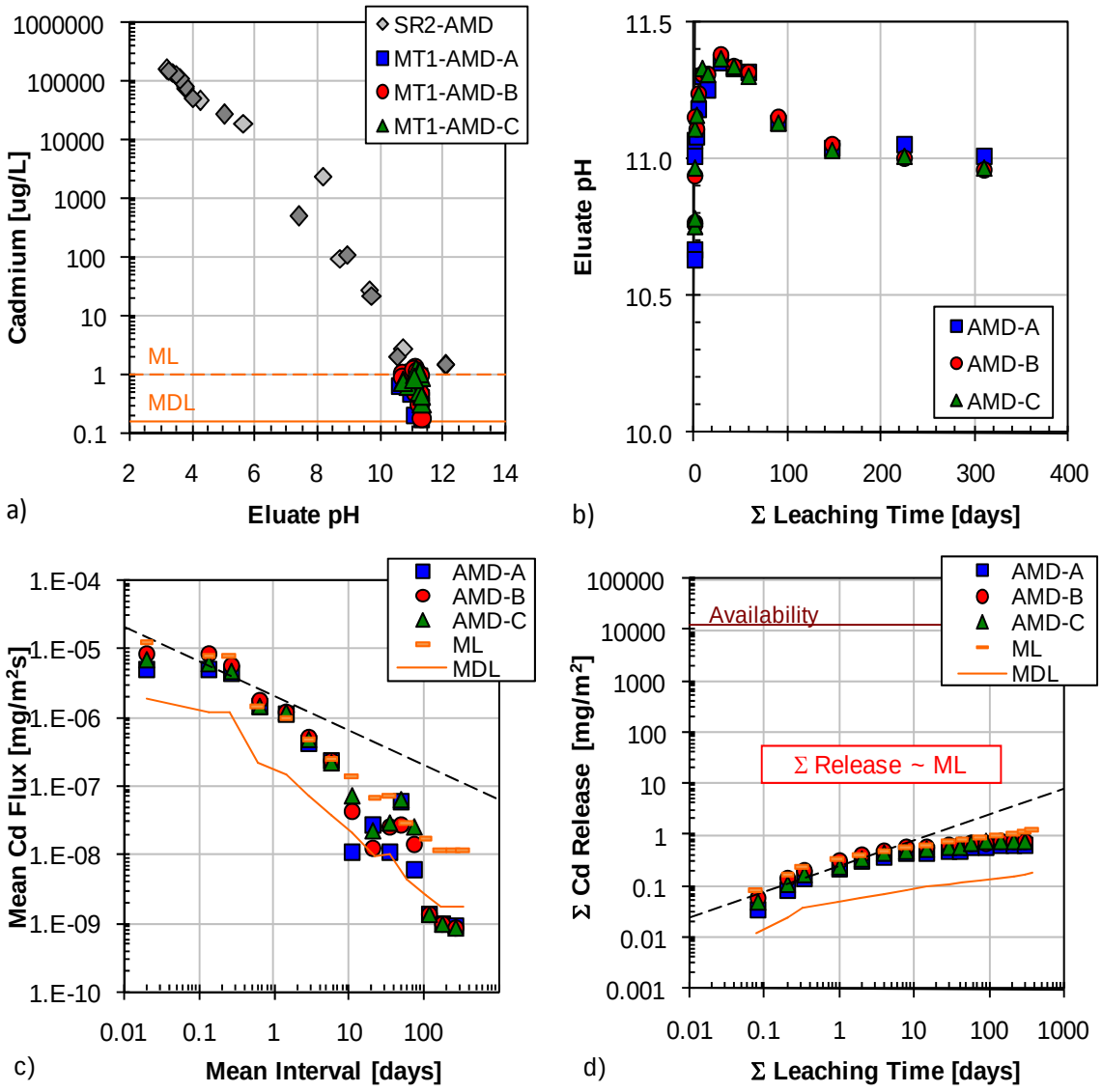

Figure A-5. Cadmium leaching test results from AMD: a) comparison of tank leach test eluants to saturation values (SR02 data) and QA/QC parameters, b) pH evolution in tank leach eluants, c) interval flux from tank leach test in comparison to flux values at the method limit ($t^{-1/2}$ model shown as dashed line), and d) cumulative mass release ($t^{1/2}$ model shown as dashed line).

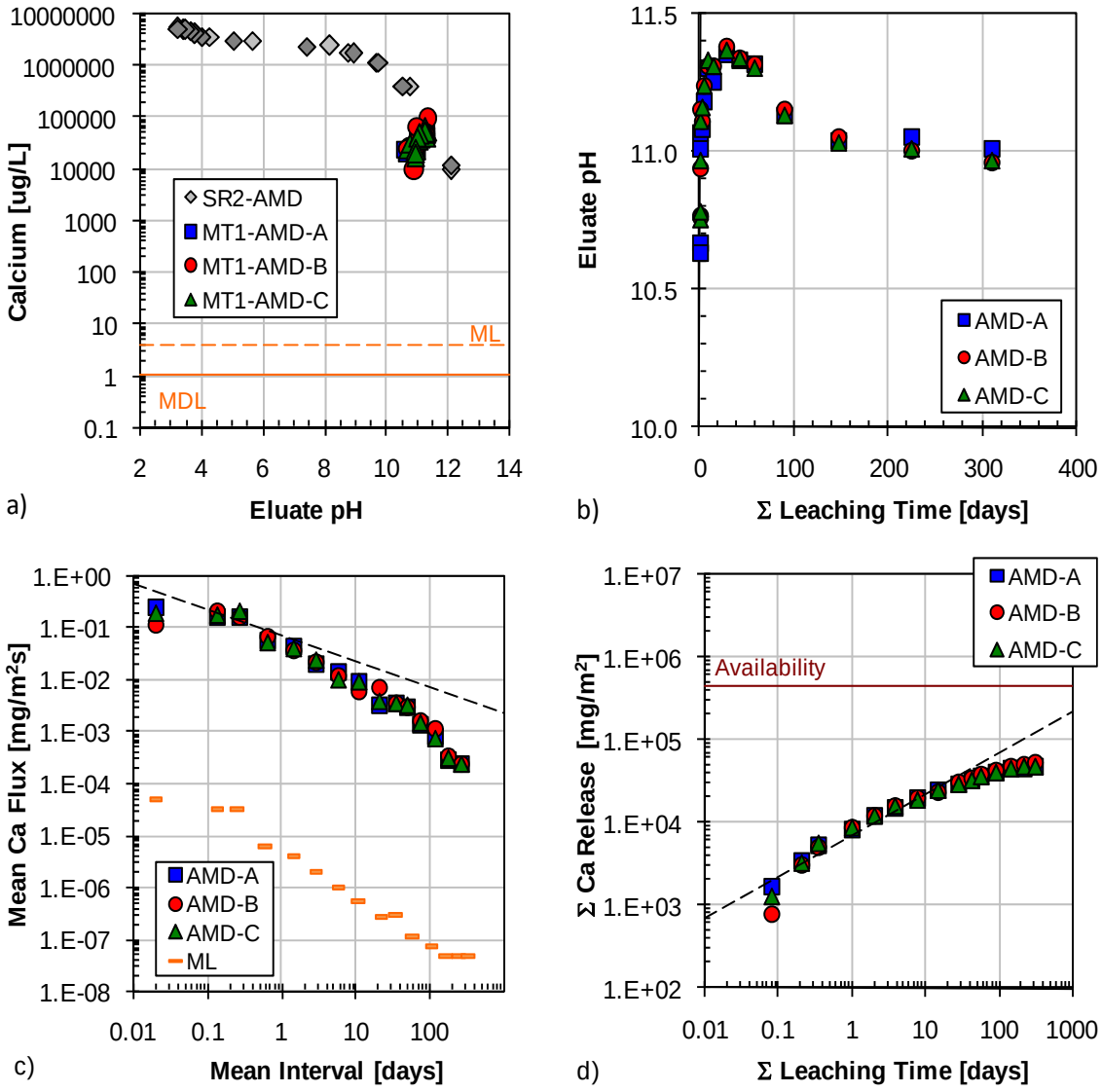

Figure A-6. Calcium leaching test results from AMD: a) comparison of tank leach test eluants to saturation values (SR02 data) and QA/QC parameters, b) pH evolution in tank leach eluants, c) interval flux from tank leach test in comparison to flux values at the method limit ($t^{-1/2}$ model shown as dashed line), and d) cumulative mass release ($t^{1/2}$ model shown as dashed line).

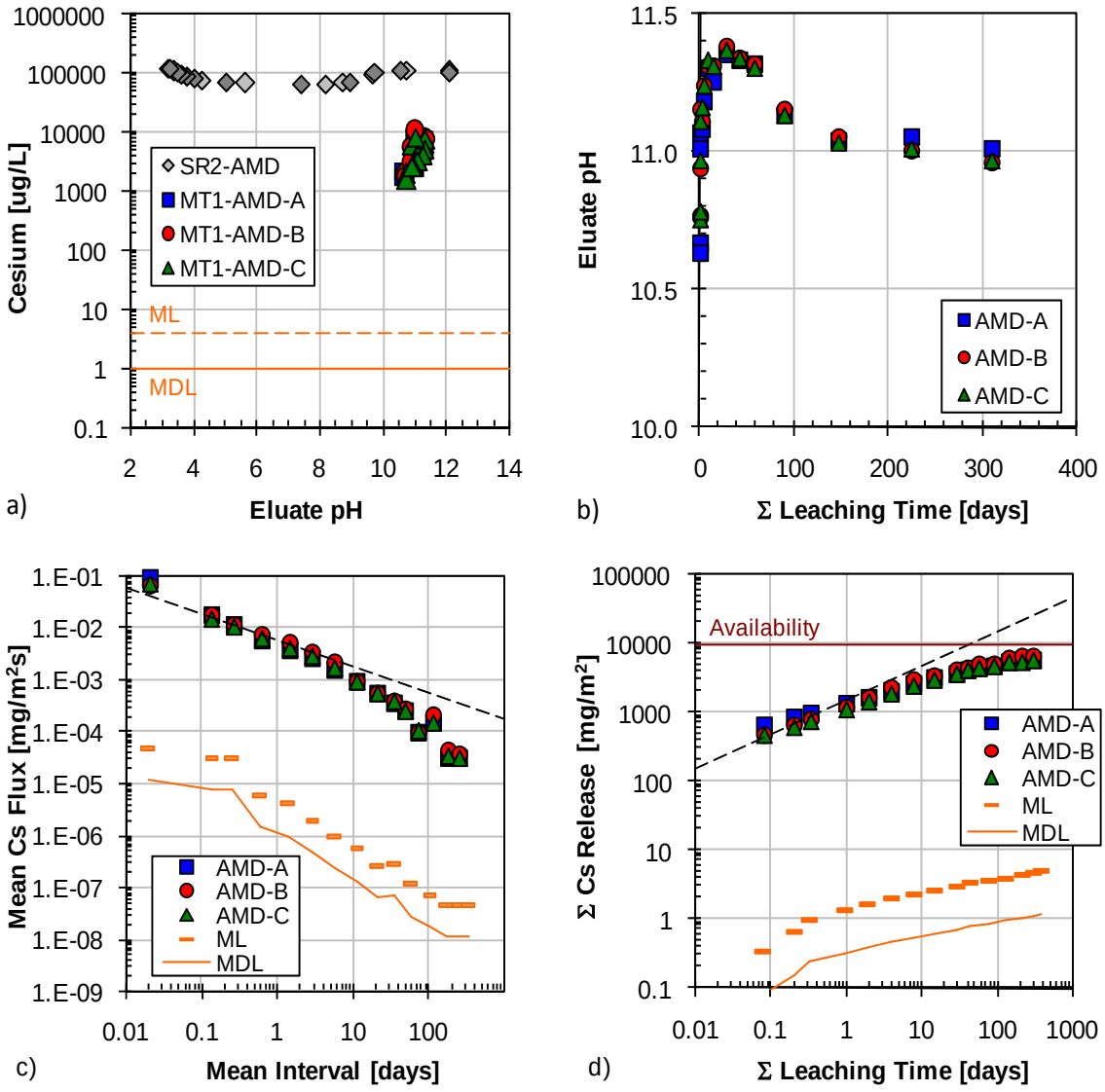

Figure A-7. Cesium leaching test results from AMD: a) comparison of tank leach test eluants to saturation values (SR02 data) and QA/QC parameters, b) pH evolution in tank leach eluants, c) interval flux from tank leach test in comparison to flux values at the method limit ($t^{-1/2}$ model shown as dashed line), and d) cumulative mass release ($t^{1/2}$ model shown as dashed line).

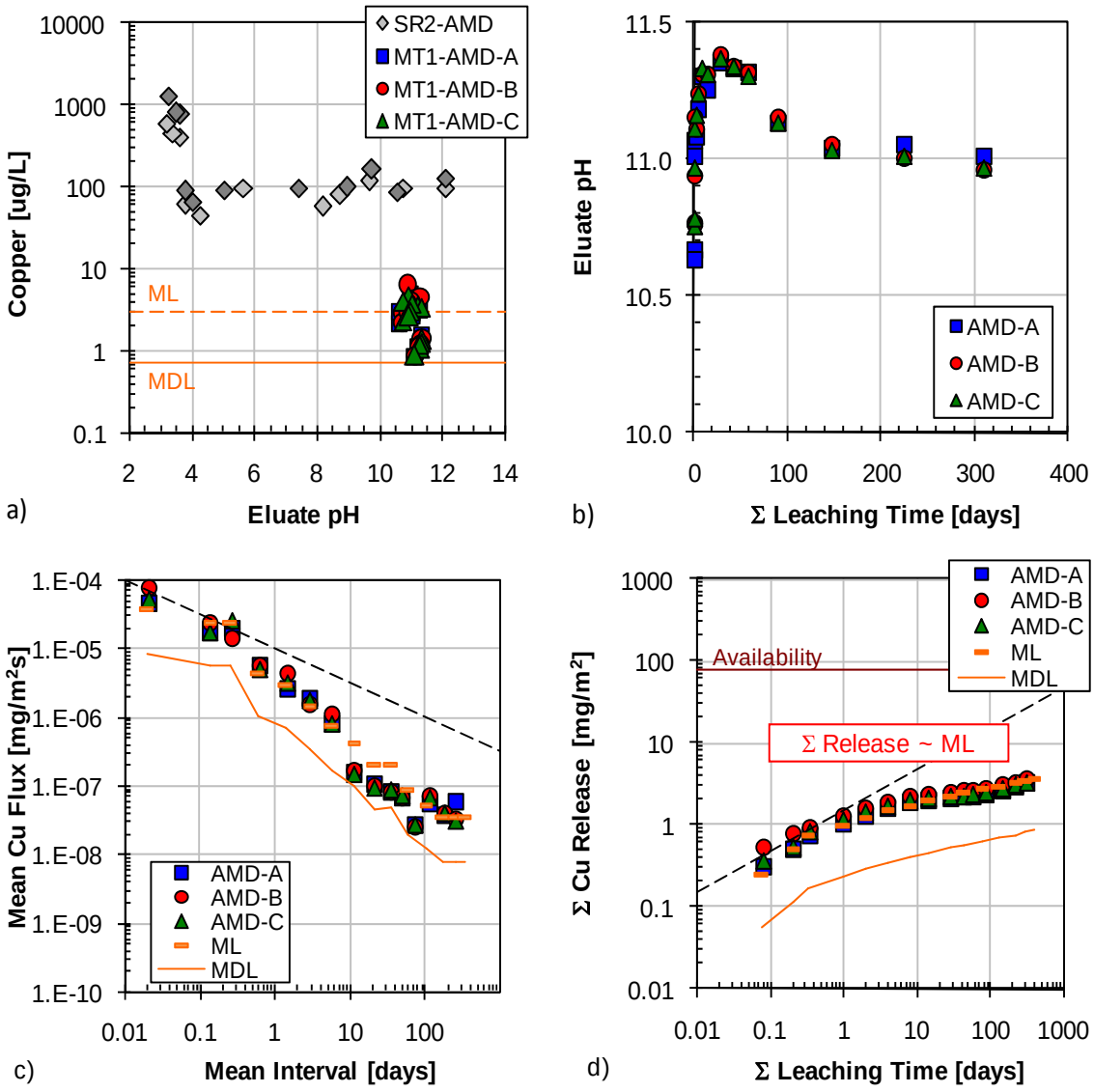

Figure A-8. Copper leaching test results from AMD: a) comparison of tank leach test eluants to saturation values (SR02 data) and QA/QC parameters, b) pH evolution in tank leach eluants, c) interval flux from tank leach test in comparison to flux values at the method limit ($t^{-1/2}$ model shown as dashed line), and d) cumulative mass release ($t^{1/2}$ model shown as dashed line).

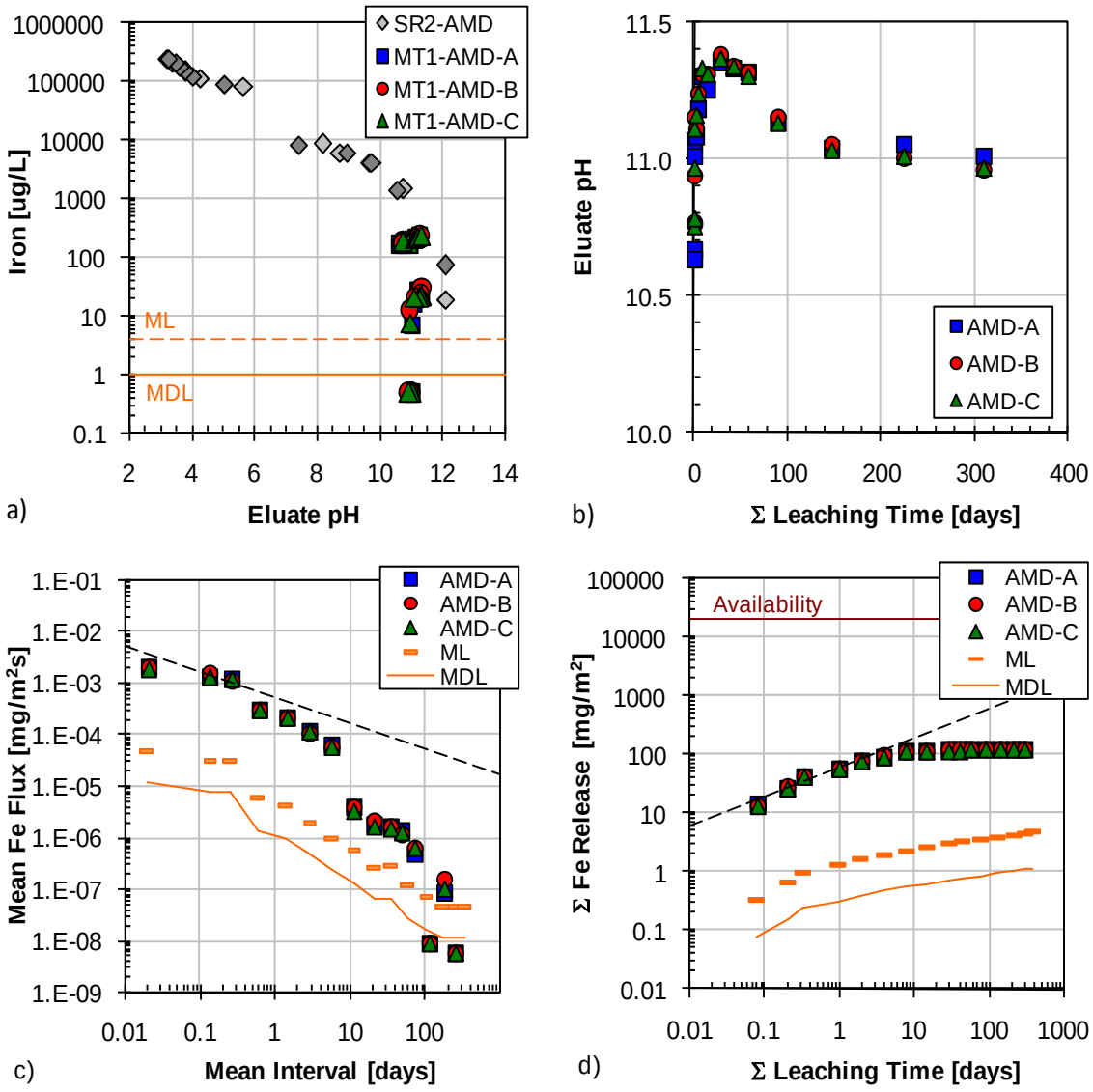

Figure A-9. Iron leaching test results from AMD: a) comparison of tank leach test eluants to saturation values (SR02 data) and QA/QC parameters, b) pH evolution in tank leach eluants, c) interval flux from tank leach test in comparison to flux values at the method limit ($t^{-1/2}$ model shown as dashed line), and d) cumulative mass release ($t^{1/2}$ model shown as dashed line).

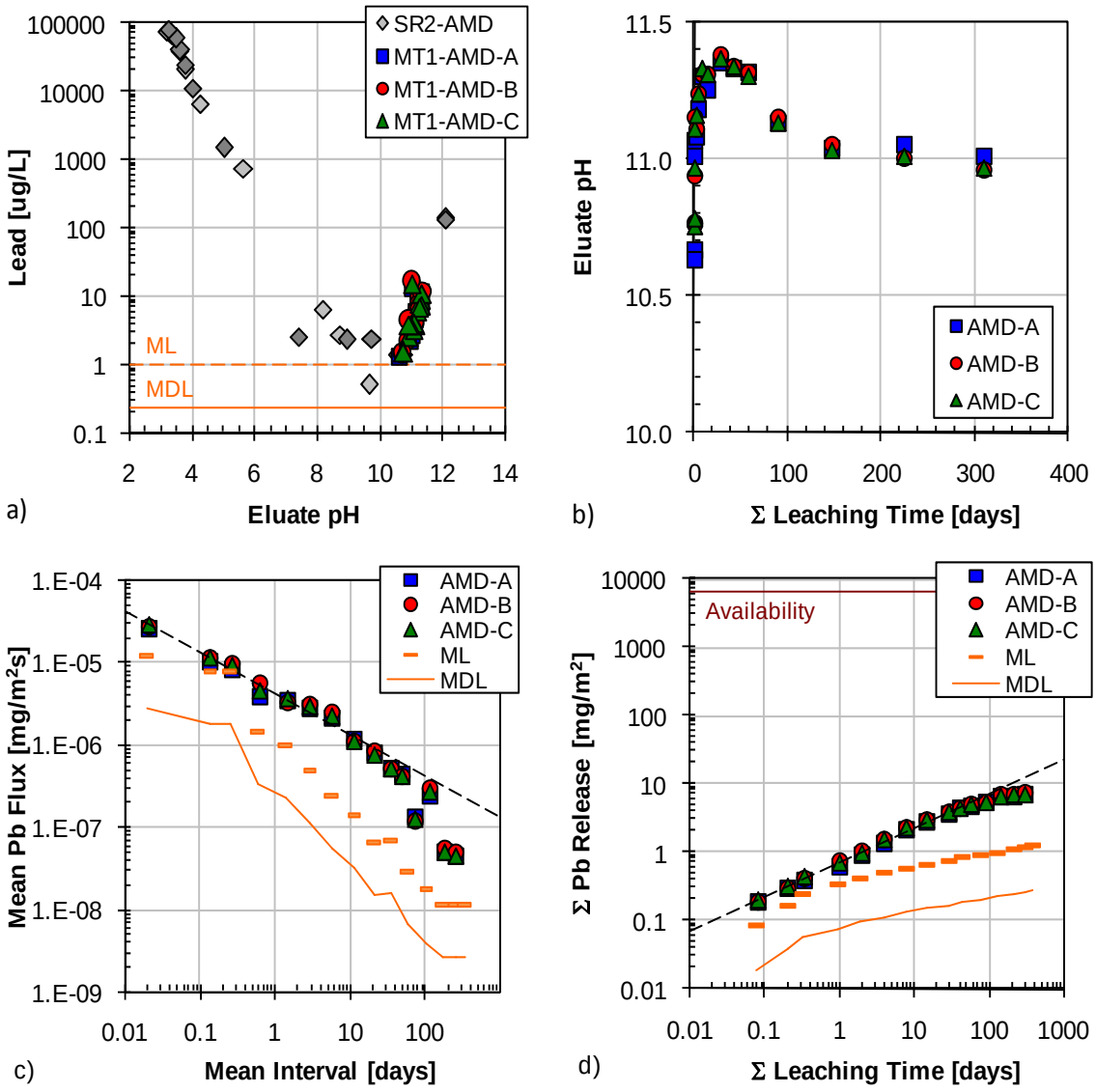

Figure A-10. Lead leaching test results from AMD: a) comparison of tank leach test eluants to saturation values (SR02 data) and QA/QC parameters, b) pH evolution in tank leach eluants, c) interval flux from tank leach test in comparison to flux values at the method limit ($t^{-1/2}$ model shown as dashed line), and d) cumulative mass release ($t^{1/2}$ model shown as dashed line).

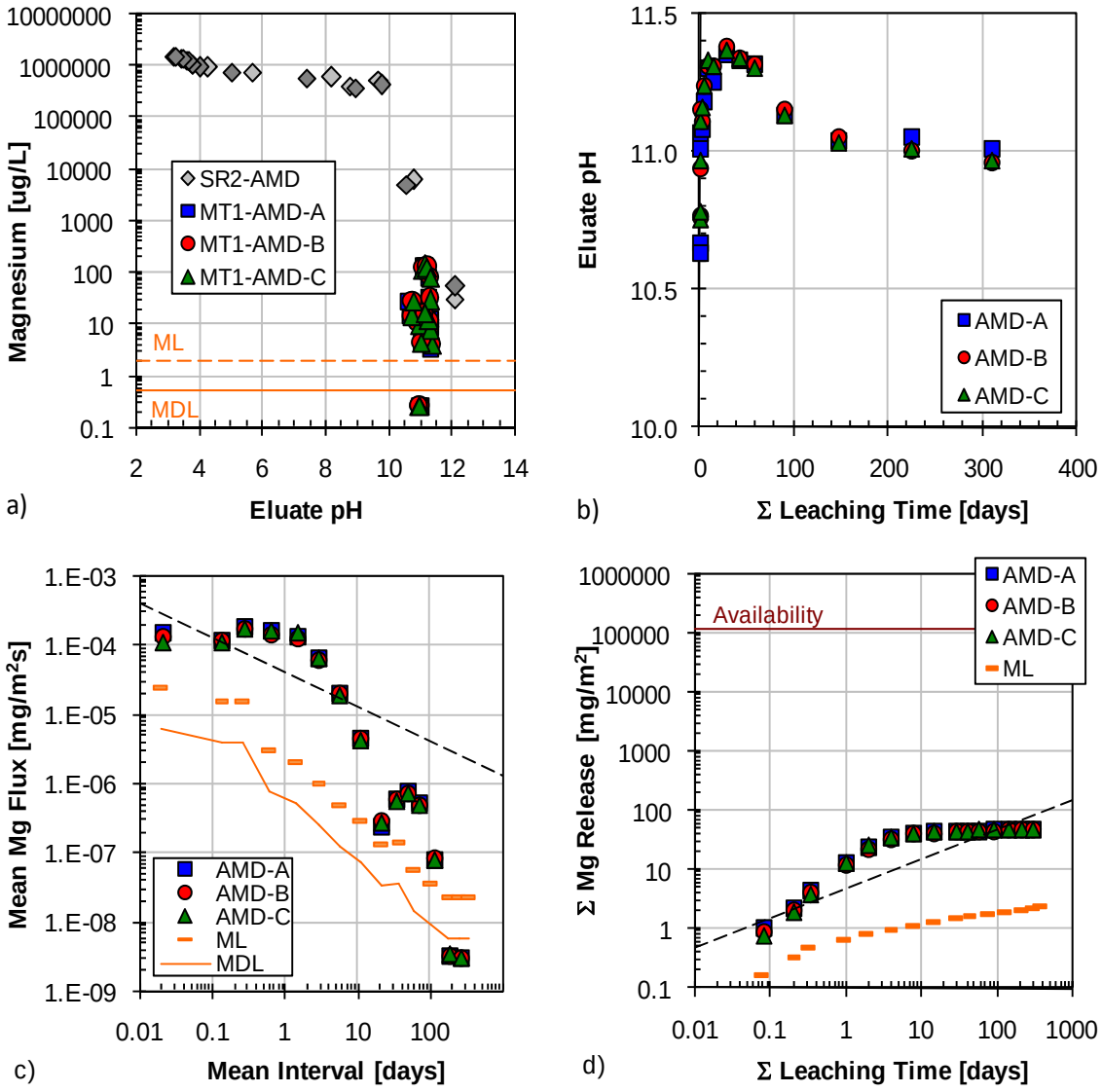

Figure A-11. Magnesium leaching test results from AMD: a) comparison of tank leach test eluants to saturation values (SR02 data) and QA/QC parameters, b) pH evolution in tank leach eluants, c) interval flux from tank leach test in comparison to flux values at the method limit ($t^{-1/2}$ model shown as dashed line), and d) cumulative mass release ($t^{1/2}$ model shown as dashed line).

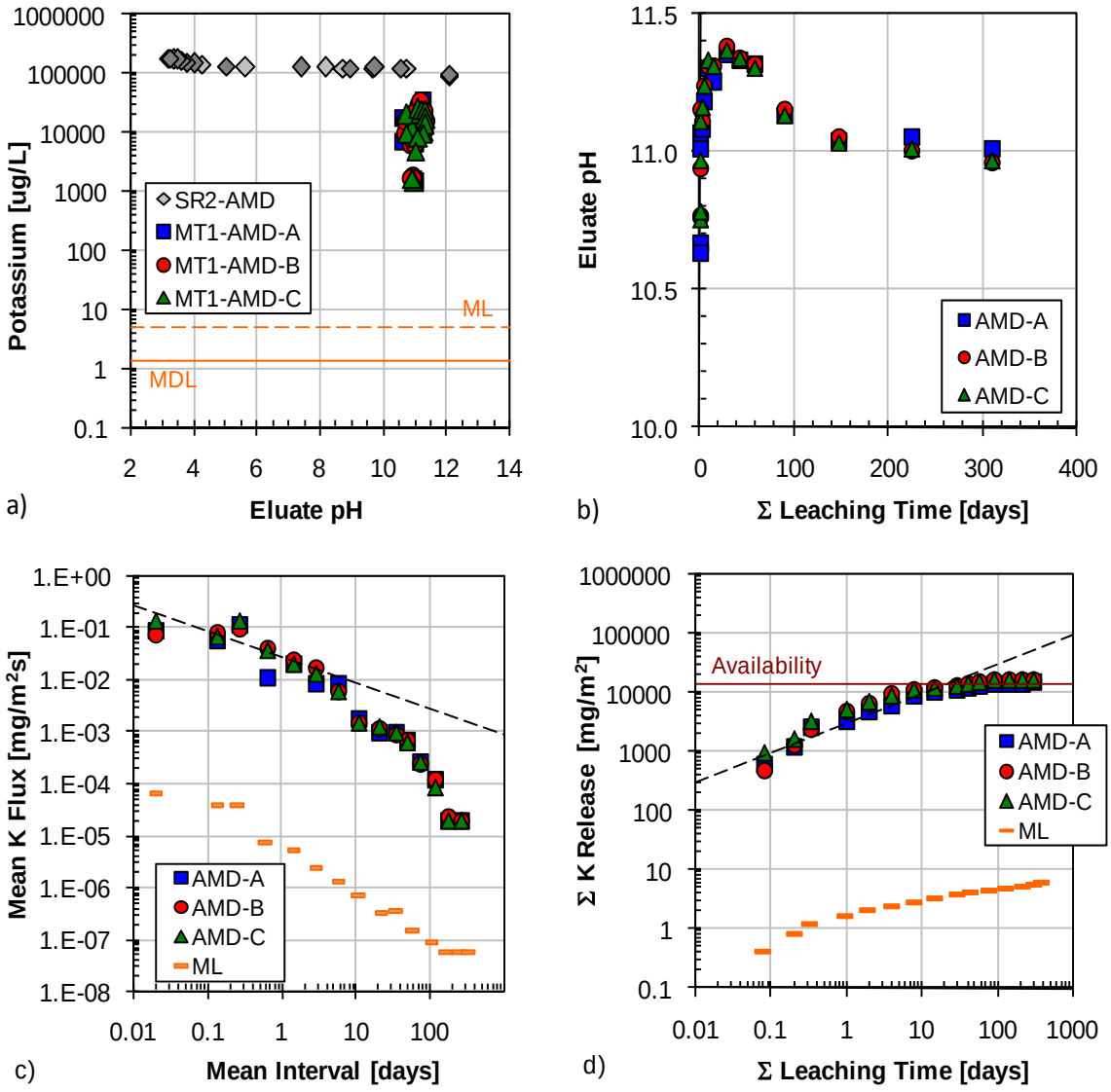

Figure A-12. Potassium leaching test results from AMD: a) comparison of tank leach test eluants to saturation values (SR02 data) and QA/QC parameters, b) pH evolution in tank leach eluants, c) interval flux from tank leach test in comparison to flux values at the method limit ($t^{-1/2}$ model shown as dashed line), and d) cumulative mass release ($t^{1/2}$ model shown as dashed line).

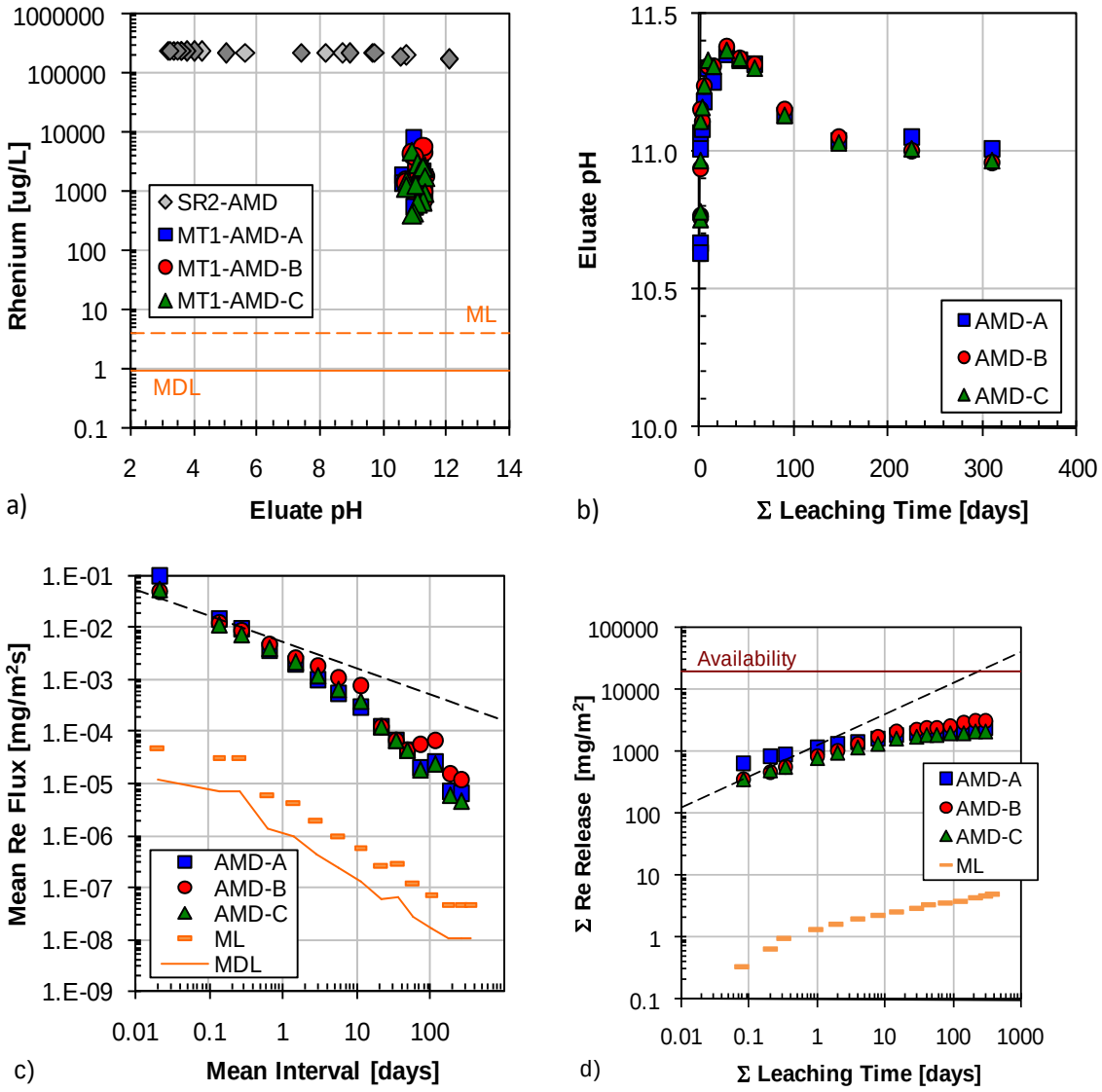

Figure A-13. Rhenium leaching test results from AMD: a) comparison of tank leach test eluants to saturation values (SR02 data) and QA/QC parameters, b) pH evolution in tank leach eluants, c) interval flux from tank leach test in comparison to flux values at the method limit ($t^{-1/2}$ model shown as dashed line), and d) cumulative mass release ($t^{1/2}$ model shown as dashed line).

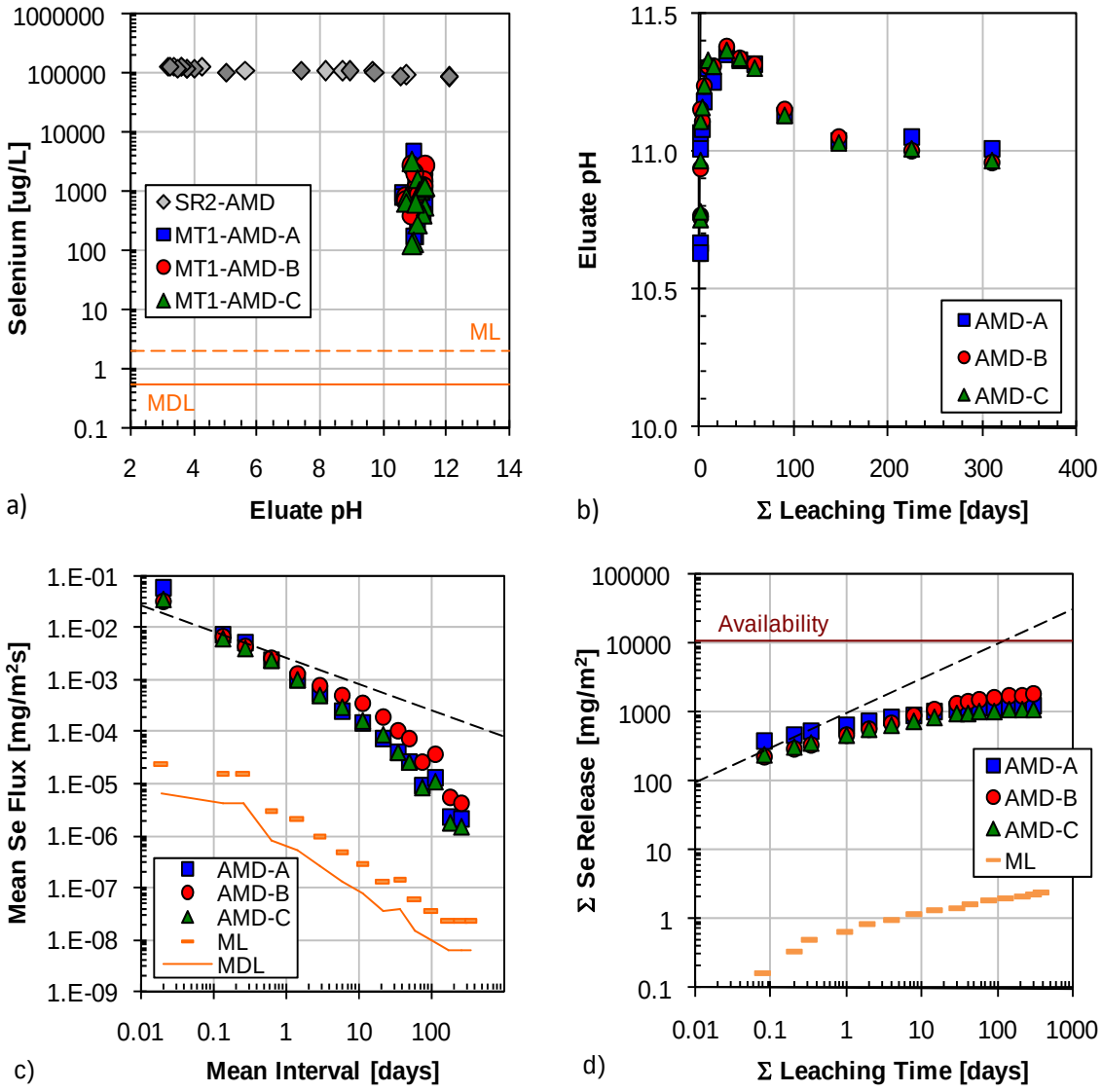

Figure A-14. Selenium leaching test results from AMD: a) comparison of tank leach test eluants to saturation values (SR02 data) and QA/QC parameters, b) pH evolution in tank leach eluants, c) interval flux from tank leach test in comparison to flux values at the method limit ($t^{-1/2}$ model shown as dashed line), and d) cumulative mass release ($t^{1/2}$ model shown as dashed line).

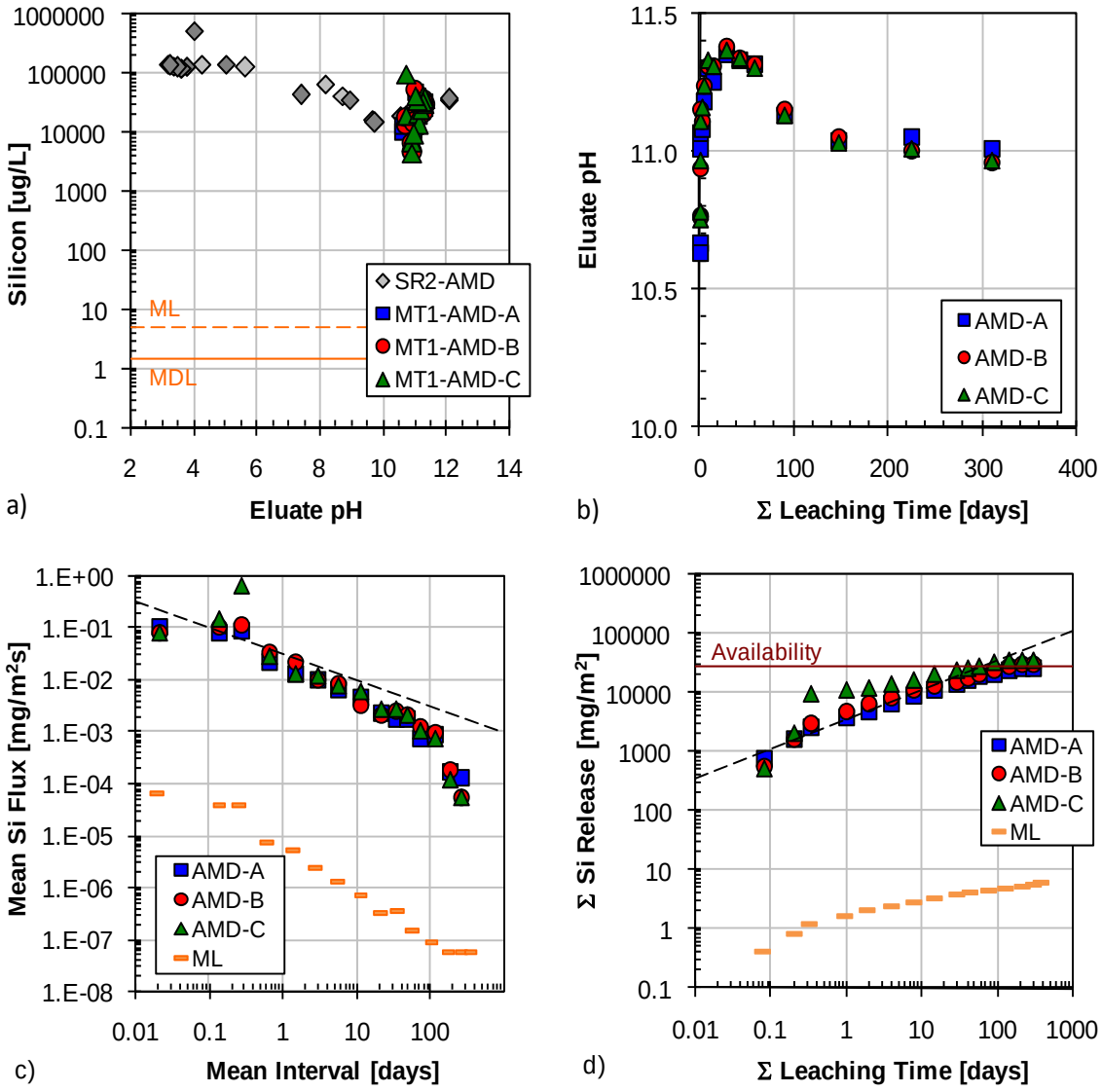

Figure A-15. Silicon leaching test results from AMD: a) comparison of tank leach test eluants to saturation values (SR02 data) and QA/QC parameters, b) pH evolution in tank leach eluants, c) interval flux from tank leach test in comparison to flux values at the method limit ($t^{-1/2}$ model shown as dashed line), and d) cumulative mass release ($t^{1/2}$ model shown as dashed line).

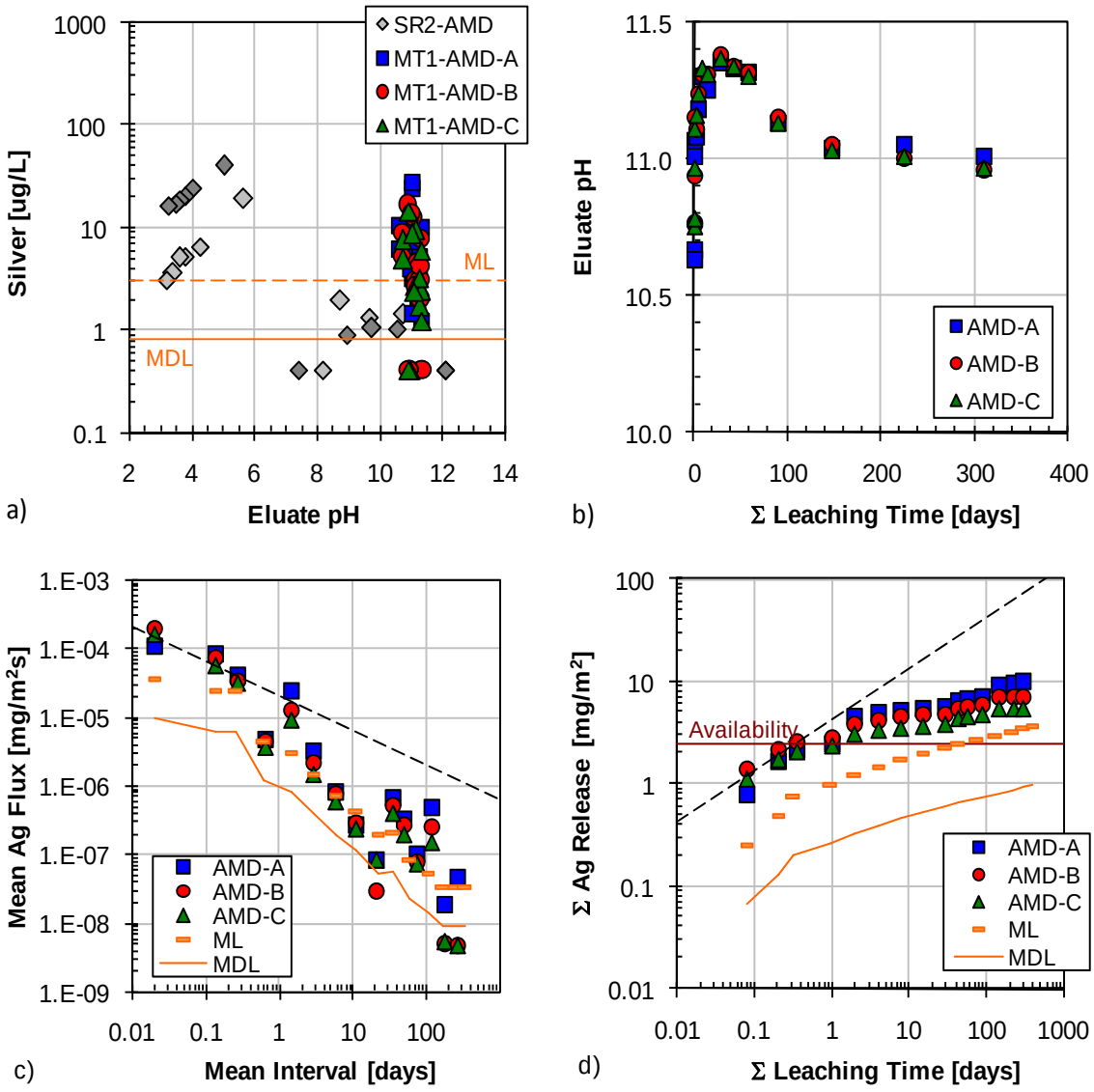

Figure A-16. Silver leaching test results from AMD: a) comparison of tank leach test eluants to saturation values (SR02 data) and QA/QC parameters, b) pH evolution in tank leach eluants, c) interval flux from tank leach test in comparison to flux values at the method limit ($t^{-1/2}$ model shown as dashed line), and d) cumulative mass release ($t^{1/2}$ model shown as dashed line).

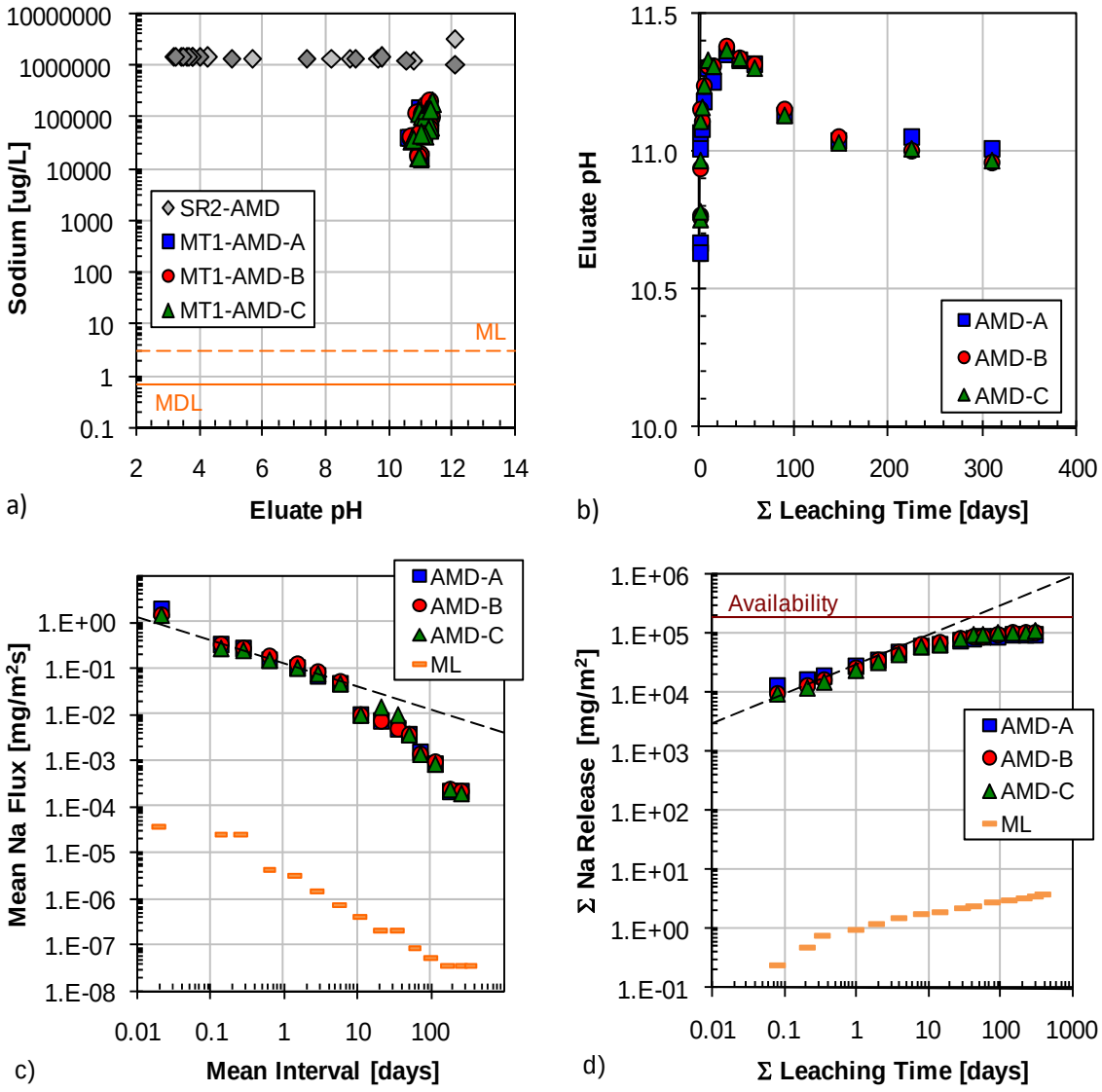

Figure A-17. Sodium leaching test results from AMD: a) comparison of tank leach test eluants to saturation values (SR02 data) and QA/QC parameters, b) pH evolution in tank leach eluants, c) interval flux from tank leach test in comparison to flux values at the method limit ($t^{-1/2}$ model shown as dashed line), and d) cumulative mass release ($t^{1/2}$ model shown as dashed line).

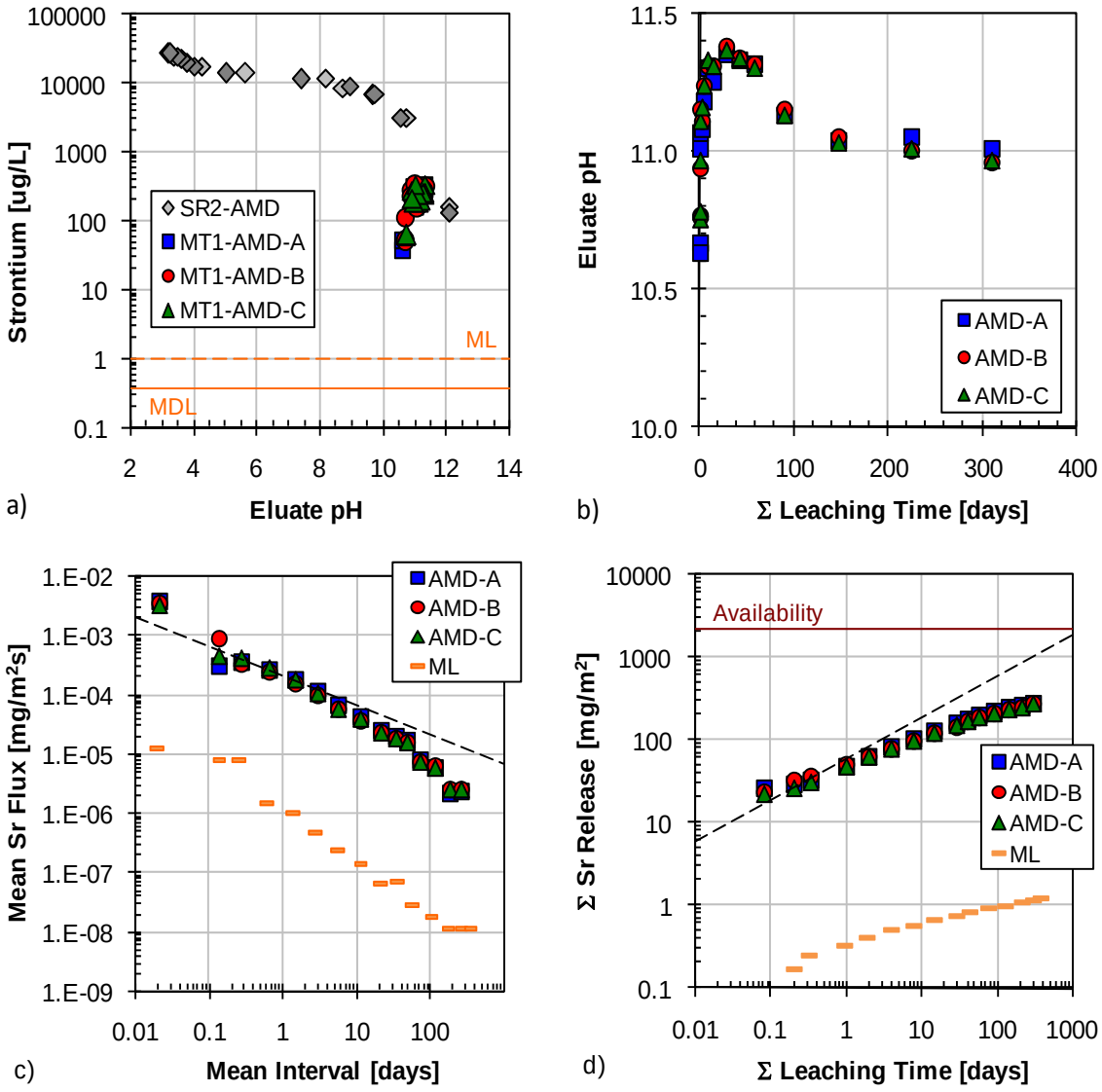

Figure A-18. Strontium leaching test results from AMD: a) comparison of tank leach test eluants to saturation values (SR02 data) and QA/QC parameters, b) pH evolution in tank leach eluants, c) interval flux from tank leach test in comparison to flux values at the method limit ($t^{-1/2}$ model shown as dashed line), and d) cumulative mass release ($t^{1/2}$ model shown as dashed line).

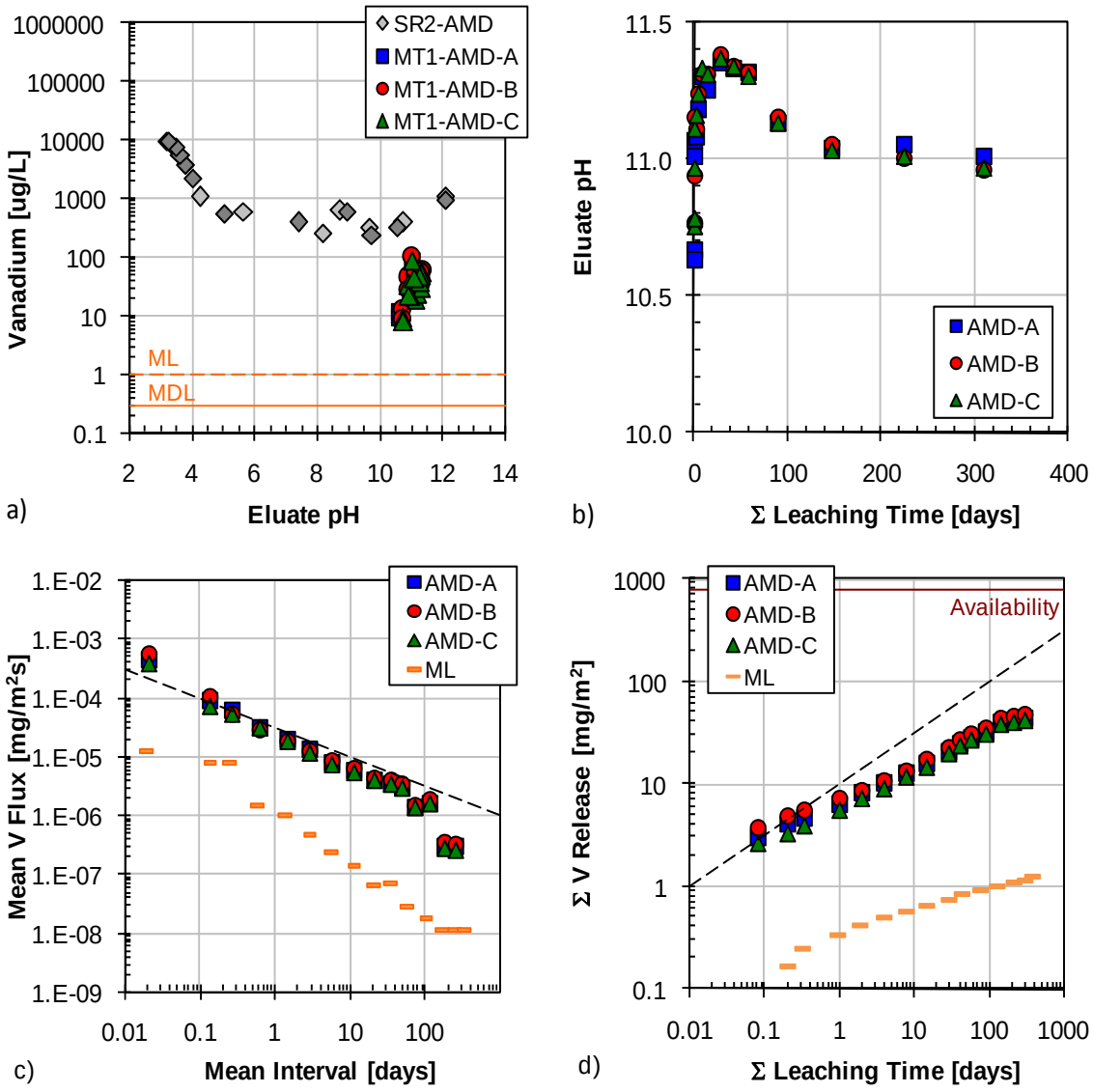

Figure A-19. Vanadium leaching test results from AMD: a) comparison of tank leach test eluants to saturation values (SR02 data) and QA/QC parameters, b) pH evolution in tank leach eluants, c) interval flux from tank leach test in comparison to flux values at the method limit ($t^{-1/2}$ model shown as dashed line), and d) cumulative mass release ($t^{1/2}$ model shown as dashed line).

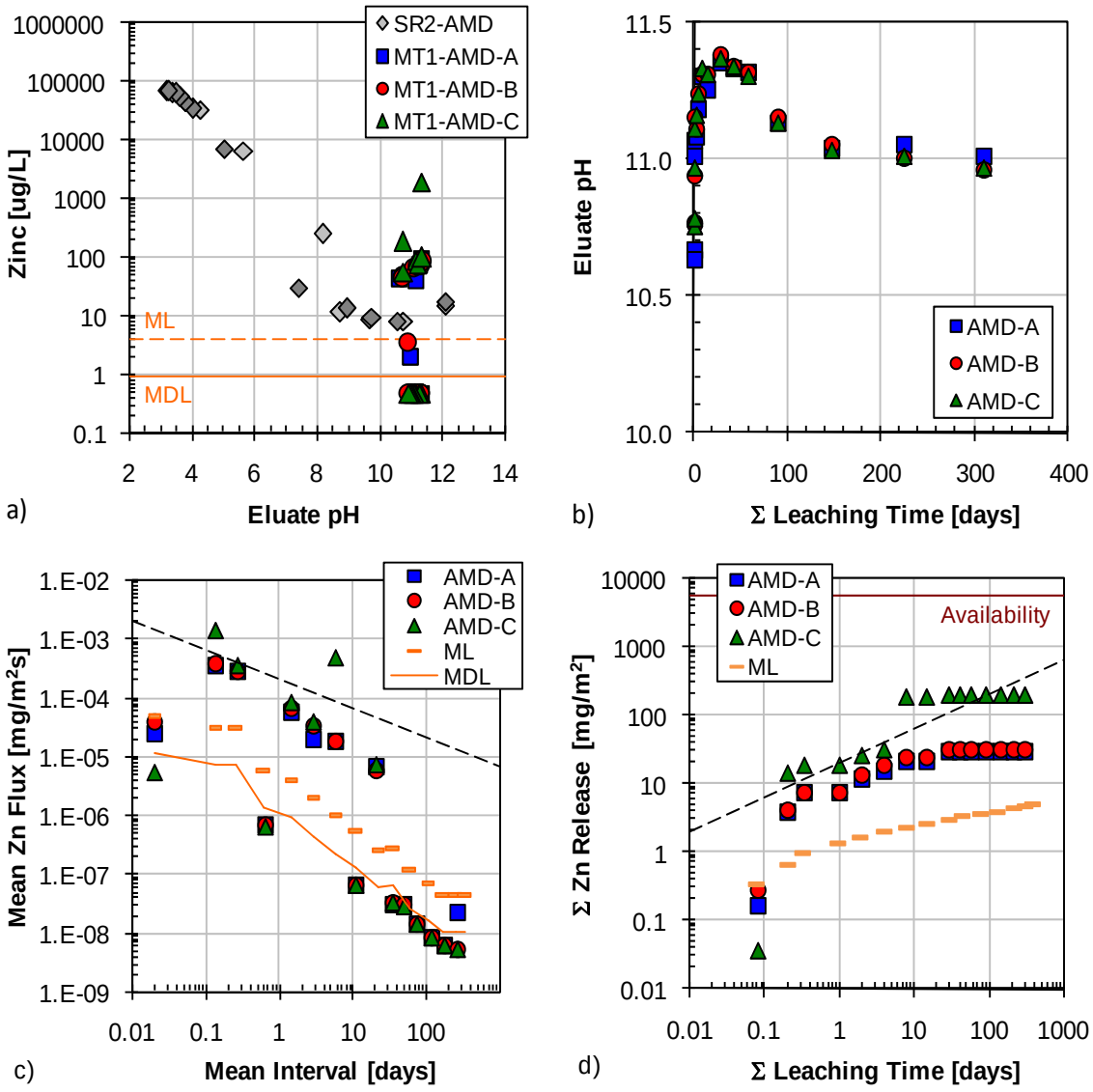

Figure A-20. Zinc leaching test results from AMD: a) comparison of tank leach test eluants to saturation values (SR02 data) and QA/QC parameters, b) pH evolution in tank leach eluants, c) interval flux from tank leach test in comparison to flux values at the method limit ($t^{-1/2}$ model shown as dashed line), and d) cumulative mass release ($t^{1/2}$ model shown as dashed line).

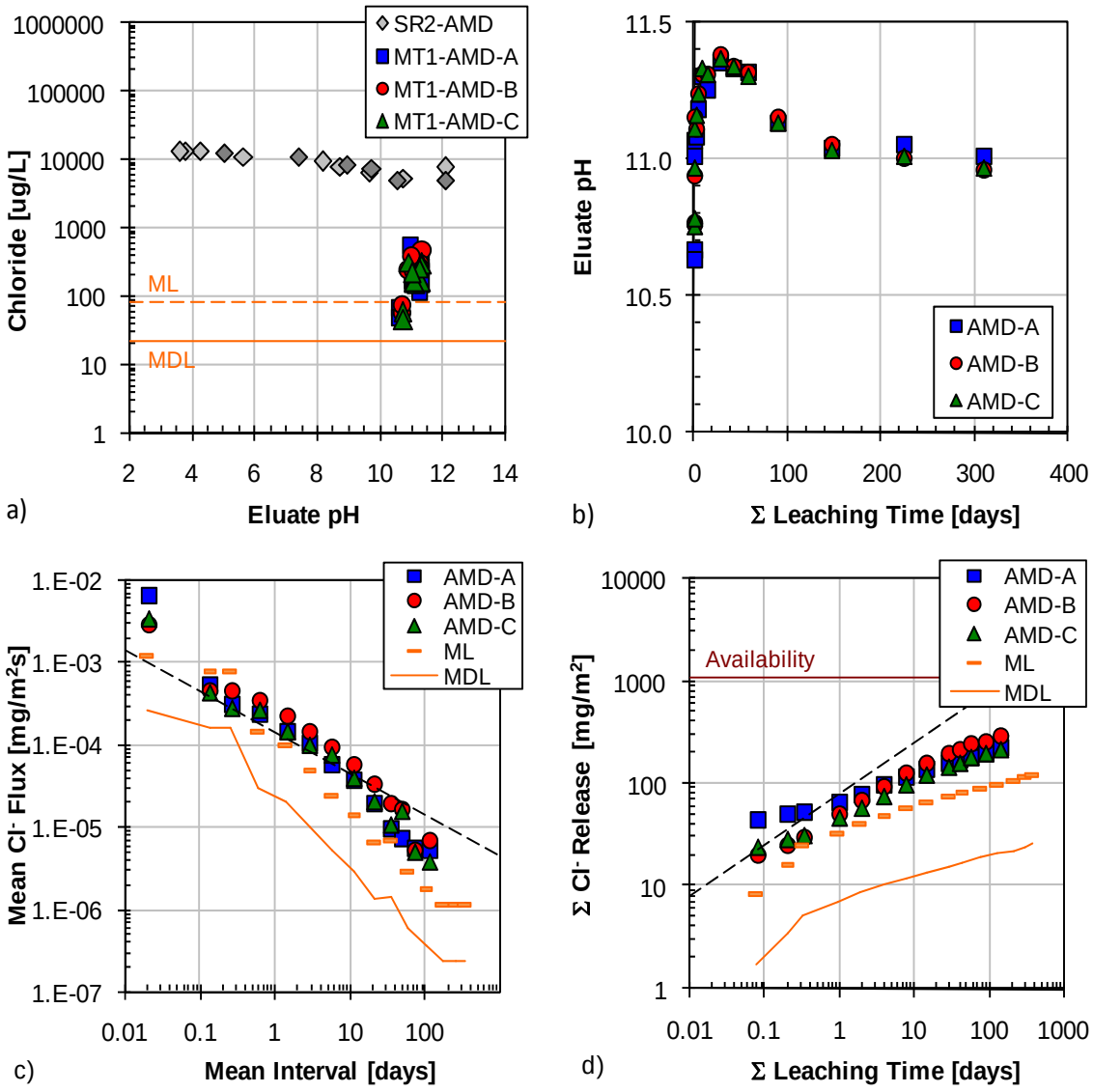

Figure A-21. Chloride leaching test results from AMD: a) comparison of tank leach test eluants to saturation values (SR02 data) and QA/QC parameters, b) pH evolution in tank leach eluants, c) interval flux from tank leach test in comparison to flux values at the method limit ($t^{-1/2}$ model shown as dashed line), and d) cumulative mass release ($t^{1/2}$ model shown as dashed line).

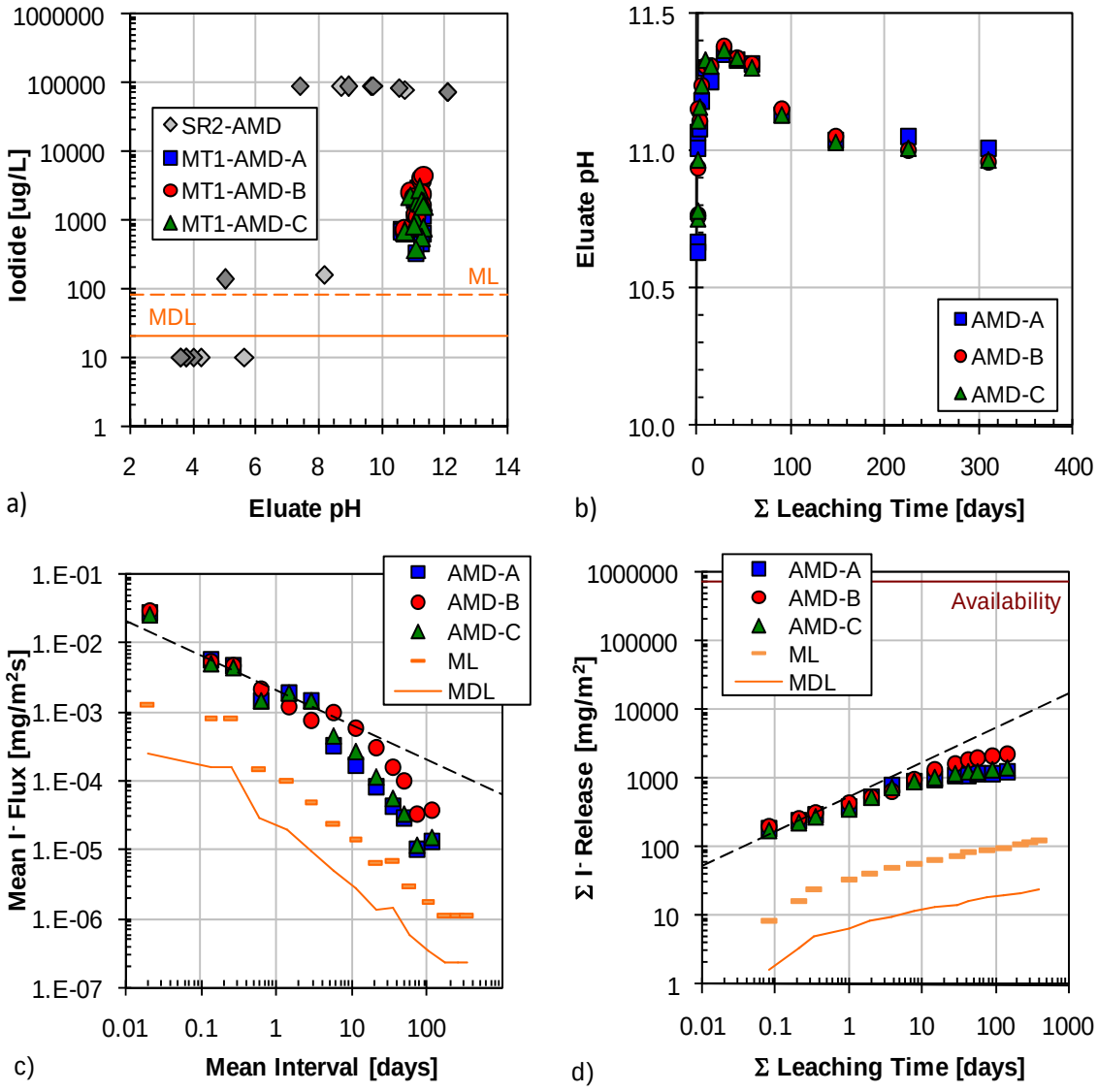

Figure A-22. Iodide leaching test results from AMD: a) comparison of tank leach test eluants to saturation values (SR02 data) and QA/QC parameters, b) pH evolution in tank leach eluants, c) interval flux from tank leach test in comparison to flux values at the method limit ($t^{-1/2}$ model shown as dashed line), and d) cumulative mass release ($t^{1/2}$ model shown as dashed line).

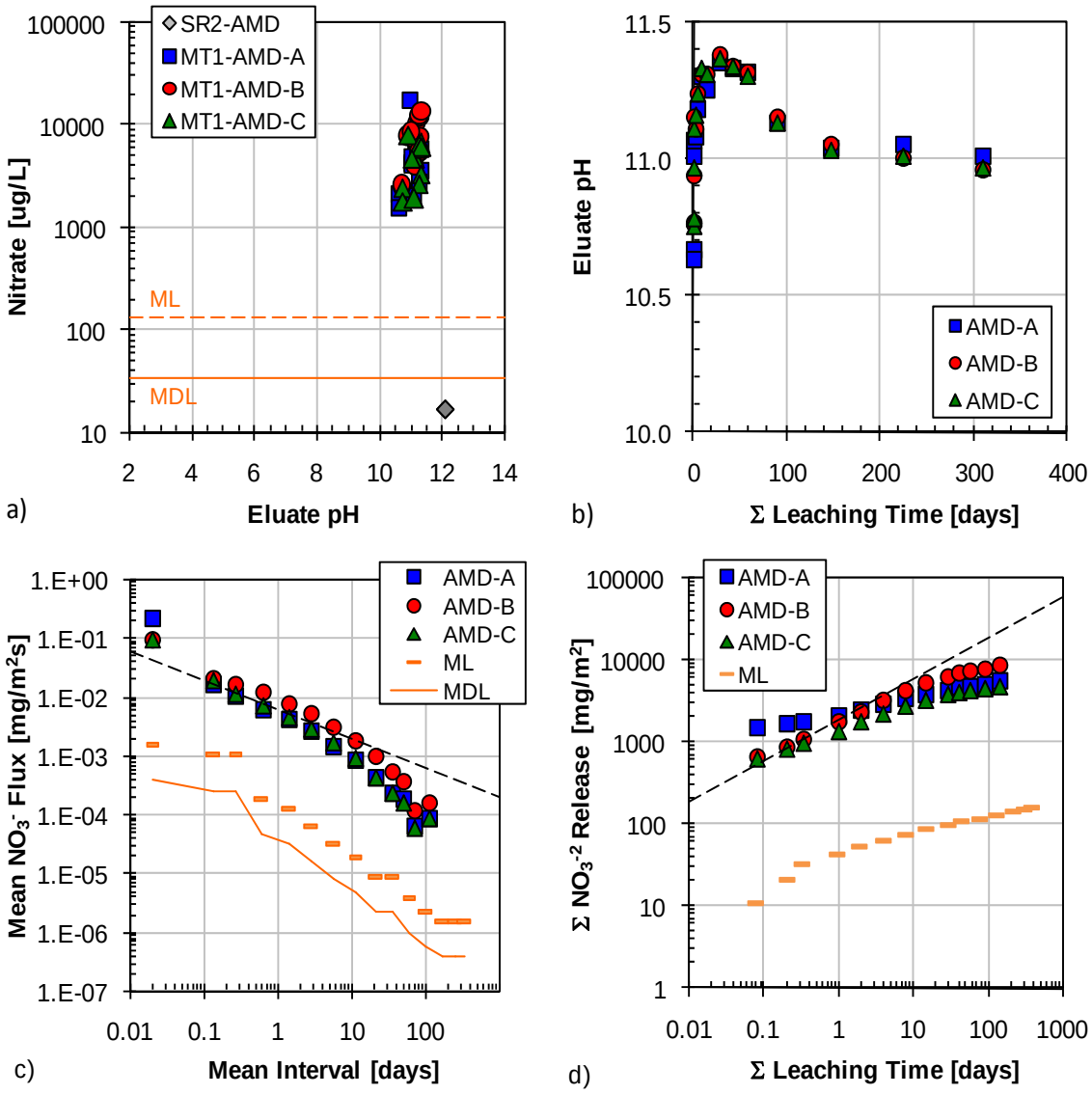

Figure A-23. Nitrate leaching test results from AMD: a) comparison of tank leach test eluants to saturation values (SR02 data) and QA/QC parameters, b) pH evolution in tank leach eluants, c) interval flux from tank leach test in comparison to flux values at the method limit ($t^{-1/2}$ model shown as dashed line), and d) cumulative mass release ($t^{1/2}$ model shown as dashed line).

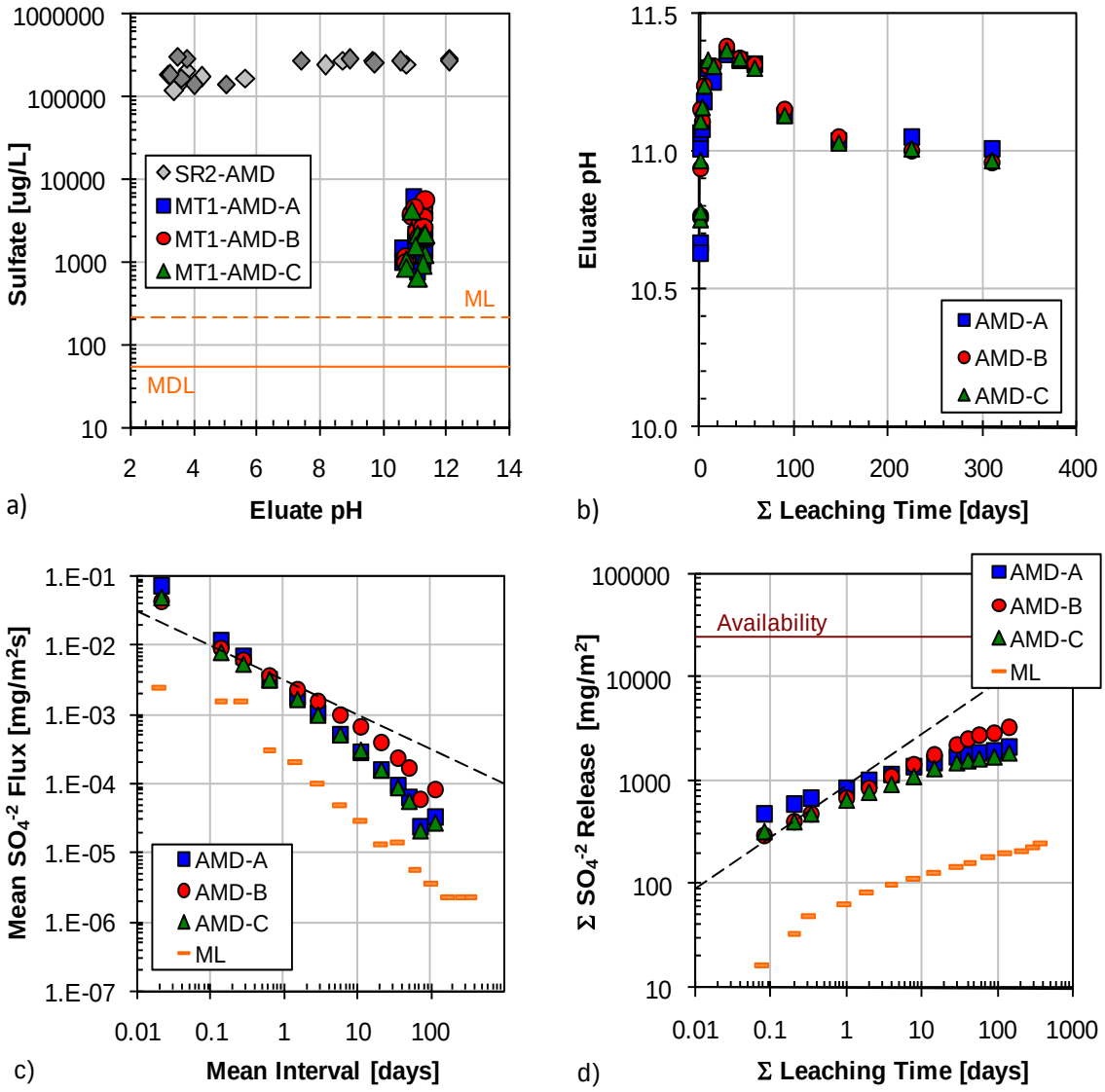

Figure A-24. Sulfate leaching test results from AMD: a) comparison of tank leach test eluants to saturation values (SR02 data) and QA/QC parameters, b) pH evolution in tank leach eluants, c) interval flux from tank leach test in comparison to flux values at the method limit ($t^{-1/2}$ model shown as dashed line), and d) cumulative mass release ($t^{1/2}$ model shown as dashed line).

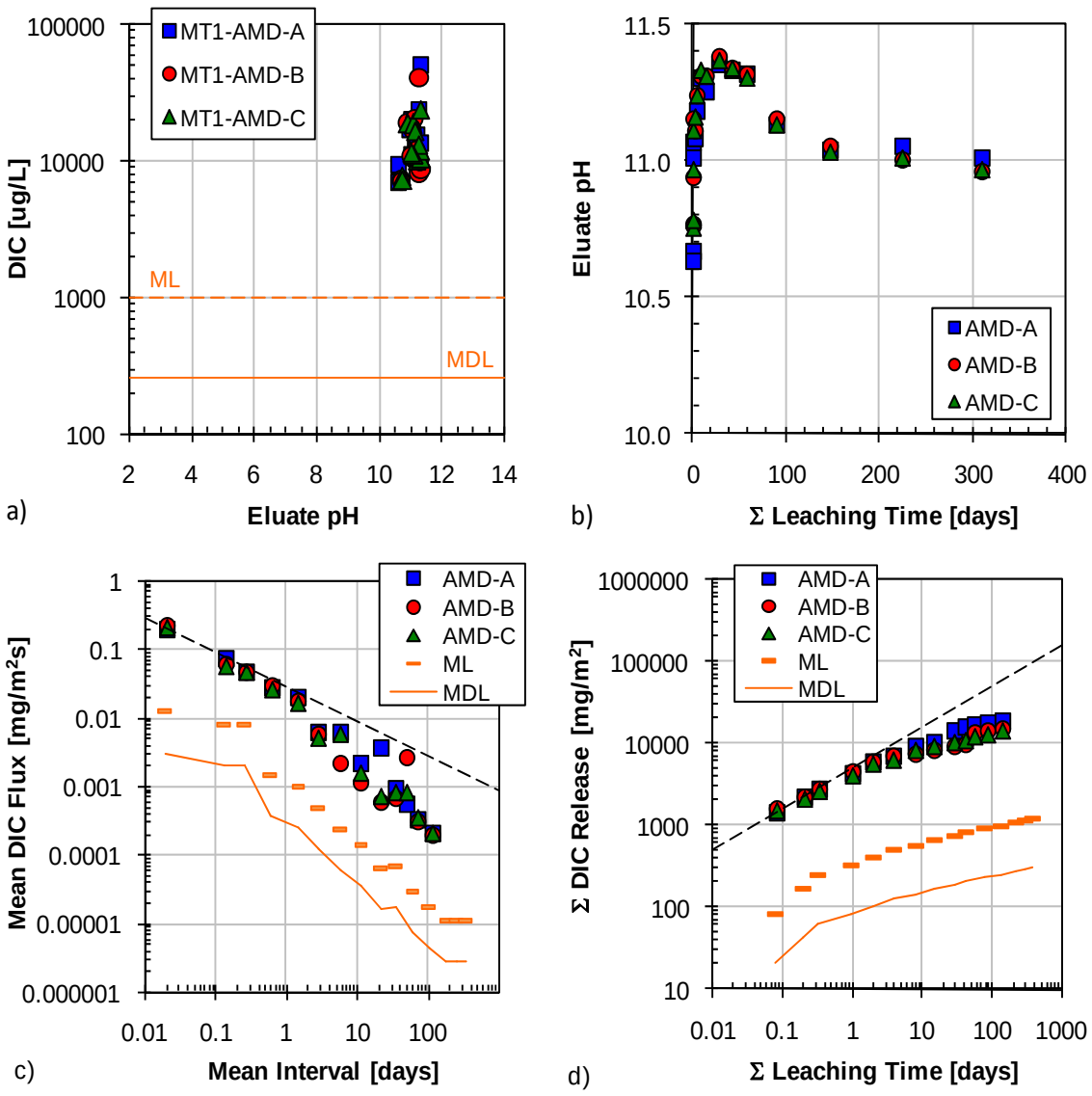

Figure A-25. Dissolved inorganic carbon (DIC) test results from AMD: a) comparison of tank leach test eluants to saturation values (SR02 data) and QA/QC parameters, b) pH evolution in tank leach eluants, c) interval flux from tank leach test in comparison to flux values at the method limit ($t^{-1/2}$ model shown as dashed line), and d) cumulative mass release ($t^{1/2}$ model shown as dashed line).

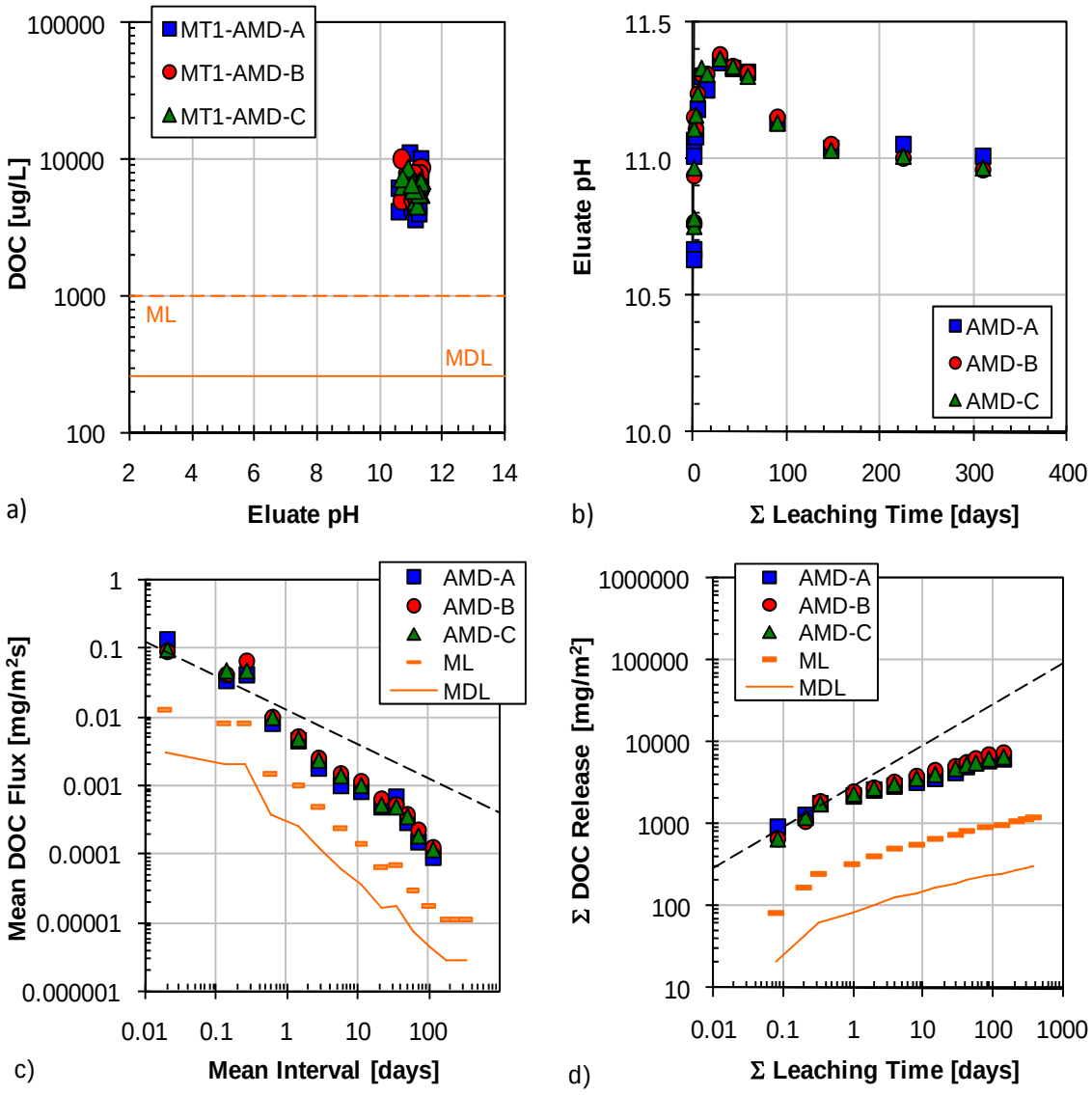

Figure A-26. Dissolved organic carbon (DOC) leaching test results from AMD: a) comparison of tank leach test eluants to saturation values (SR02 data) and QA/QC parameters, b) pH evolution in tank leach eluants, c) interval flux from tank leach test in comparison to flux values at the method limit ($t^{-1/2}$ model shown as dashed line), and d) cumulative mass release ($t^{1/2}$ model shown as dashed line).

Secondary Waste in DI Water (SWD)

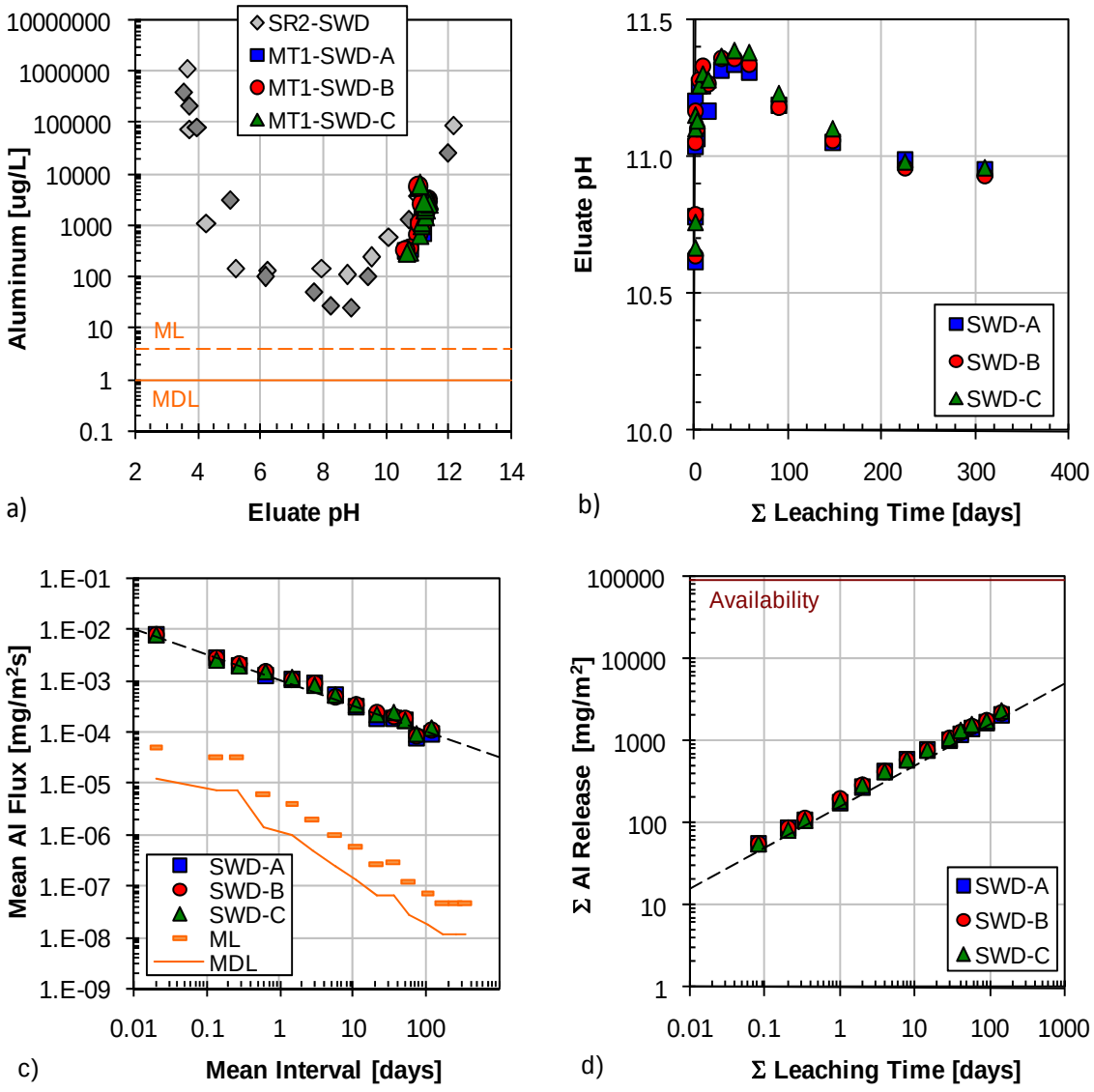

Figure A-27. Aluminum leaching test results from SWD: a) comparison of tank leach test eluants to saturation values (SR02 data) and QA/QC parameters, b) pH evolution in tank leach eluants, c) interval flux from tank leach test in comparison to flux values at the method limit ($t^{-1/2}$ model for AMD shown as dashed line), and d) cumulative mass release ($t^{1/2}$ model for AMD shown as dashed line).

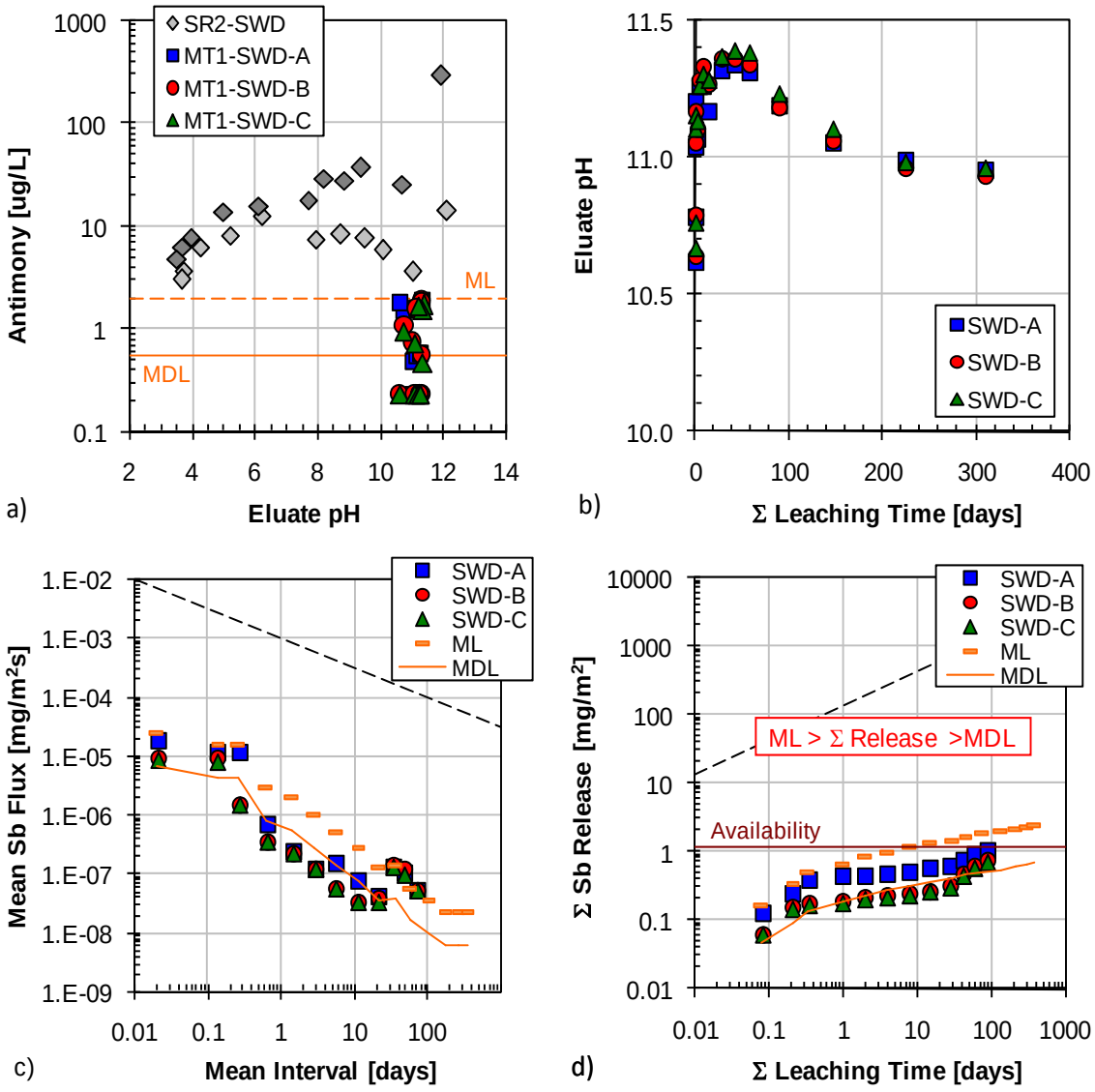

Figure A-28. Antimony leaching test results from SWD: a) comparison of tank leach test eluants to saturation values (SR02 data) and QA/QC parameters, b) pH evolution in tank leach eluants, c) interval flux from tank leach test in comparison to flux values at the method limit ($t^{-1/2}$ model for AMD shown as dashed line), and d) cumulative mass release ($t^{1/2}$ model for AMD shown as dashed line).

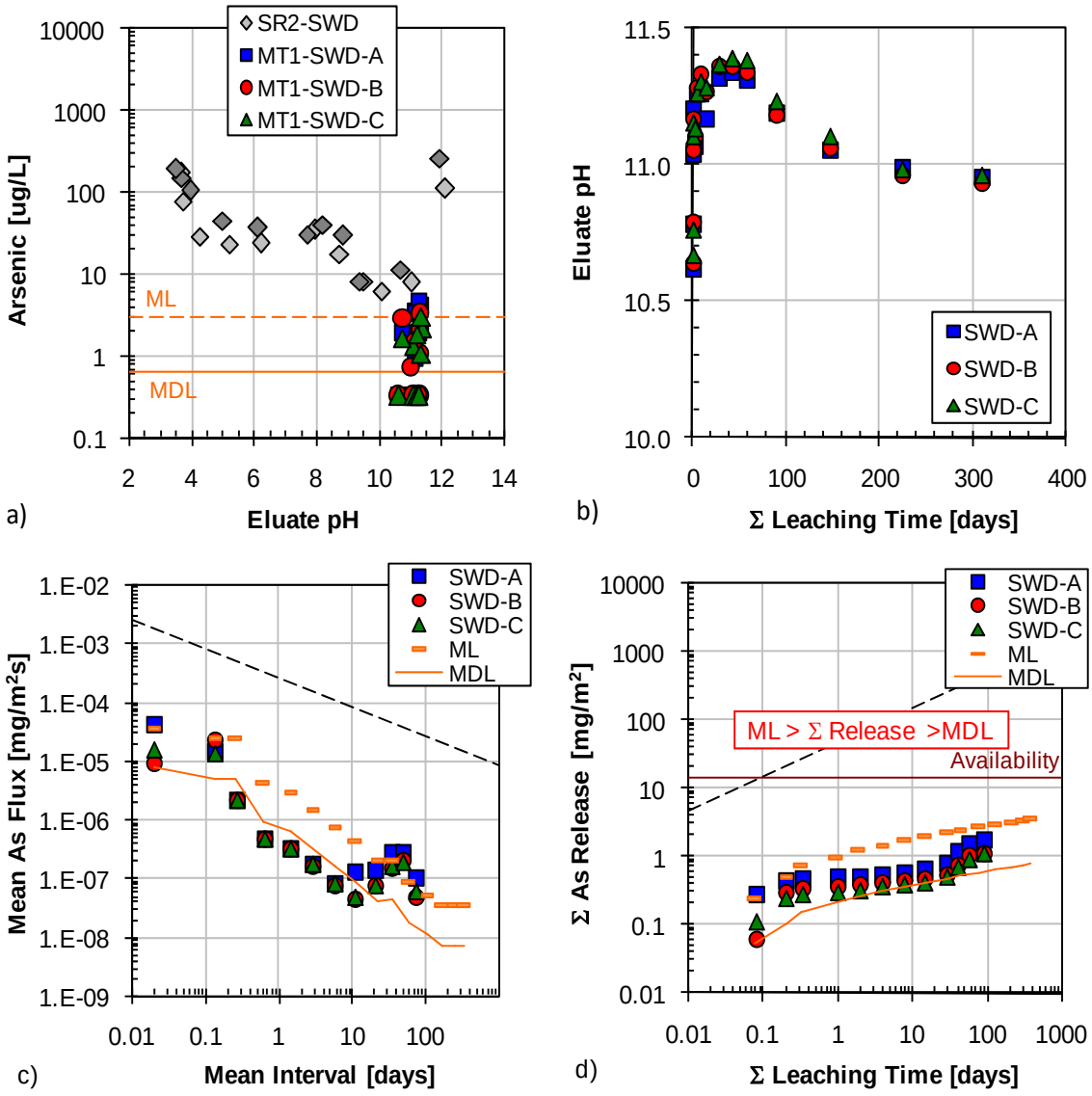

Figure A-29. Arsenic leaching test results from SWD: a) comparison of tank leach test eluants to saturation values (SR02 data) and QA/QC parameters, b) pH evolution in tank leach eluants, c) interval flux from tank leach test in comparison to flux values at the method limit ($t^{-1/2}$ model for AMD shown as dashed line), and d) cumulative mass release ($t^{1/2}$ model for AMD shown as dashed line).

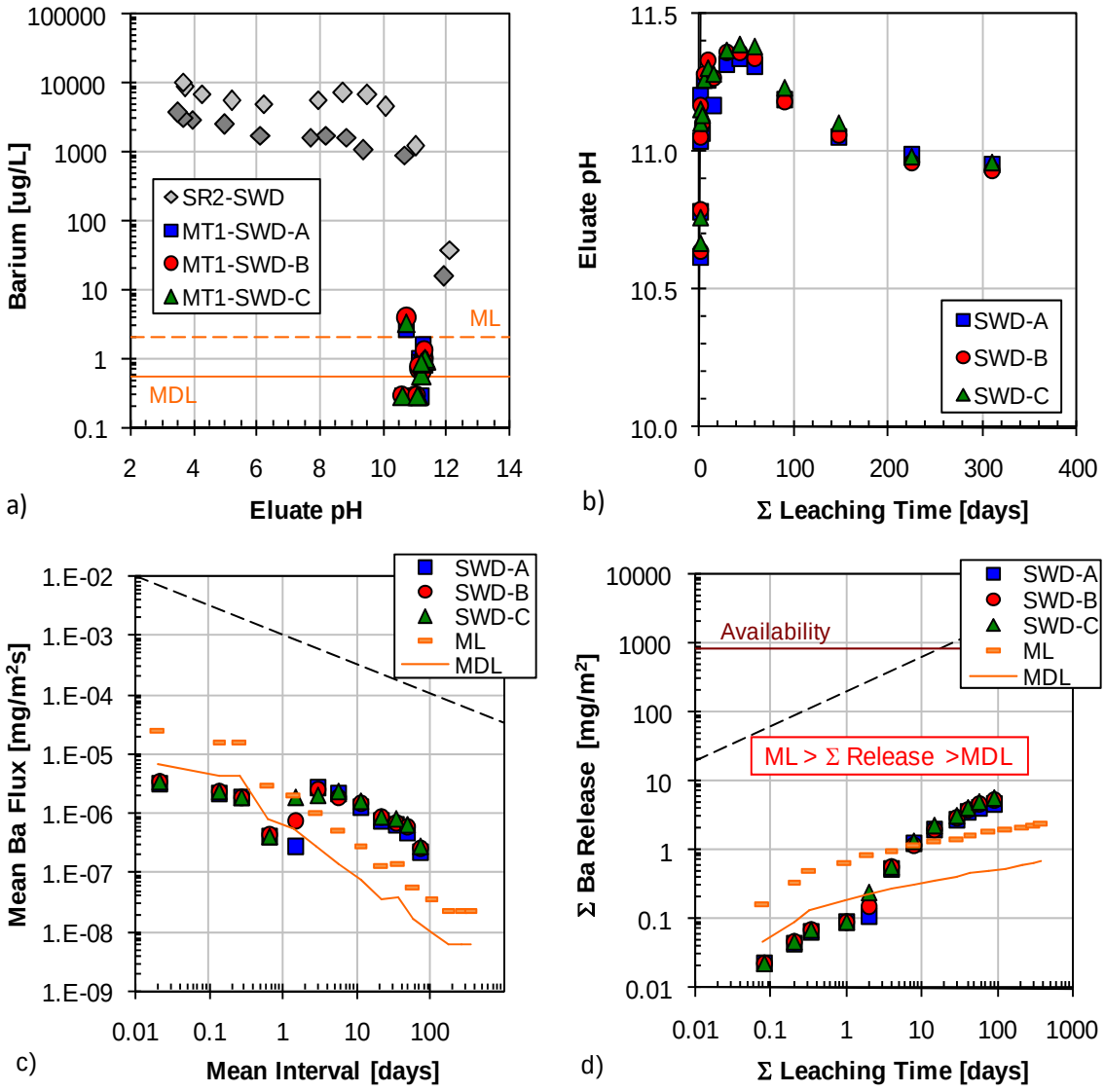

Figure A-30. Barium leaching test results from SWD: a) comparison of tank leach test eluants to saturation values (SR02 data) and QA/QC parameters, b) pH evolution in tank leach eluants, c) interval flux from tank leach test in comparison to flux values at the method limit ($t^{-1/2}$ model for AMD shown as dashed line), and d) cumulative mass release ($t^{1/2}$ model for AMD shown as dashed line).

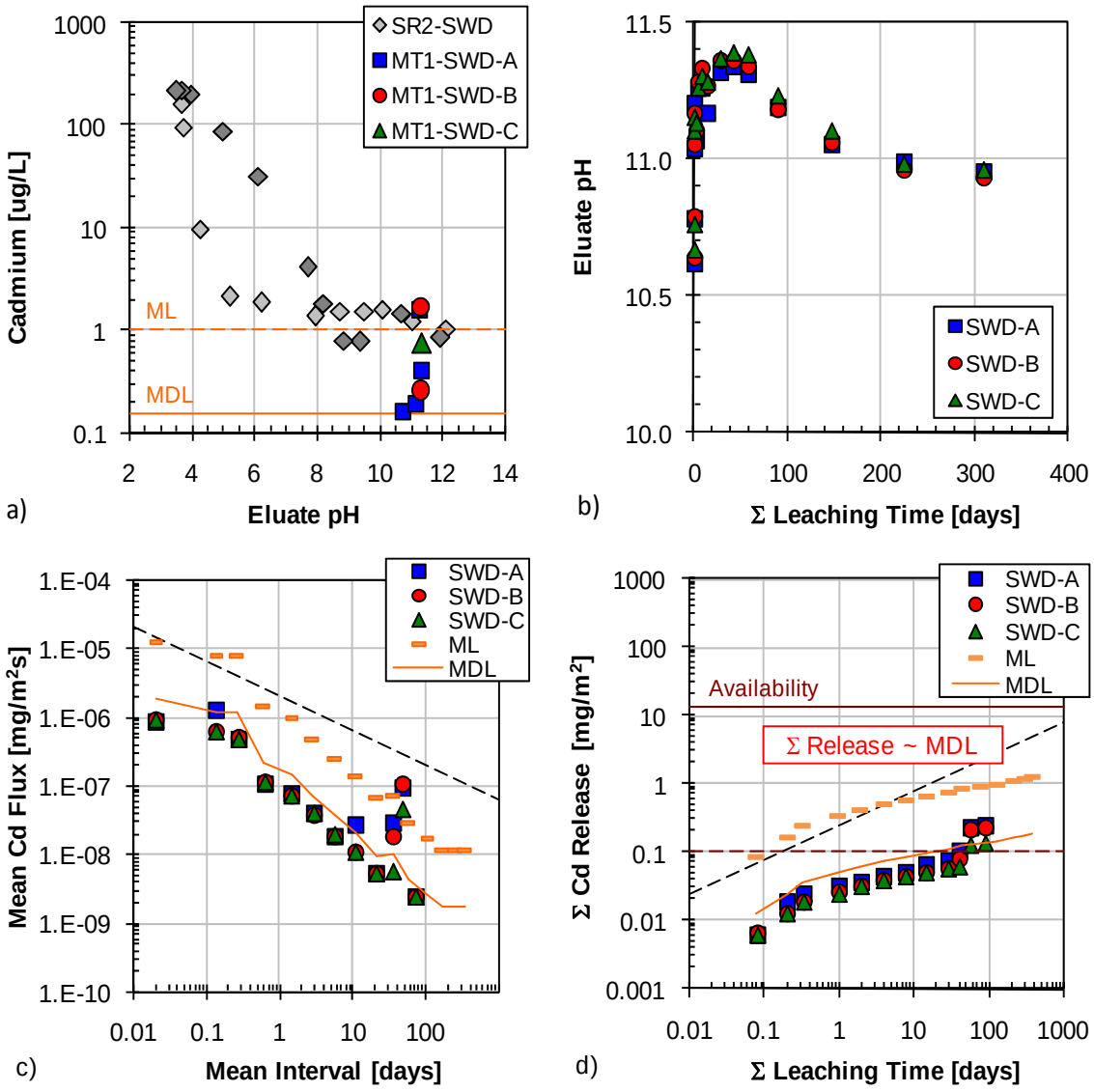

Figure A-31. Cadmium leaching test results from SWD: a) comparison of tank leach test eluants to saturation values (SR02 data) and QA/QC parameters, b) pH evolution in tank leach eluants, c) interval flux from tank leach test in comparison to flux values at the method limit ($t^{-1/2}$ model for AMD shown as dashed line), and d) cumulative mass release ($t^{1/2}$ model for AMD shown as dashed line).

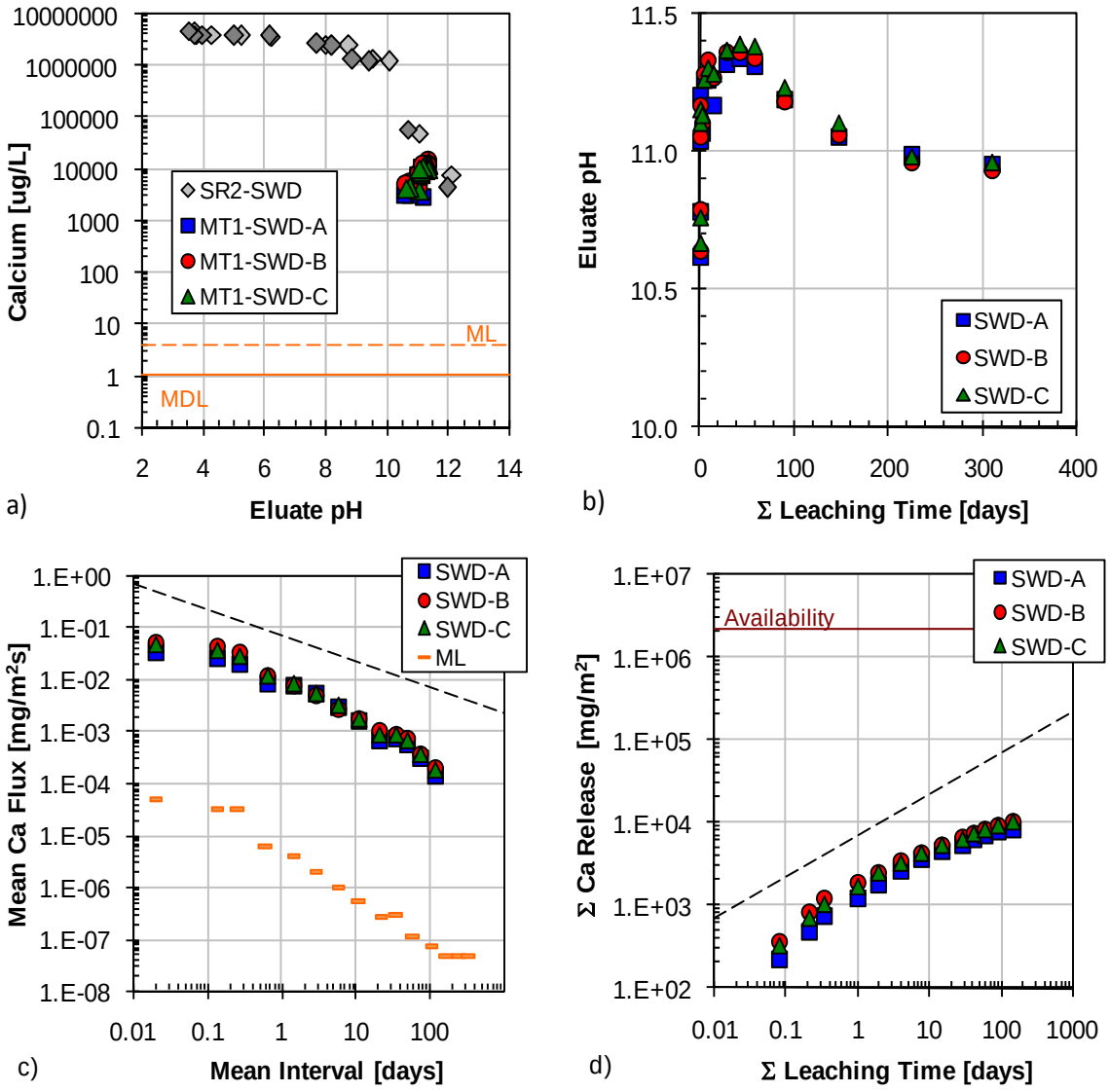

Figure A-32. Calcium leaching test results from SWD: a) comparison of tank leach test eluants to saturation values (SR02 data) and QA/QC parameters, b) pH evolution in tank leach eluants, c) interval flux from tank leach test in comparison to flux values at the method limit ($t^{-1/2}$ model for AMD shown as dashed line), and d) cumulative mass release ($t^{1/2}$ model for AMD shown as dashed line).

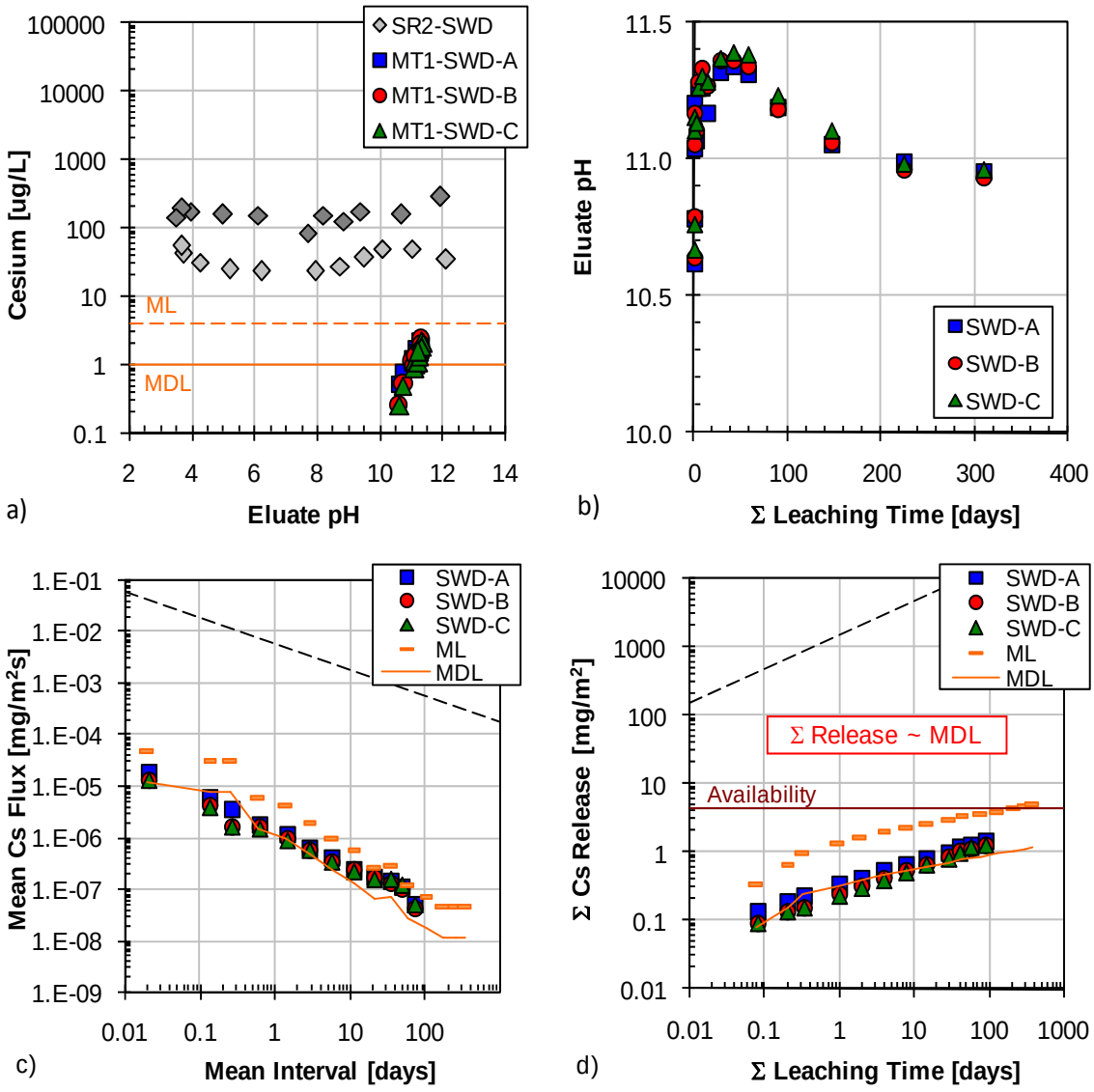

Figure A-33. Cesium leaching test results from SWD: a) comparison of tank leach test eluants to saturation values (SR02 data) and QA/QC parameters, b) pH evolution in tank leach eluants, c) interval flux from tank leach test in comparison to flux values at the method limit ($t^{-1/2}$ model for AMD shown as dashed line), and d) cumulative mass release ($t^{1/2}$ model for AMD shown as dashed line).

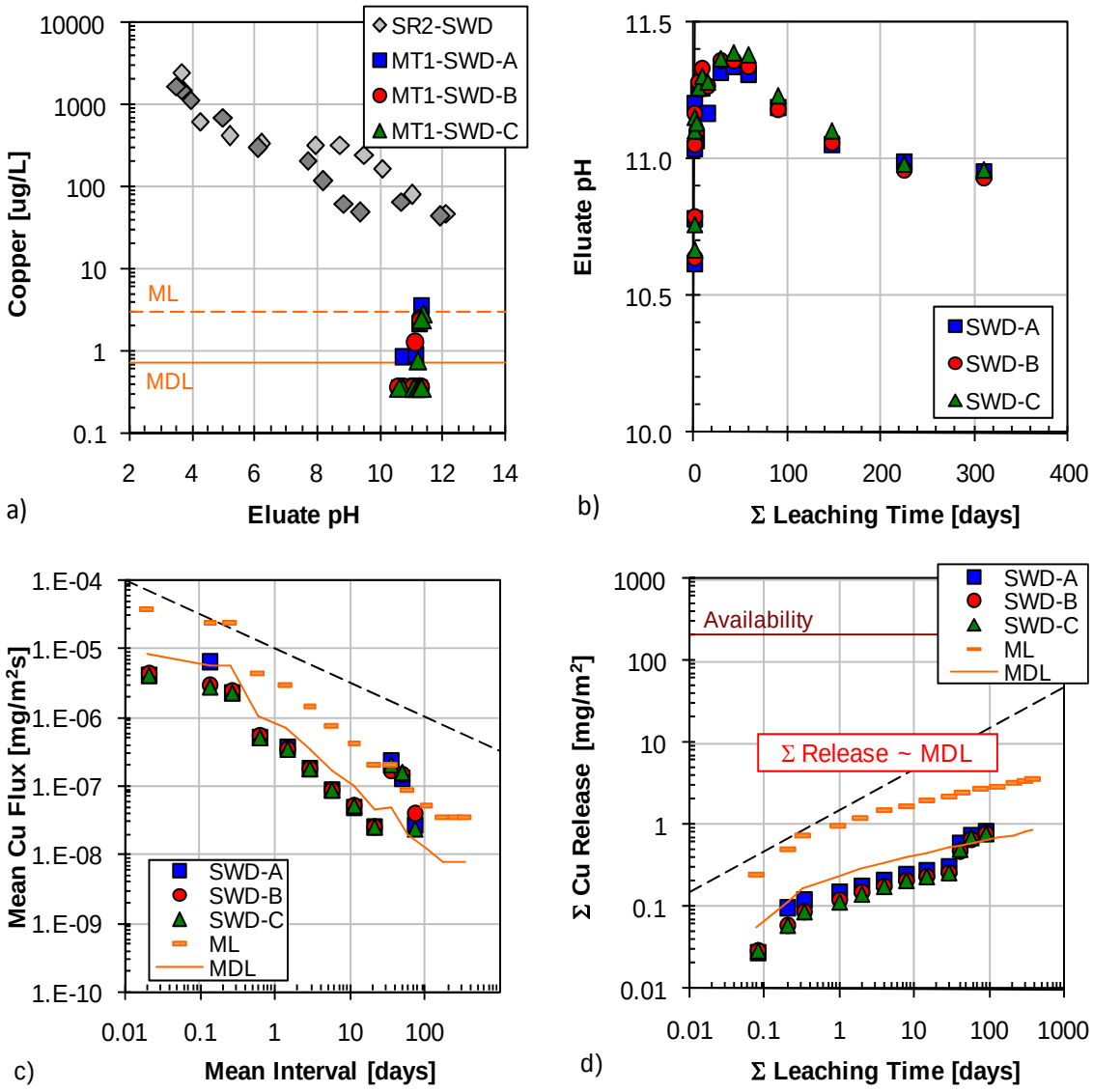

Figure A-34. Copper leaching test results from SWD: a) comparison of tank leach test eluants to saturation values (SR02 data) and QA/QC parameters, b) pH evolution in tank leach eluants, c) interval flux from tank leach test in comparison to flux values at the method limit ($t^{-1/2}$ model for AMD shown as dashed line), and d) cumulative mass release ($t^{1/2}$ model for AMD shown as dashed line).

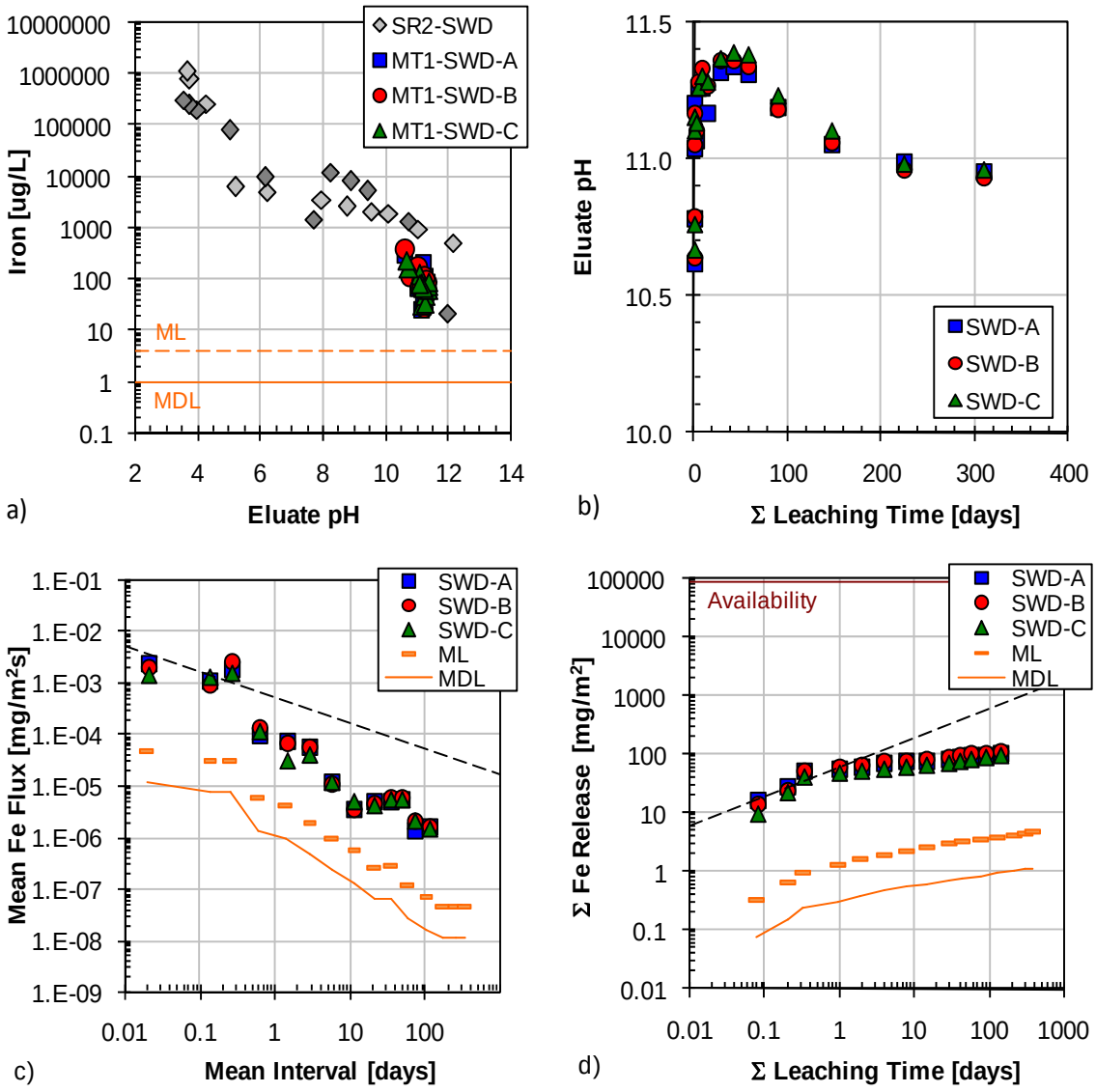

Figure A-35. Iron leaching test results from SWD: a) comparison of tank leach test eluants to saturation values (SR02 data) and QA/QC parameters, b) pH evolution in tank leach eluants, c) interval flux from tank leach test in comparison to flux values at the method limit ($t^{-1/2}$ model for AMD shown as dashed line), and d) cumulative mass release ($t^{1/2}$ model for AMD shown as dashed line).

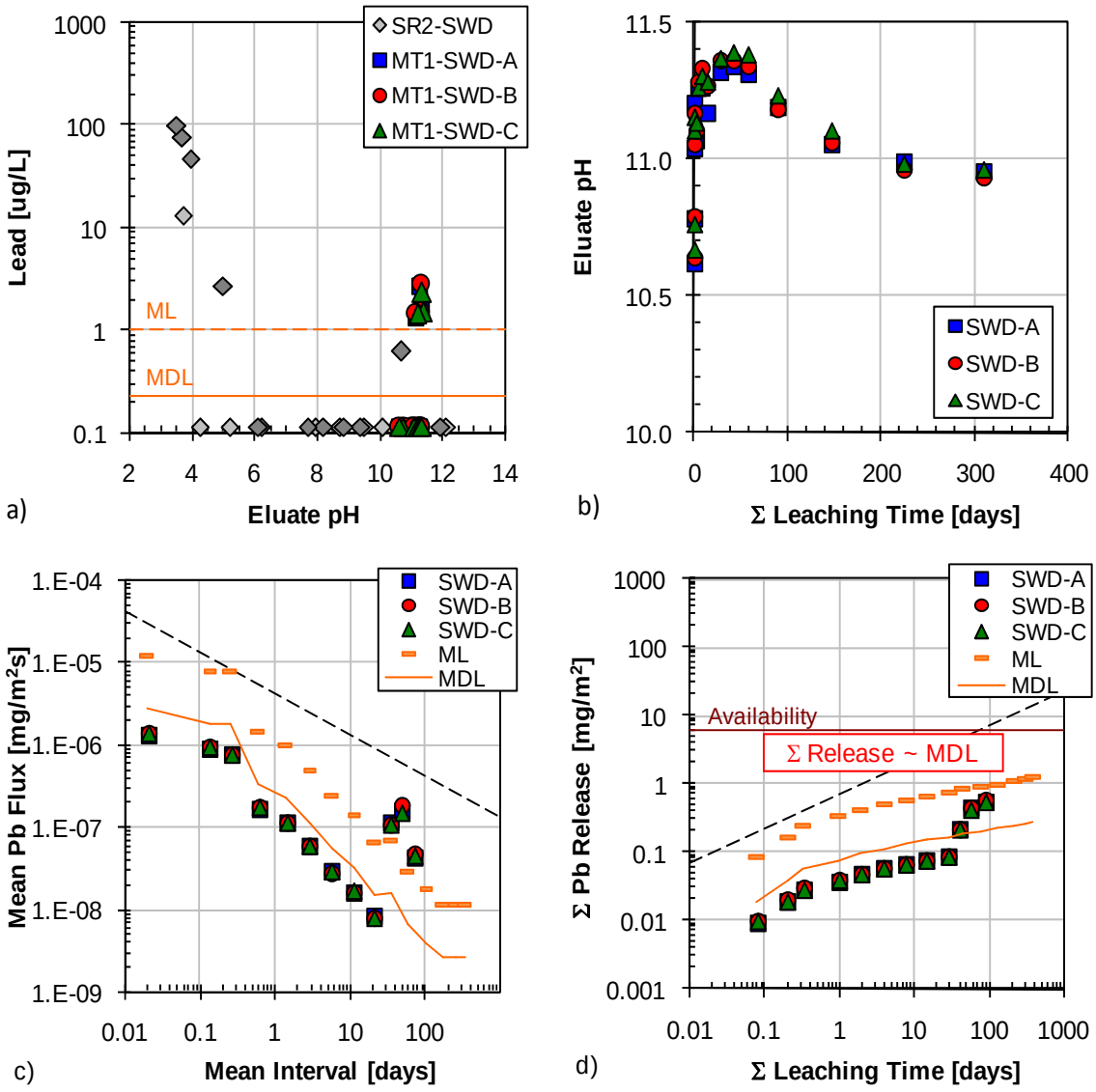

Figure A-36. Lead leaching test results from SWD: a) comparison of tank leach test eluants to saturation values (SR02 data) and QA/QC parameters, b) pH evolution in tank leach eluants, c) interval flux from tank leach test in comparison to flux values at the method limit ($t^{-1/2}$ model for AMD shown as dashed line), and d) cumulative mass release ($t^{1/2}$ model for AMD shown as dashed line).

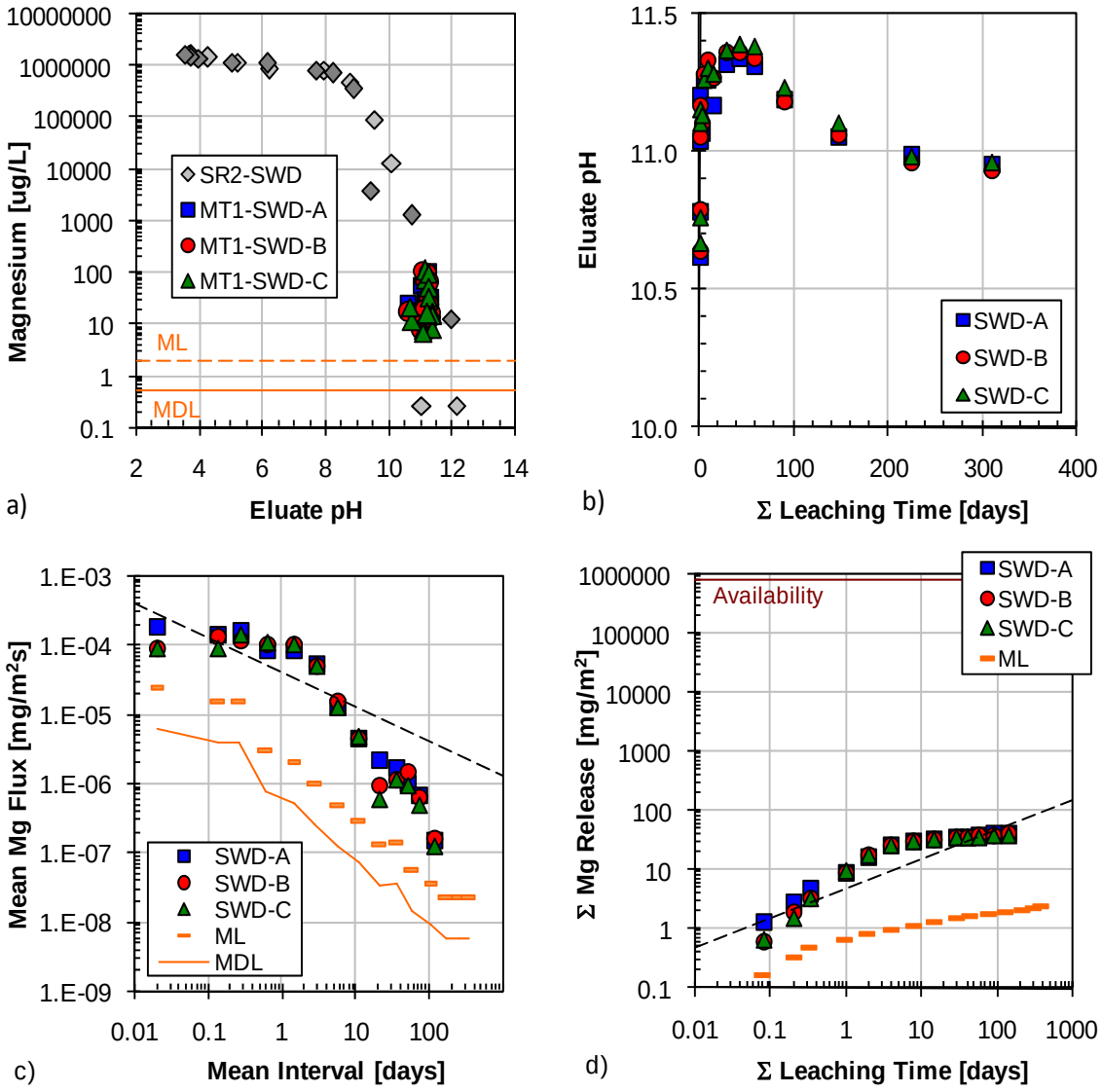

Figure A-37. Magnesium leaching test results from SWD matrix: a) comparison of tank leach test eluants to saturation values (SR02 data) and QA/QC parameters, b) pH evolution in tank leach eluants, c) interval flux from tank leach test in comparison to flux values at the method limit ($t^{-1/2}$ model for AMD shown as dashed line), and d) cumulative mass release ($t^{1/2}$ model for AMD shown as dashed line).

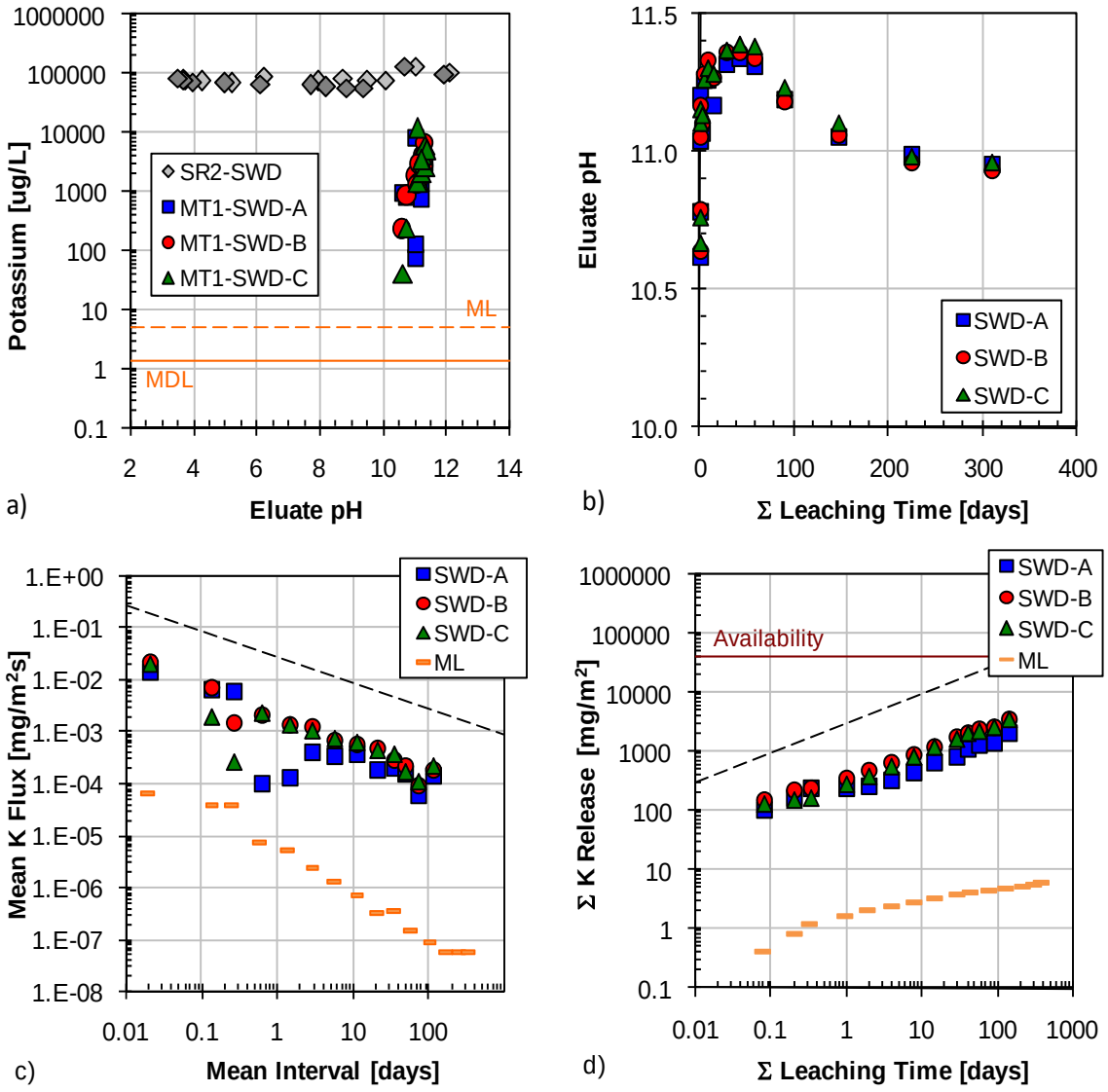

Figure A-38. Potassium leaching test results from SWD matrix: a) comparison of tank leach test eluants to saturation values (SR02 data) and QA/QC parameters, b) pH evolution in tank leach eluants, c) interval flux from tank leach test in comparison to flux values at the method limit ($t^{-1/2}$ model for AMD shown as dashed line), and d) cumulative mass release ($t^{1/2}$ model for AMD shown as dashed line).

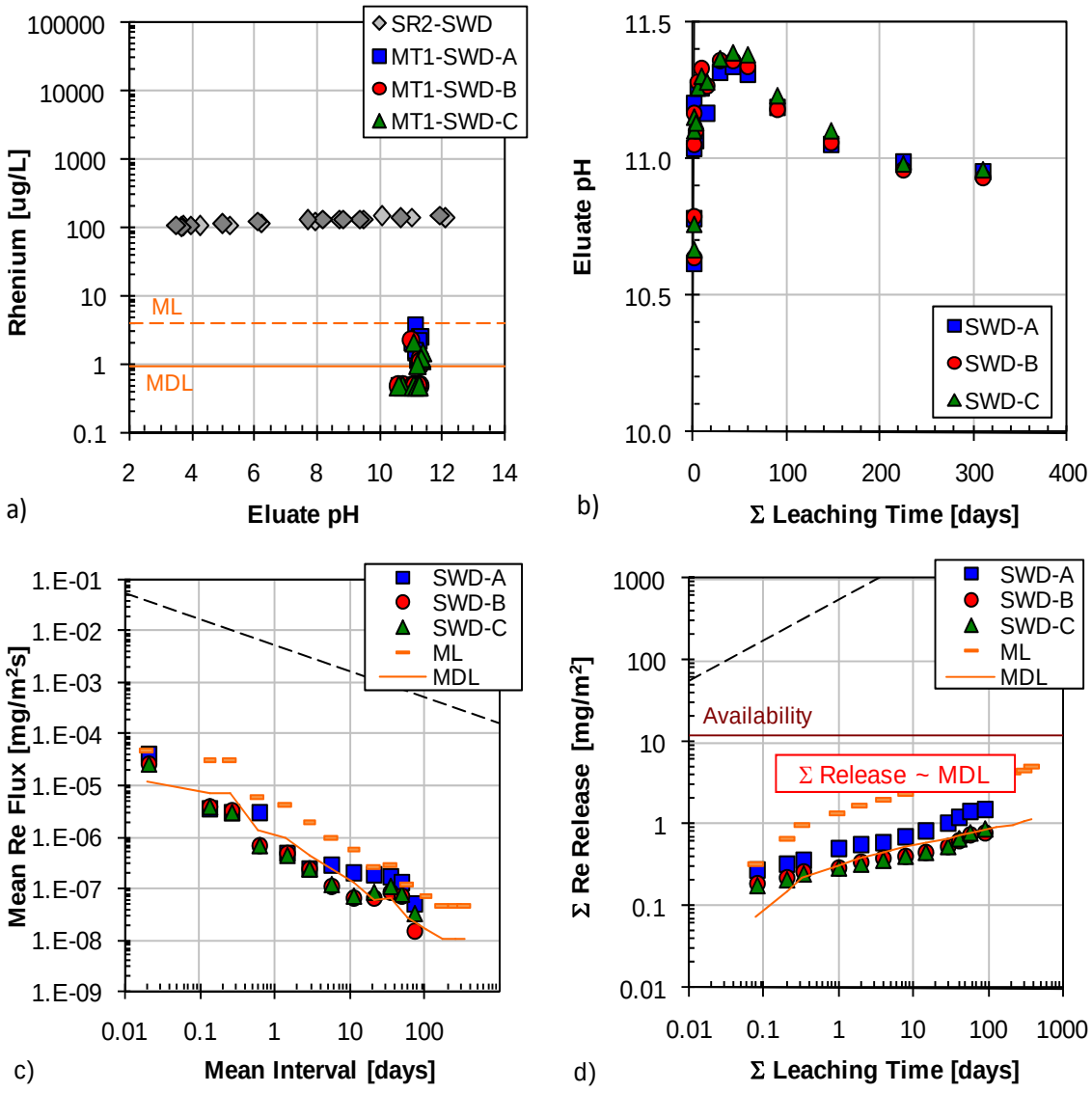

Figure A-39. Rhenium leaching test results from SWD matrix: a) comparison of tank leach test eluants to saturation values (SR02 data) and QA/QC parameters, b) pH evolution in tank leach eluants, c) interval flux from tank leach test in comparison to flux values at the method limit ($t^{-1/2}$ model for AMD shown as dashed line), and d) cumulative mass release ($t^{1/2}$ model for AMD shown as dashed line).

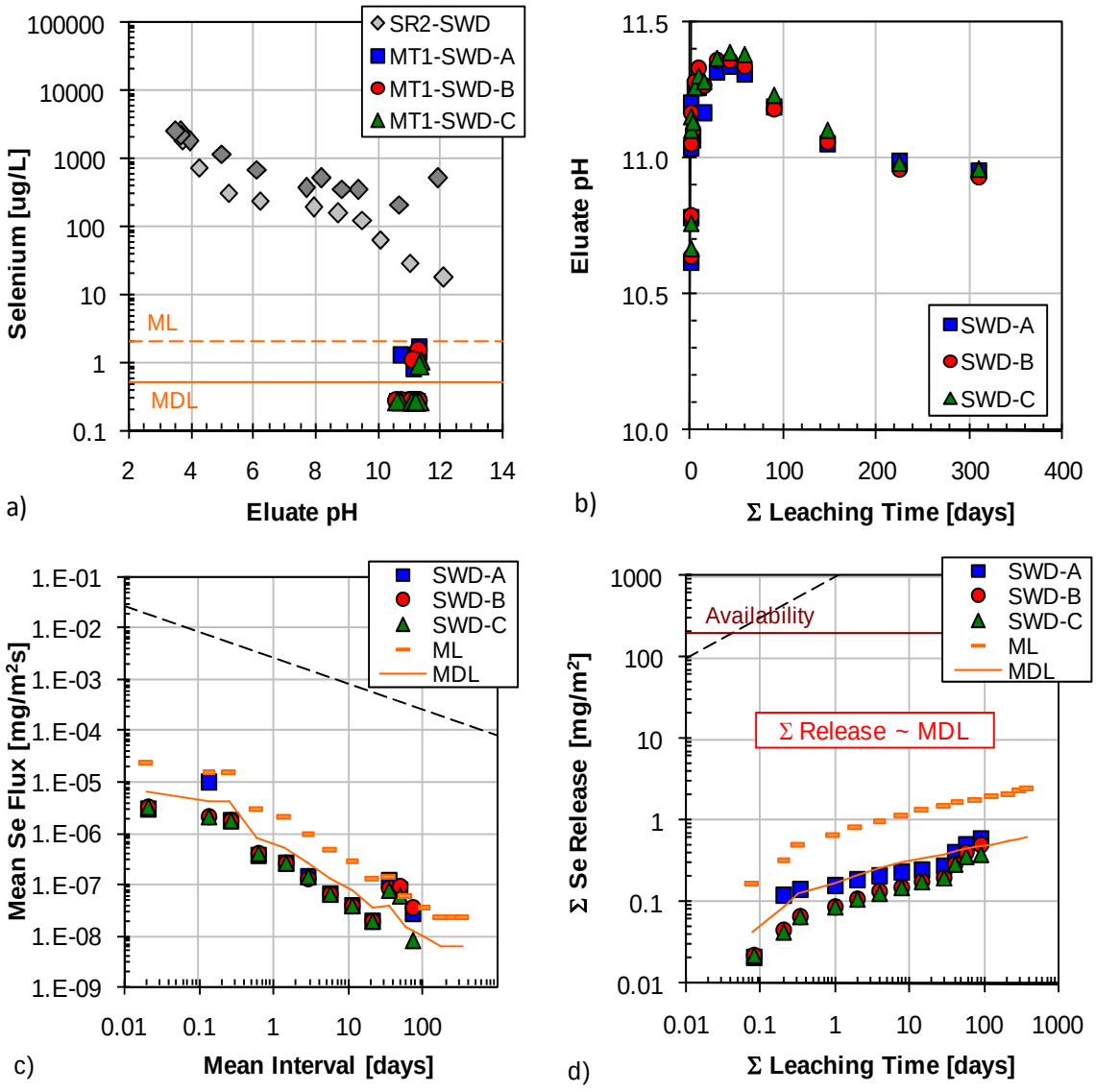

Figure A-40. Selenium leaching test results from SWD matrix: a) comparison of tank leach test eluants to saturation values (SR02 data) and QA/QC parameters, b) pH evolution in tank leach eluants, c) interval flux from tank leach test in comparison to flux values at the method limit ($t^{-1/2}$ model for AMD shown as dashed line), and d) cumulative mass release ($t^{1/2}$ model for AMD shown as dashed line).

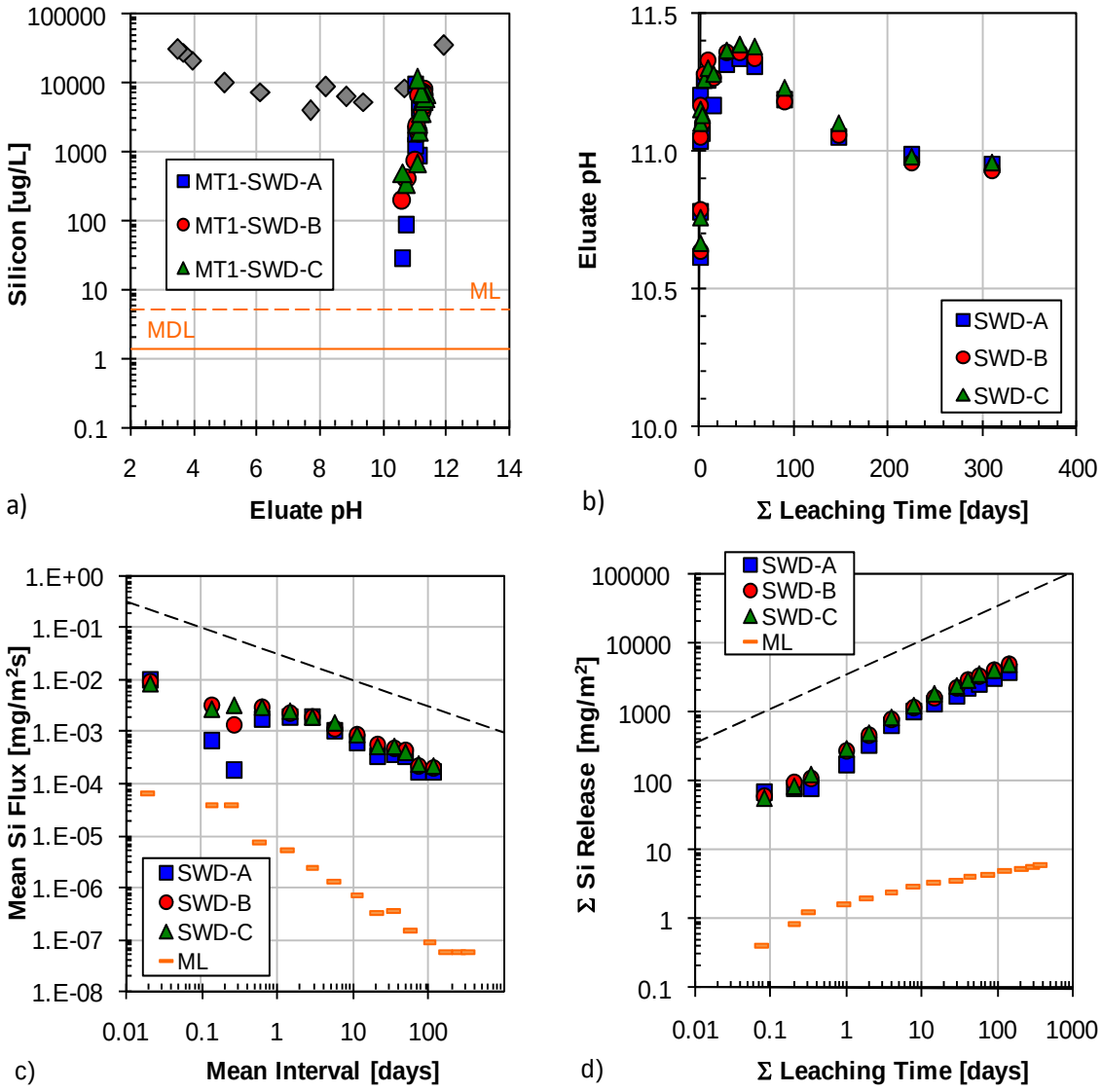

Figure A-41. Silicon leaching test results from SWD matrix: a) comparison of tank leach test eluants to saturation values (SR02 data) and QA/QC parameters, b) pH evolution in tank leach eluants, c) interval flux from tank leach test in comparison to flux values at the method limit ($t^{-1/2}$ model for AMD shown as dashed line), and d) cumulative mass release ($t^{1/2}$ model for AMD shown as dashed line).

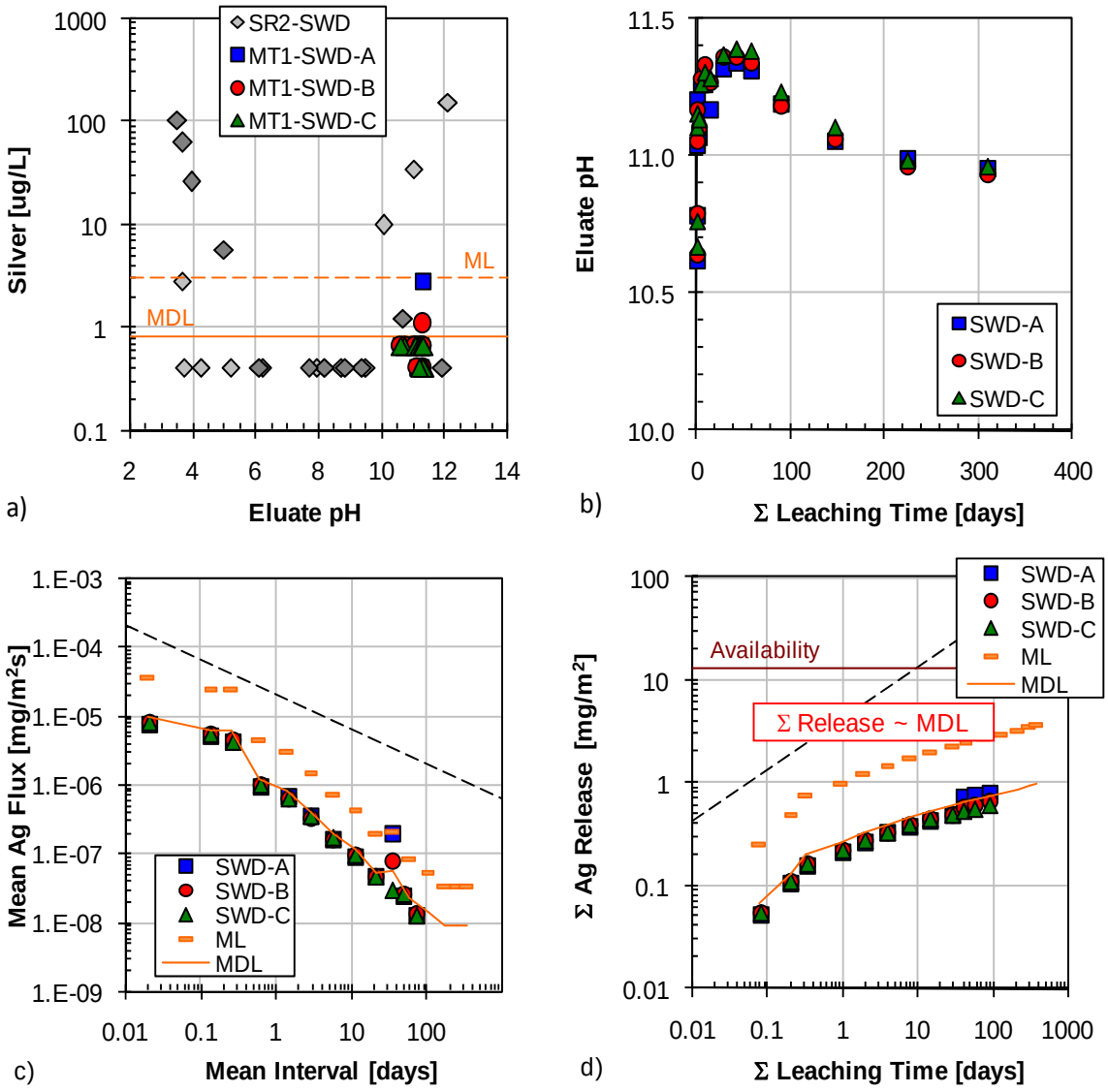

Figure A-42. Silver leaching test results from SWD matrix: a) comparison of tank leach test eluants to saturation values (SR02 data) and QA/QC parameters, b) pH evolution in tank leach eluants, c) interval flux from tank leach test in comparison to flux values at the method limit ($t^{-1/2}$ model for AMD shown as dashed line), and d) cumulative mass release ($t^{1/2}$ model for AMD shown as dashed line).

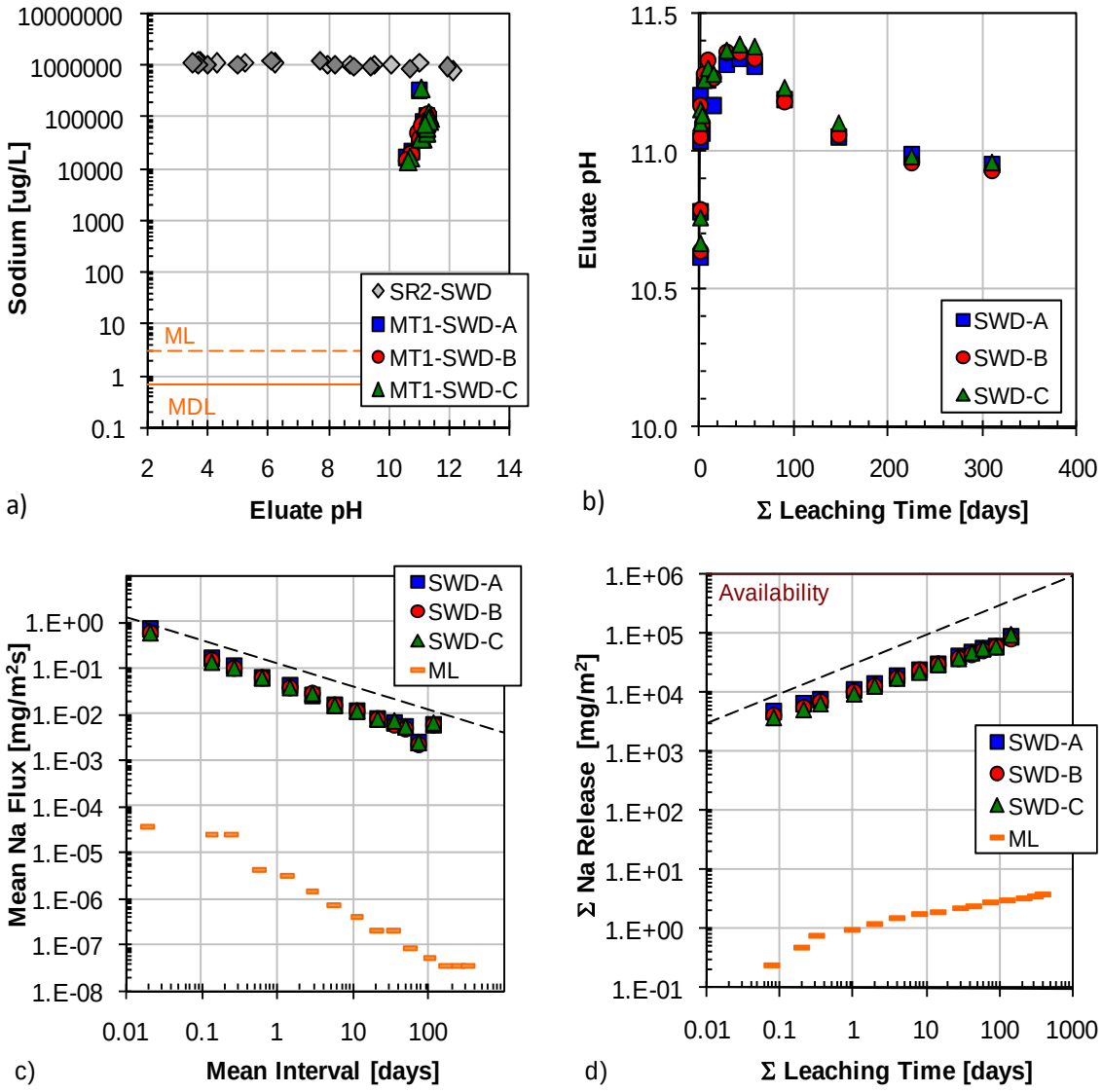

Figure A-43. Sodium leaching test results from SWD matrix: a) comparison of tank leach test eluants to saturation values (SR02 data) and QA/QC parameters, b) pH evolution in tank leach eluants, c) interval flux from tank leach test in comparison to flux values at the method limit ($t^{-1/2}$ model for AMD shown as dashed line), and d) cumulative mass release ($t^{1/2}$ model for AMD shown as dashed line).

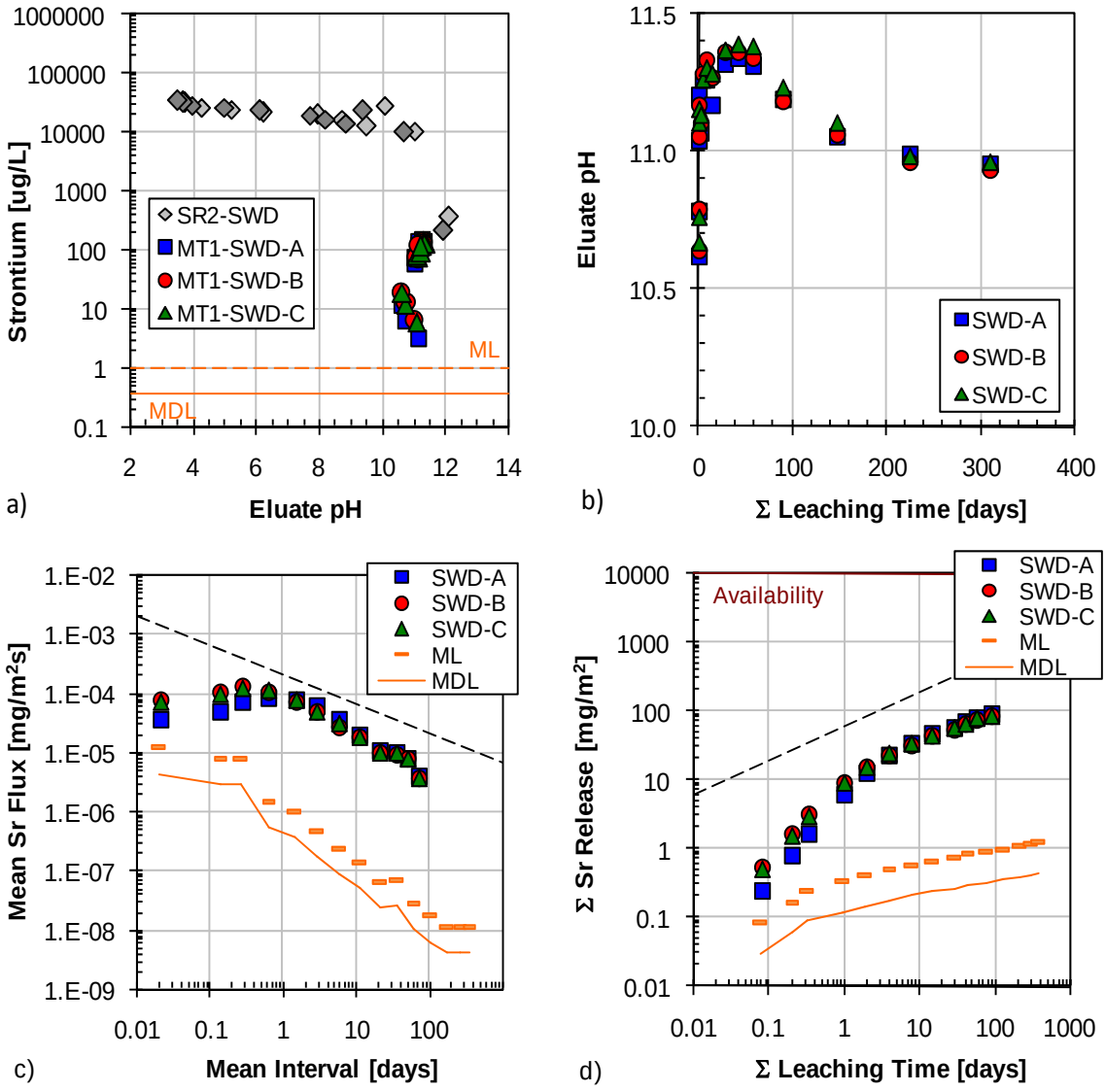

Figure A-44. Strontium leaching test results from SWD matrix: a) comparison of tank leach test eluants to saturation values (SR02 data) and QA/QC parameters, b) pH evolution in tank leach eluants, c) interval flux from tank leach test in comparison to flux values at the method limit ($t^{-1/2}$ model for AMD shown as dashed line), and d) cumulative mass release ($t^{1/2}$ model for AMD shown as dashed line).

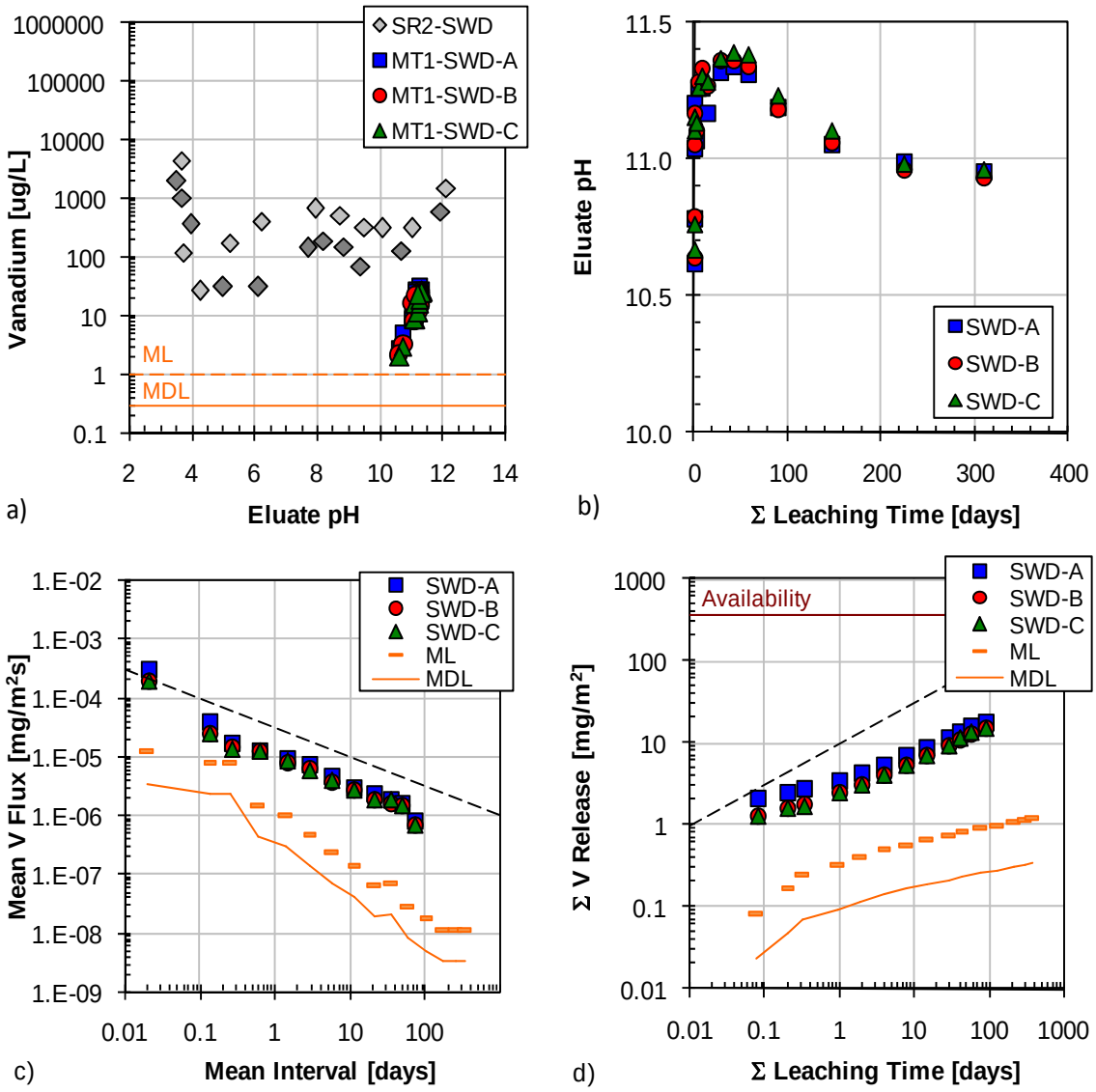

Figure A-45. Vanadium leaching test results from SWD matrix: a) comparison of tank leach test eluants to saturation values (SR02 data) and QA/QC parameters, b) pH evolution in tank leach eluants, c) interval flux from tank leach test in comparison to flux values at the method limit ($t^{-1/2}$ model for AMD shown as dashed line), and d) cumulative mass release ($t^{1/2}$ model for AMD shown as dashed line).

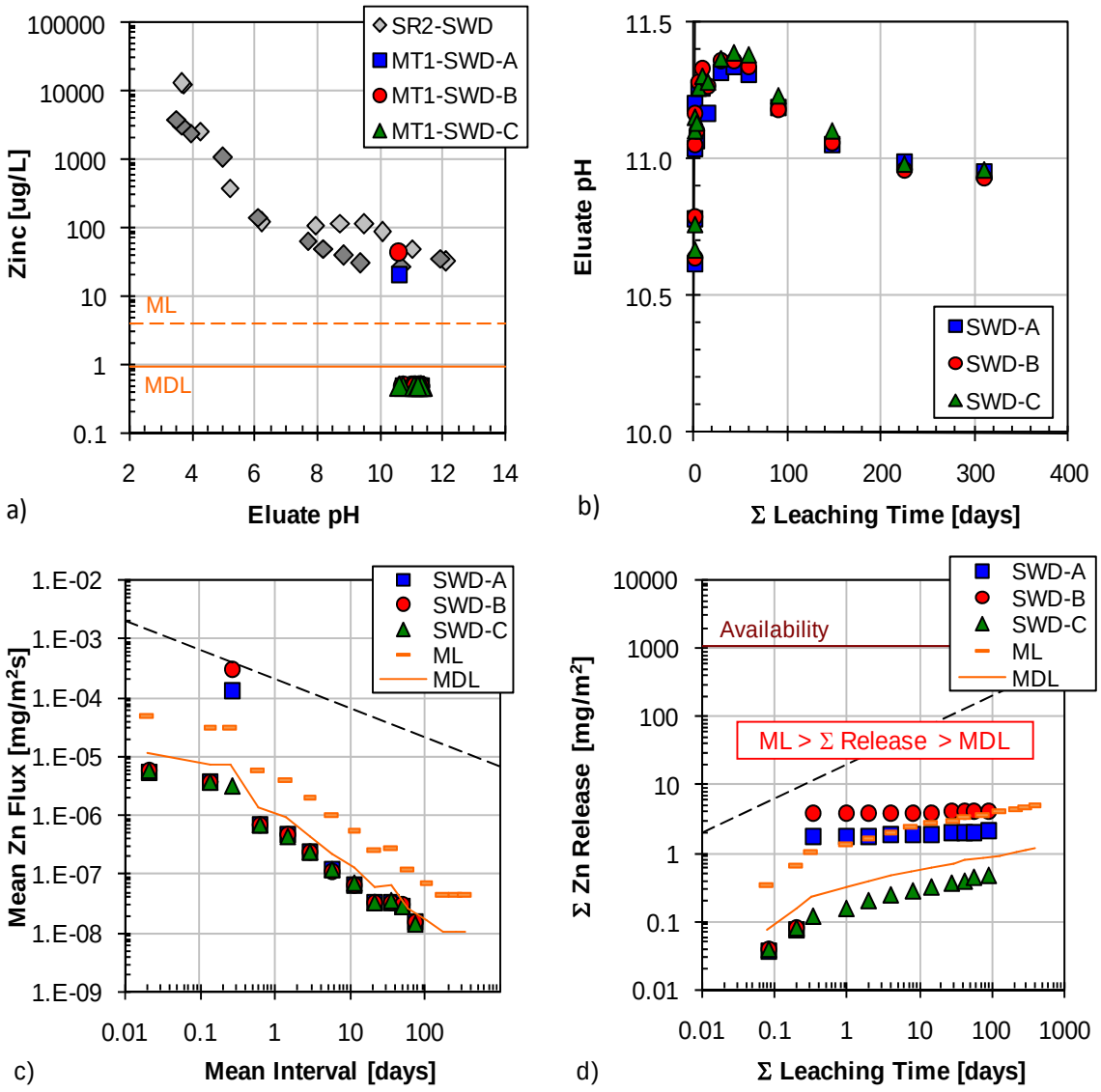

Figure A-46. Zinc leaching test results from SWD matrix: a) comparison of tank leach test eluants to saturation values (SR02 data) and QA/QC parameters, b) pH evolution in tank leach eluants, c) interval flux from tank leach test in comparison to flux values at the method limit ($t^{-1/2}$ model for AMD shown as dashed line), and d) cumulative mass release ($t^{1/2}$ model for AMD shown as dashed line).

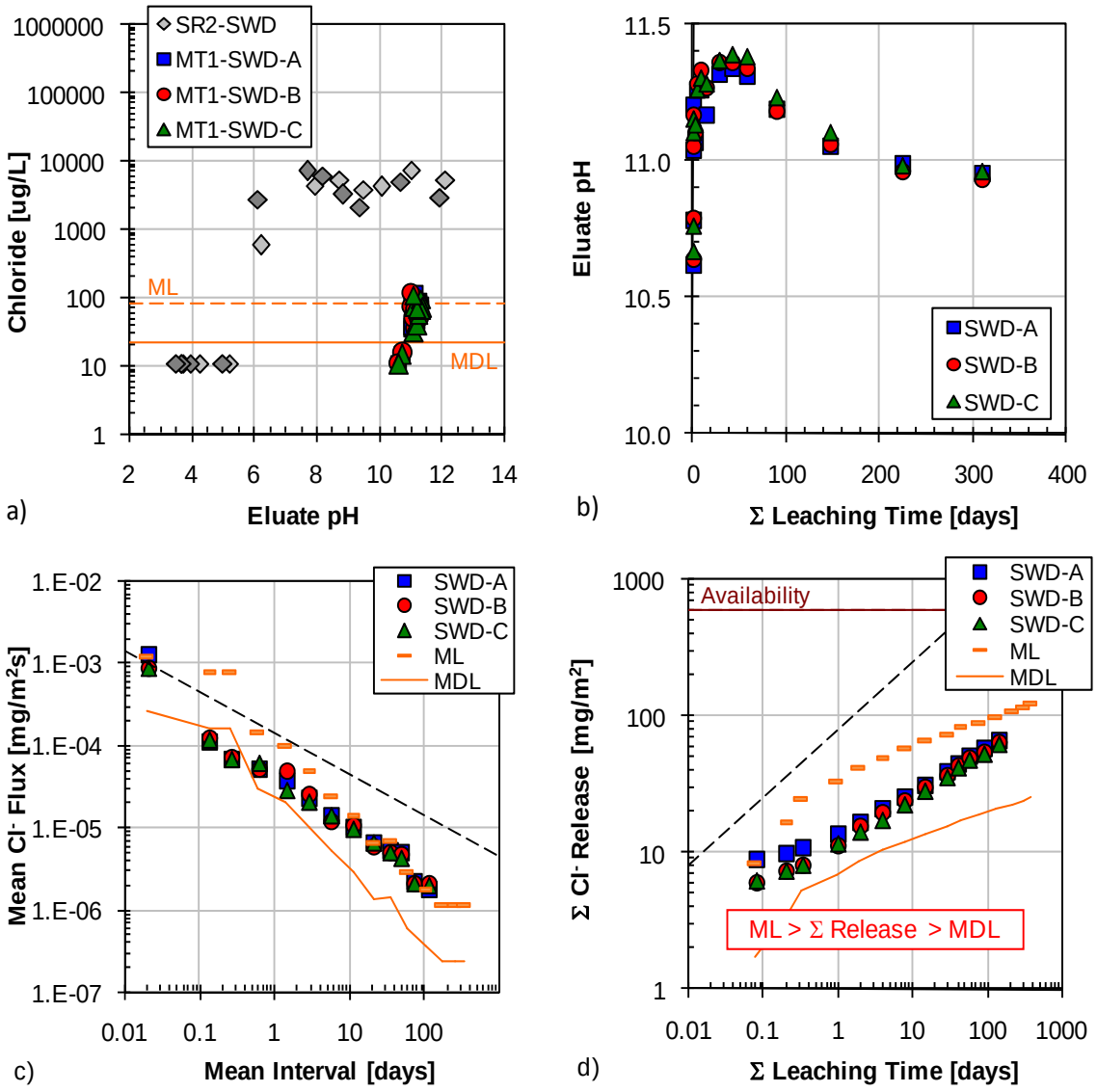

Figure A-47. Chloride leaching test results from SWD matrix: a) comparison of tank leach test eluants to saturation values (SR02 data) and QA/QC parameters, b) pH evolution in tank leach eluants, c) interval flux from tank leach test in comparison to flux values at the method limit ($t^{-1/2}$ model for AMD shown as dashed line), and d) cumulative mass release ($t^{1/2}$ model for AMD shown as dashed line).

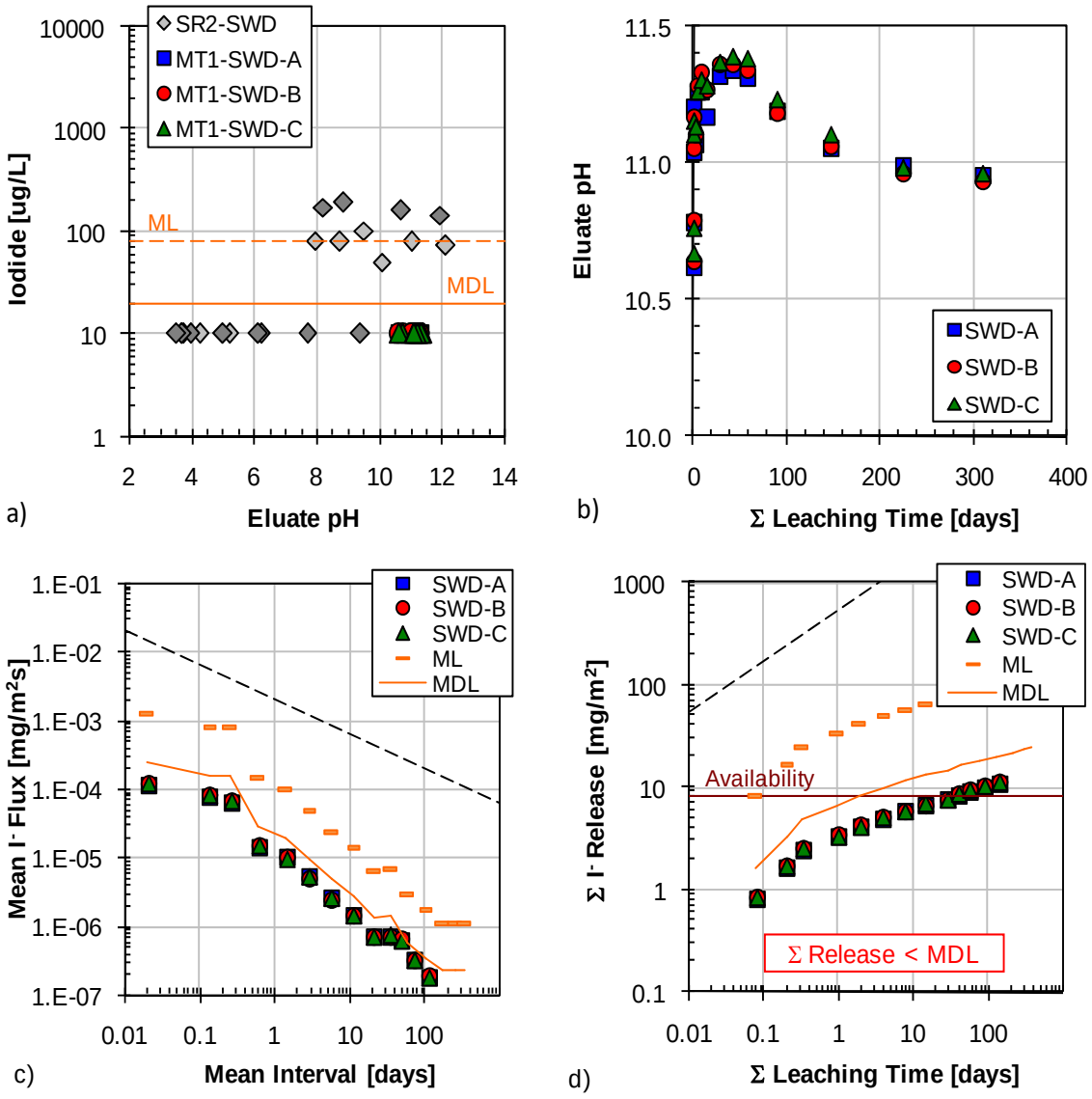

Figure A-48. Iodide leaching test results from SWD matrix: a) comparison of tank leach test eluants to saturation values (SR02 data) and QA/QC parameters, b) pH evolution in tank leach eluants, c) interval flux from tank leach test in comparison to flux values at the method limit ($t^{-1/2}$ model for AMD shown as dashed line), and d) cumulative mass release ($t^{1/2}$ model for AMD shown as dashed line).

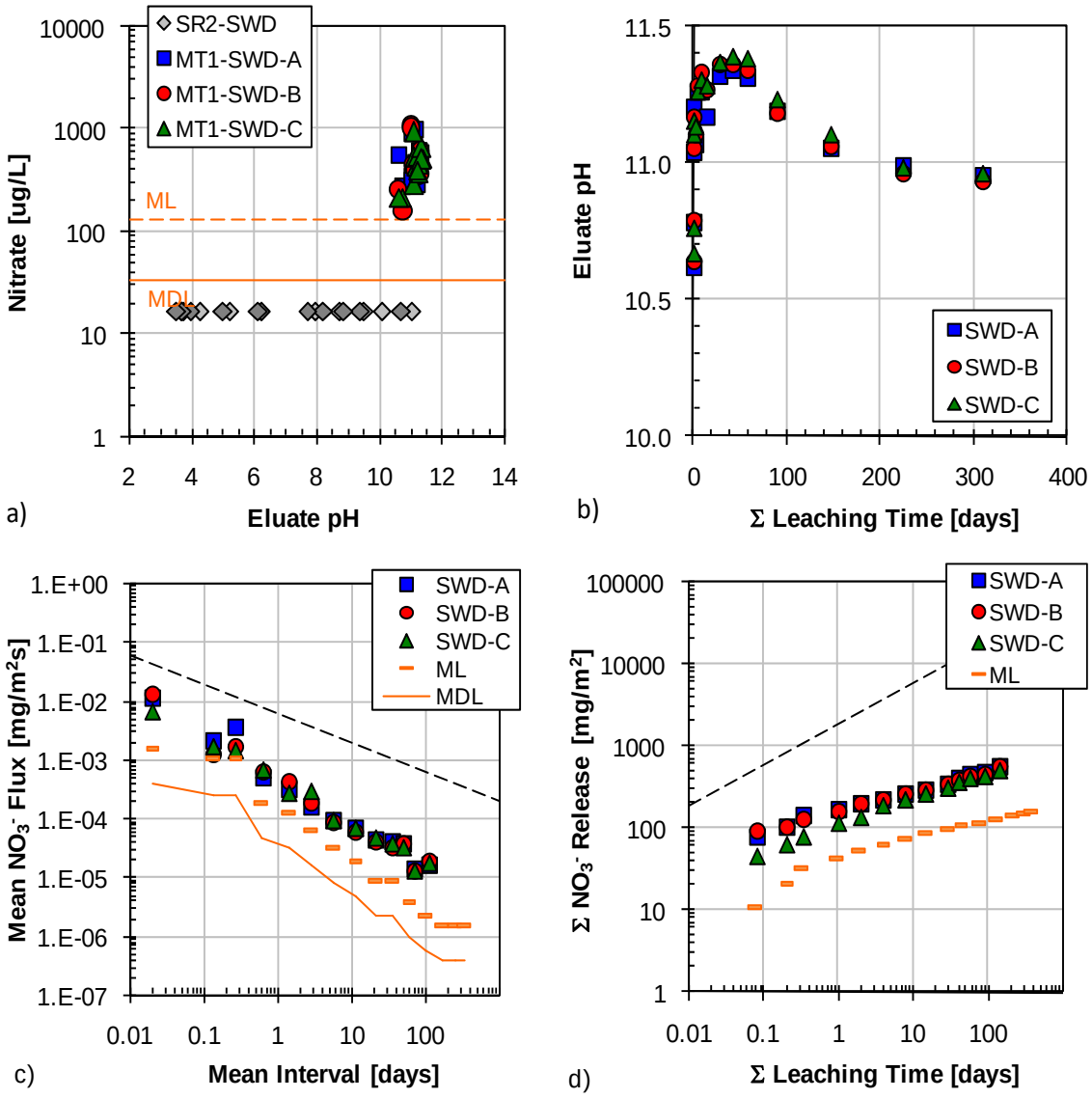

Figure A-49. Nitrate leaching test results from SWD matrix: a) comparison of tank leach test eluants to saturation values (SR02 data) and QA/QC parameters, b) pH evolution in tank leach eluants, c) interval flux from tank leach test in comparison to flux values at the method limit ($t^{-1/2}$ model for AMD shown as dashed line), and d) cumulative mass release ($t^{1/2}$ model for AMD shown as dashed line).

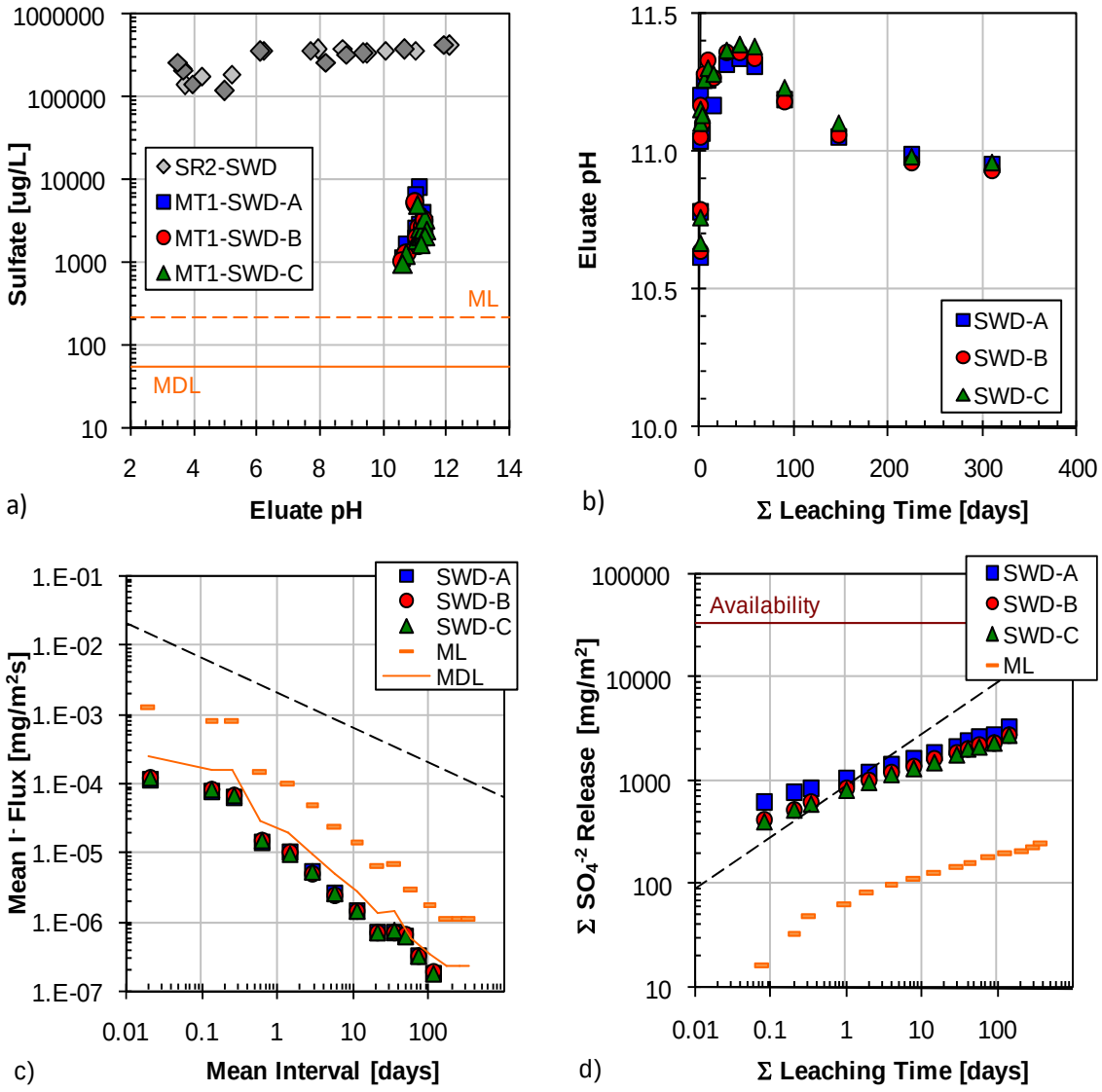

Figure A-50. Sulfate leaching test results from SWD matrix: a) comparison of tank leach test eluants to saturation values (SR02 data) and QA/QC parameters, b) pH evolution in tank leach eluants, c) interval flux from tank leach test in comparison to flux values at the method limit ($t^{-1/2}$ model for AMD shown as dashed line), and d) cumulative mass release ($t^{1/2}$ model for AMD shown as dashed line).

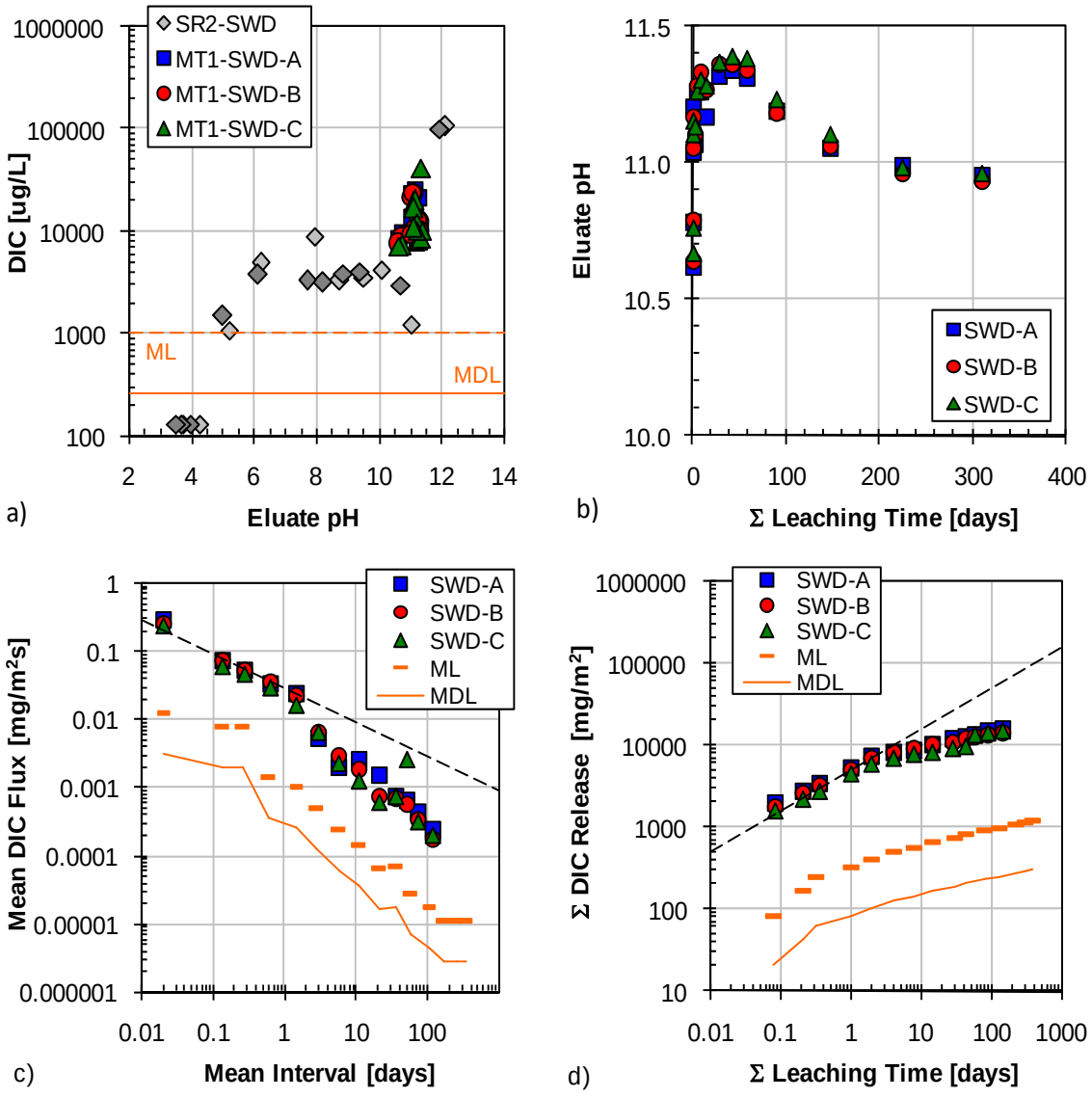

Figure A-51. Dissolved inorganic carbon test results from SWD matrix: a) comparison of tank leach test eluants to saturation values (SR02 data) and QA/QC parameters, b) pH evolution in tank leach eluants, c) interval flux from tank leach test in comparison to flux values at the method limit ($t^{-1/2}$ model for AMD shown as dashed line), and d) cumulative mass release ($t^{1/2}$ model for AMD shown as dashed line).

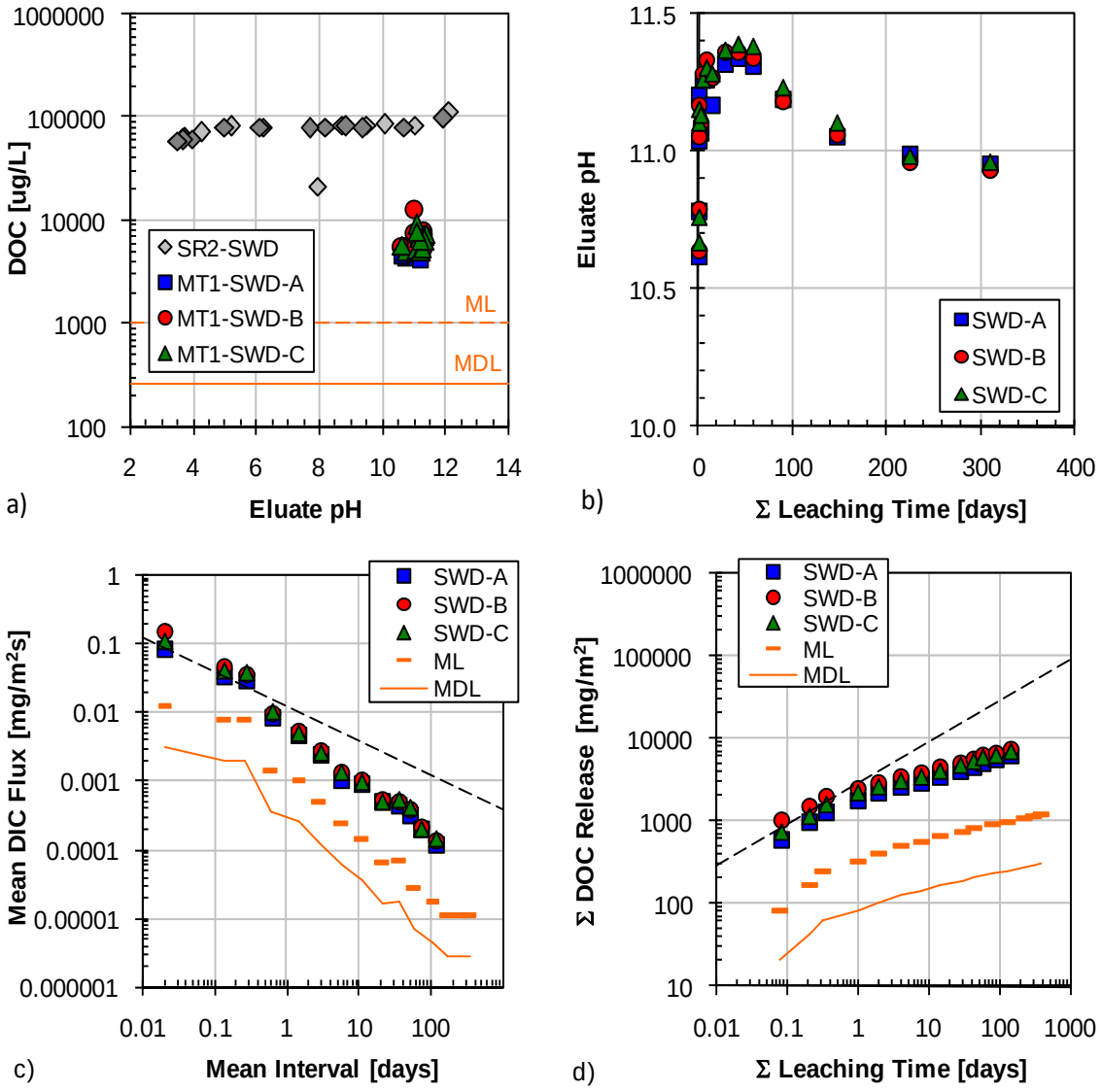

Figure A-52. Dissolved organic carbon leaching test results from SWD matrix: a) comparison of tank leach test eluants to saturation values (SR02 data) and QA/QC parameters, b) pH evolution in tank leach eluants, c) interval flux from tank leach test in comparison to flux values at the method limit ($t^{-1/2}$ model for AMD shown as dashed line), and d) cumulative mass release ($t^{1/2}$ model for AMD shown as dashed line).

Matrix Blank in DI Water (MBD)

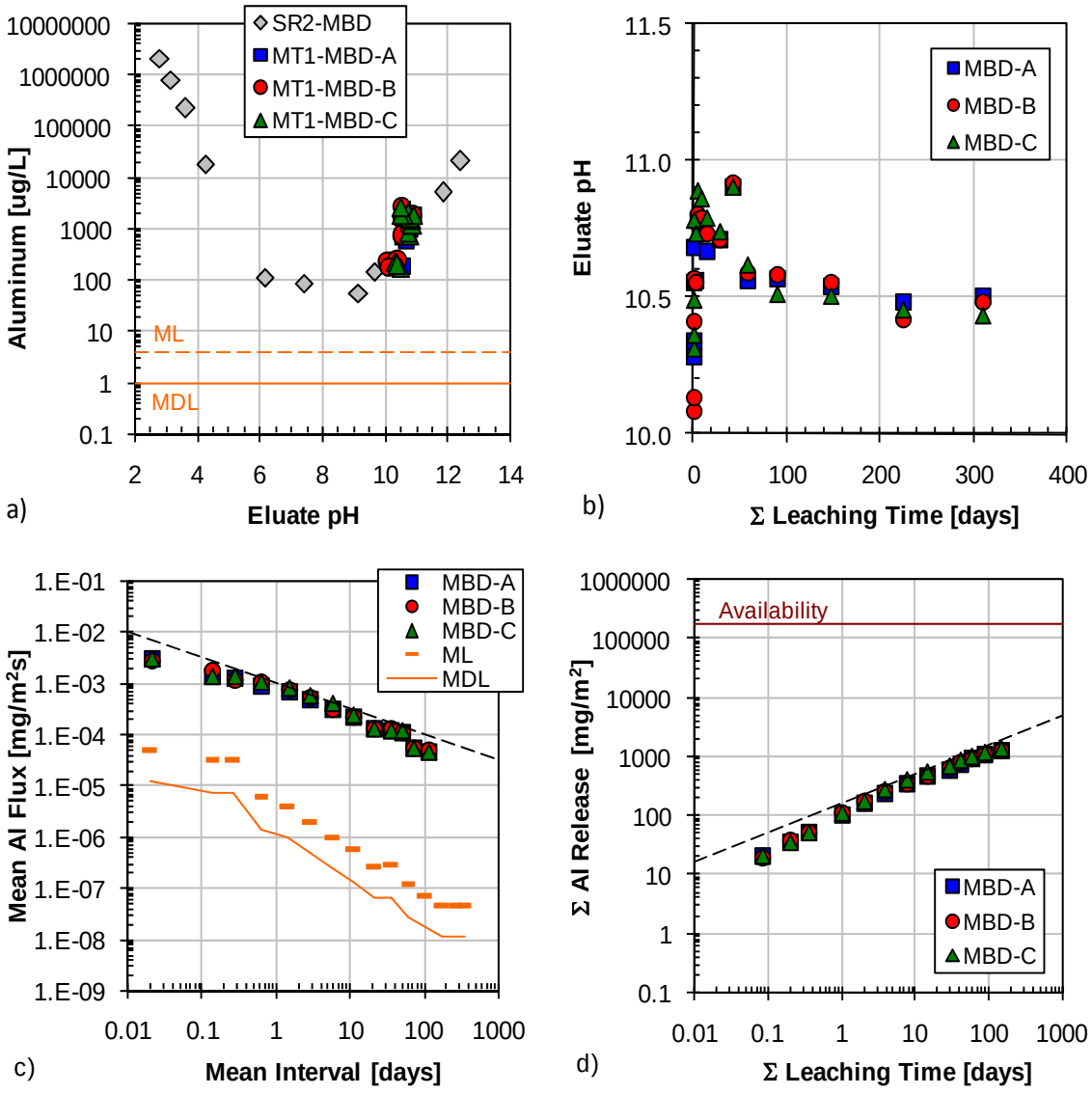

Figure A-53. Aluminum leaching test results from MBD matrix: a) comparison of tank leach test eluants to saturation values (SR02 data) and QA/QC parameters, b) pH evolution in tank leach eluants, c) interval flux from tank leach test in comparison to flux values at the method limit ($t^{-1/2}$ model for AMD shown as dashed line), and d) cumulative mass release ($t^{1/2}$ model for AMD shown as dashed line).

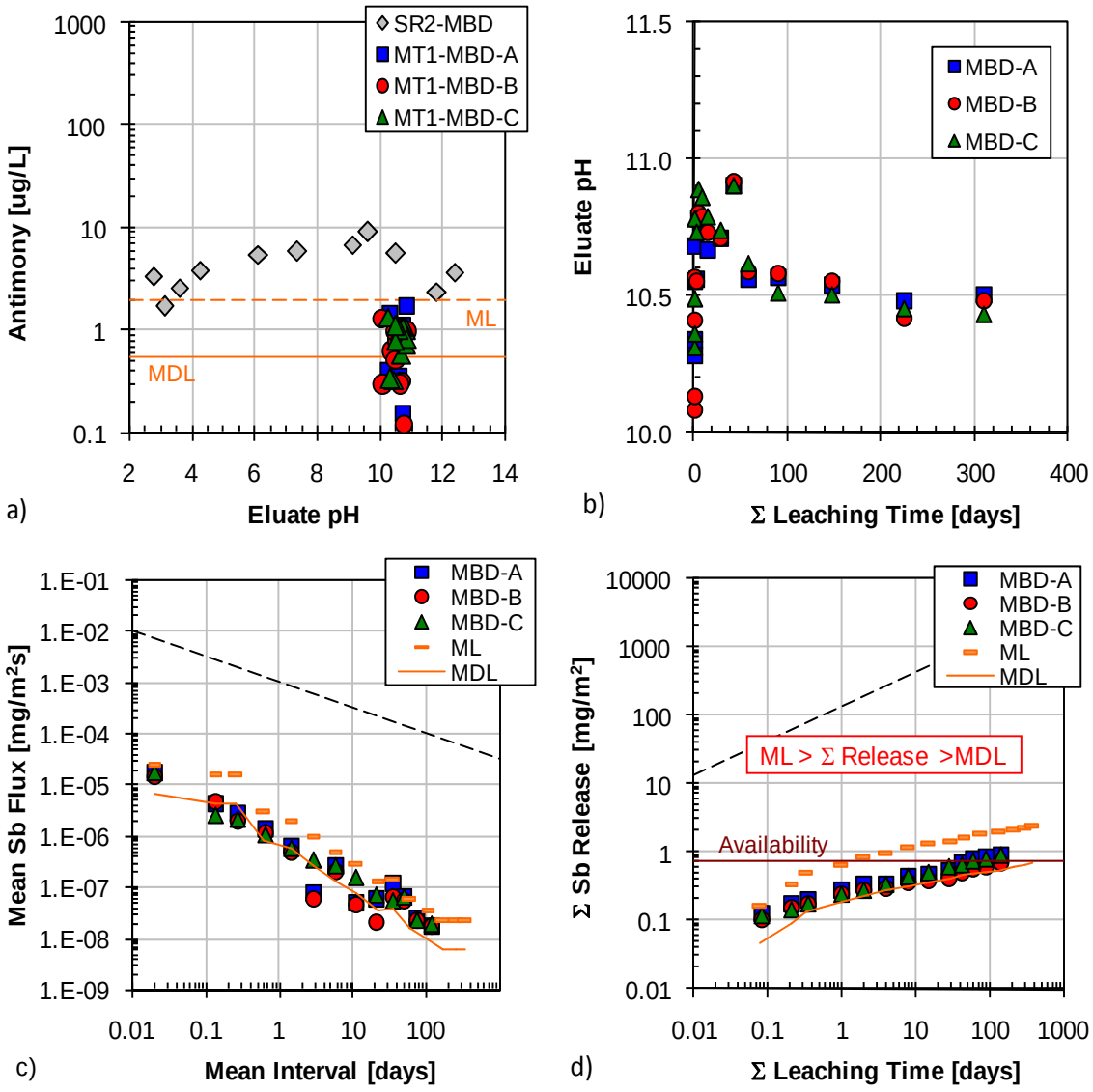

Figure A-54. Antimony leaching test results from MBD matrix: a) comparison of tank leach test eluants to saturation values (SR02 data) and QA/QC parameters, b) pH evolution in tank leach eluants, c) interval flux from tank leach test in comparison to flux values at the method limit ($t^{-1/2}$ model for AMD shown as dashed line), and d) cumulative mass release ($t^{1/2}$ model for AMD shown as dashed line).

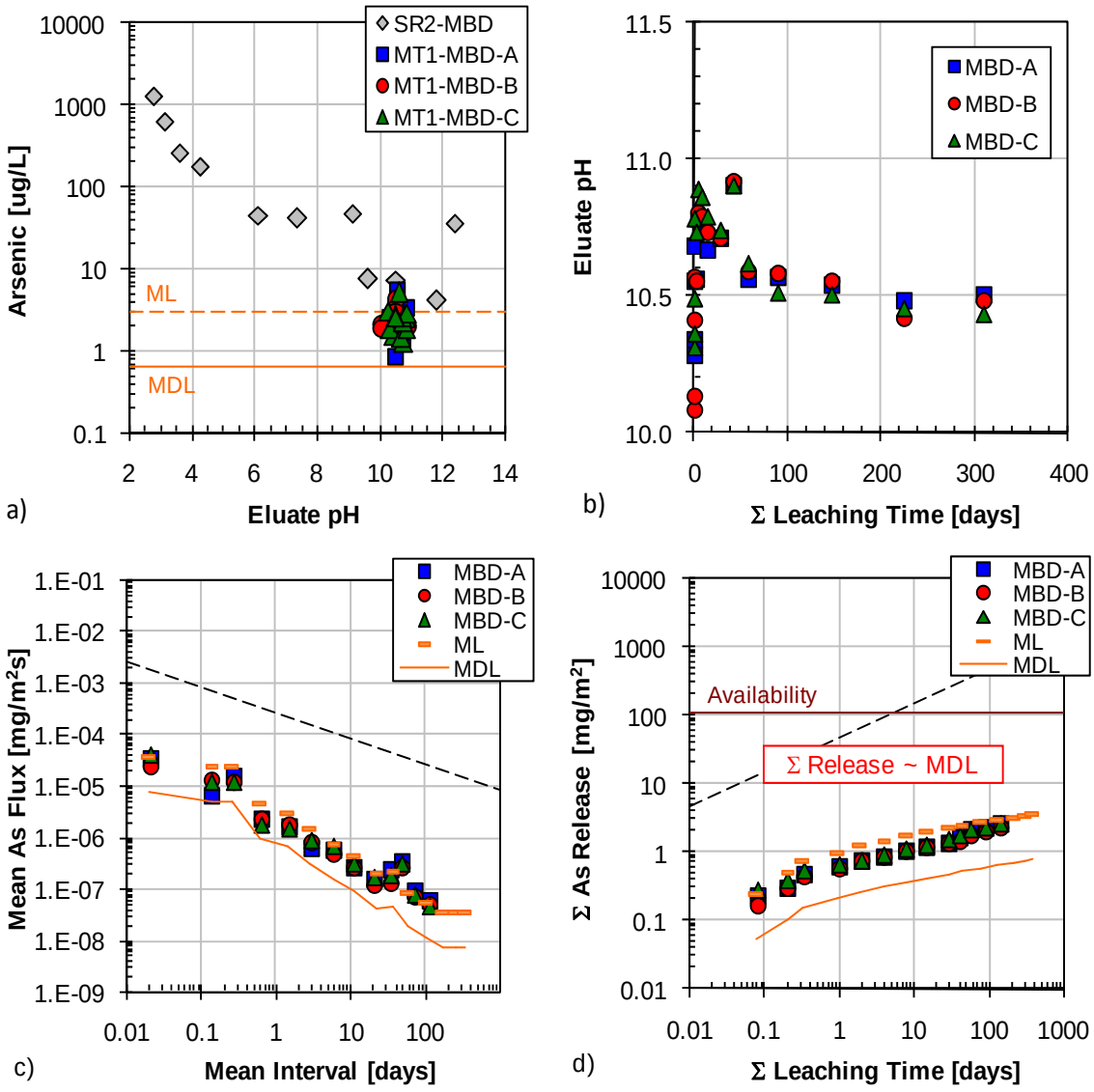

Figure A-55. Arsenic leaching test results from MBD matrix: a) comparison of tank leach test eluants to saturation values (SR02 data) and QA/QC parameters, b) pH evolution in tank leach eluants, c) interval flux from tank leach test in comparison to flux values at the method limit ($t^{-1/2}$ model for AMD shown as dashed line), and d) cumulative mass release ($t^{1/2}$ model for AMD shown as dashed line).

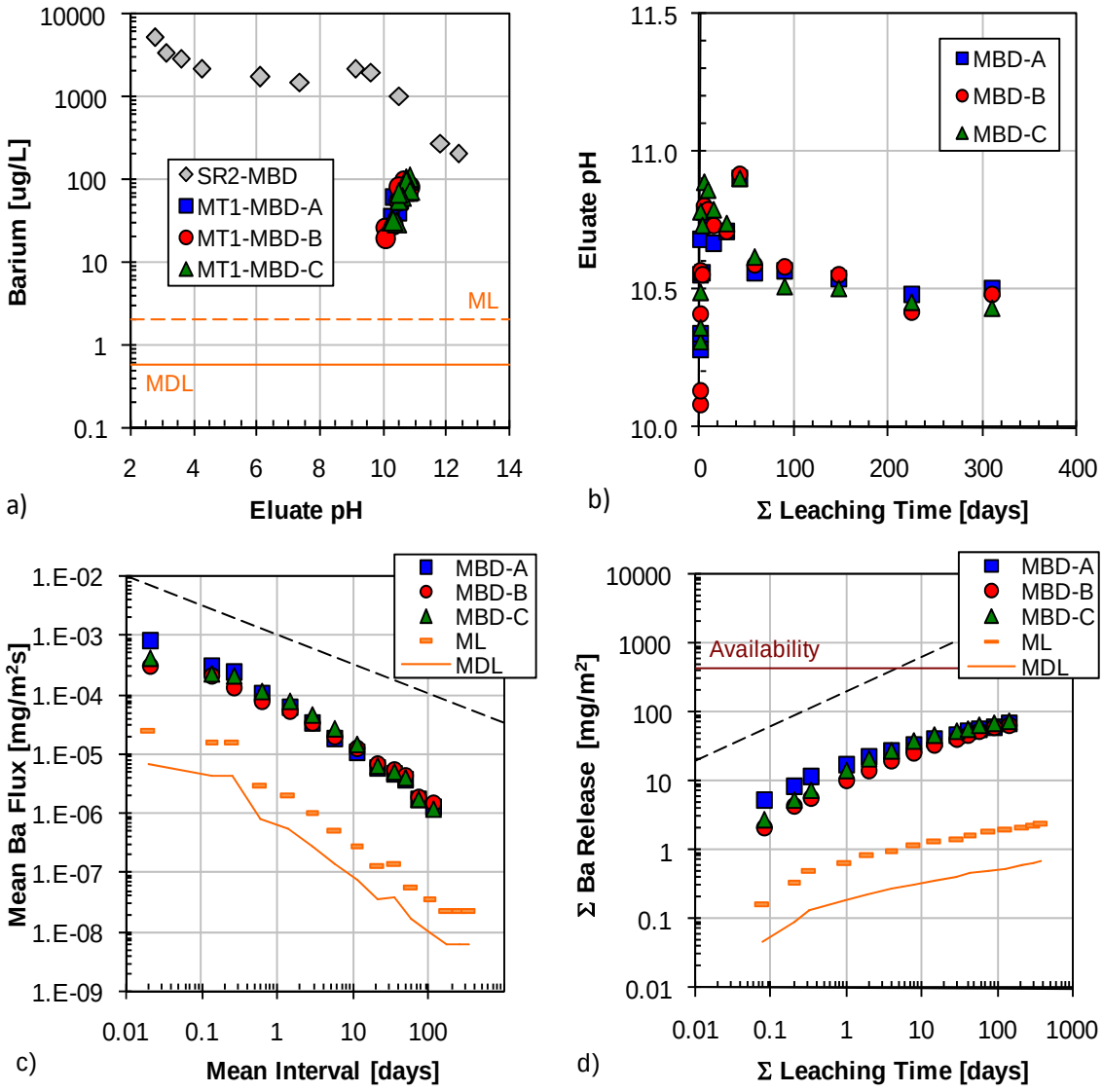

Figure A-56. Barium leaching test results from MBD matrix: a) comparison of tank leach test eluants to saturation values (SR02 data) and QA/QC parameters, b) pH evolution in tank leach eluants, c) interval flux from tank leach test in comparison to flux values at the method limit ($t^{-1/2}$ model for AMD shown as dashed line), and d) cumulative mass release ($t^{1/2}$ model for AMD shown as dashed line).

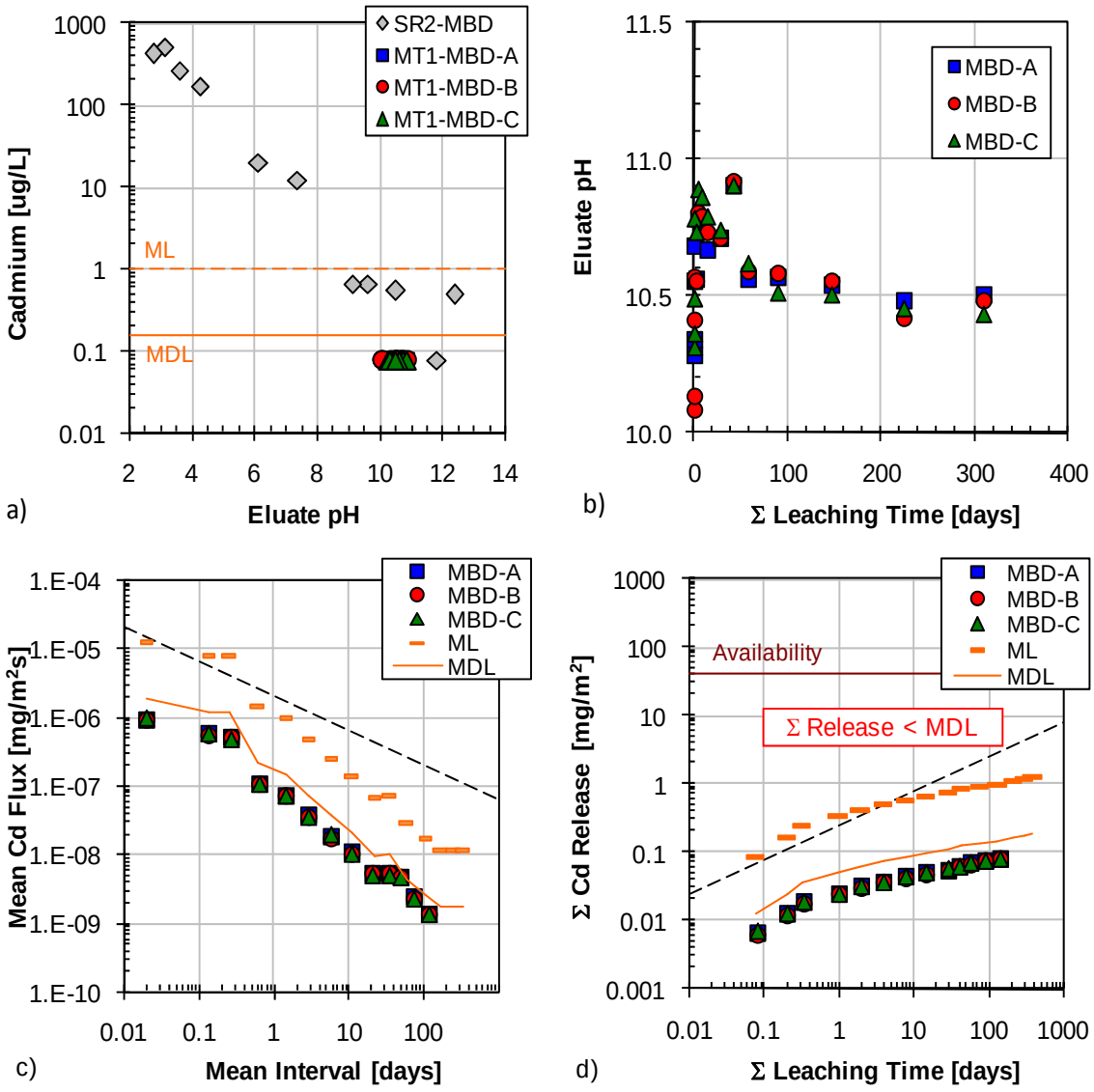

Figure A-57. Cadmium leaching test results from MBD matrix: a) comparison of tank leach test eluants to saturation values (SR02 data) and QA/QC parameters, b) pH evolution in tank leach eluants, c) interval flux from tank leach test in comparison to flux values at the method limit ($t^{-1/2}$ model for AMD shown as dashed line), and d) cumulative mass release ($t^{1/2}$ model for AMD shown as dashed line).

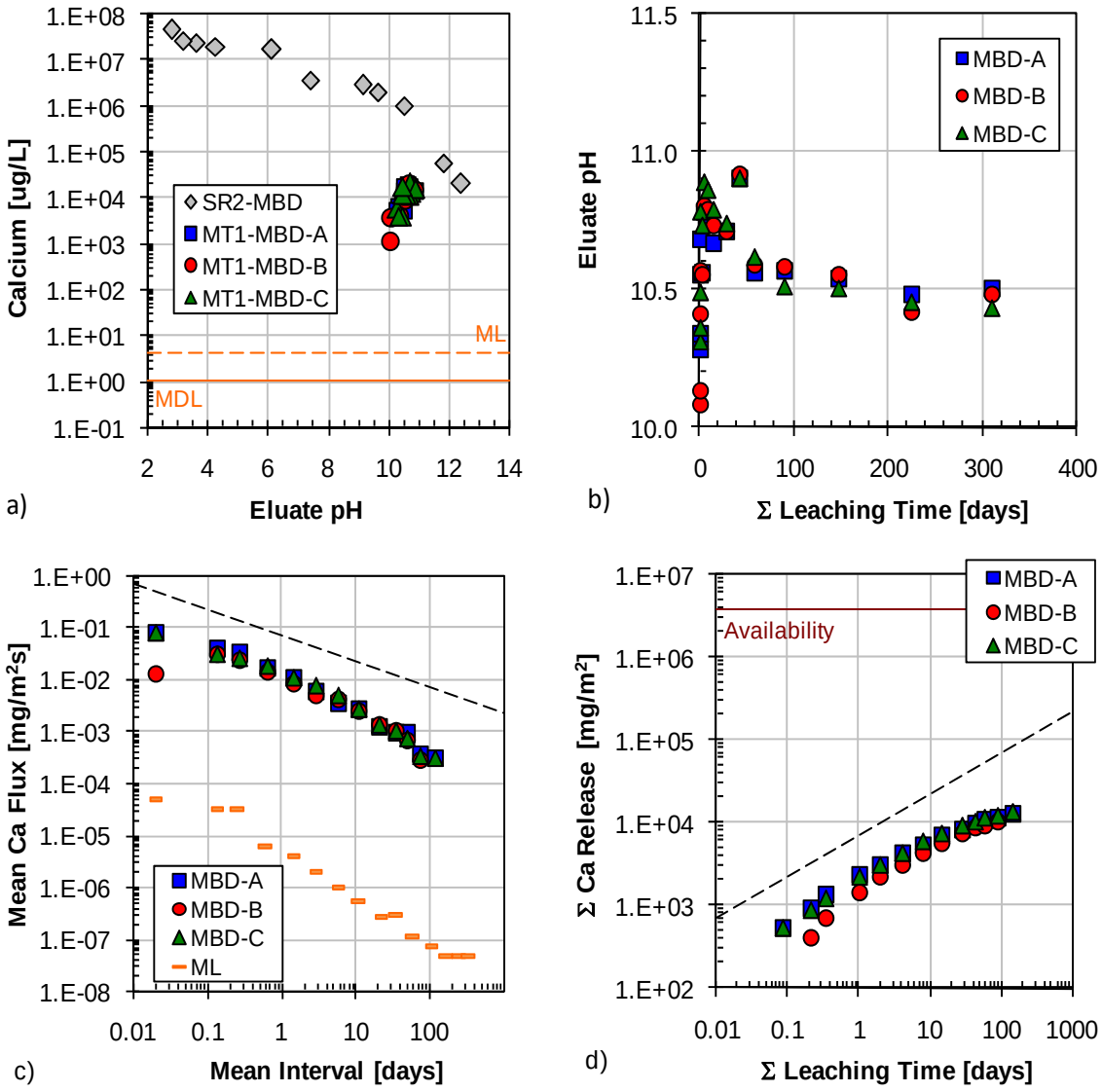

Figure A-58. Calcium leaching test results from MBD matrix: a) comparison of tank leach test eluants to saturation values (SR02 data) and QA/QC parameters, b) pH evolution in tank leach eluants, c) interval flux from tank leach test in comparison to flux values at the method limit ($t^{-1/2}$ model for AMD shown as dashed line), and d) cumulative mass release ($t^{1/2}$ model for AMD shown as dashed line).

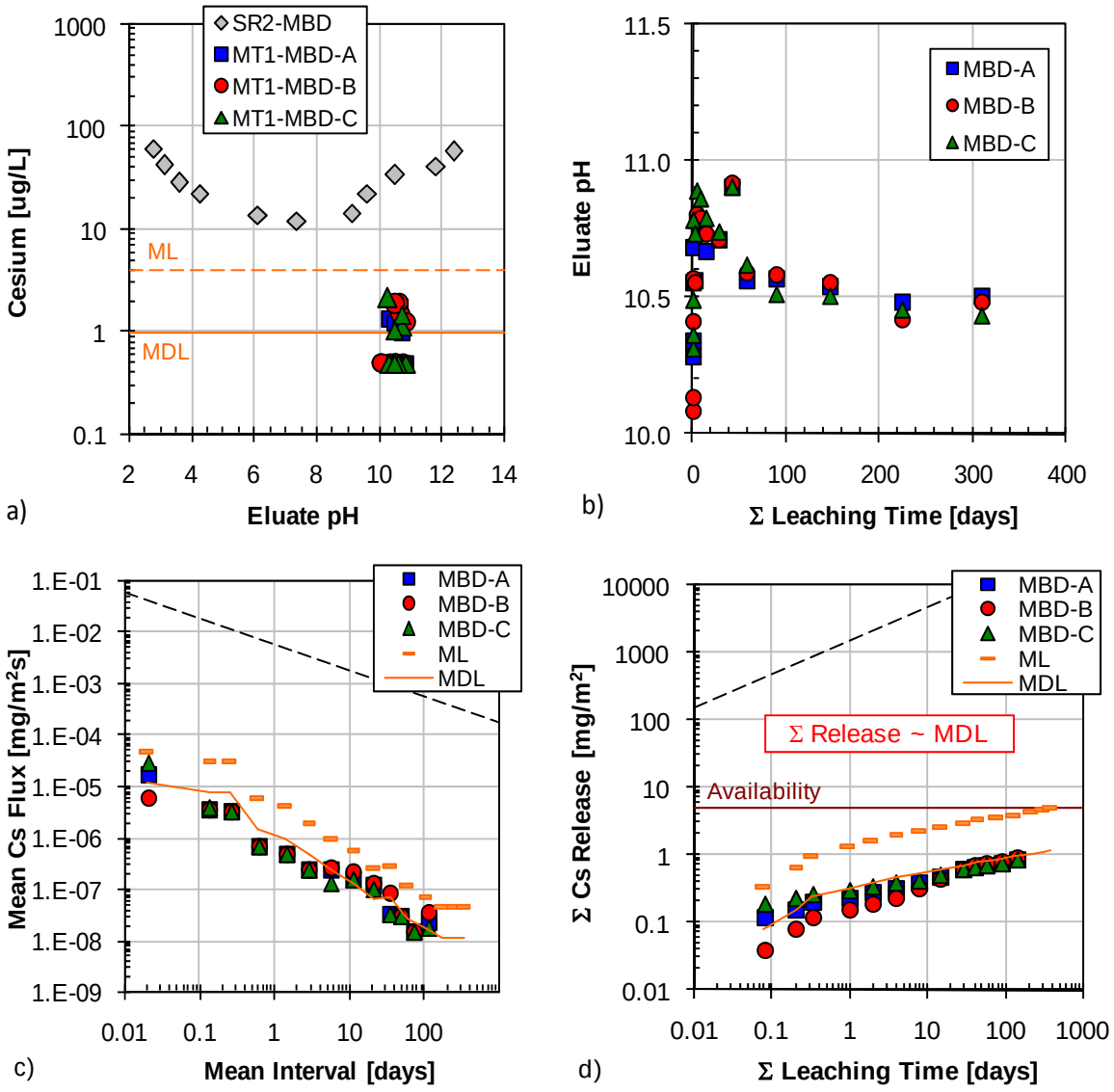

Figure A-59. Cesium leaching test results from MBD matrix: a) comparison of tank leach test eluants to saturation values (SR02 data) and QA/QC parameters, b) pH evolution in tank leach eluants, c) interval flux from tank leach test in comparison to flux values at the method limit ($t^{-1/2}$ model for AMD shown as dashed line), and d) cumulative mass release ($t^{1/2}$ model for AMD shown as dashed line).

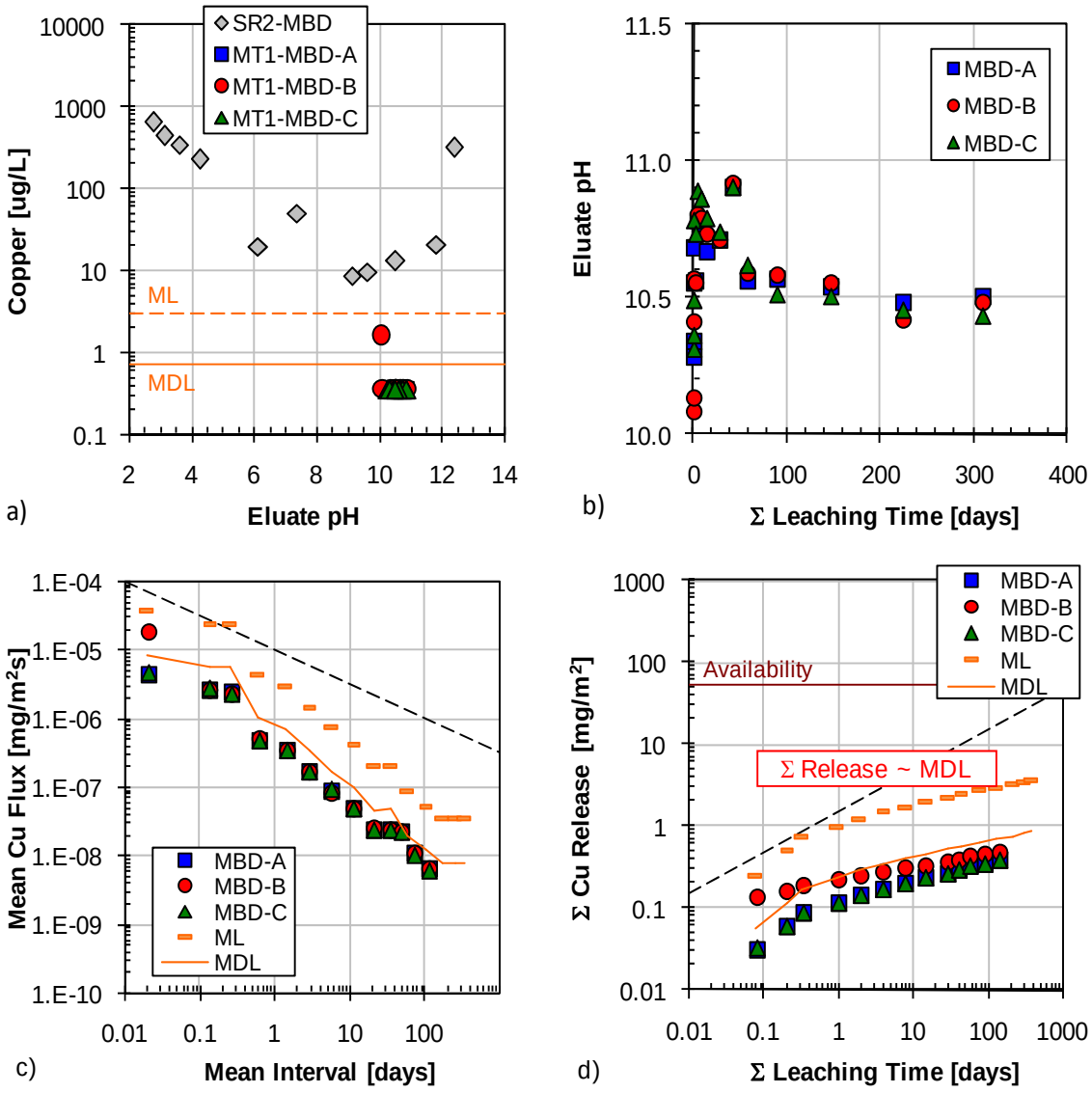

Figure A-60. Copper leaching test results from MBD matrix: a) comparison of tank leach test eluants to saturation values (SR02 data) and QA/QC parameters, b) pH evolution in tank leach eluants, c) interval flux from tank leach test in comparison to flux values at the method limit ($t^{-1/2}$ model for AMD shown as dashed line), and d) cumulative mass release ($t^{1/2}$ model for AMD shown as dashed line).

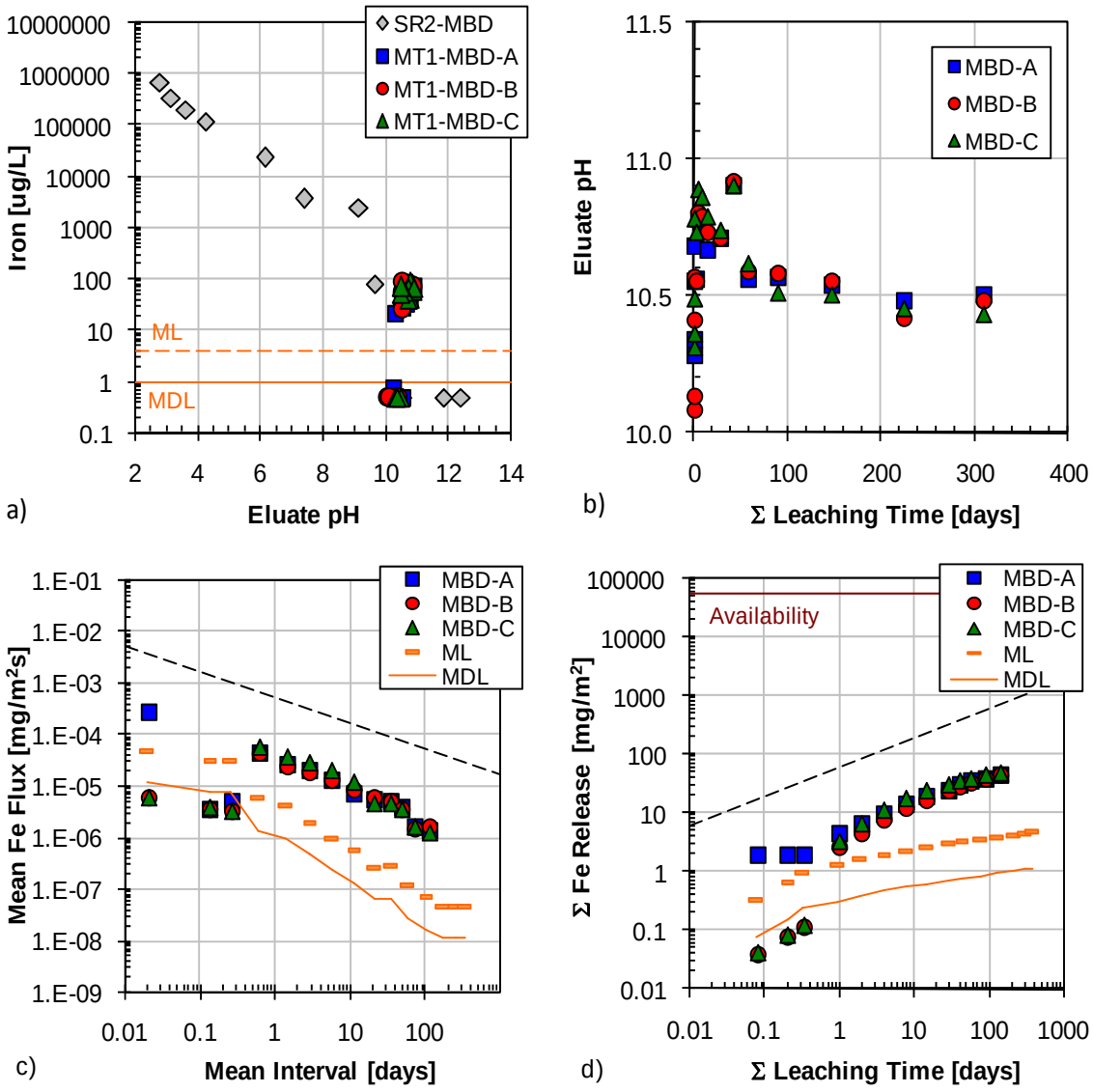

Figure A-61. Iron leaching test results from MBD matrix: a) comparison of tank leach test eluants to saturation values (SR02 data) and QA/QC parameters, b) pH evolution in tank leach eluants, c) interval flux from tank leach test in comparison to flux values at the method limit ($t^{-1/2}$ model for AMD shown as dashed line), and d) cumulative mass release ($t^{1/2}$ model for AMD shown as dashed line).

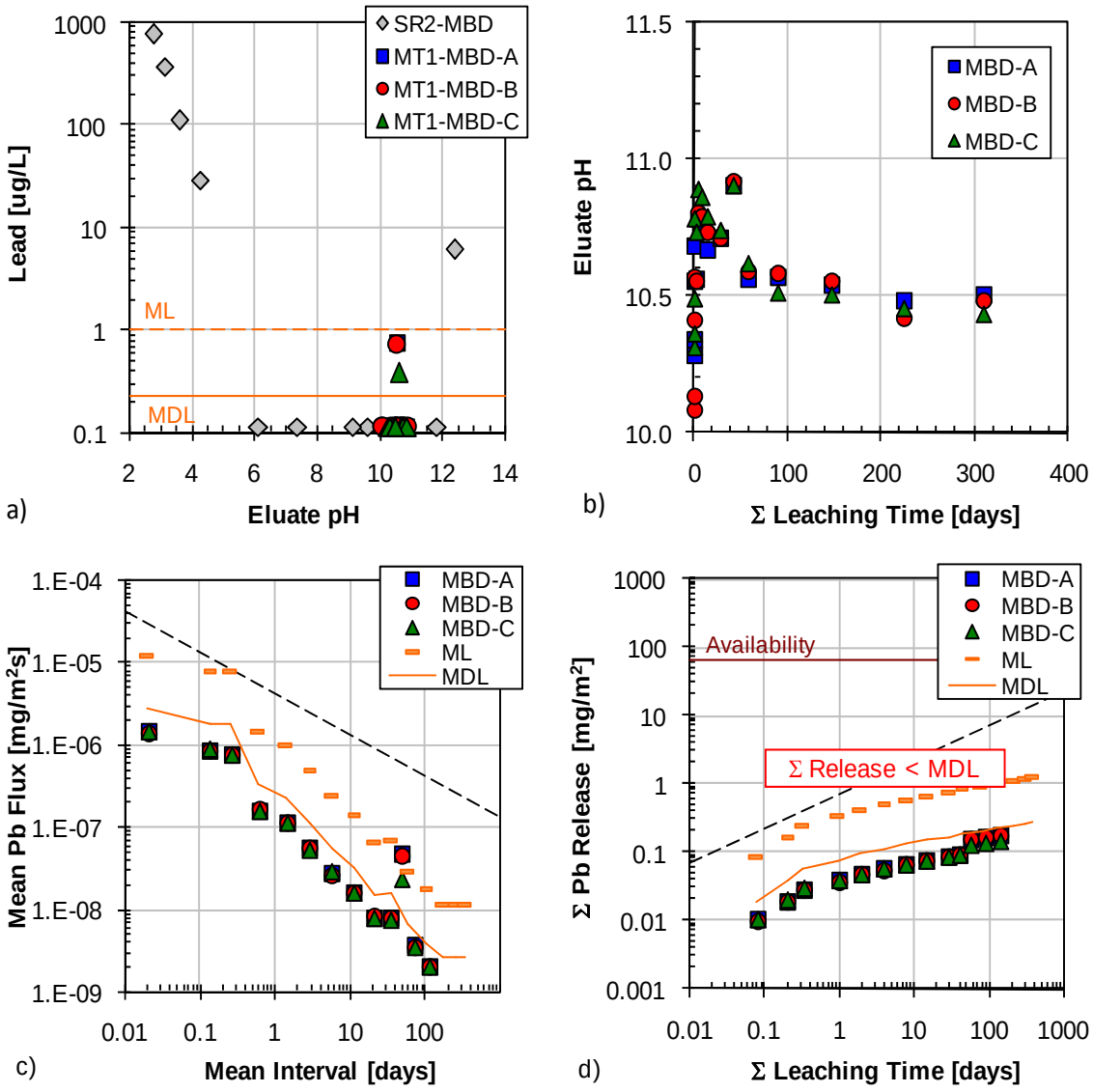

Figure A-62. Lead leaching test results from MBD matrix: a) comparison of tank leach test eluants to saturation values (SR02 data) and QA/QC parameters, b) pH evolution in tank leach eluants, c) interval flux from tank leach test in comparison to flux values at the method limit ($t^{-1/2}$ model for AMD shown as dashed line), and d) cumulative mass release ($t^{1/2}$ model for AMD shown as dashed line).

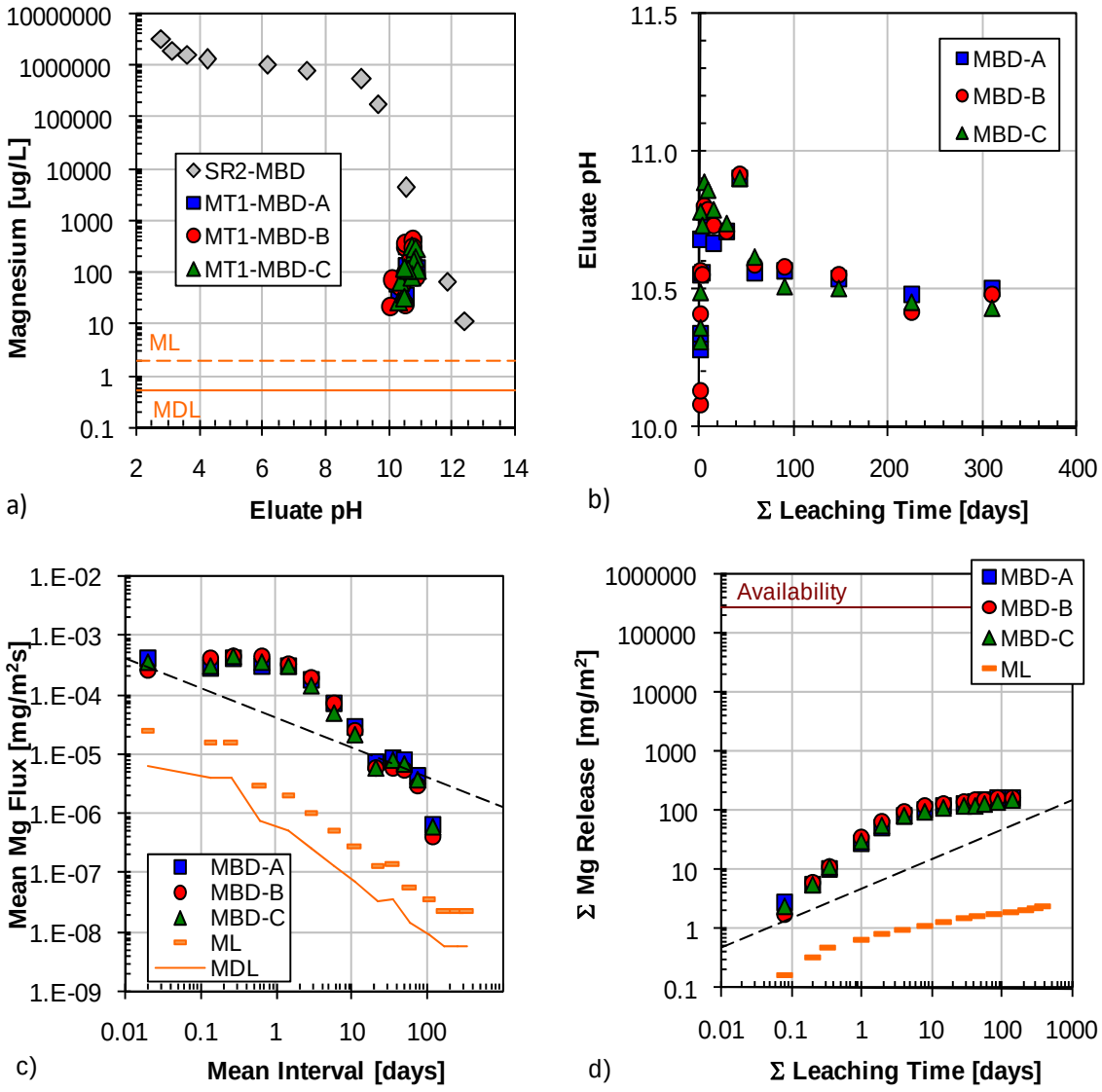

Figure A-63. Magnesium leaching test results from MBD matrix: a) comparison of tank leach test eluants to saturation values (SR02 data) and QA/QC parameters, b) pH evolution in tank leach eluants, c) interval flux from tank leach test in comparison to flux values at the method limit ($t^{-1/2}$ model for AMD shown as dashed line), and d) cumulative mass release ($t^{1/2}$ model for AMD shown as dashed line).

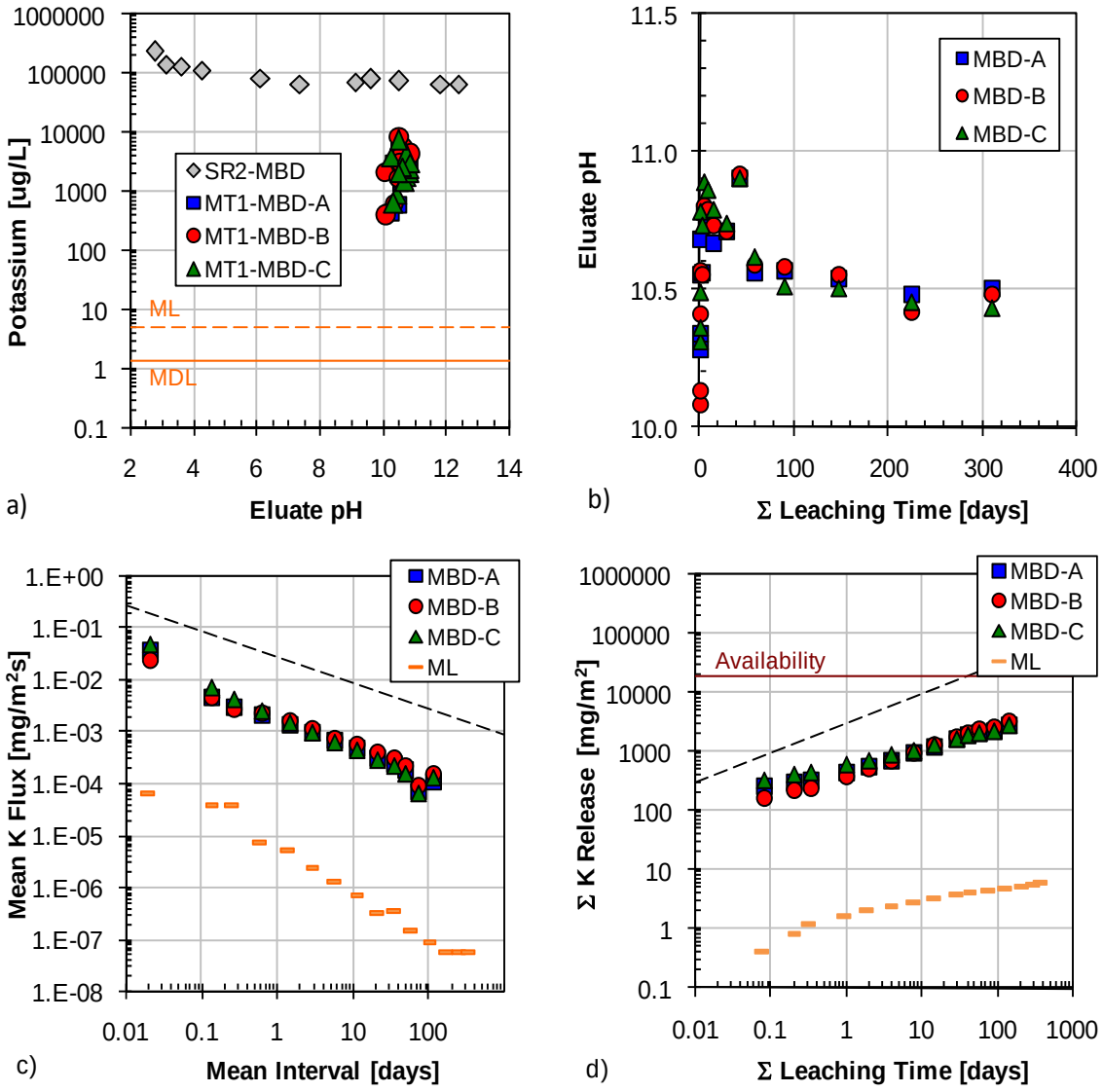

Figure A-64. Potassium leaching test results from MBD matrix: a) comparison of tank leach test eluants to saturation values (SR02 data) and QA/QC parameters, b) pH evolution in tank leach eluants, c) interval flux from tank leach test in comparison to flux values at the method limit ($t^{-1/2}$ model for AMD shown as dashed line), and d) cumulative mass release ($t^{1/2}$ model for AMD shown as dashed line).

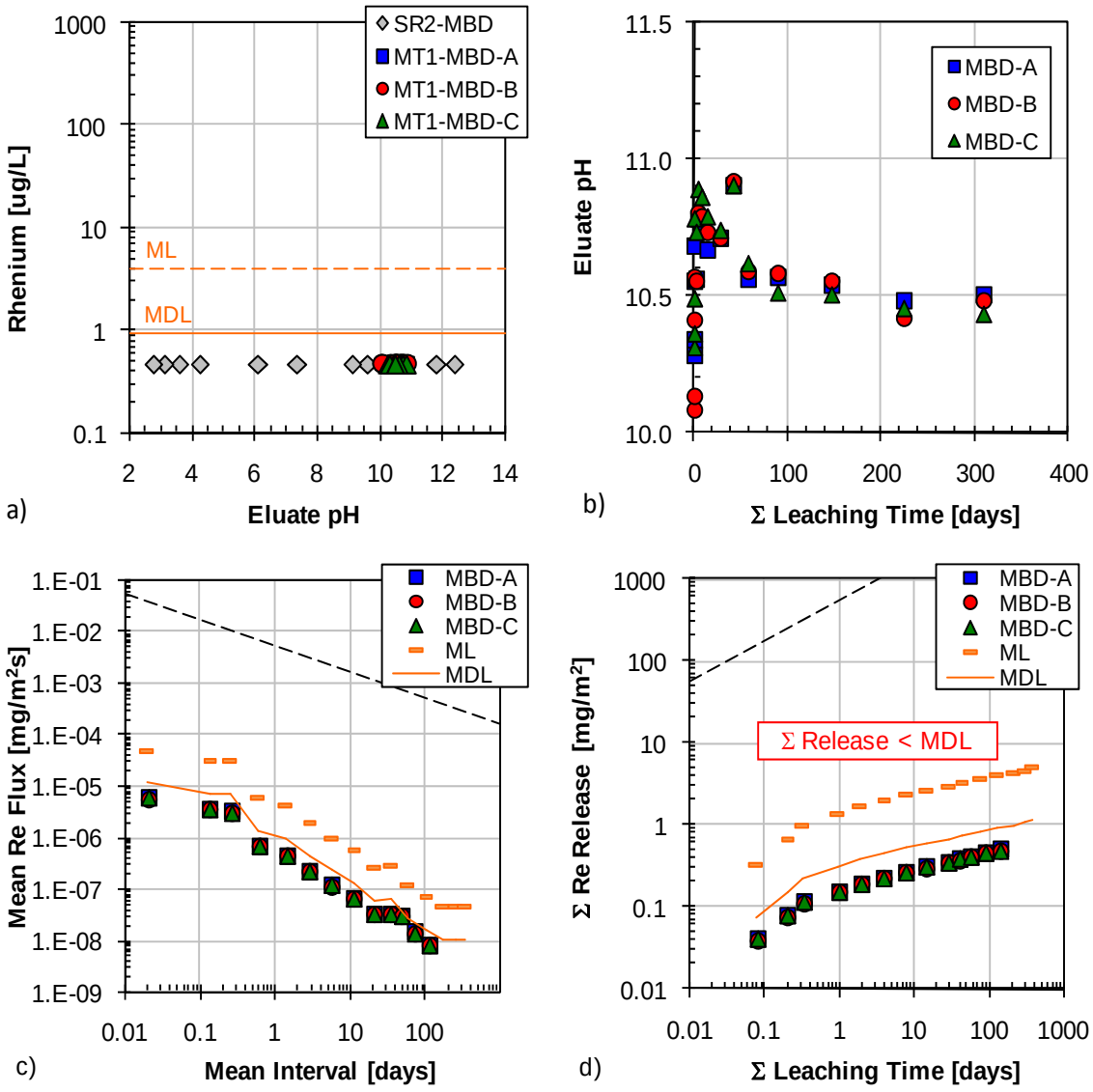

Figure A-65. Rhenium leaching test results from MBD matrix: a) comparison of tank leach test eluants to saturation values (SR02 data) and QA/QC parameters, b) pH evolution in tank leach eluants, c) interval flux from tank leach test in comparison to flux values at the method limit ($t^{-1/2}$ model for AMD shown as dashed line), and d) cumulative mass release ($t^{1/2}$ model for AMD shown as dashed line).

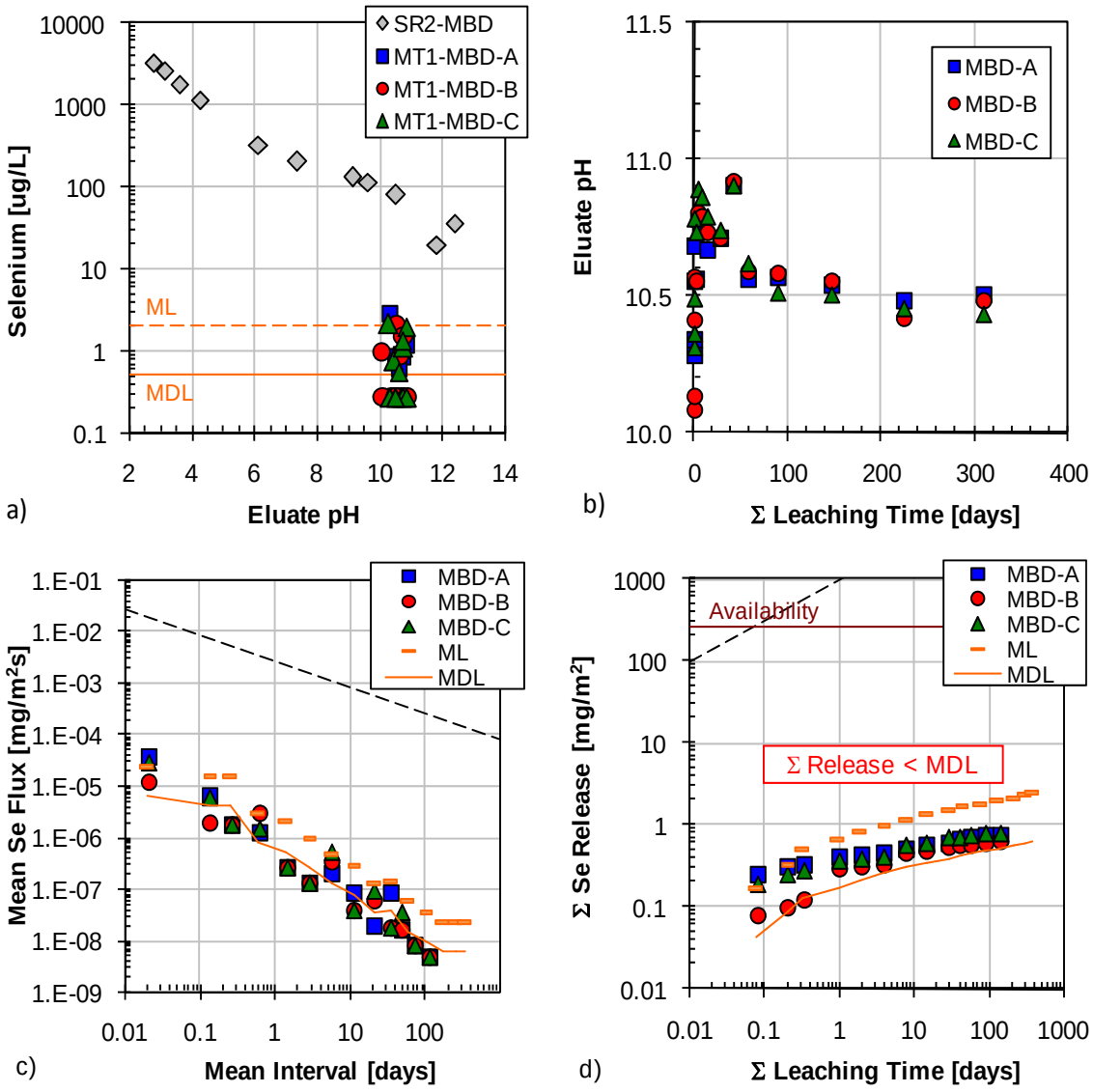

Figure A-66. Selenium leaching test results from MBD matrix: a) comparison of tank leach test eluants to saturation values (SR02 data) and QA/QC parameters, b) pH evolution in tank leach eluants, c) interval flux from tank leach test in comparison to flux values at the method limit ($t^{-1/2}$ model for AMD shown as dashed line), and d) cumulative mass release ($t^{1/2}$ model for AMD shown as dashed line).

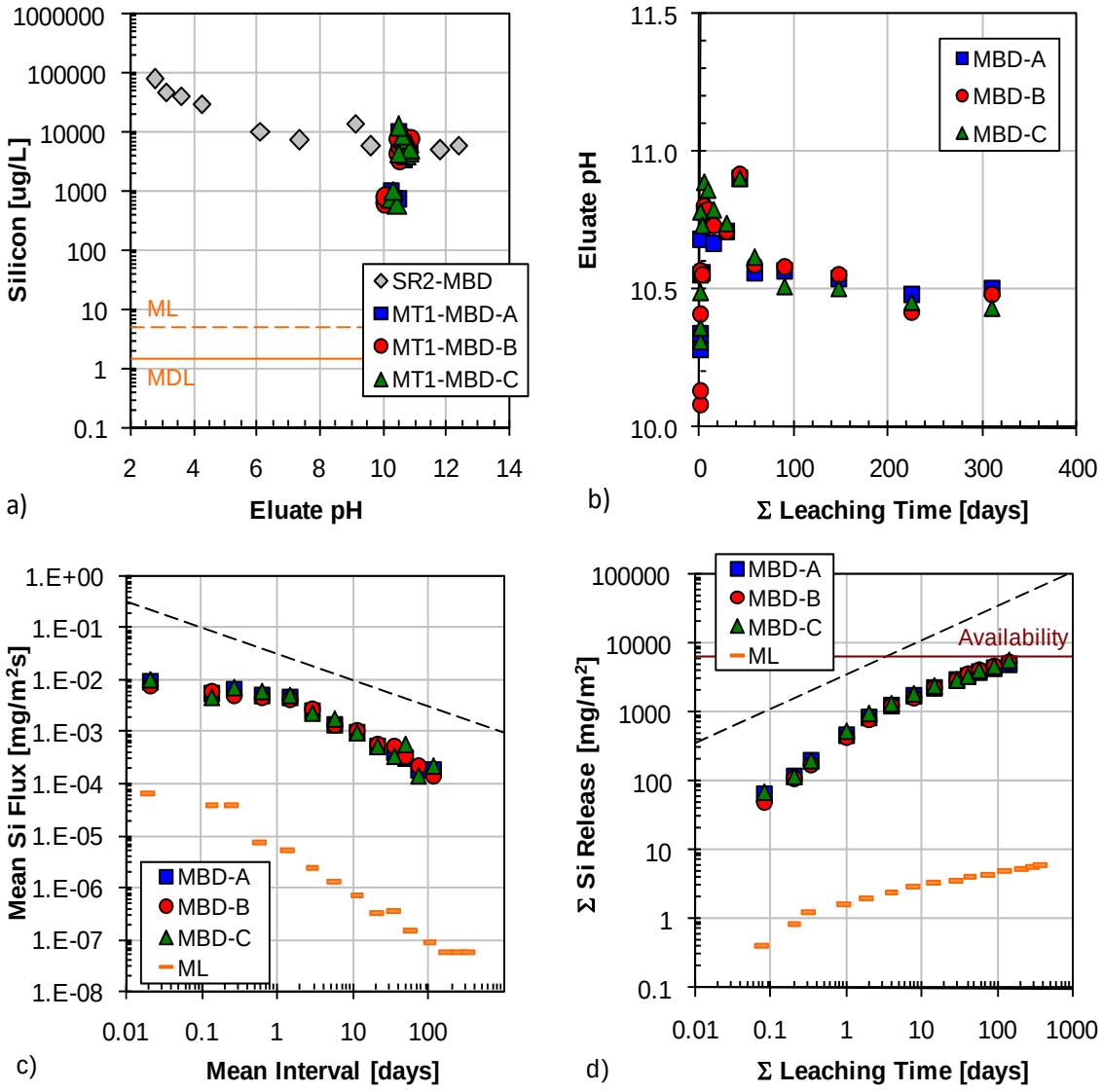

Figure A-67. Silicon leaching test results from MBD matrix: a) comparison of tank leach test eluants to saturation values (SR02 data) and QA/QC parameters, b) pH evolution in tank leach eluants, c) interval flux from tank leach test in comparison to flux values at the method limit ($t^{-1/2}$ model for AMD shown as dashed line), and d) cumulative mass release ($t^{1/2}$ model for AMD shown as dashed line).

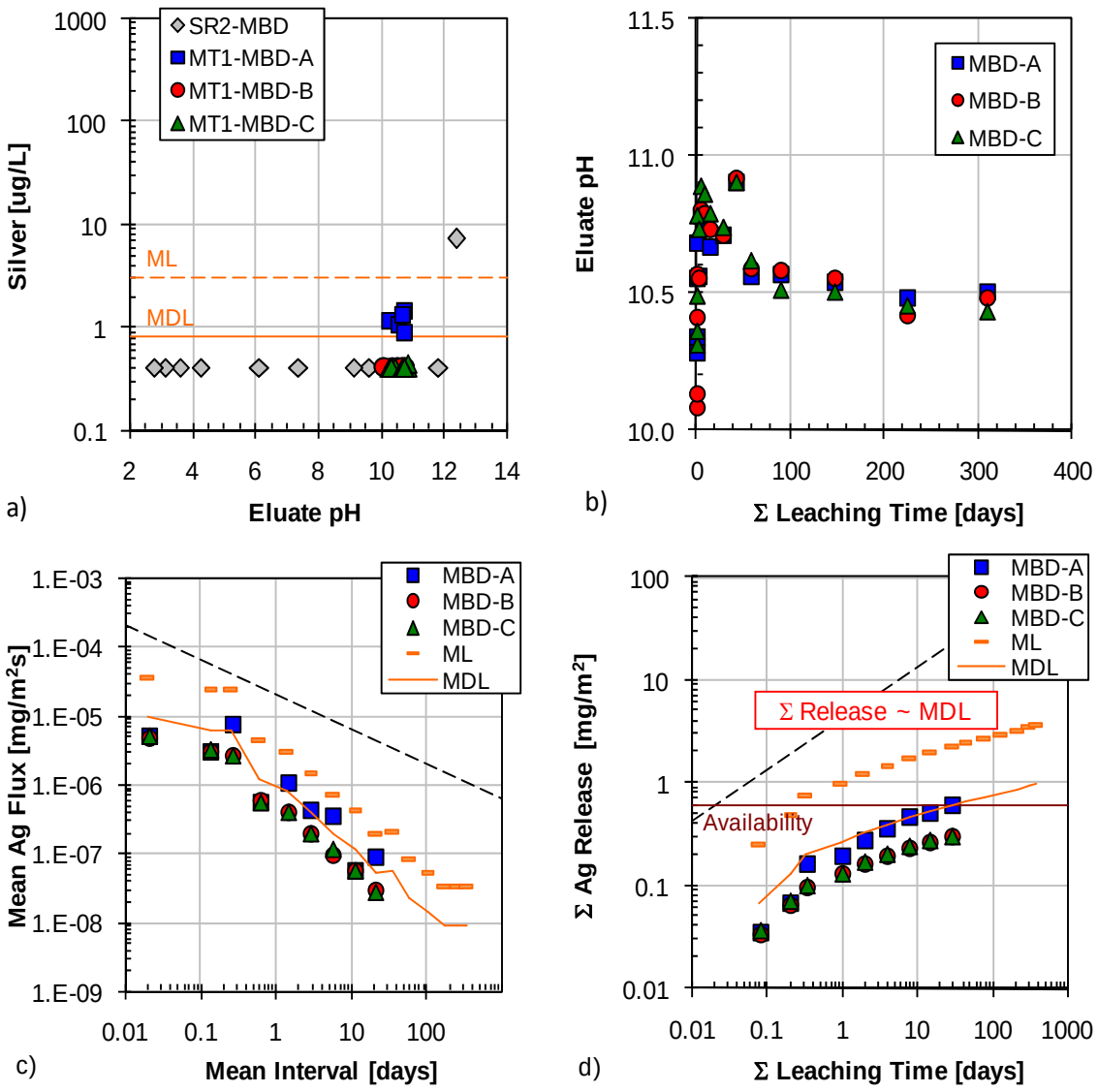

Figure A-68. Silver leaching test results from MBD matrix: a) comparison of tank leach test eluants to saturation values (SR02 data) and QA/QC parameters, b) pH evolution in tank leach eluants, c) interval flux from tank leach test in comparison to flux values at the method limit ($t^{-1/2}$ model for AMD shown as dashed line), and d) cumulative mass release ($t^{1/2}$ model for AMD shown as dashed line).

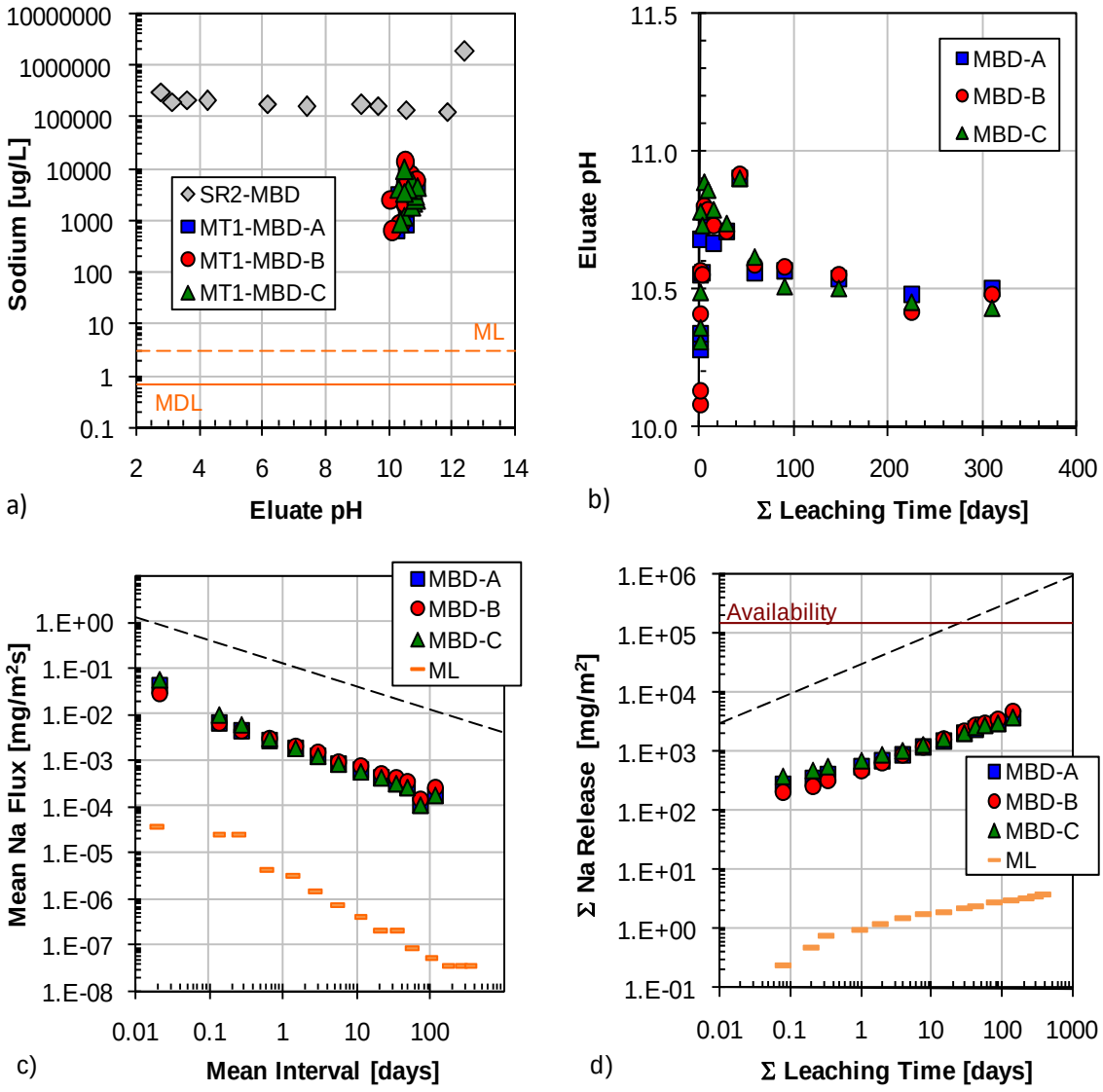

Figure A-69. Sodium leaching test results from MBD matrix: a) comparison of tank leach test eluants to saturation values (SR02 data) and QA/QC parameters, b) pH evolution in tank leach eluants, c) interval flux from tank leach test in comparison to flux values at the method limit ($t^{-1/2}$ model for AMD shown as dashed line), and d) cumulative mass release ($t^{1/2}$ model for AMD shown as dashed line).

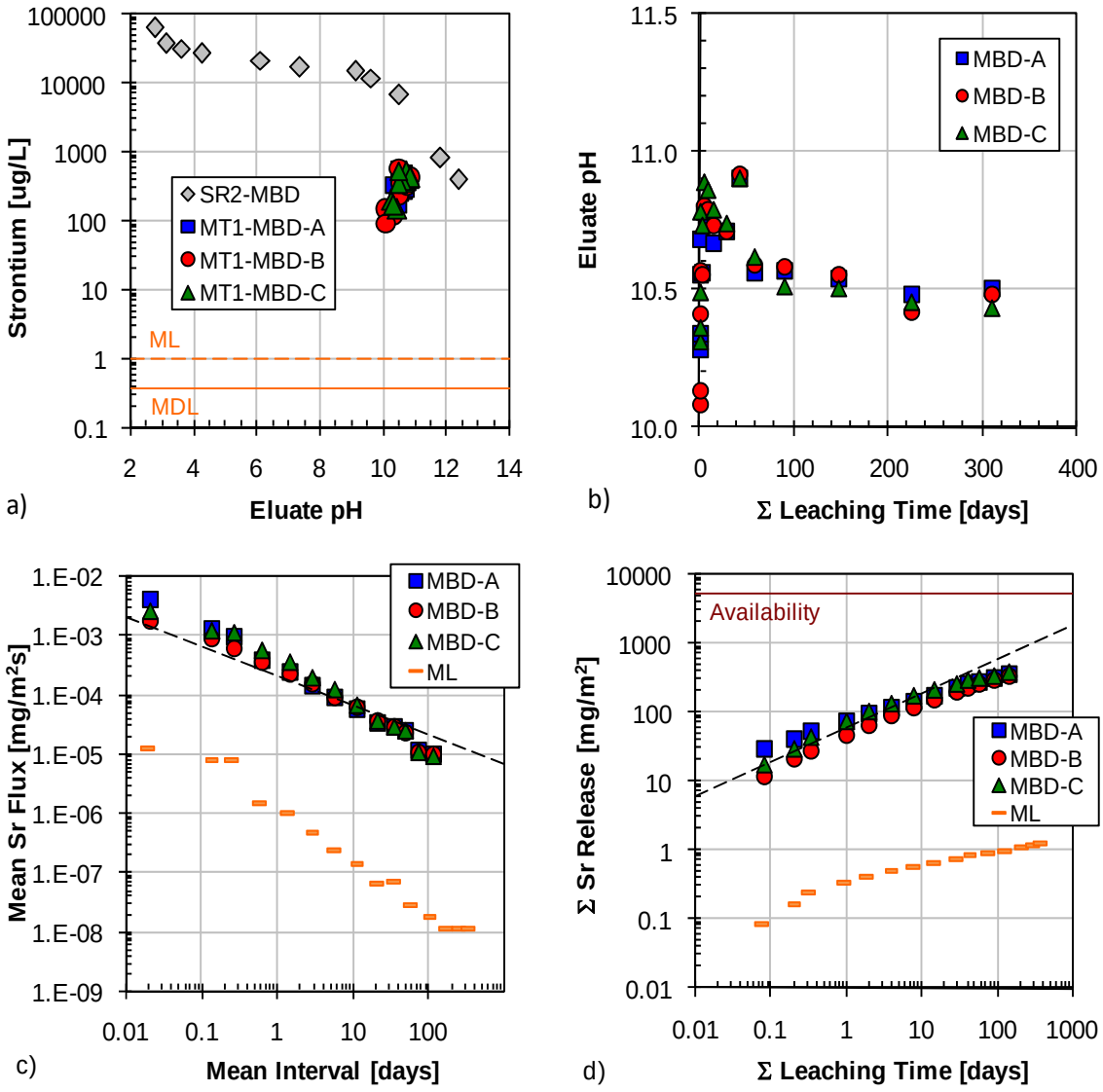

Figure A-70. Strontium leaching test results from MBD matrix: a) comparison of tank leach test eluants to saturation values (SR02 data) and QA/QC parameters, b) pH evolution in tank leach eluants, c) interval flux from tank leach test in comparison to flux values at the method limit ($t^{-1/2}$ model for AMD shown as dashed line), and d) cumulative mass release ($t^{1/2}$ model for AMD shown as dashed line).

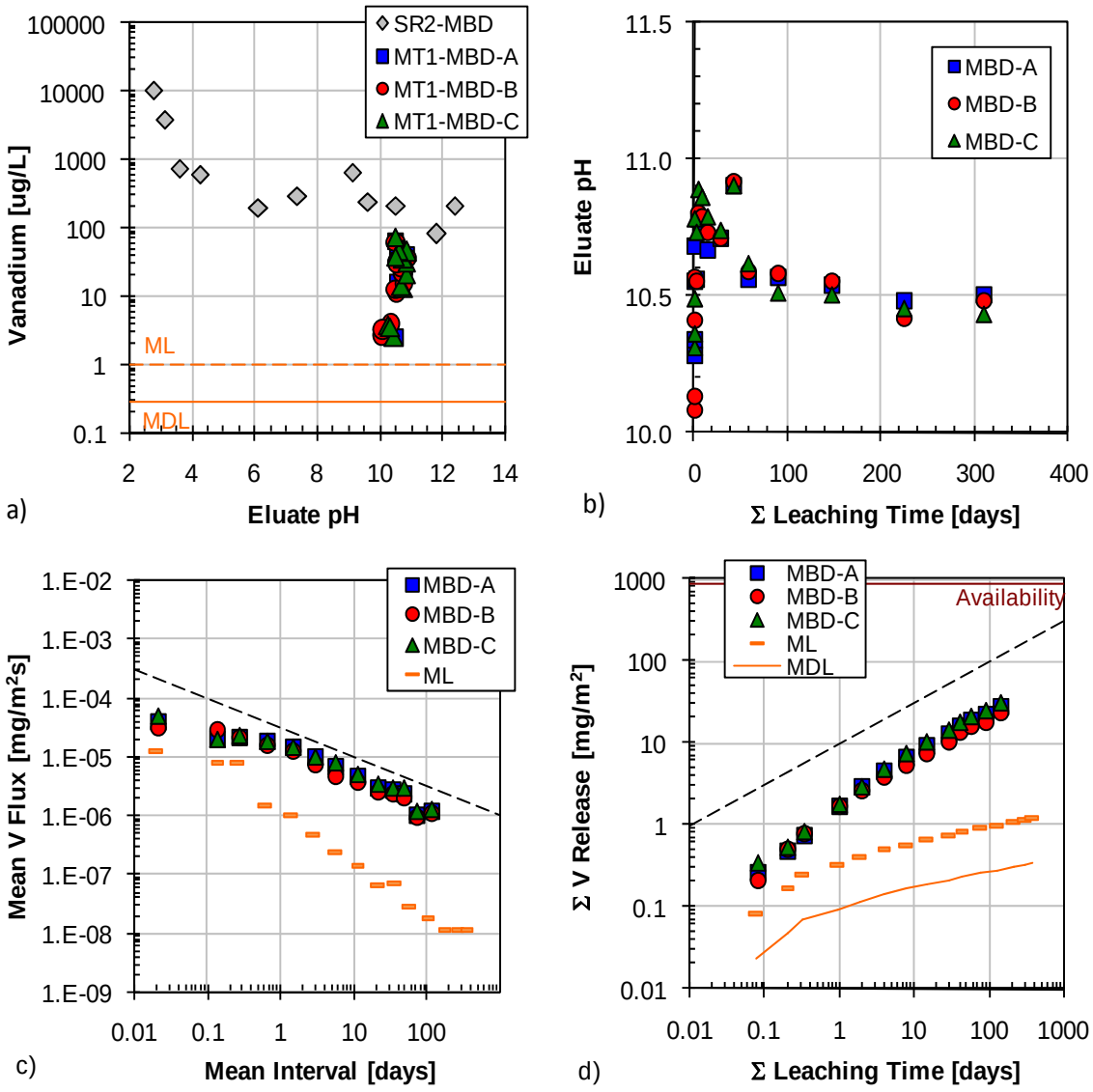

Figure A-71. Vanadium leaching test results from MBD matrix: a) comparison of tank leach test eluants to saturation values (SR02 data) and QA/QC parameters, b) pH evolution in tank leach eluants, c) interval flux from tank leach test in comparison to flux values at the method limit ($t^{-1/2}$ model for AMD shown as dashed line), and d) cumulative mass release ($t^{1/2}$ model for AMD shown as dashed line).

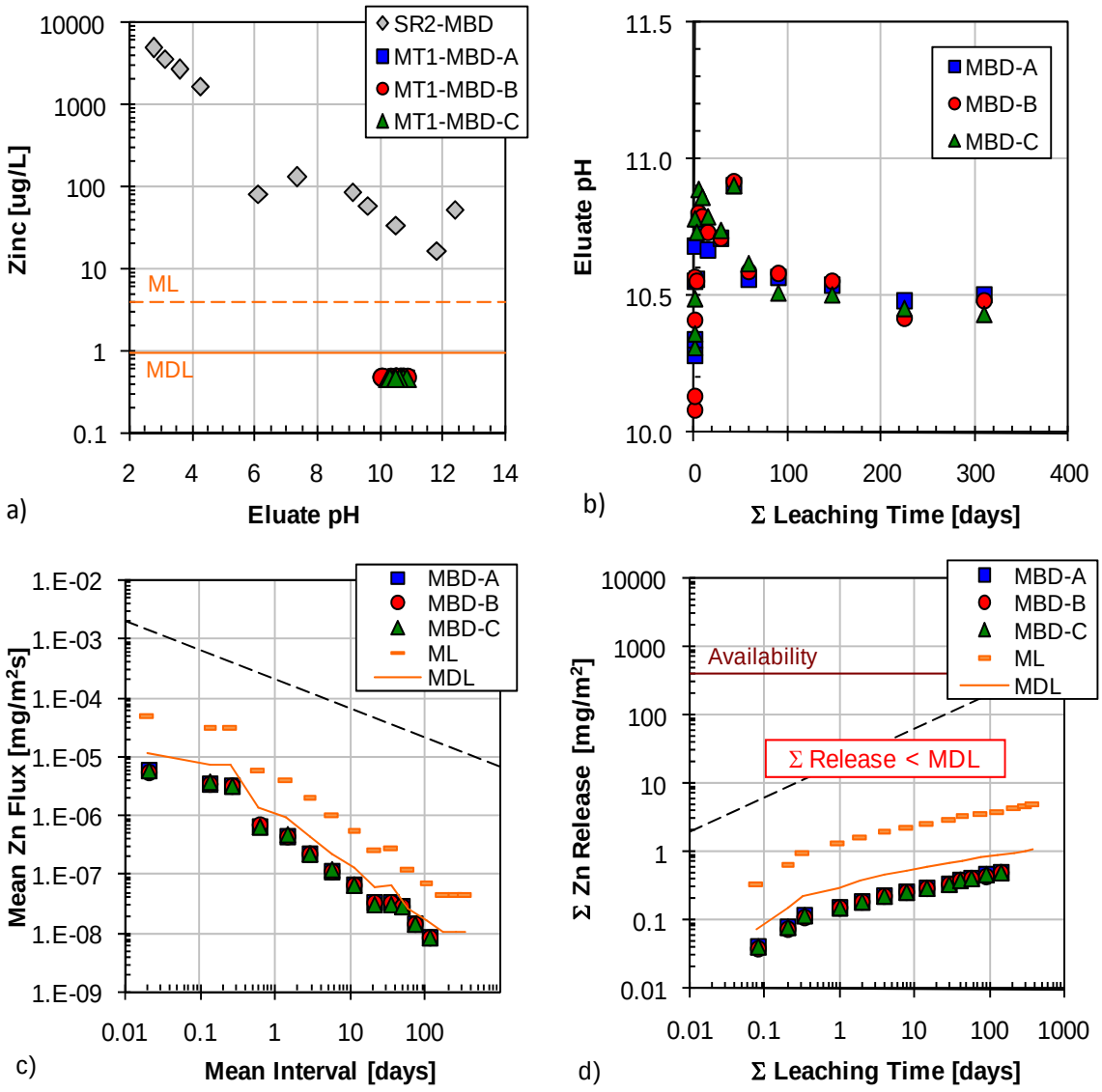

Figure A-72. Zinc leaching test results from MBD matrix: a) comparison of tank leach test eluants to saturation values (SR02 data) and QA/QC parameters, b) pH evolution in tank leach eluants, c) interval flux from tank leach test in comparison to flux values at the method limit ($t^{-1/2}$ model for AMD shown as dashed line), and d) cumulative mass release ($t^{1/2}$ model for AMD shown as dashed line).

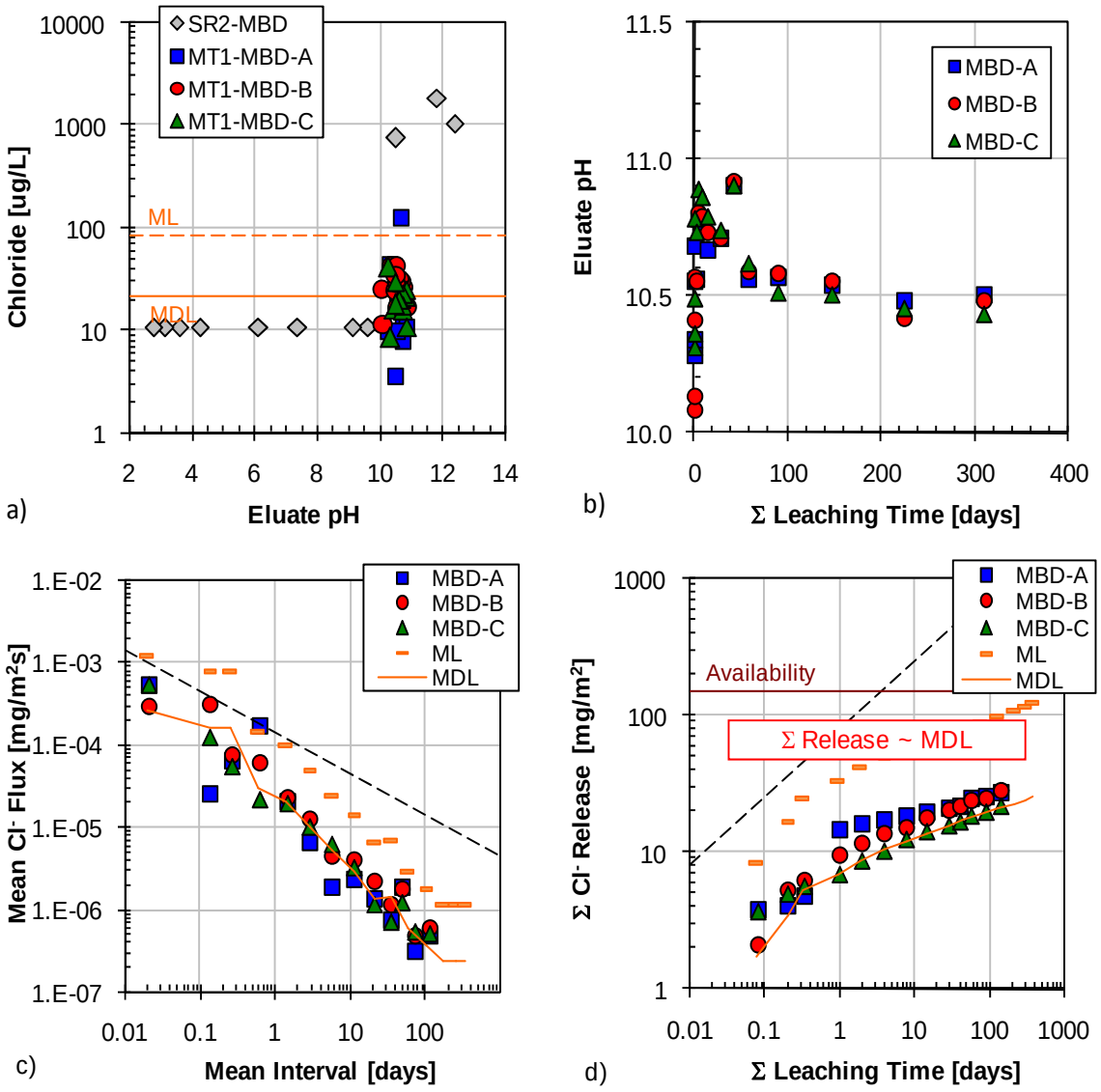

Figure A-73. Chloride leaching test results from MBD matrix: a) comparison of tank leach test eluants to saturation values (SR02 data) and QA/QC parameters, b) pH evolution in tank leach eluants, c) interval flux from tank leach test in comparison to flux values at the method limit ($t^{-1/2}$ model for AMD shown as dashed line), and d) cumulative mass release ($t^{1/2}$ model for AMD shown as dashed line).

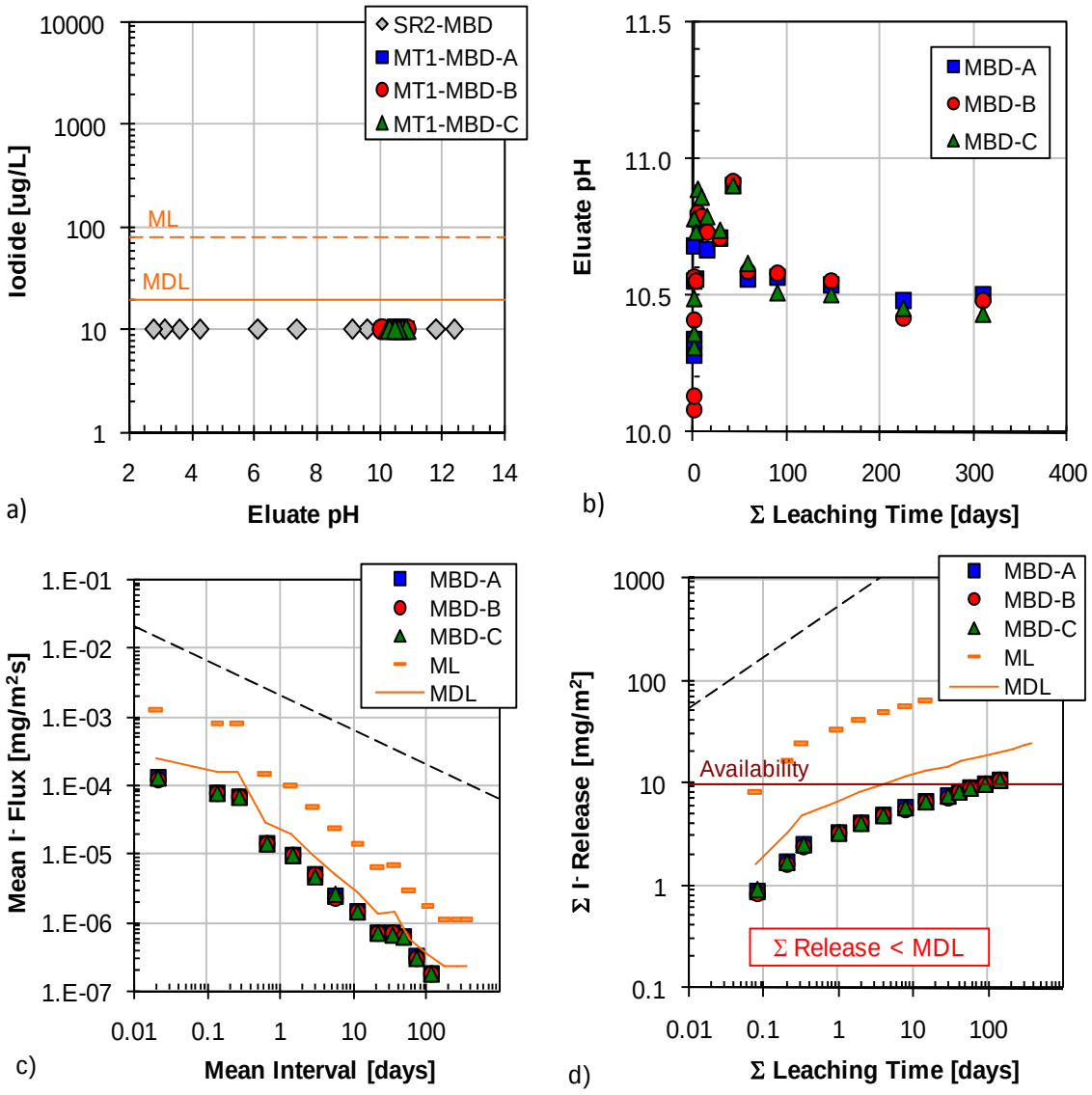

Figure A-74. Iodide leaching test results from MBD matrix: a) comparison of tank leach test eluants to saturation values (SR02 data) and QA/QC parameters, b) pH evolution in tank leach eluants, c) interval flux from tank leach test in comparison to flux values at the method limit ($t^{-1/2}$ model for AMD shown as dashed line), and d) cumulative mass release ($t^{1/2}$ model for AMD shown as dashed line).

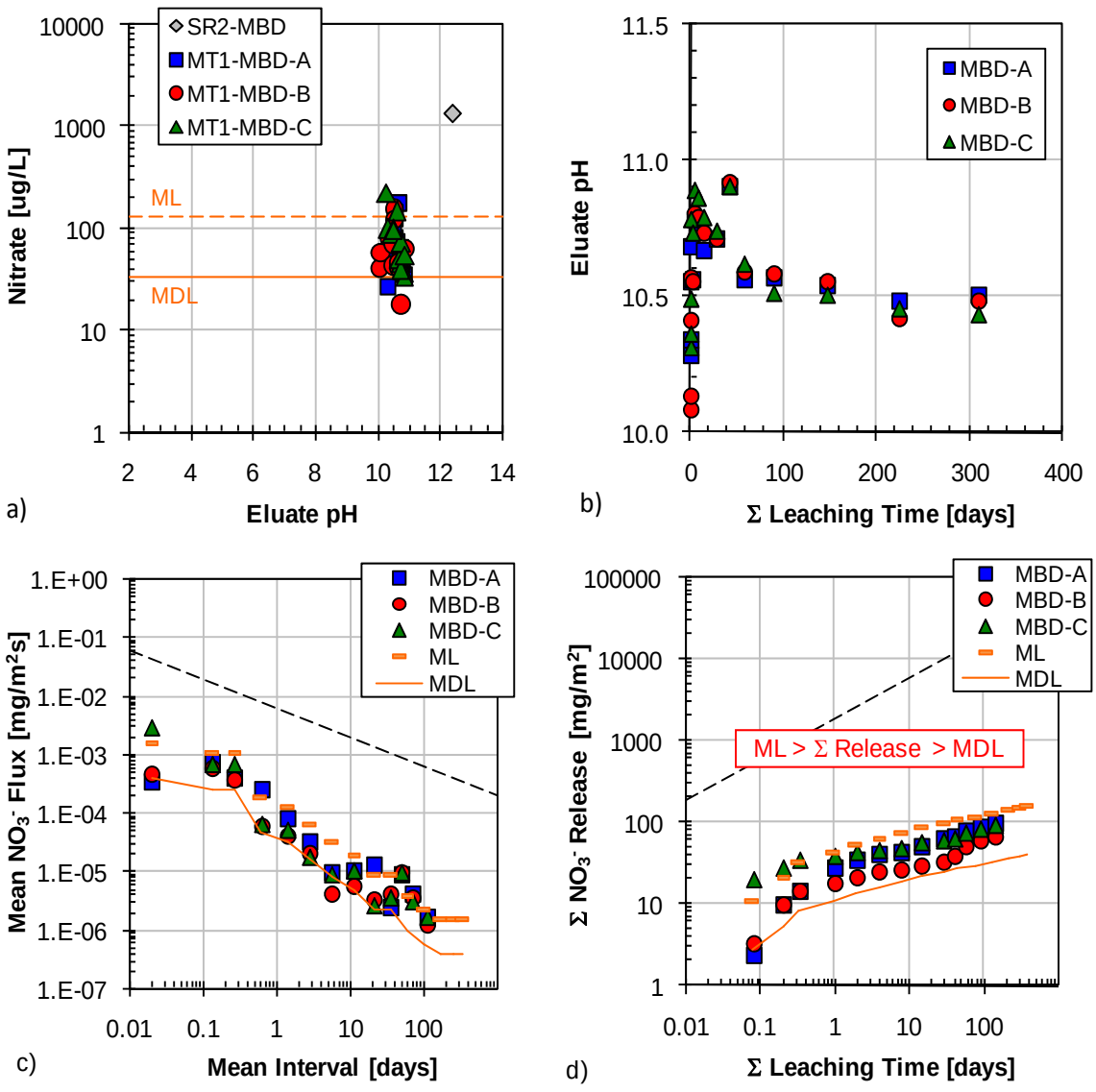

Figure A-75. Nitrate leaching test results from MBD matrix: a) comparison of tank leach test eluants to saturation values (SR02 data) and QA/QC parameters, b) pH evolution in tank leach eluants, c) interval flux from tank leach test in comparison to flux values at the method limit ($t^{-1/2}$ model for AMD shown as dashed line), and d) cumulative mass release ($t^{1/2}$ model for AMD shown as dashed line).

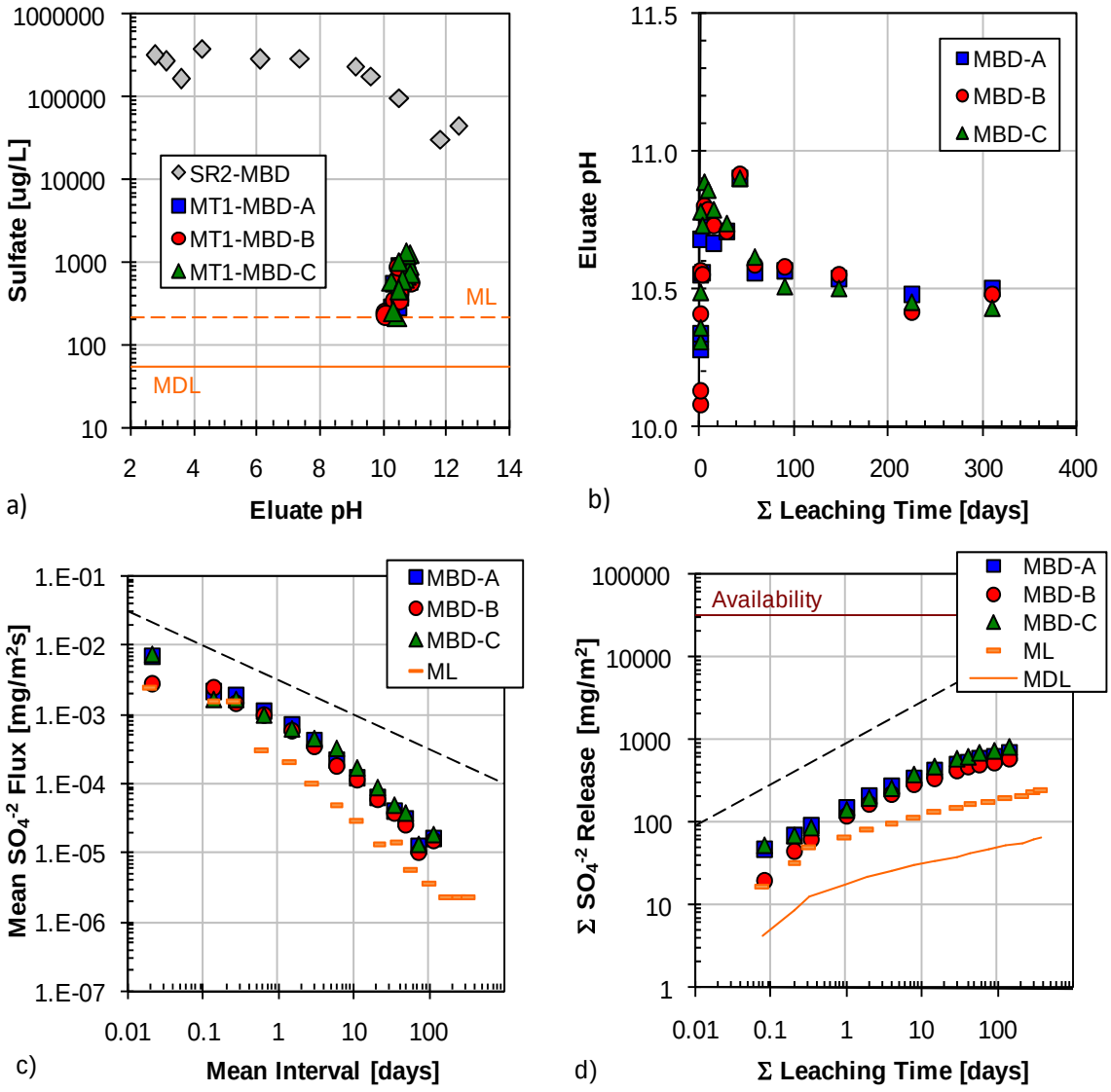

Figure A-76. Sulfate leaching test results from MBD matrix: a) comparison of tank leach test eluants to saturation values (SR02 data) and QA/QC parameters, b) pH evolution in tank leach eluants, c) interval flux from tank leach test in comparison to flux values at the method limit ($t^{-1/2}$ model for AMD shown as dashed line), and d) cumulative mass release ($t^{1/2}$ model for AMD shown as dashed line).

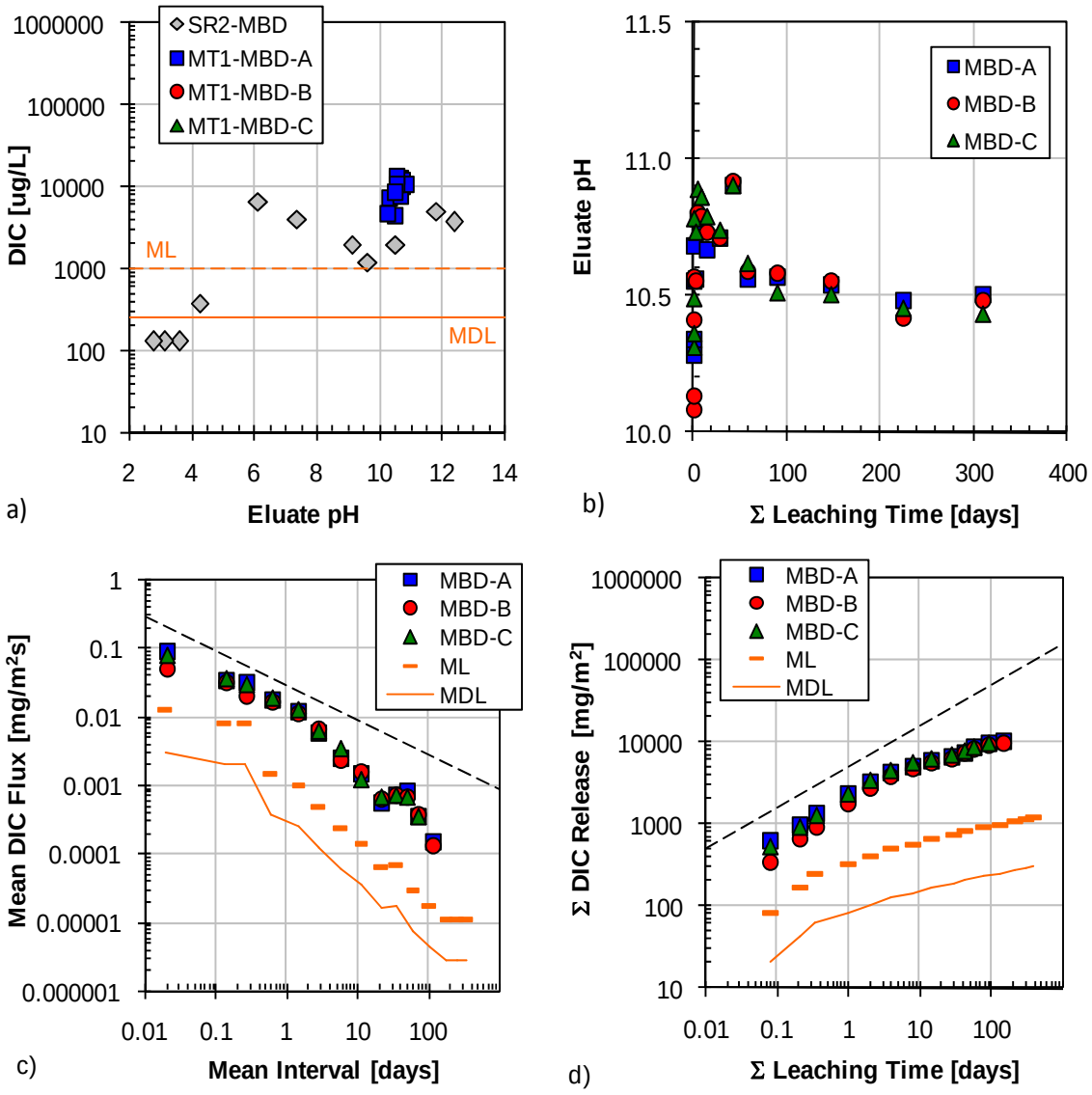

Figure A-77. Dissolved inorganic carbon (DIC) leaching test results from MBD matrix: a) comparison of tank leach test eluants to saturation values (SR02 data) and QA/QC parameters, b) pH evolution in tank leach eluants, c) interval flux from tank leach test in comparison to flux values at the method limit ($t^{-1/2}$ model for AMD shown as dashed line), and d) cumulative mass release ($t^{1/2}$ model for AMD shown as dashed line).

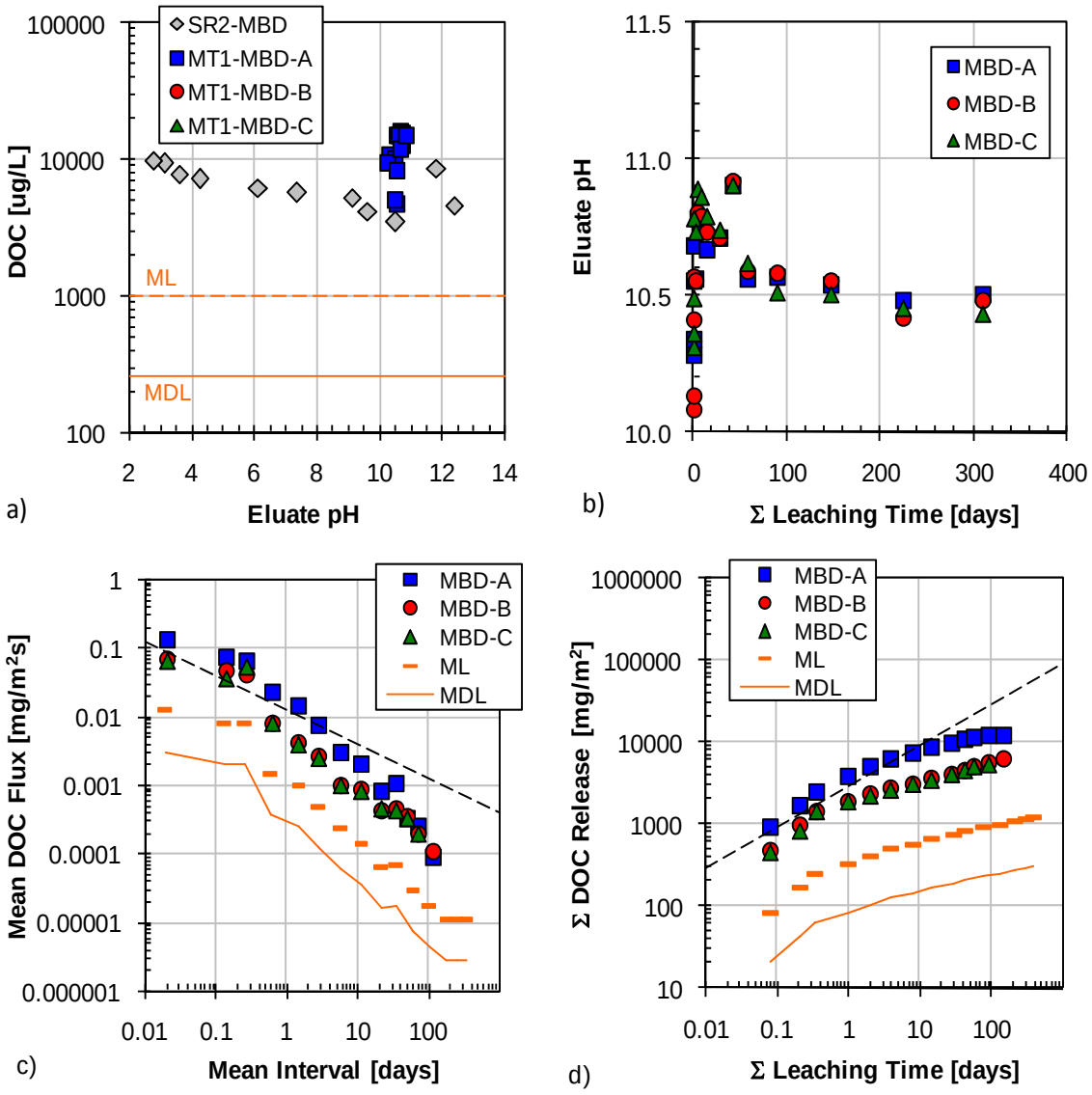

Figure A-78. Dissolved organic carbon (DOC) leaching test results from MBD matrix: a) comparison of tank leach test eluants to saturation values (SR02 data) and QA/QC parameters, b) pH evolution in tank leach eluants, c) interval flux from tank leach test in comparison to flux values at the method limit ($t^{-1/2}$ model for AMD shown as dashed line), and d) cumulative mass release ($t^{1/2}$ model for AMD shown as dashed line).

APPENDIX B: SIMULATED HANFORD GROUNDWATER LEACHING TEST RESULTS

Academic Matrix in SHG (AMG Material)

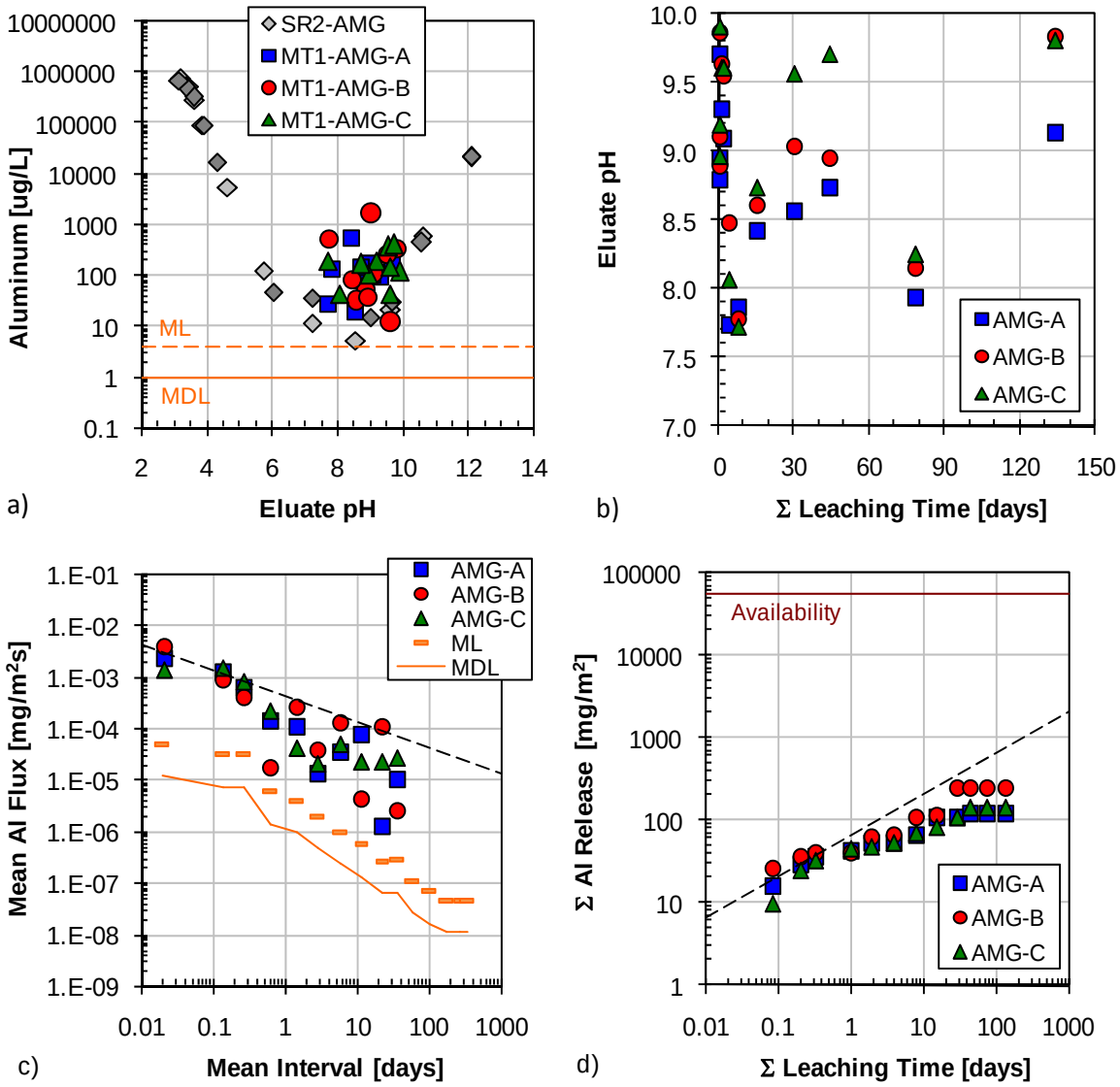

Figure B-1. Aluminum leaching test results from AMG: a) comparison of tank leach test eluants to saturation values (SR02 data) and QA/QC parameters, b) pH evolution in tank leach eluants, c) interval flux from tank leach test in comparison to flux values at the method limit ($t^{-1/2}$ model shown as dashed line), and d) cumulative mass release ($t^{1/2}$ model shown as dashed line).

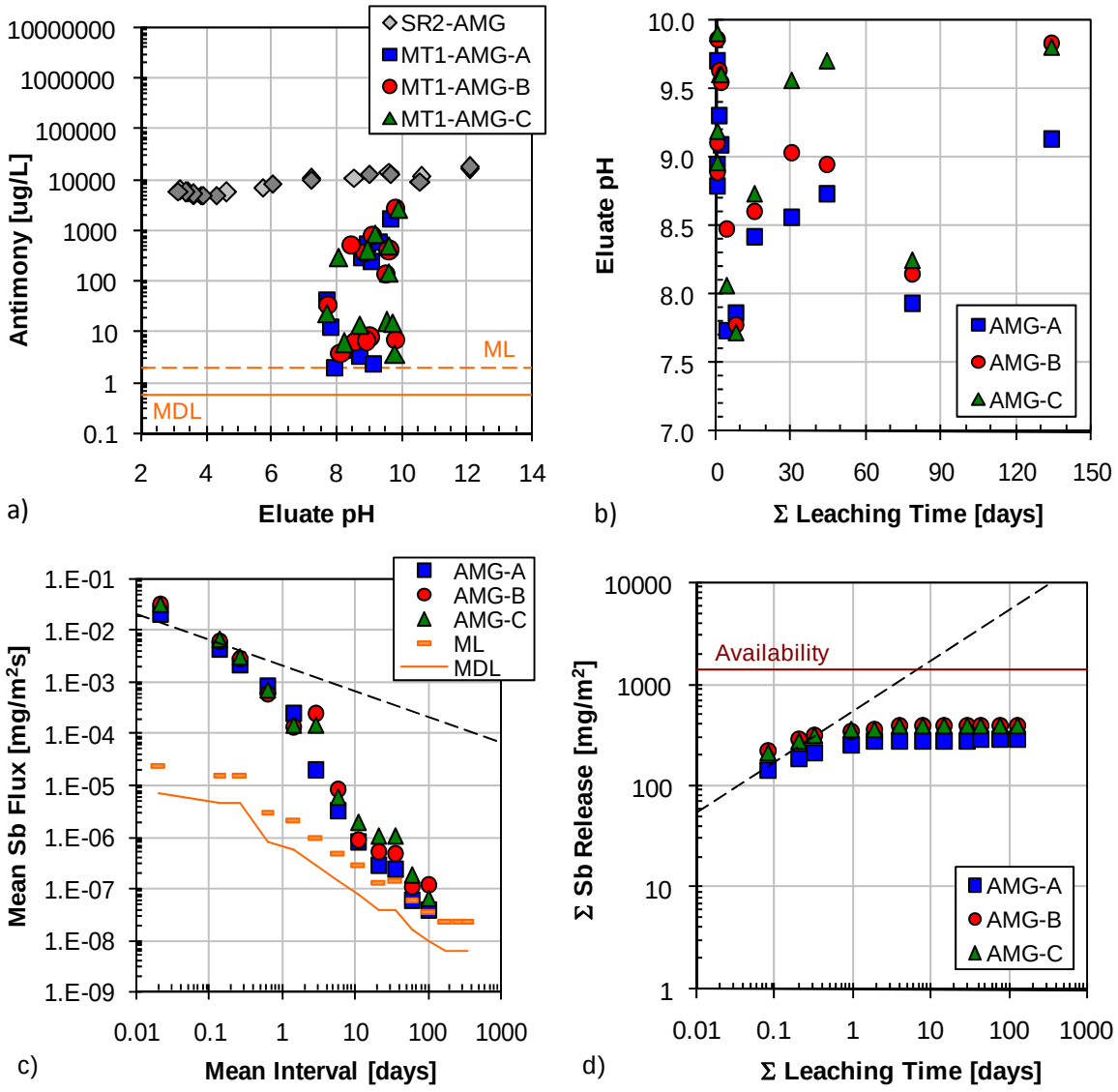

Figure B-2. Antimony leaching test results from AMG: a) comparison of tank leach test eluants to saturation values (SR02 data) and QA/QC parameters, b) pH evolution in tank leach eluants, c) interval flux from tank leach test in comparison to flux values at the method limit ($t^{-1/2}$ model shown as dashed line), and d) cumulative mass release ($t^{1/2}$ model shown as dashed line).

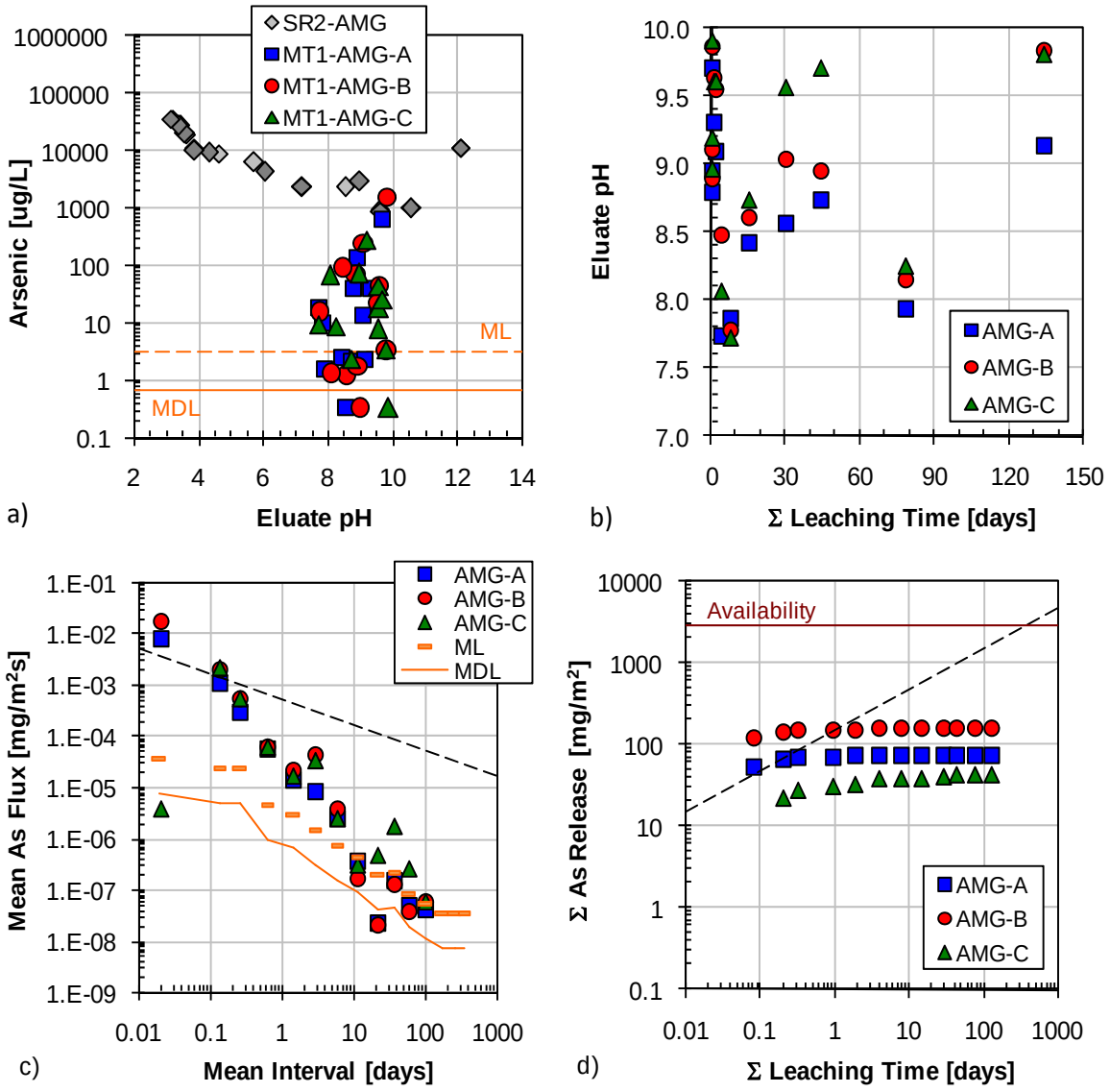

Figure B-3. Arsenic leaching test results from AMG: a) comparison of tank leach test eluants to saturation values (SR02 data) and QA/QC parameters, b) pH evolution in tank leach eluants, c) interval flux from tank leach test in comparison to flux values at the method limit ($t^{-1/2}$ model shown as dashed line), and d) cumulative mass release ($t^{1/2}$ model shown as dashed line).

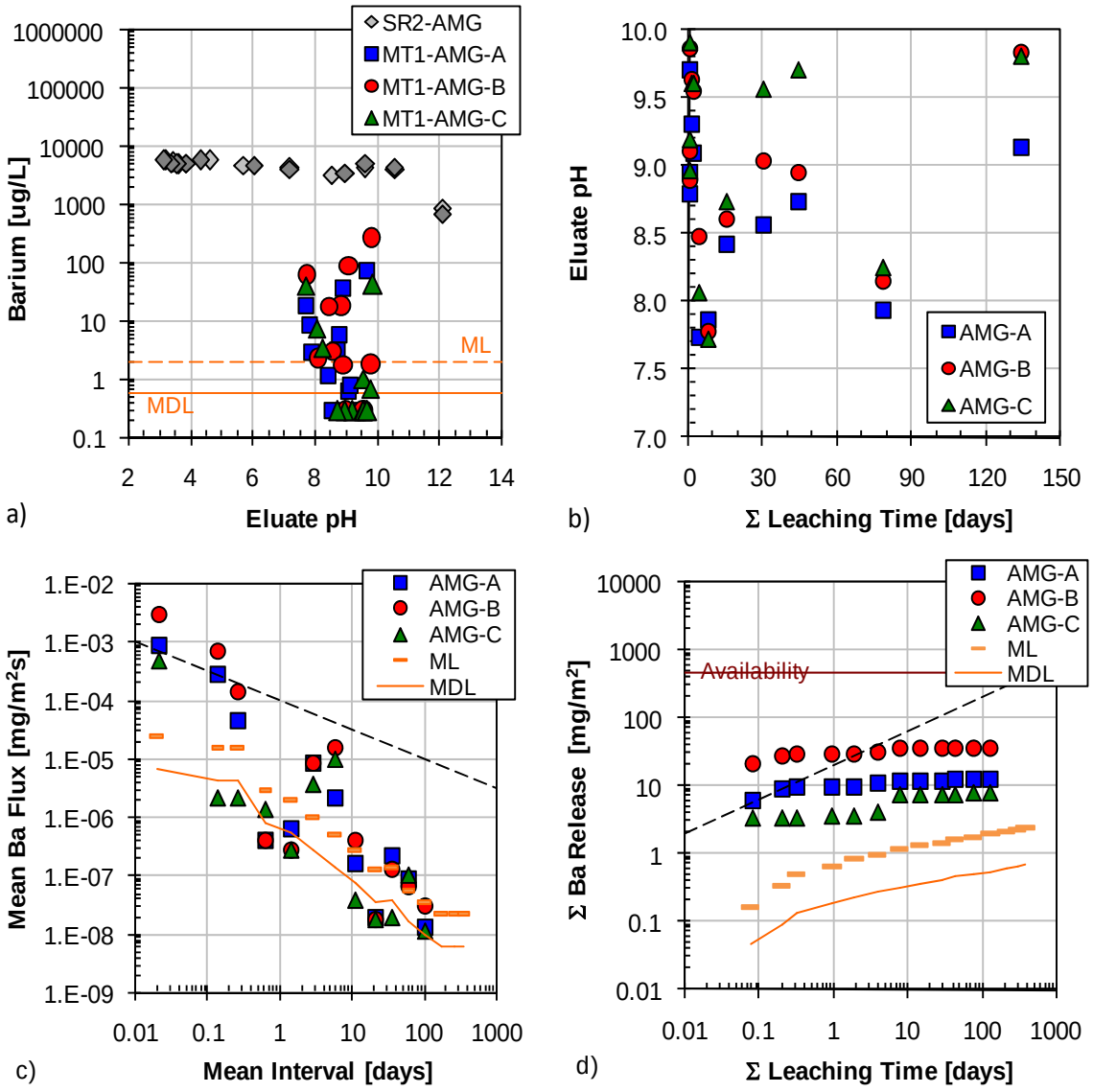

Figure B-4. Barium leaching test results from AMG: a) comparison of tank leach test eluants to saturation values (SR02 data) and QA/QC parameters, b) pH evolution in tank leach eluants, c) interval flux from tank leach test in comparison to flux values at the method limit ($t^{-1/2}$ model shown as dashed line), and d) cumulative mass release ($t^{1/2}$ model shown as dashed line).

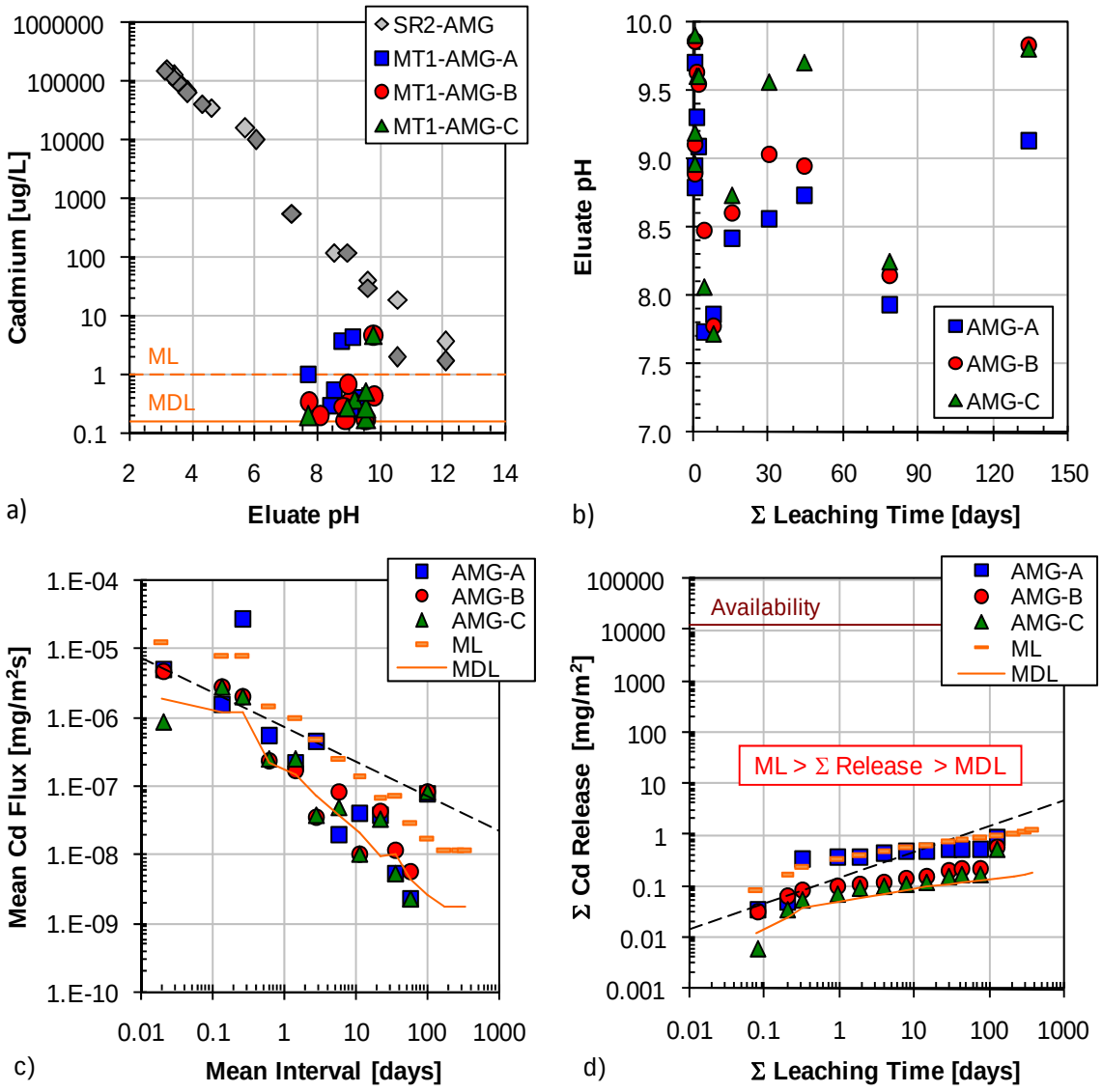

Figure B-5. Cadmium leaching test results from AMG: a) comparison of tank leach test eluants to saturation values (SR02 data) and QA/QC parameters, b) pH evolution in tank leach eluants, c) interval flux from tank leach test in comparison to flux values at the method limit ($t^{-1/2}$ model shown as dashed line), and d) cumulative mass release ($t^{1/2}$ model shown as dashed line).

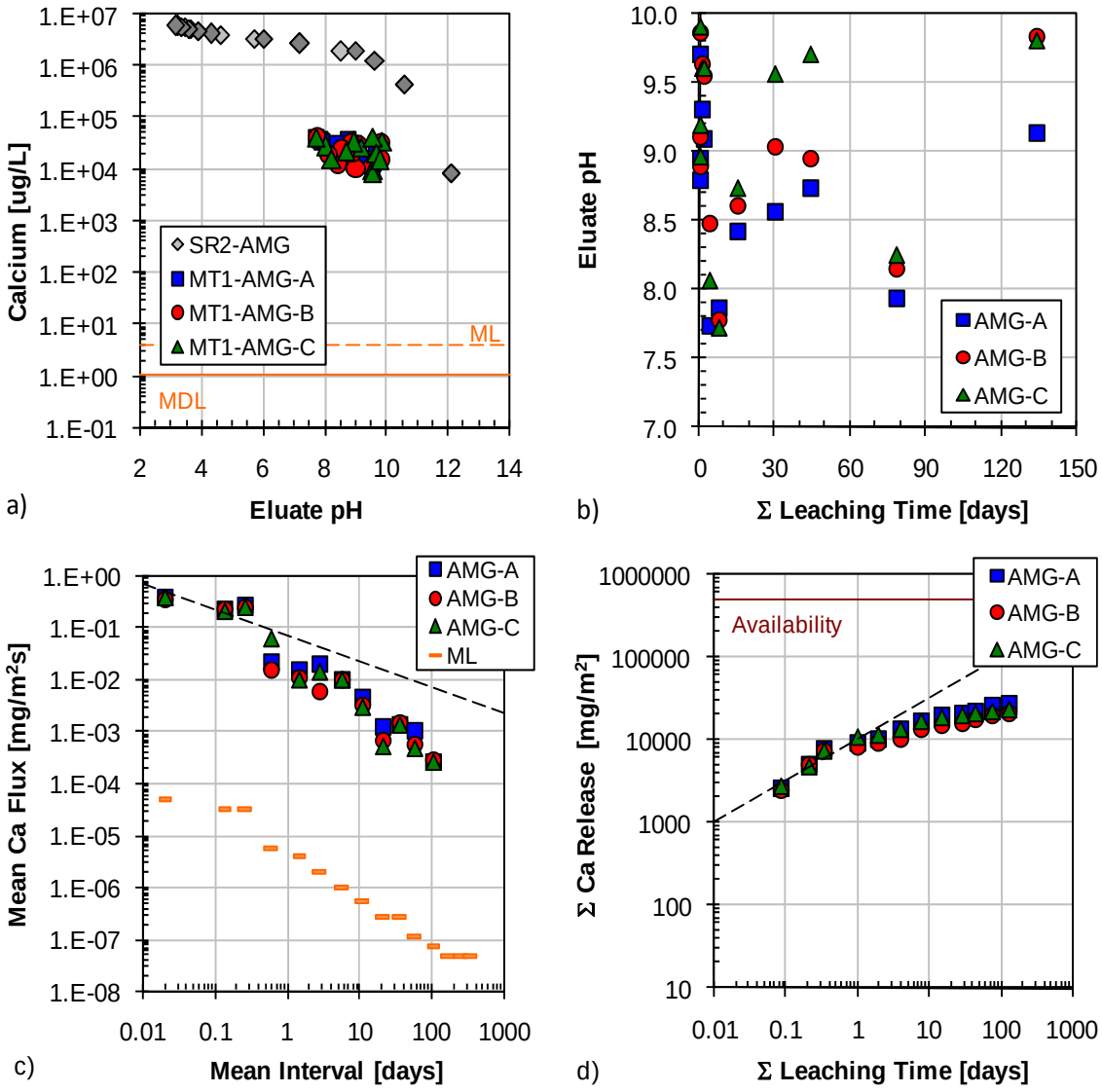

Figure B-6. Calcium leaching test results from AMG: a) comparison of tank leach test eluants to saturation values (SR02 data) and QA/QC parameters, b) pH evolution in tank leach eluants, c) interval flux from tank leach test in comparison to flux values at the method limit ($t^{-1/2}$ model shown as dashed line), and d) cumulative mass release ($t^{1/2}$ model shown as dashed line).

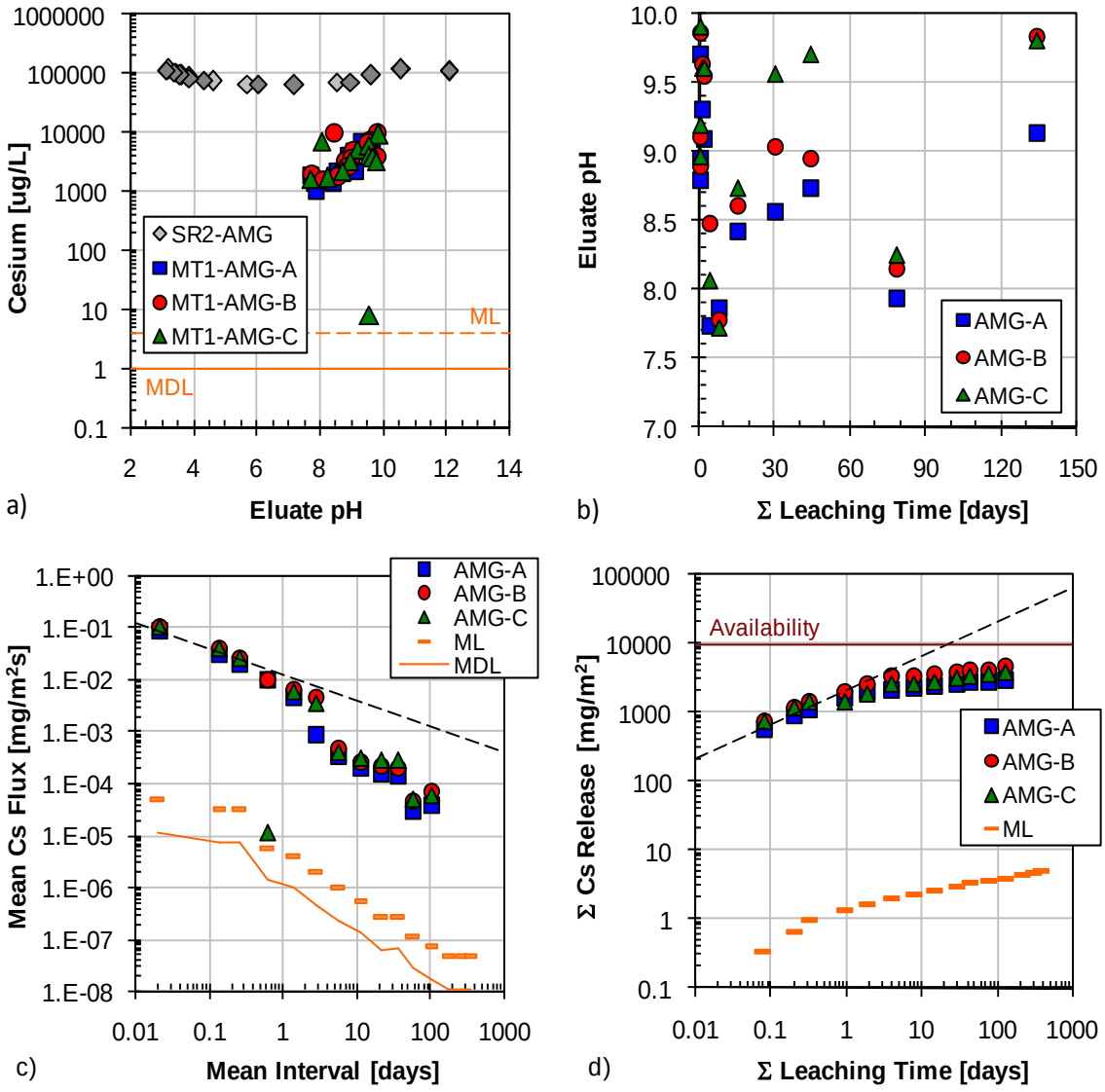

Figure B-7. Cesium leaching test results from AMG: a) comparison of tank leach test eluants to saturation values (SR02 data) and QA/QC parameters, b) pH evolution in tank leach eluants, c) interval flux from tank leach test in comparison to flux values at the method limit ($t^{-1/2}$ model shown as dashed line), and d) cumulative mass release ($t^{1/2}$ model shown as dashed line).

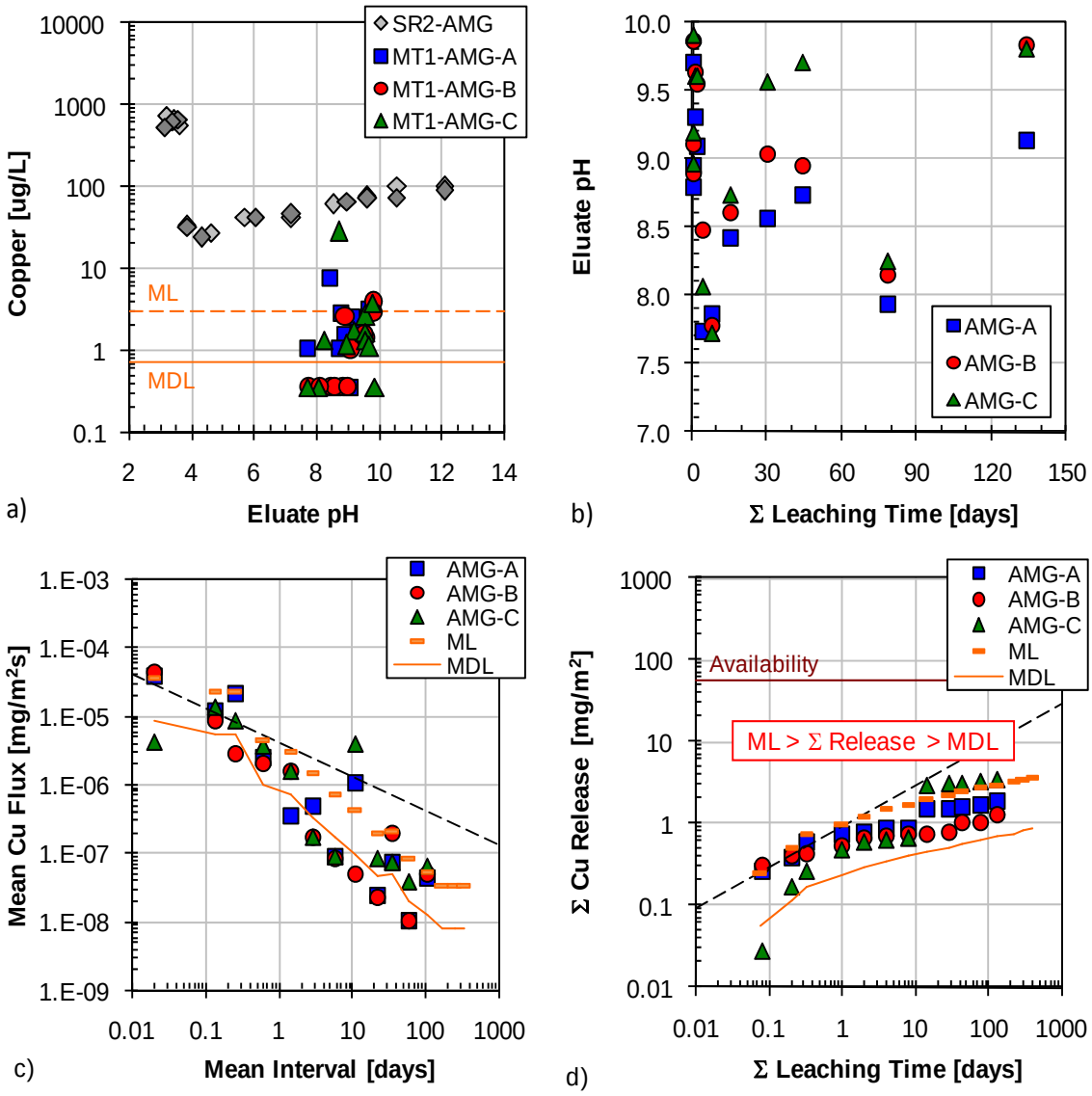

Figure B-8. Copper leaching test results from AMG: a) comparison of tank leach test eluants to saturation values (SR02 data) and QA/QC parameters, b) pH evolution in tank leach eluants, c) interval flux from tank leach test in comparison to flux values at the method limit ($t^{-1/2}$ model shown as dashed line), and d) cumulative mass release ($t^{1/2}$ model shown as dashed line).

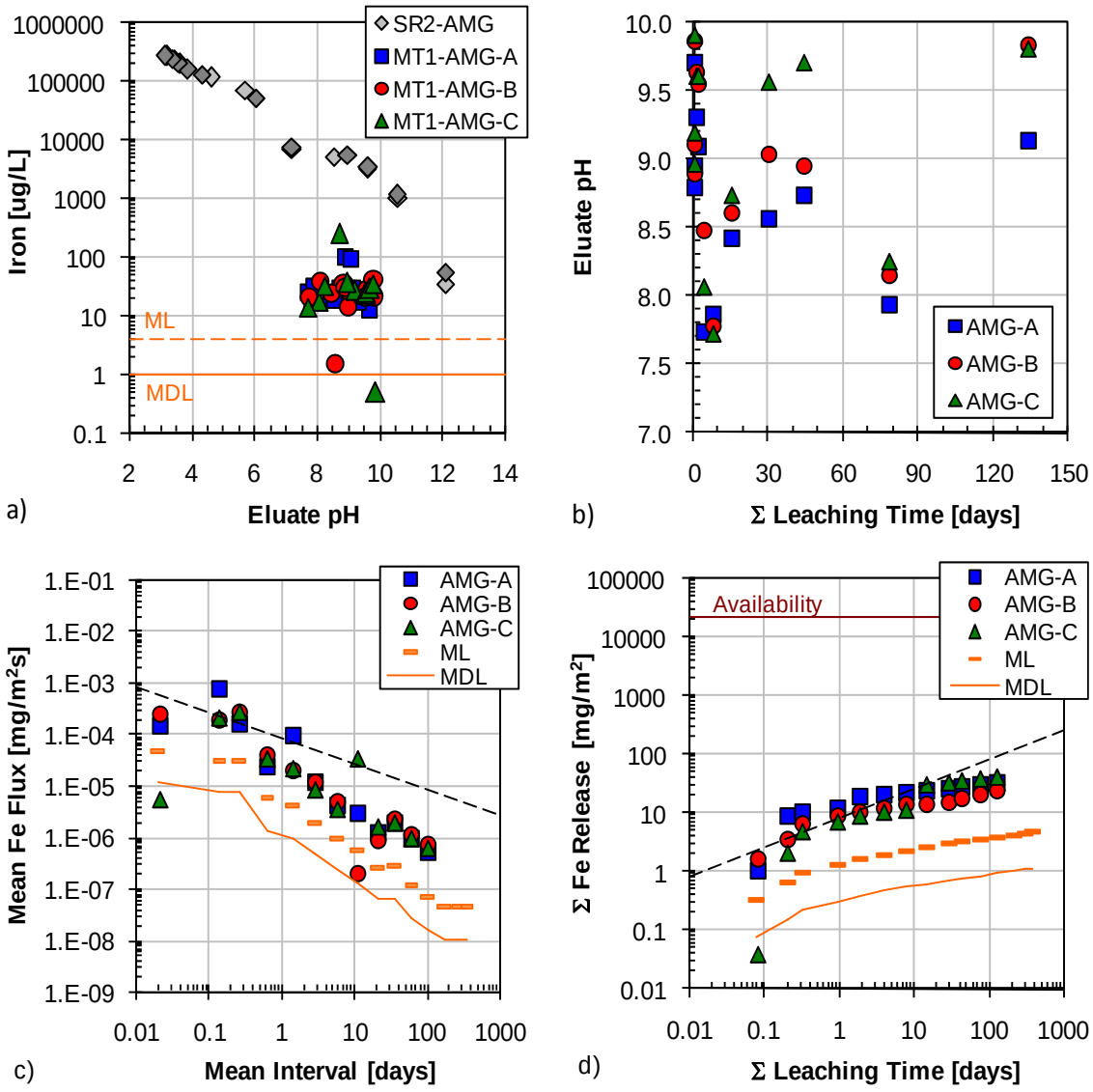

Figure B-9. Iron leaching test results from AMG: a) comparison of tank leach test eluants to saturation values (SR02 data) and QA/QC parameters, b) pH evolution in tank leach eluants, c) interval flux from tank leach test in comparison to flux values at the method limit ($t^{-1/2}$ model shown as dashed line), and d) cumulative mass release ($t^{1/2}$ model shown as dashed line).

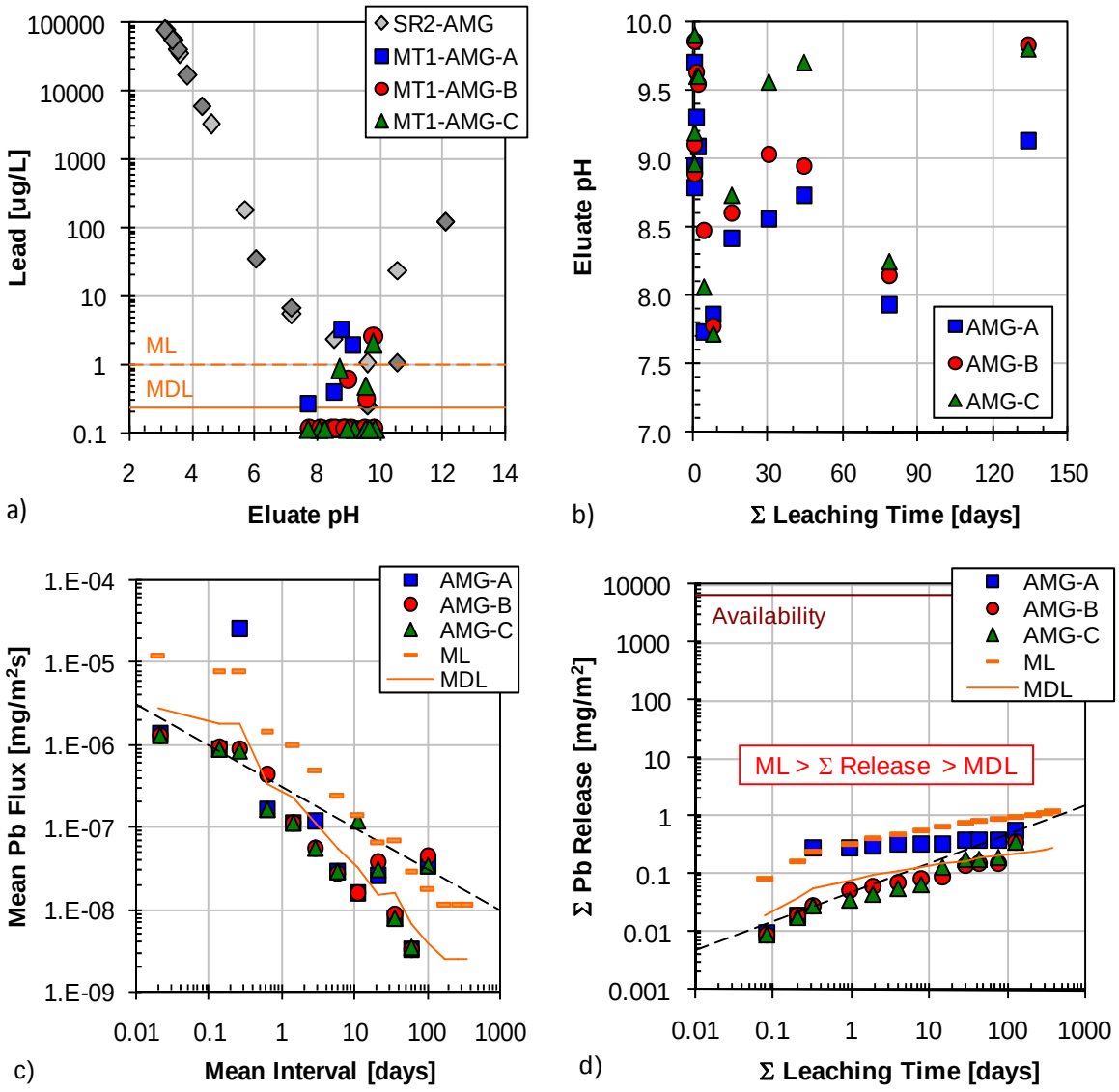

Figure B-10. Lead leaching test results from AMG: a) comparison of tank leach test eluants to saturation values (SR02 data) and QA/QC parameters, b) pH evolution in tank leach eluants, c) interval flux from tank leach test in comparison to flux values at the method limit ($t^{-1/2}$ model shown as dashed line), and d) cumulative mass release ($t^{1/2}$ model shown as dashed line).

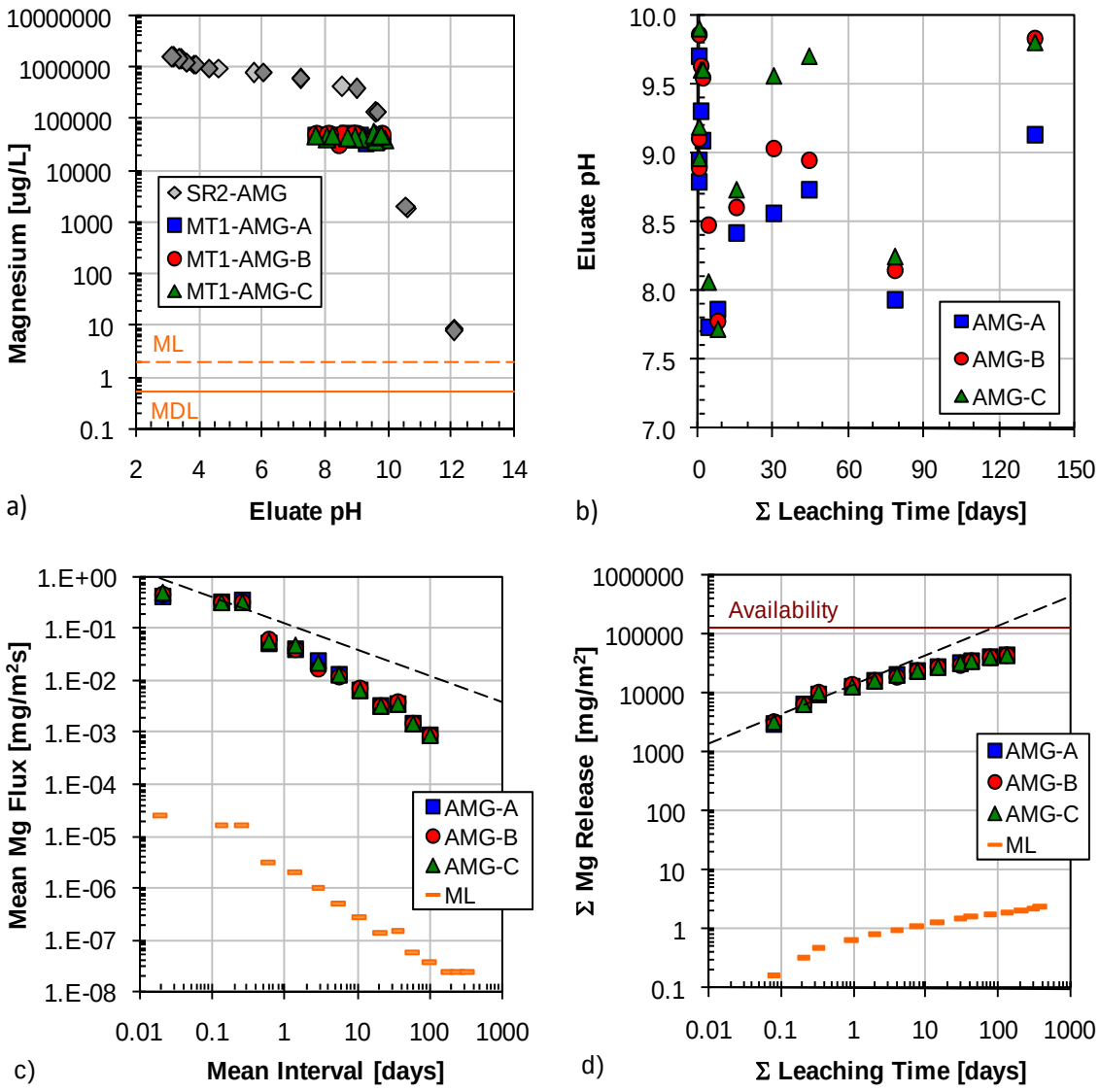

Figure B-11. Magnesium leaching test results from AMG: a) comparison of tank leach test eluants to saturation values (SR02 data) and QA/QC parameters, b) pH evolution in tank leach eluants, c) interval flux from tank leach test in comparison to flux values at the method limit ($t^{-1/2}$ model shown as dashed line), and d) cumulative mass release ($t^{1/2}$ model shown as dashed line).

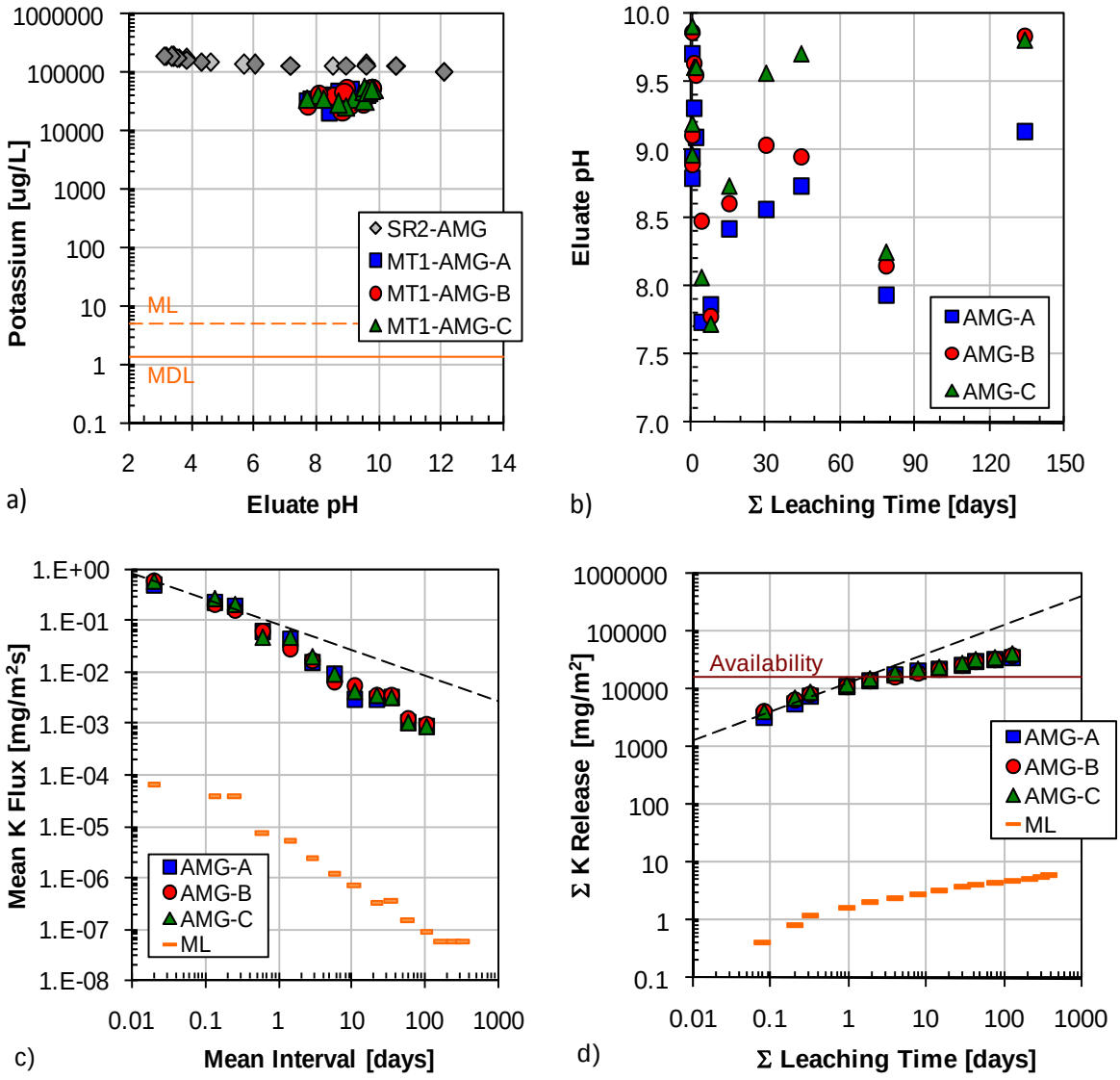

Figure B-12. Potassium leaching test results from AMG: a) comparison of tank leach test eluants to saturation values (SR02 data) and QA/QC parameters, b) pH evolution in tank leach eluants, c) interval flux from tank leach test in comparison to flux values at the method limit ($t^{-1/2}$ model shown as dashed line), and d) cumulative mass release ($t^{1/2}$ model shown as dashed line).

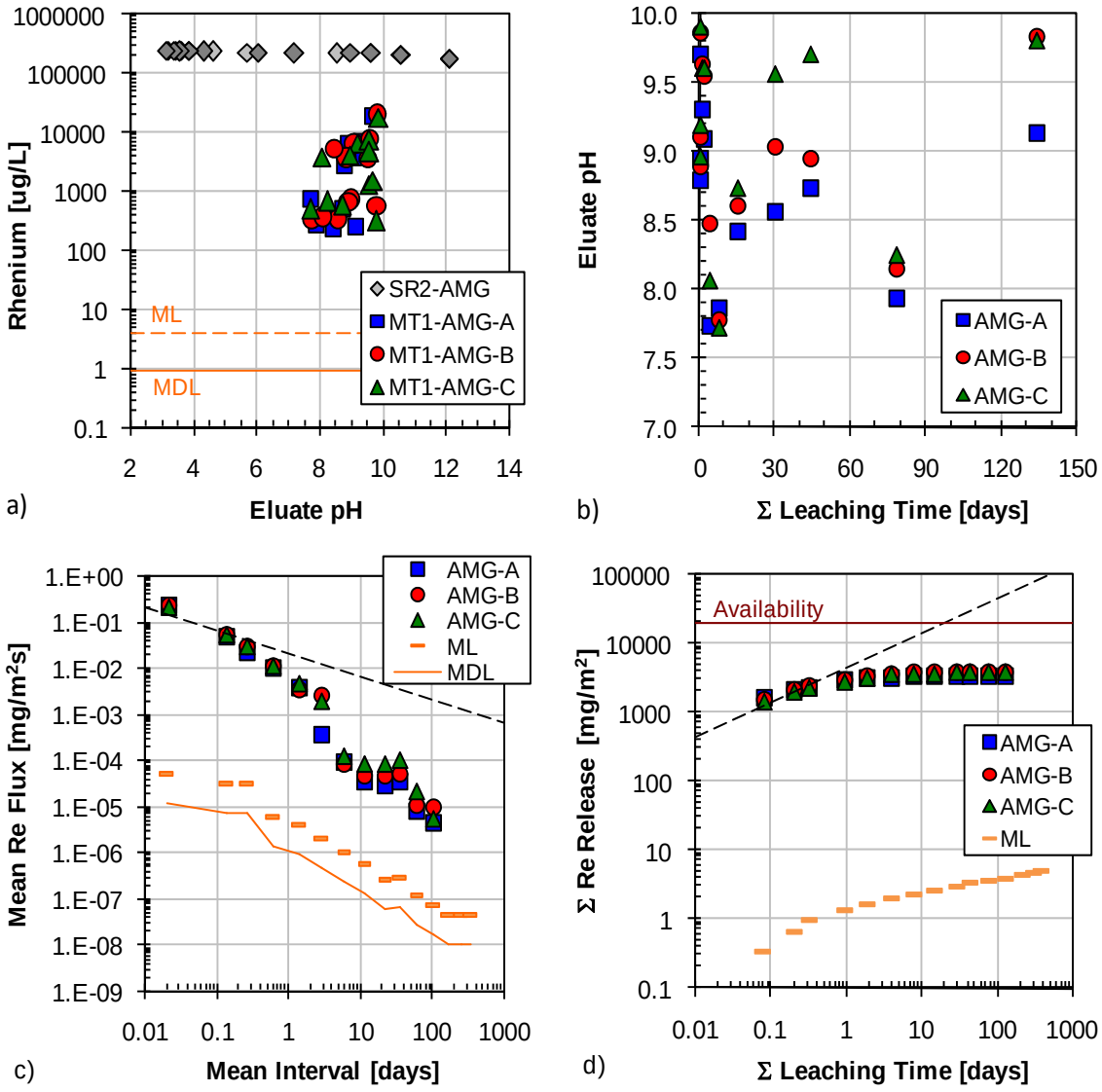

Figure B-13. Rhenium leaching test results from AMG: a) comparison of tank leach test eluants to saturation values (SR02 data) and QA/QC parameters, b) pH evolution in tank leach eluants, c) interval flux from tank leach test in comparison to flux values at the method limit ($t^{-1/2}$ model shown as dashed line), and d) cumulative mass release ($t^{1/2}$ model shown as dashed line).

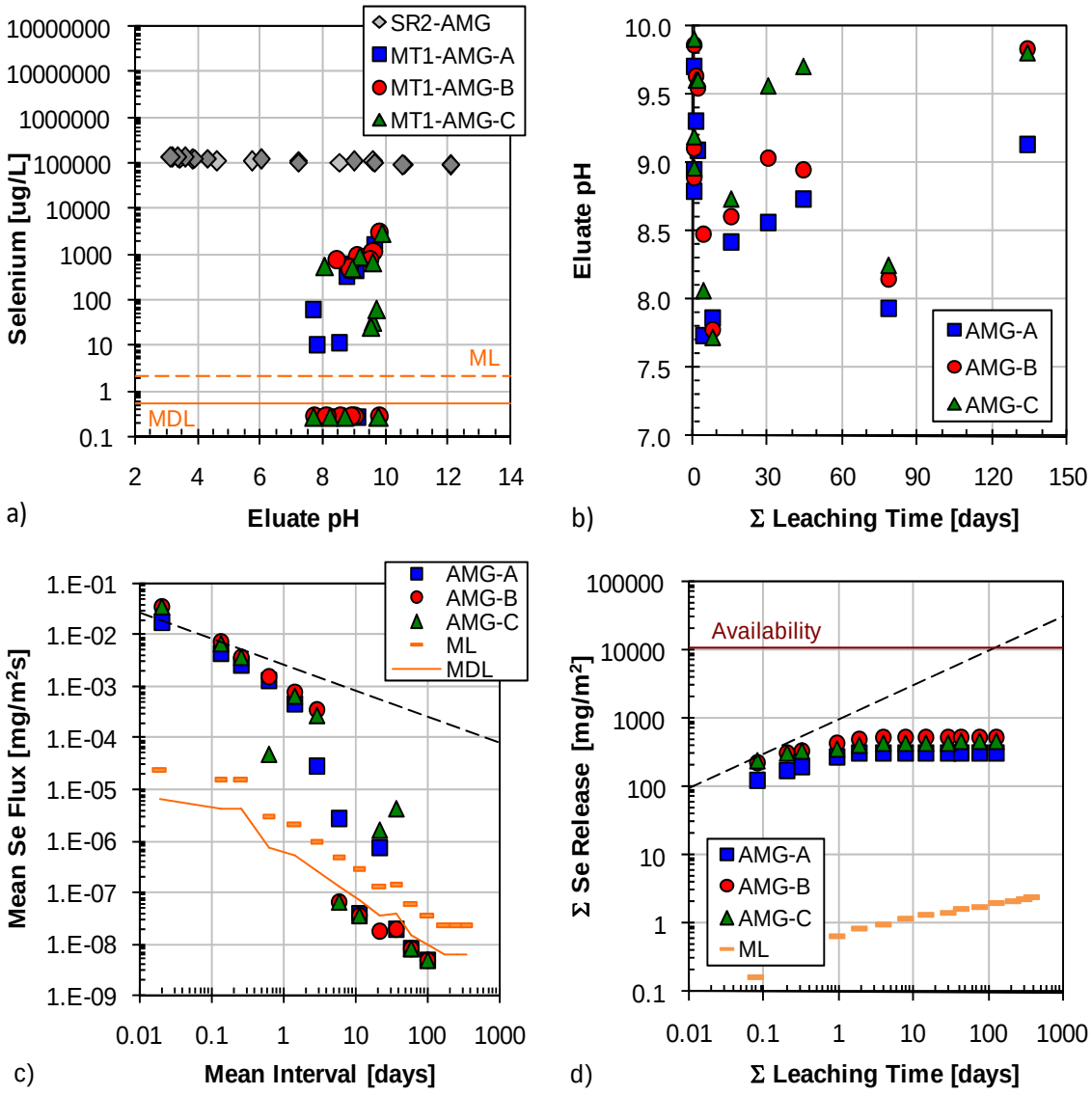

Figure B-14. Selenium leaching test results from AMG: a) comparison of tank leach test eluants to saturation values (SR02 data) and QA/QC parameters, b) pH evolution in tank leach eluants, c) interval flux from tank leach test in comparison to flux values at the method limit ($t^{-1/2}$ model shown as dashed line), and d) cumulative mass release ($t^{1/2}$ model shown as dashed line).

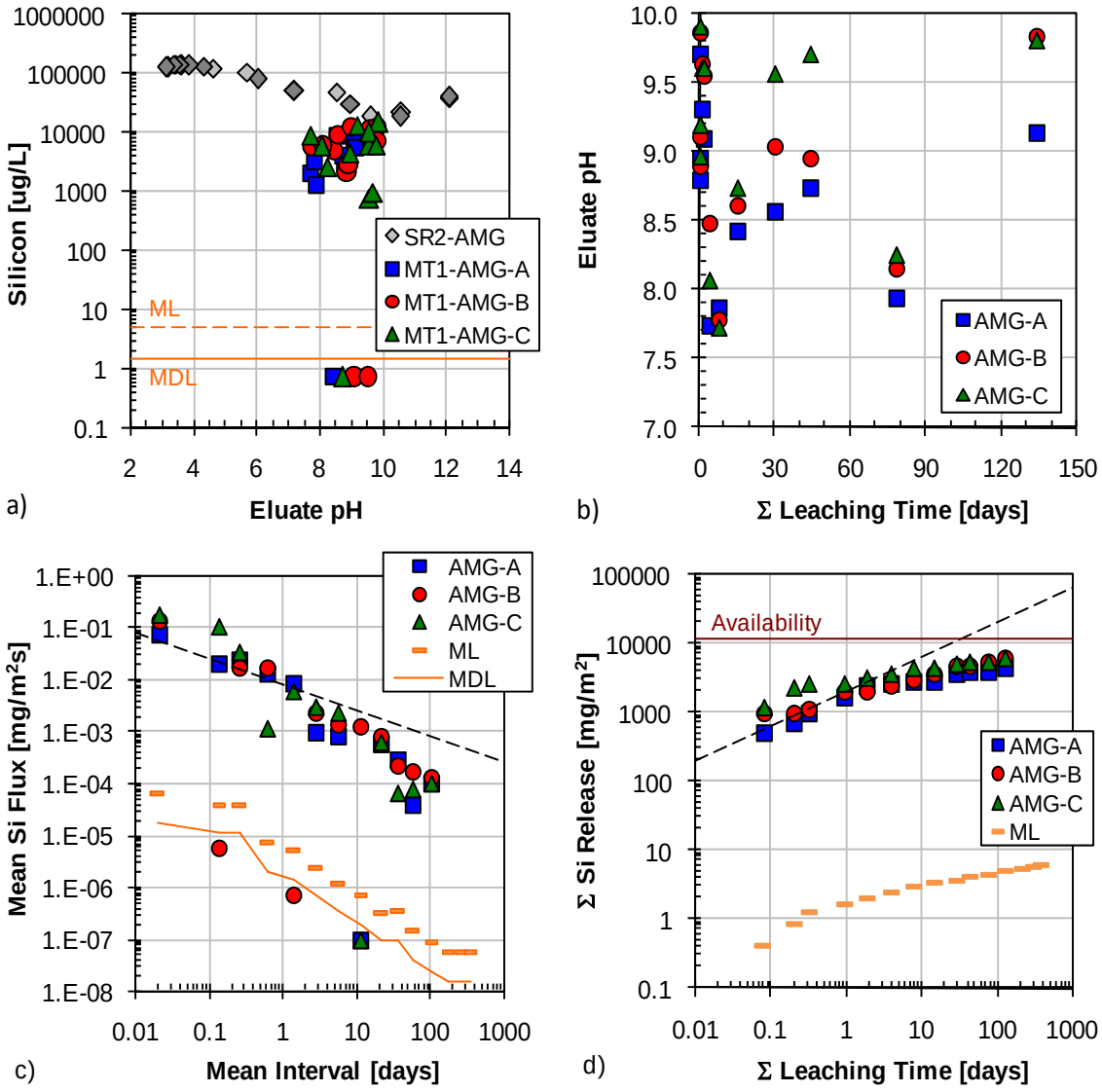

Figure B-15. Silicon leaching test results from AMG: a) comparison of tank leach test eluants to saturation values (SR02 data) and QA/QC parameters, b) pH evolution in tank leach eluants, c) interval flux from tank leach test in comparison to flux values at the method limit ($t^{-1/2}$ model shown as dashed line), and d) cumulative mass release ($t^{1/2}$ model shown as dashed line).

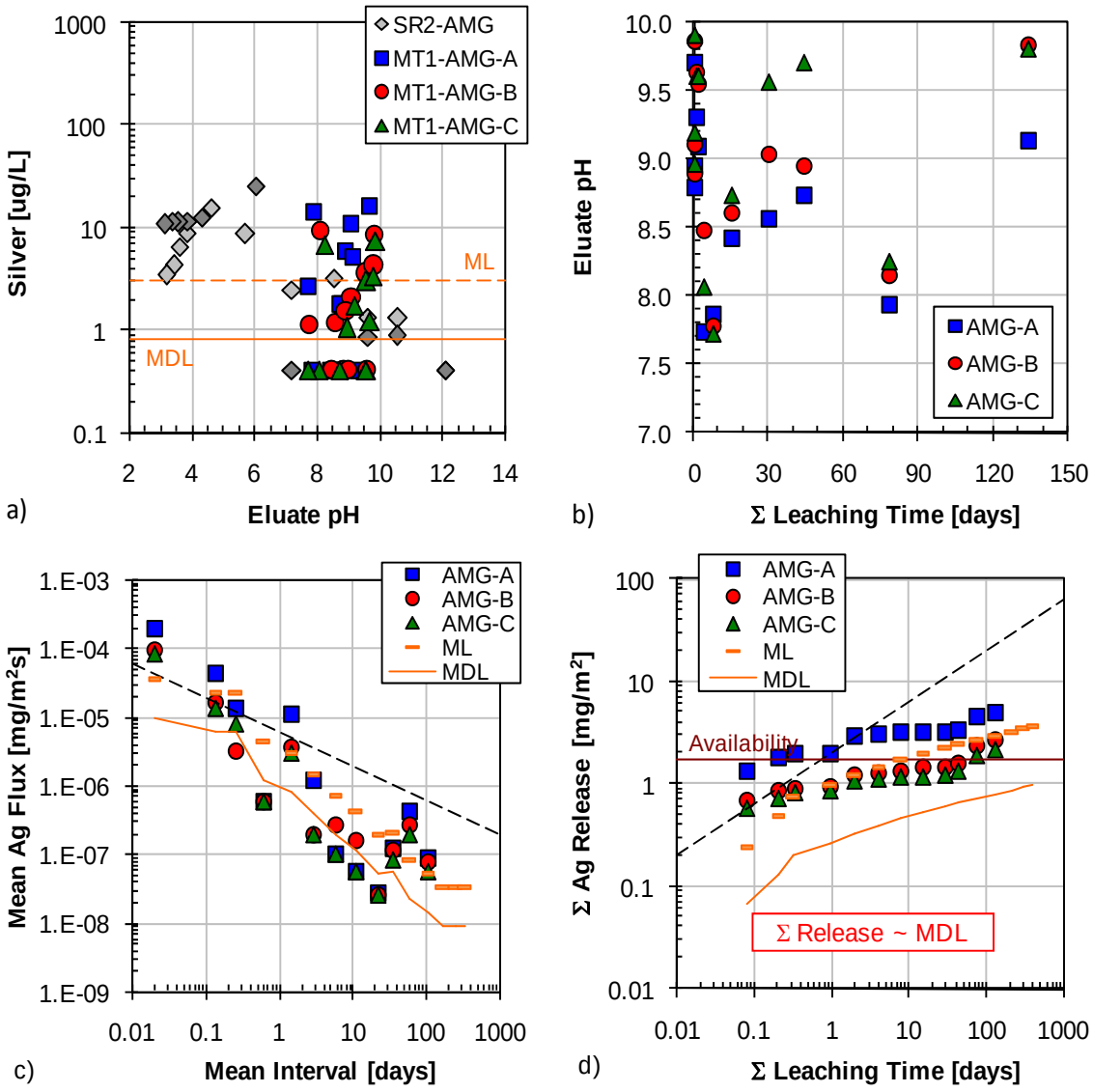

Figure B-16. Silver leaching test results from AMG: a) comparison of tank leach test eluants to saturation values (SR02 data) and QA/QC parameters, b) pH evolution in tank leach eluants, c) interval flux from tank leach test in comparison to flux values at the method limit ($t^{-1/2}$ model shown as dashed line), and d) cumulative mass release ($t^{1/2}$ model shown as dashed line).

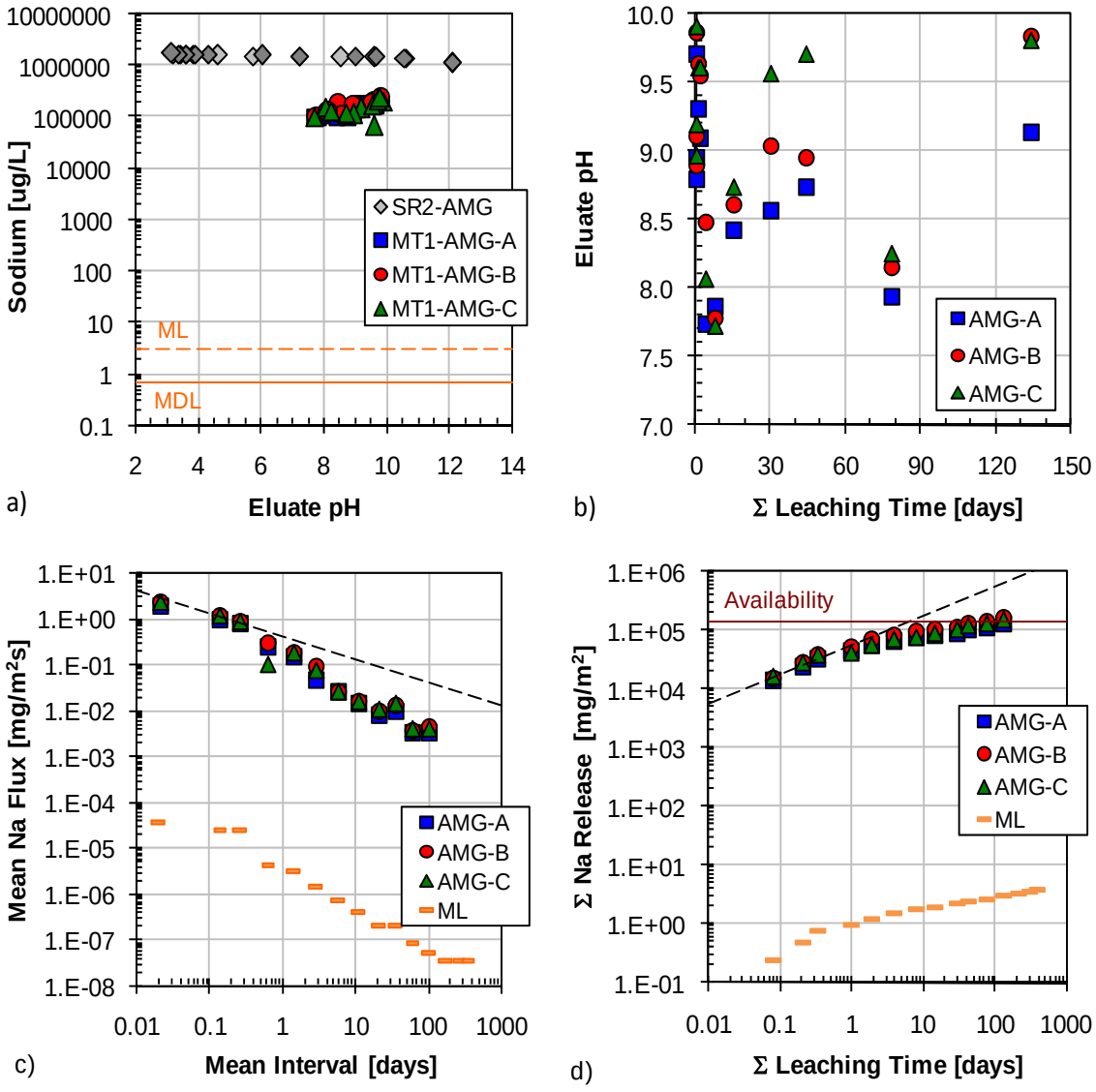

Figure B-17. Sodium leaching test results from AMG: a) comparison of tank leach test eluants to saturation values (SR02 data) and QA/QC parameters, b) pH evolution in tank leach eluants, c) interval flux from tank leach test in comparison to flux values at the method limit ($t^{-1/2}$ model shown as dashed line), and d) cumulative mass release ($t^{1/2}$ model shown as dashed line).

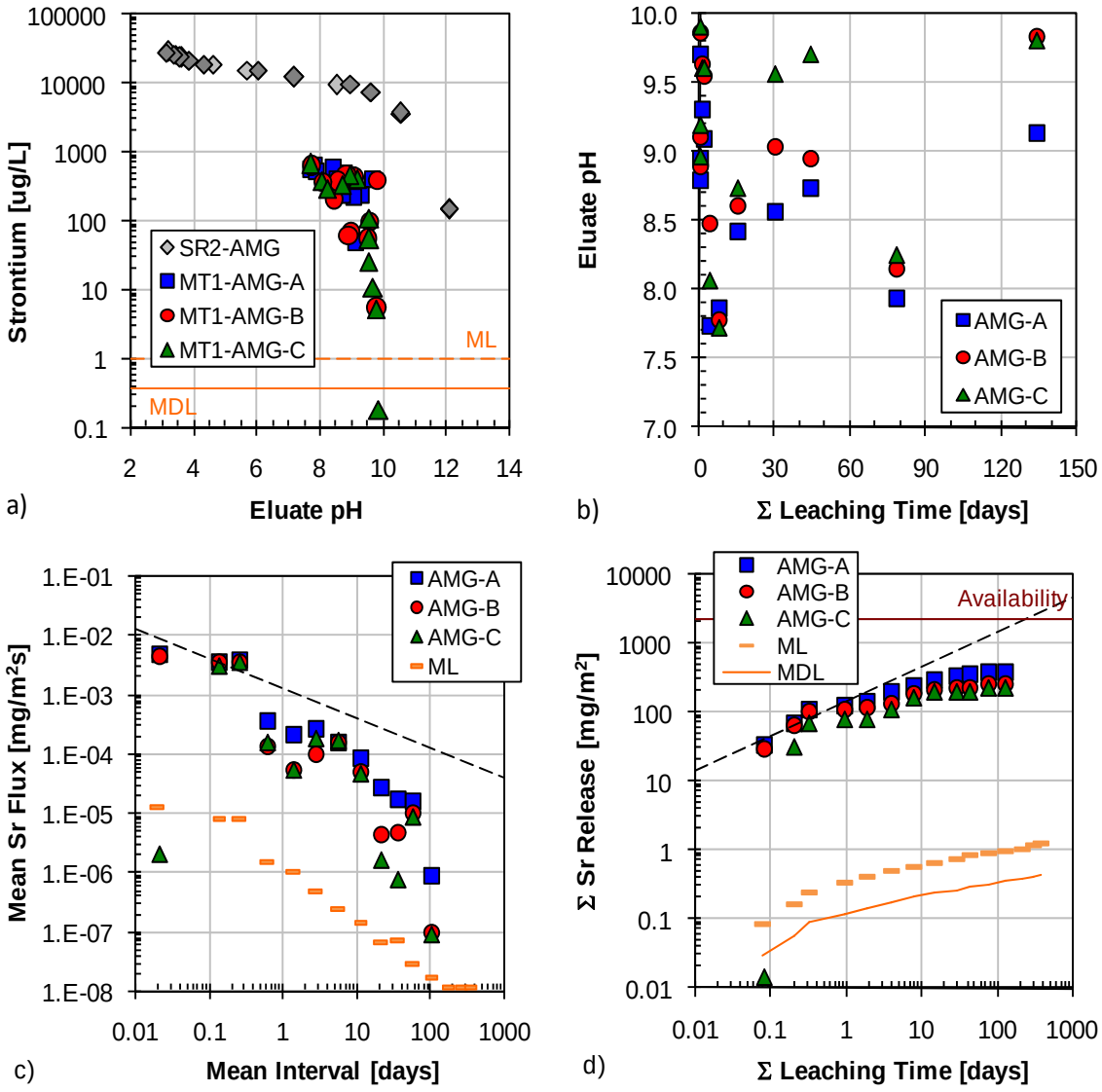

Figure B-18. Strontium leaching test results from AMG: a) comparison of tank leach test eluants to saturation values (SR02 data) and QA/QC parameters, b) pH evolution in tank leach eluants, c) interval flux from tank leach test in comparison to flux values at the method limit ($t^{-1/2}$ model shown as dashed line), and d) cumulative mass release ($t^{1/2}$ model shown as dashed line).

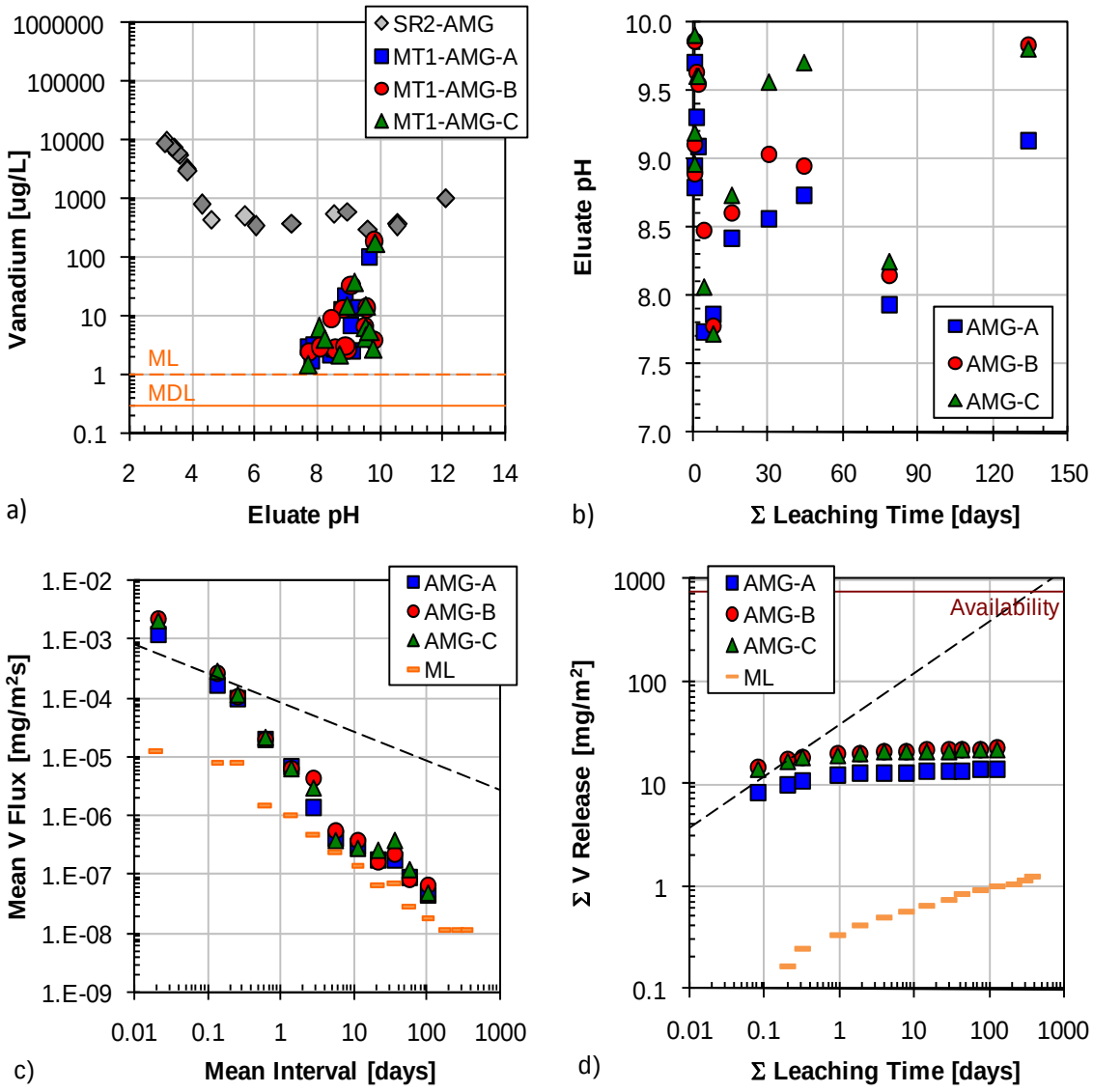

Figure B-19. Vanadium leaching test results from AMG: a) comparison of tank leach test eluants to saturation values (SR02 data) and QA/QC parameters, b) pH evolution in tank leach eluants, c) interval flux from tank leach test in comparison to flux values at the method limit ($t^{-1/2}$ model shown as dashed line), and d) cumulative mass release ($t^{1/2}$ model shown as dashed line).

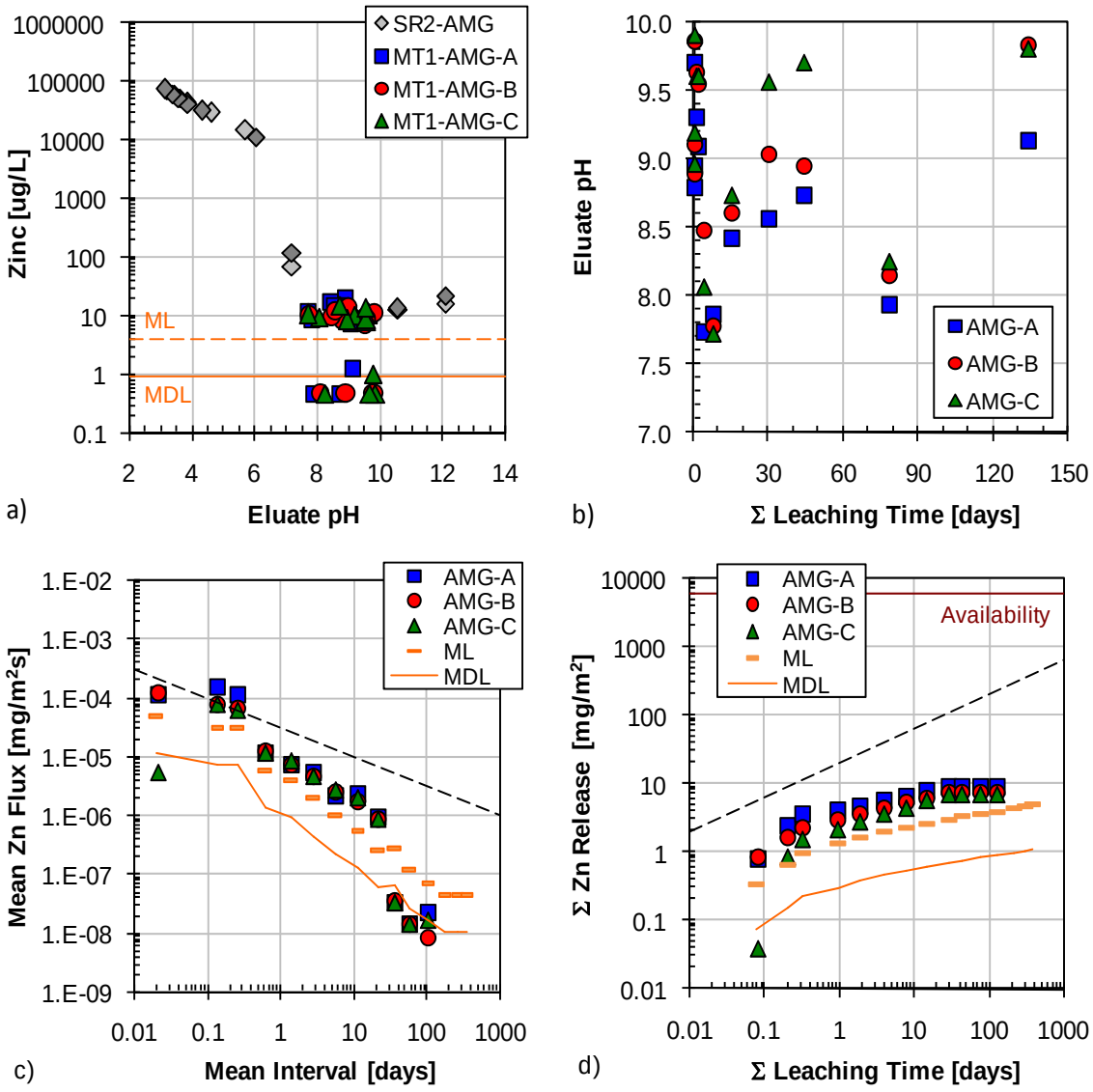

Figure B-20. Zinc leaching test results from AMG: a) comparison of tank leach test eluants to saturation values (SR02 data) and QA/QC parameters, b) pH evolution in tank leach eluants, c) interval flux from tank leach test in comparison to flux values at the method limit ($t^{-1/2}$ model shown as dashed line), and d) cumulative mass release ($t^{1/2}$ model shown as dashed line).

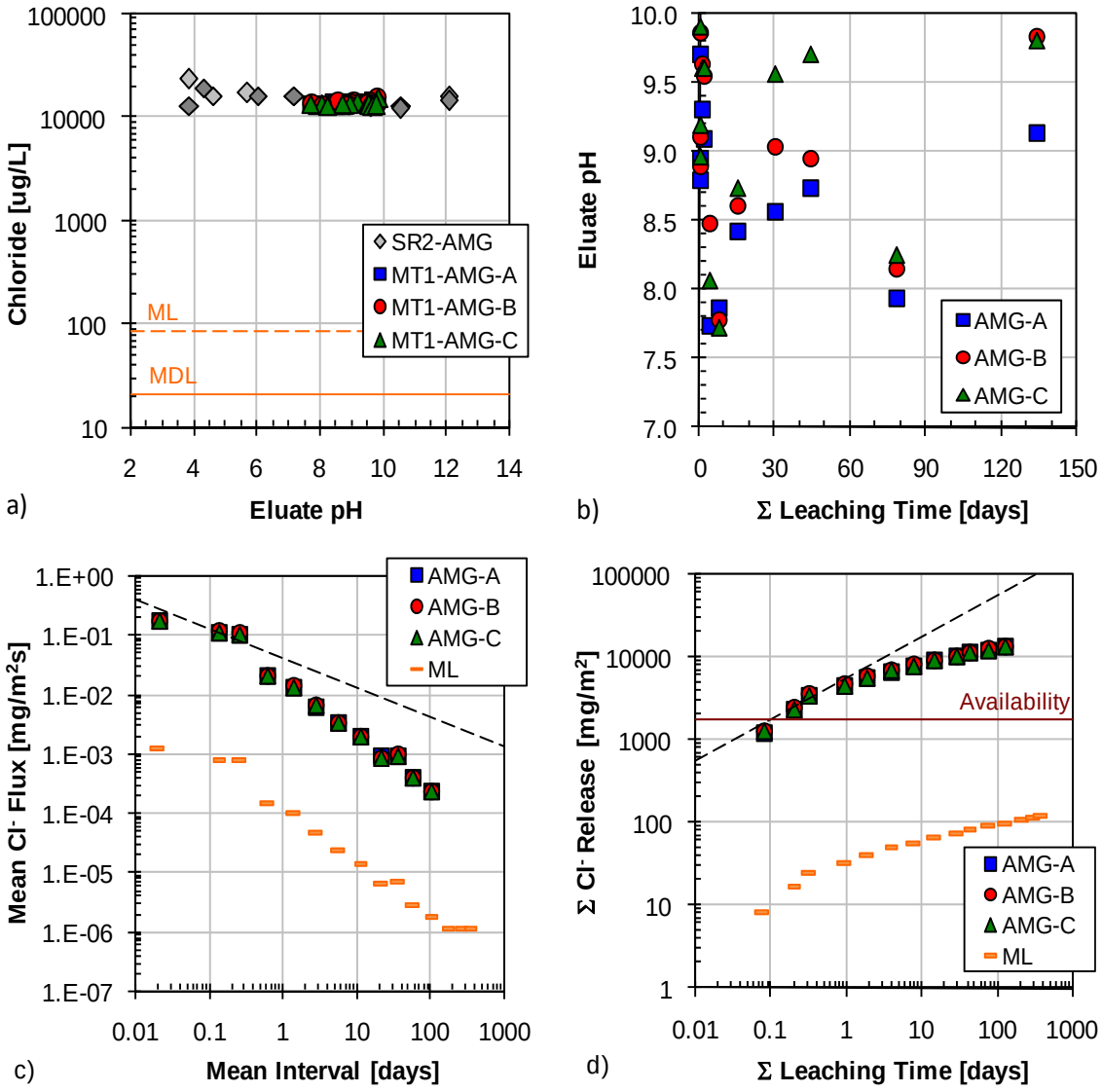

Figure B-21. Chloride leaching test results from AMG: a) comparison of tank leach test eluants to saturation values (SR02 data) and QA/QC parameters, b) pH evolution in tank leach eluants, c) interval flux from tank leach test in comparison to flux values at the method limit ($t^{-1/2}$ model shown as dashed line), and d) cumulative mass release ($t^{1/2}$ model shown as dashed line).

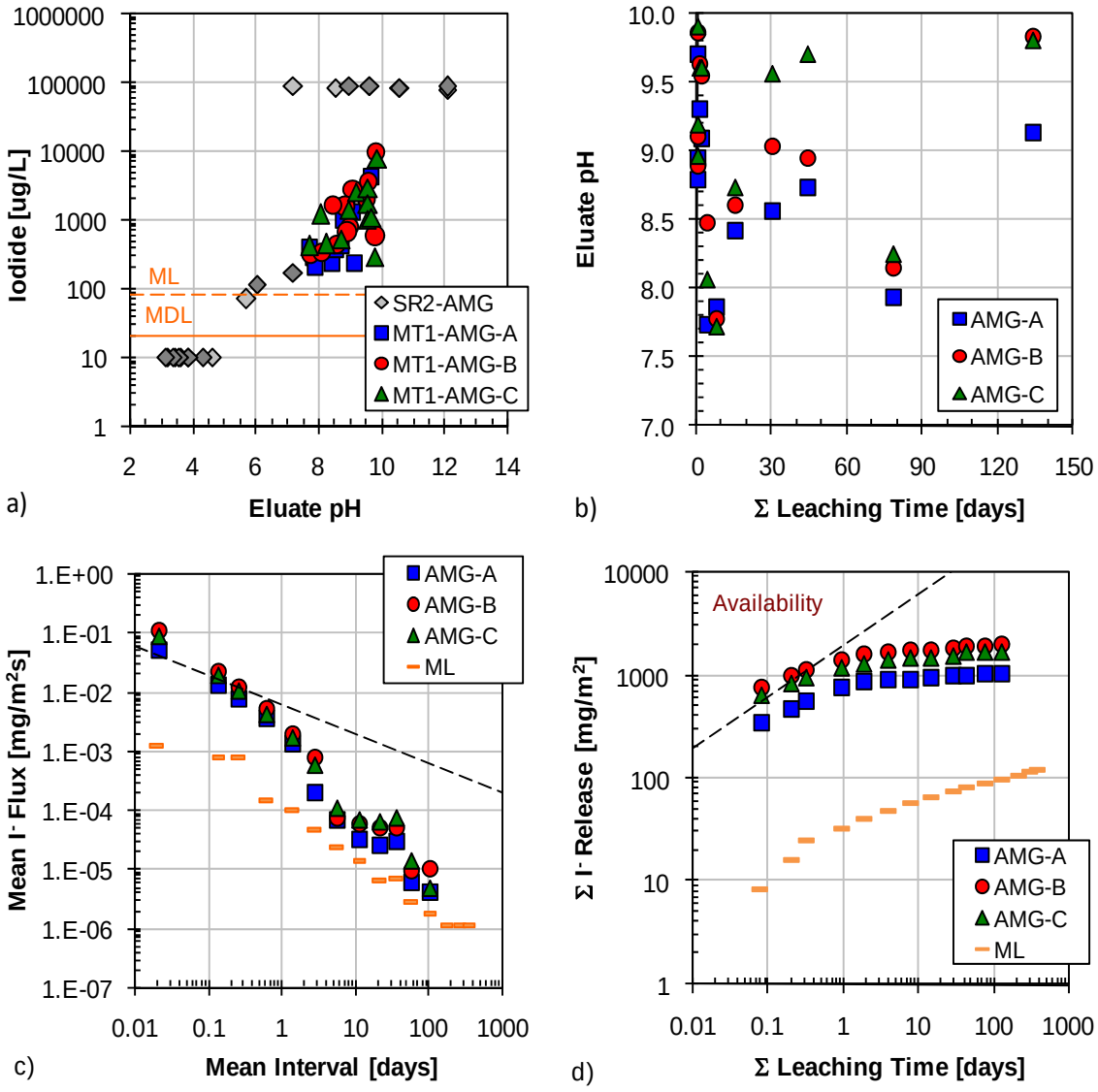

Figure B-22. Iodide leaching test results from AMG: a) comparison of tank leach test eluants to saturation values (SR02 data) and QA/QC parameters, b) pH evolution in tank leach eluants, c) interval flux from tank leach test in comparison to flux values at the method limit ($t^{-1/2}$ model shown as dashed line), and d) cumulative mass release ($t^{1/2}$ model shown as dashed line).

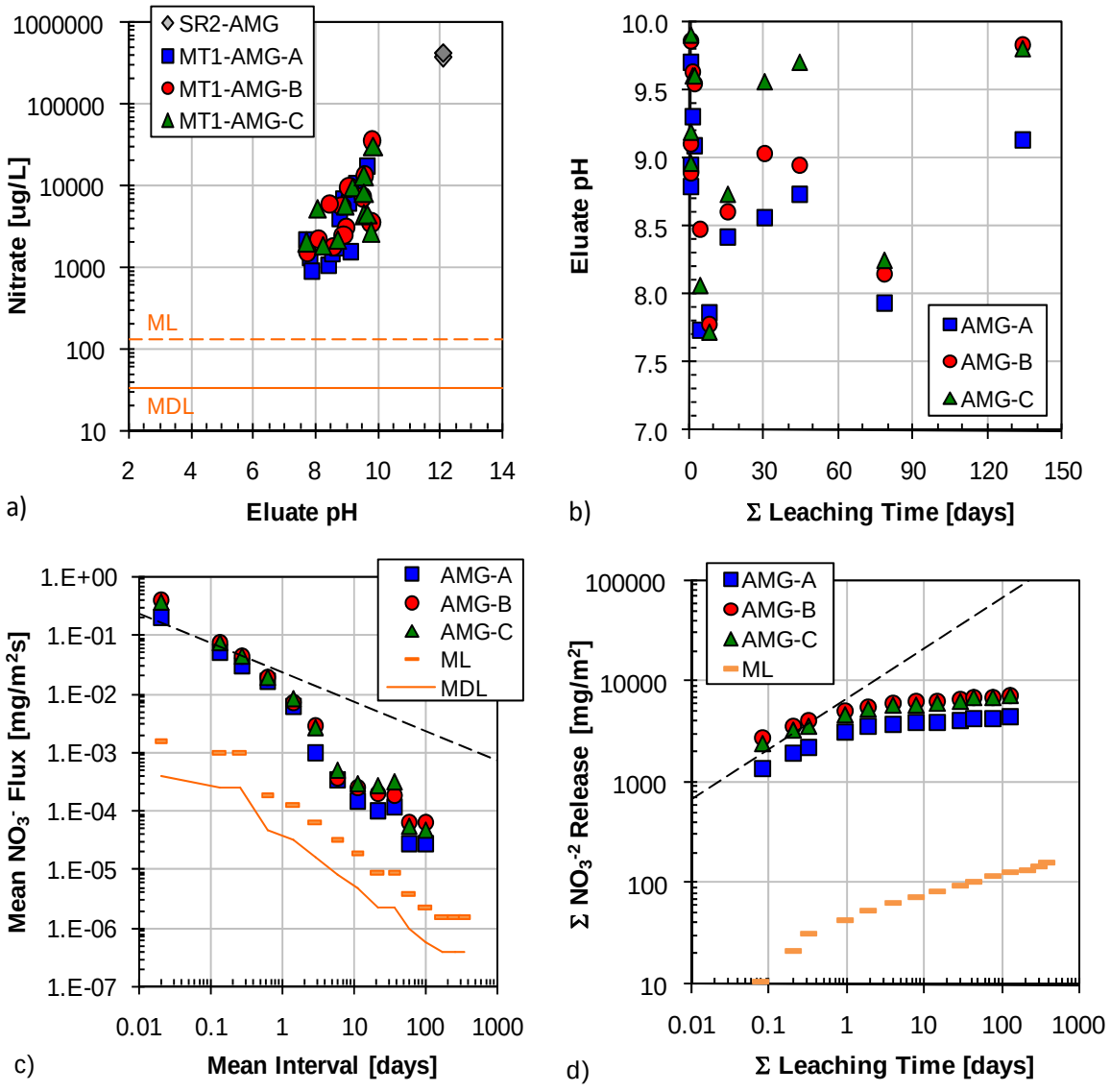

Figure B-23. Nitrate leaching test results from AMG: a) comparison of tank leach test eluants to saturation values (SR02 data) and QA/QC parameters, b) pH evolution in tank leach eluants, c) interval flux from tank leach test in comparison to flux values at the method limit ($t^{-1/2}$ model shown as dashed line), and d) cumulative mass release ($t^{1/2}$ model shown as dashed line).

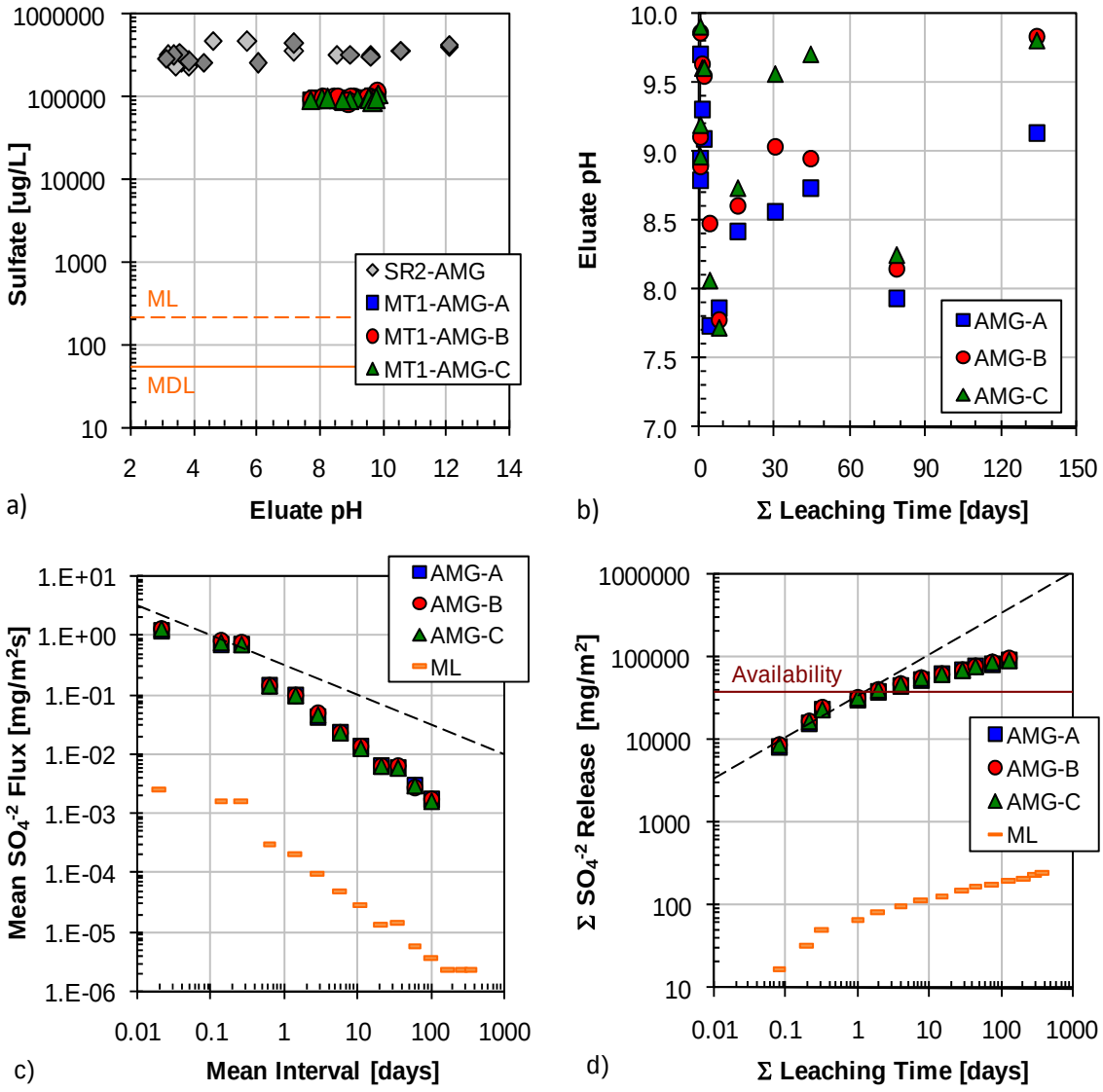

Figure B-24. Sulfate leaching test results from AMG: a) comparison of tank leach test eluants to saturation values (SR02 data) and QA/QC parameters, b) pH evolution in tank leach eluants, c) interval flux from tank leach test in comparison to flux values at the method limit ($t^{-1/2}$ model shown as dashed line), and d) cumulative mass release ($t^{1/2}$ model shown as dashed line).

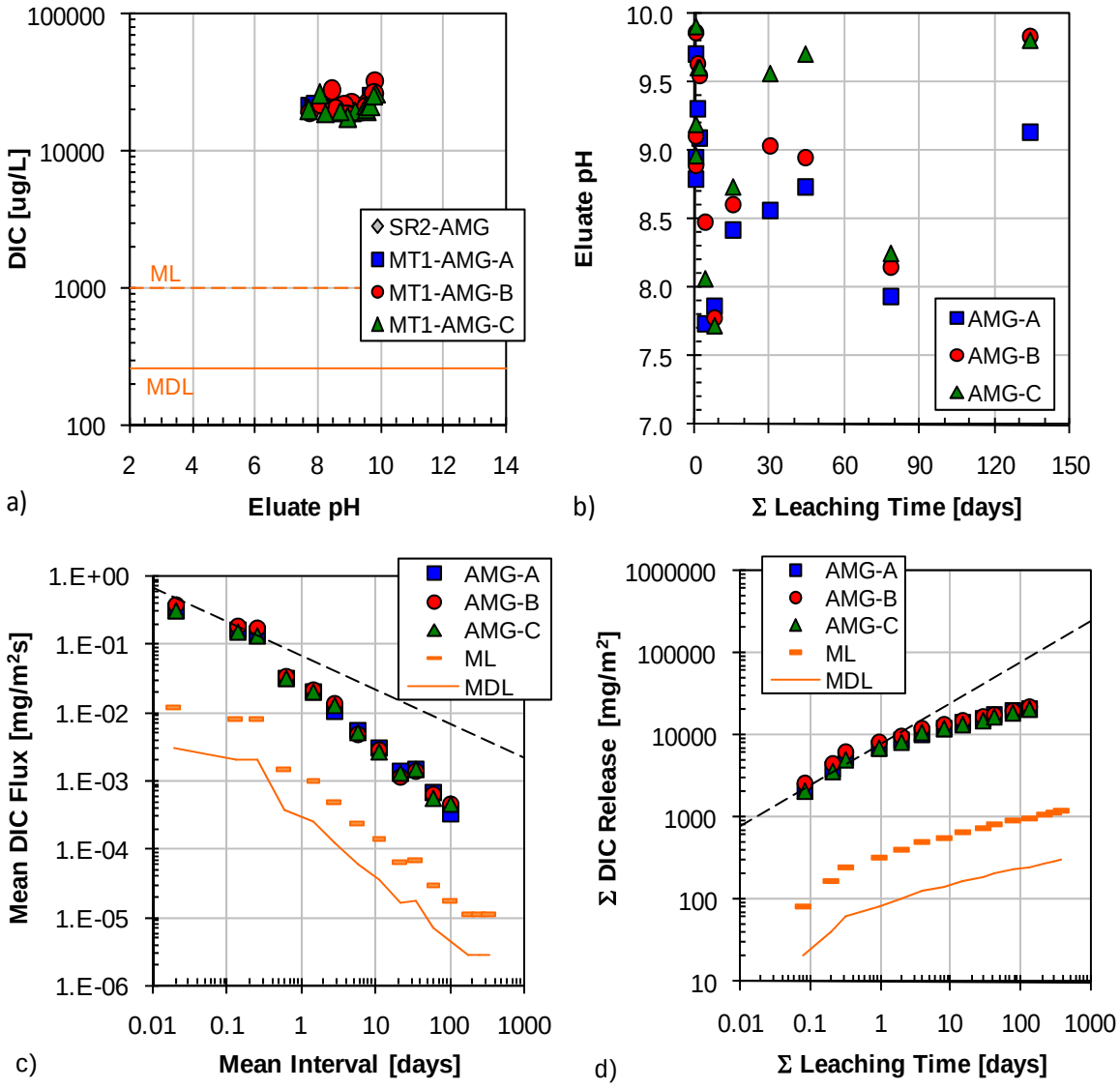

Figure B-25. Dissolved inorganic carbon (DIC) test results from AMG: a) comparison of tank leach test eluants to saturation values (SR02 data) and QA/QC parameters, b) pH evolution in tank leach eluants, c) interval flux from tank leach test in comparison to flux values at the method limit ($t^{-1/2}$ model shown as dashed line), and d) cumulative mass release ($t^{1/2}$ model shown as dashed line).

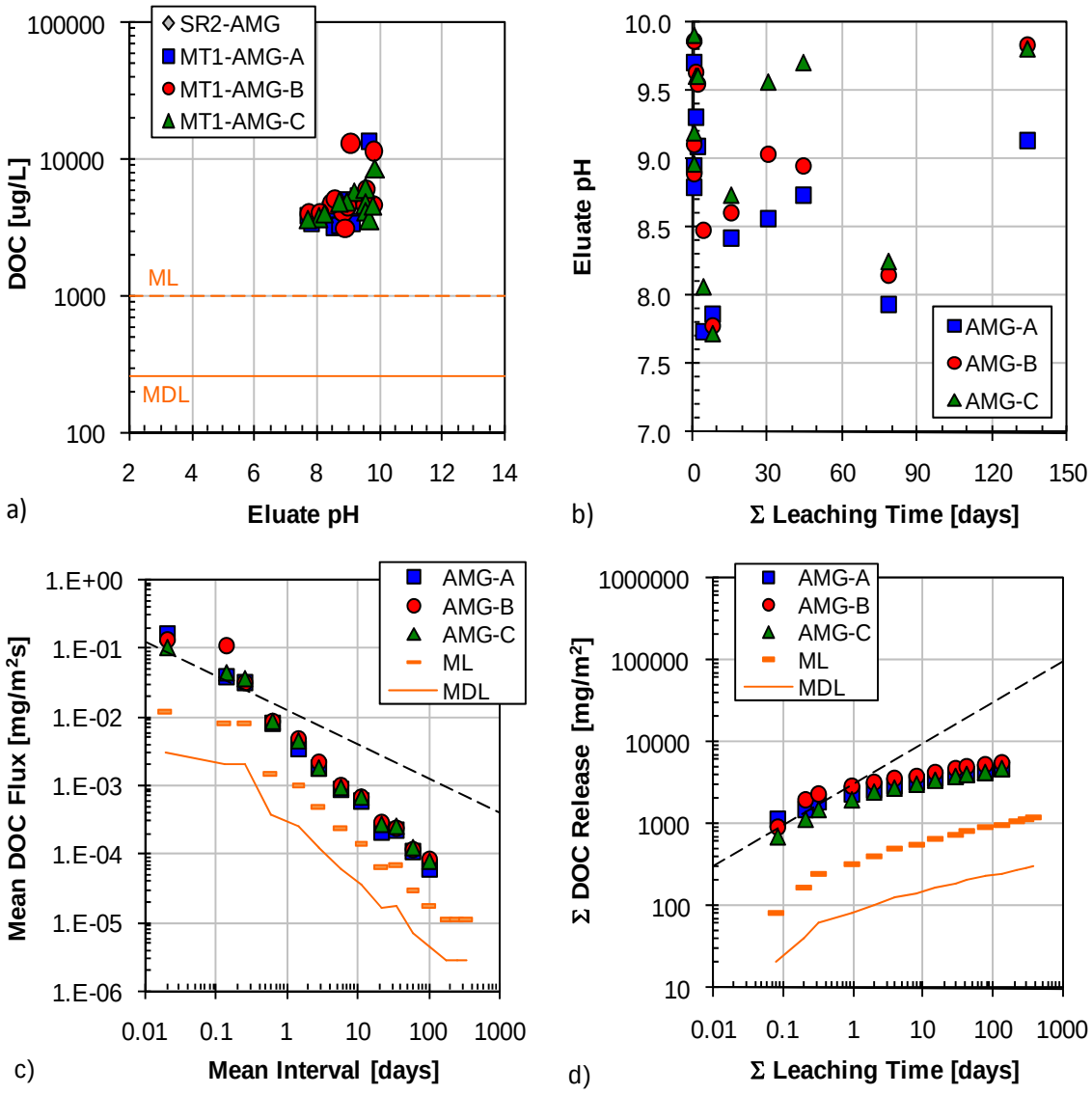

Figure B-26. Dissolved organic carbon (DOC) leaching test results from AMG: a) comparison of tank leach test eluants to saturation values (SR02 data) and QA/QC parameters, b) pH evolution in tank leach eluants, c) interval flux from tank leach test in comparison to flux values at the method limit ($t^{-1/2}$ model shown as dashed line), and d) cumulative mass release ($t^{1/2}$ model shown as dashed line).

Secondary Waste in SHG (SWG)

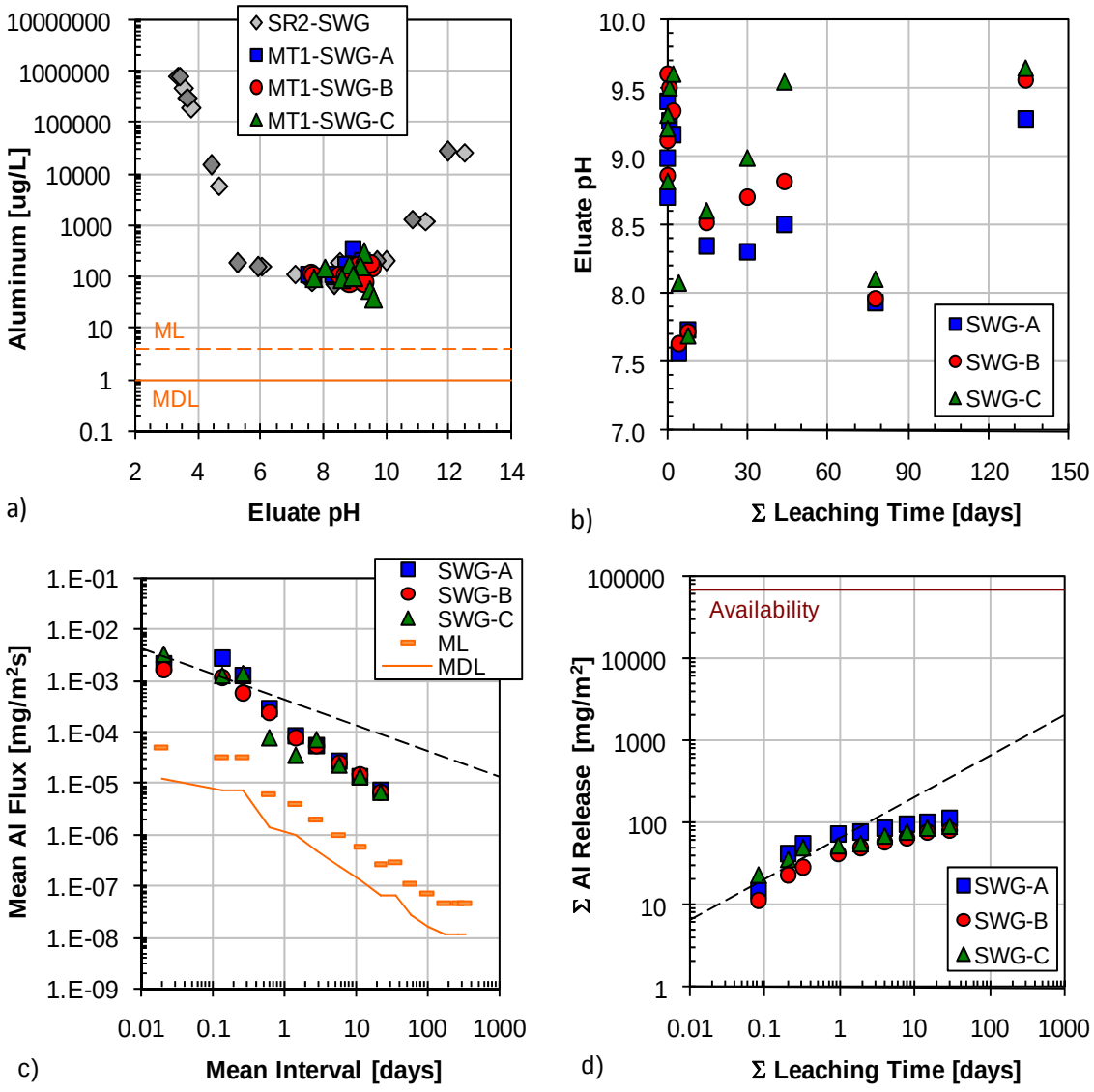

Figure B-27. Aluminum leaching test results from SWG: a) comparison of tank leach test eluants to saturation values (SR02 data) and QA/QC parameters, b) pH evolution in tank leach eluants, c) interval flux from tank leach test in comparison to flux values at the method limit ($t^{-1/2}$ model for AMG shown as dashed line), and d) cumulative mass release ($t^{1/2}$ model for AMG shown as dashed line).

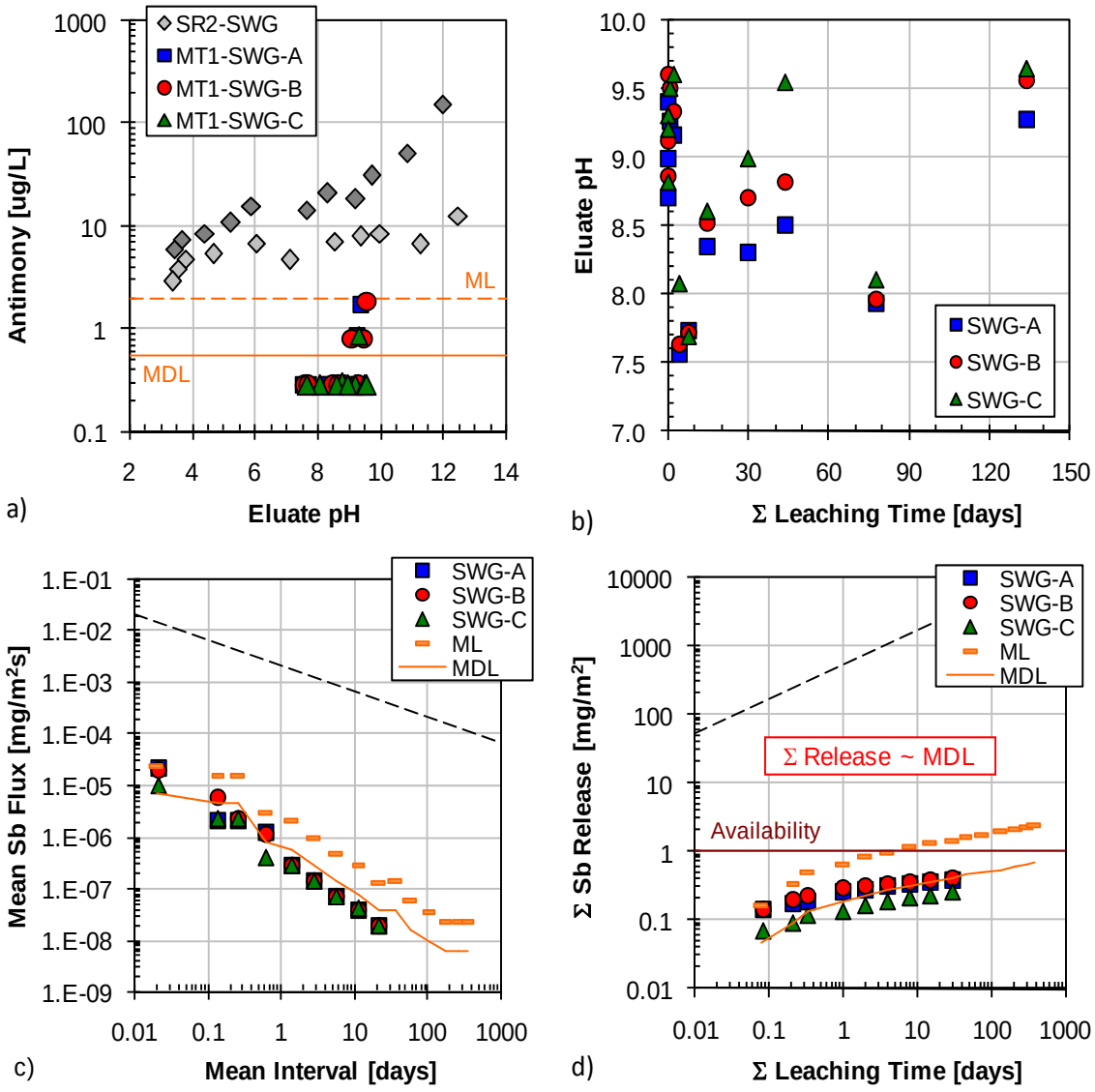

Figure B-28. Antimony leaching test results from SWG: a) comparison of tank leach test eluants to saturation values (SR02 data) and QA/QC parameters, b) pH evolution in tank leach eluants, c) interval flux from tank leach test in comparison to flux values at the method limit ($t^{-1/2}$ model for AMG shown as dashed line), and d) cumulative mass release ($t^{1/2}$ model for AMG shown as dashed line).

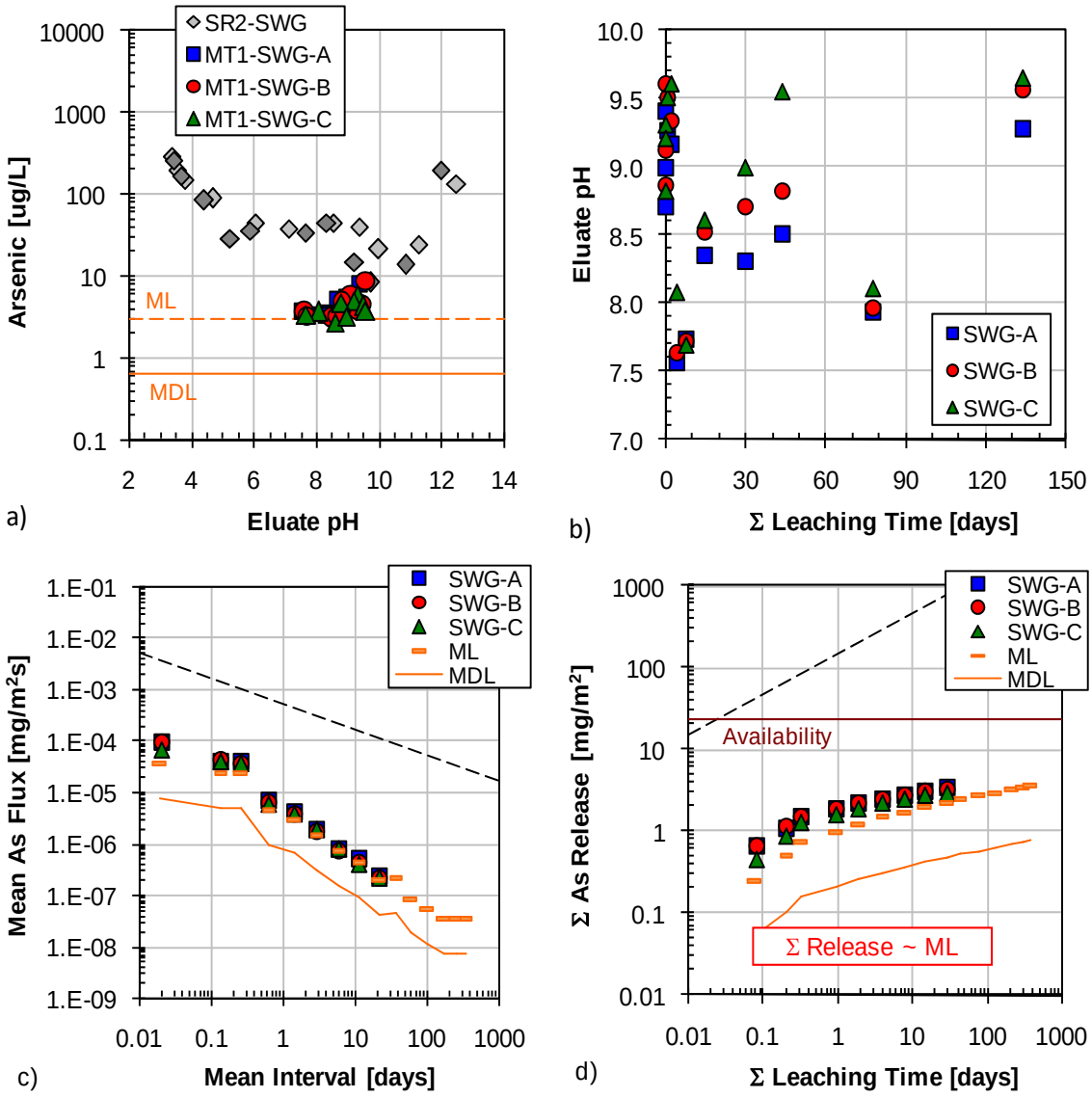

Figure B-29. Arsenic leaching test results from SWG: a) comparison of tank leach test eluants to saturation values (SR02 data) and QA/QC parameters, b) pH evolution in tank leach eluants, c) interval flux from tank leach test in comparison to flux values at the method limit ($t^{-1/2}$ model for AMG shown as dashed line), and d) cumulative mass release ($t^{1/2}$ model for AMG shown as dashed line).

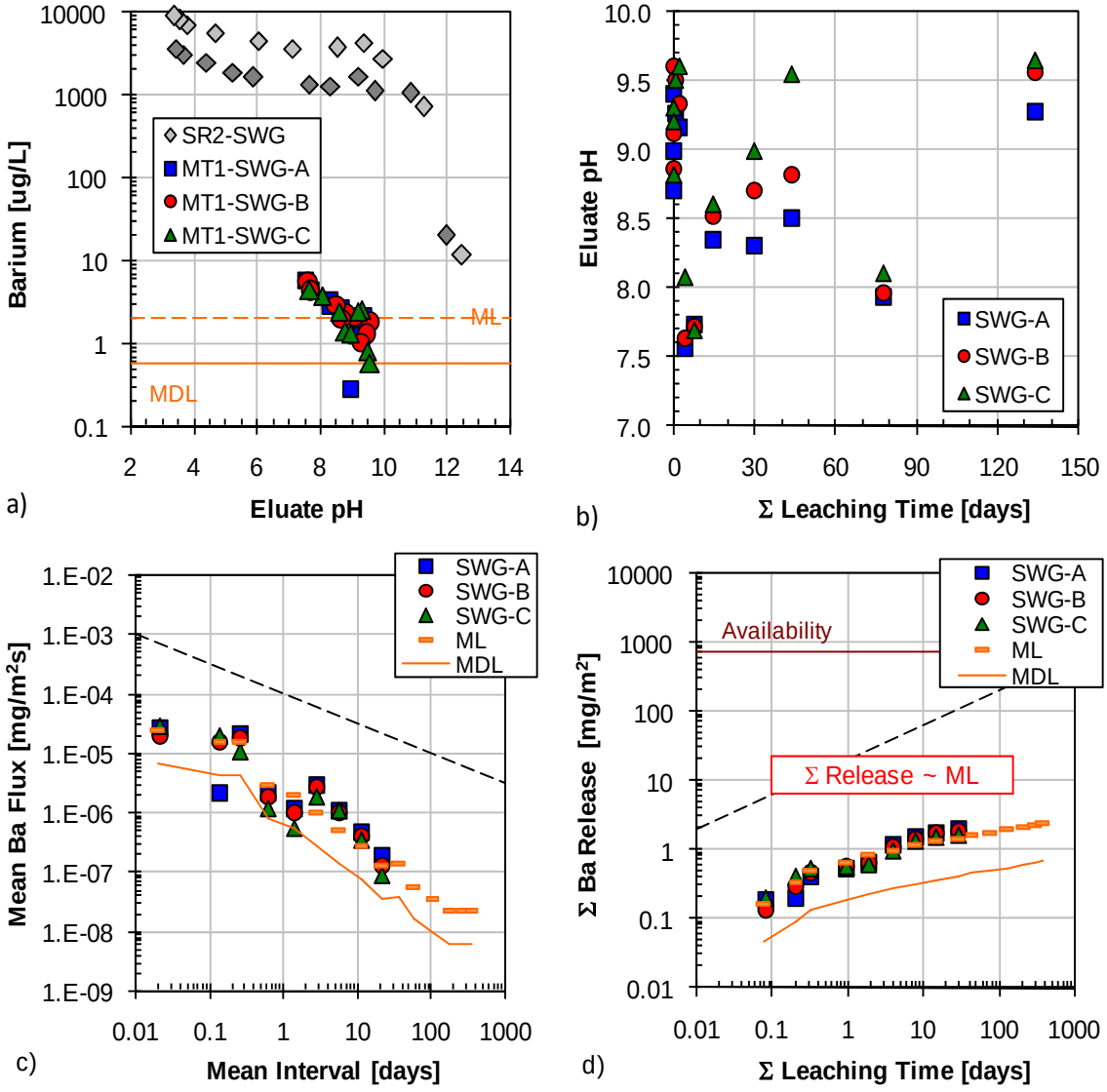

Figure B-30. Barium leaching test results from SWG: a) comparison of tank leach test eluants to saturation values (SR02 data) and QA/QC parameters, b) pH evolution in tank leach eluants, c) interval flux from tank leach test in comparison to flux values at the method limit ($t^{-1/2}$ model for AMG shown as dashed line), and d) cumulative mass release ($t^{1/2}$ model for AMG shown as dashed line).

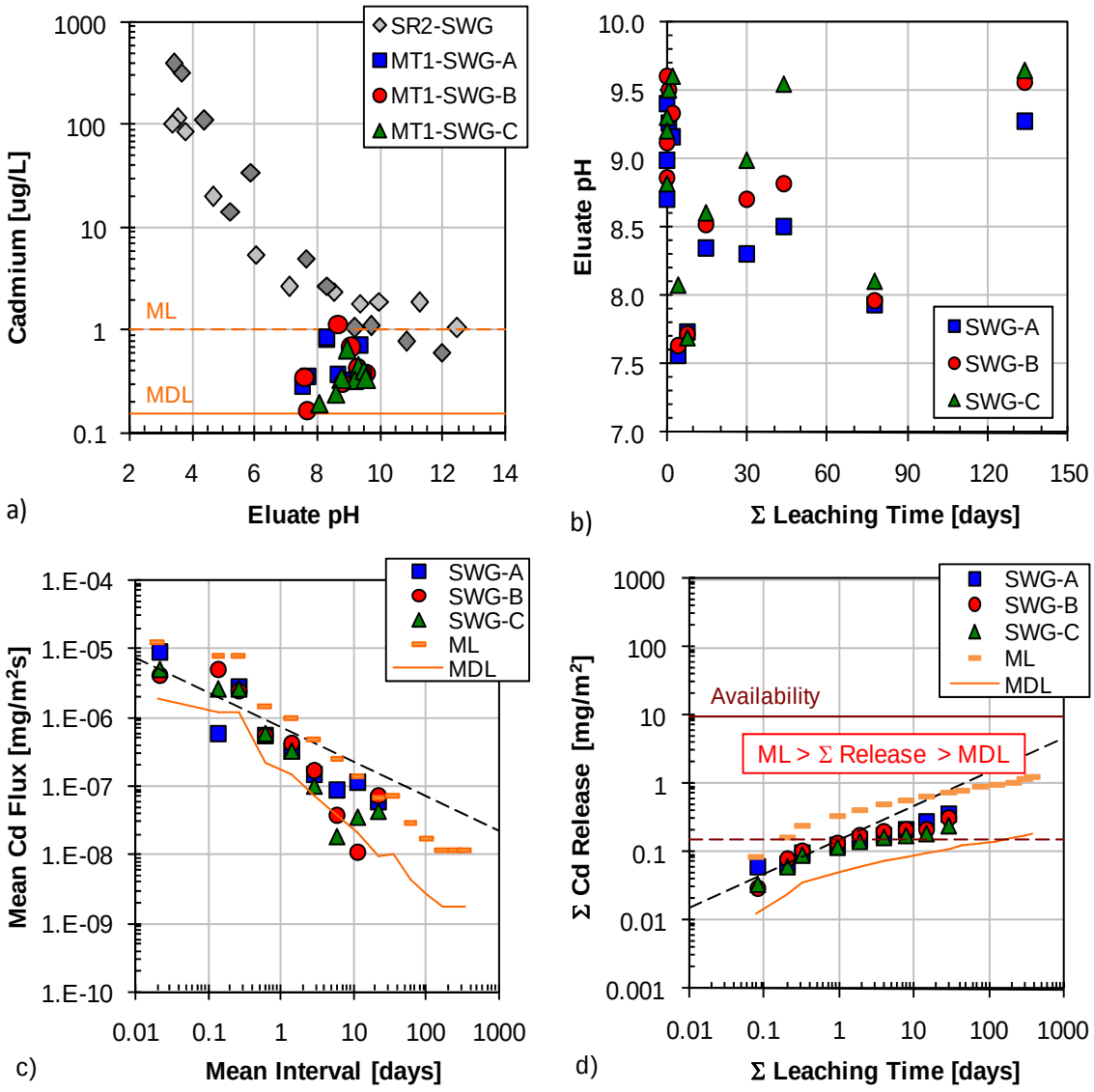

Figure B-31. Cadmium leaching test results from SWG: a) comparison of tank leach test eluants to saturation values (SR02 data) and QA/QC parameters, b) pH evolution in tank leach eluants, c) interval flux from tank leach test in comparison to flux values at the method limit ($t^{-1/2}$ model for AMG shown as dashed line), and d) cumulative mass release ($t^{1/2}$ model for AMG shown as dashed line).

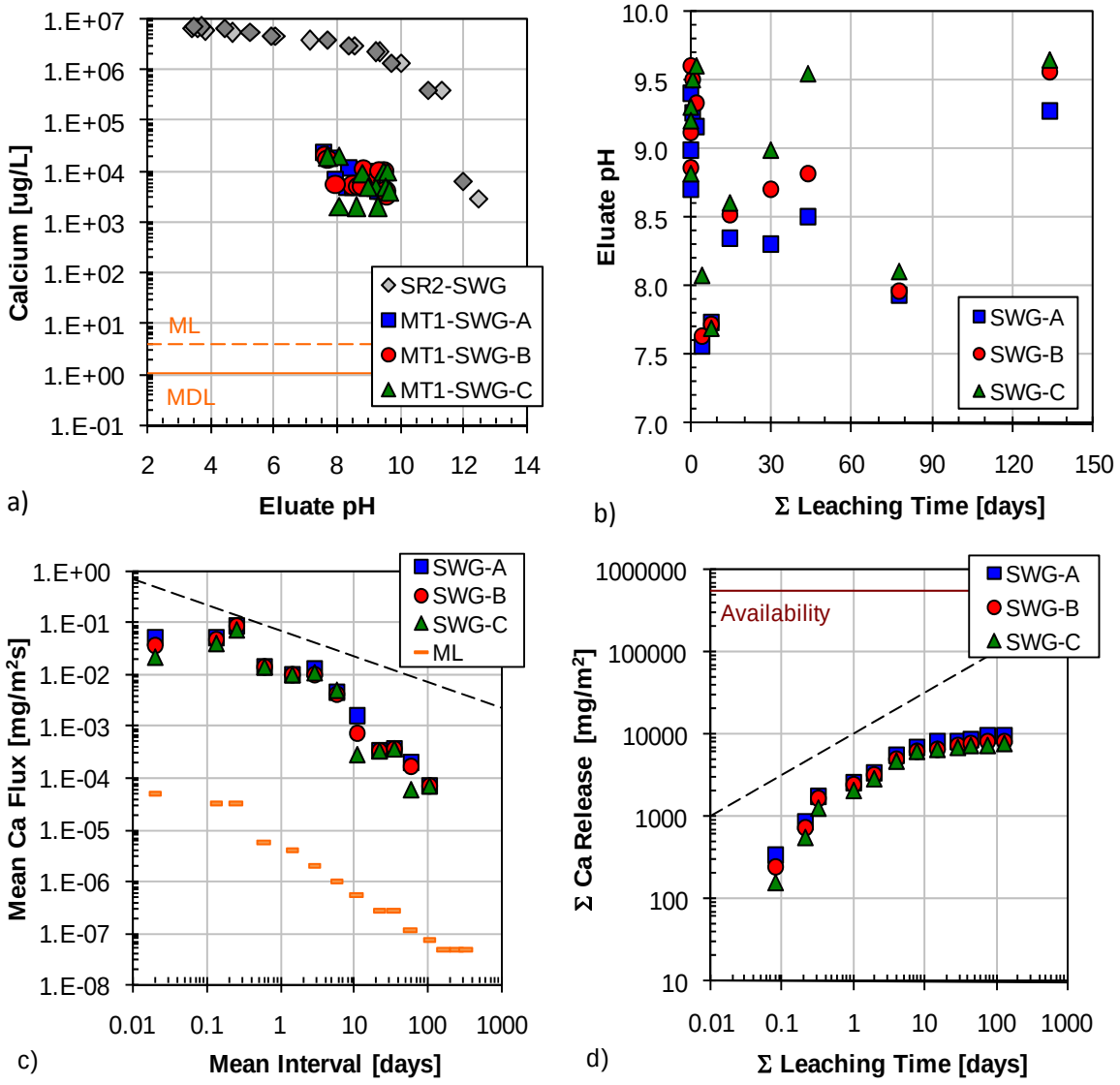

Figure B-32. Calcium leaching test results from SWG: a) comparison of tank leach test eluants to saturation values (SR02 data) and QA/QC parameters, b) pH evolution in tank leach eluants, c) interval flux from tank leach test in comparison to flux values at the method limit ($t^{-1/2}$ model for AMG shown as dashed line), and d) cumulative mass release ($t^{1/2}$ model for AMG shown as dashed line).

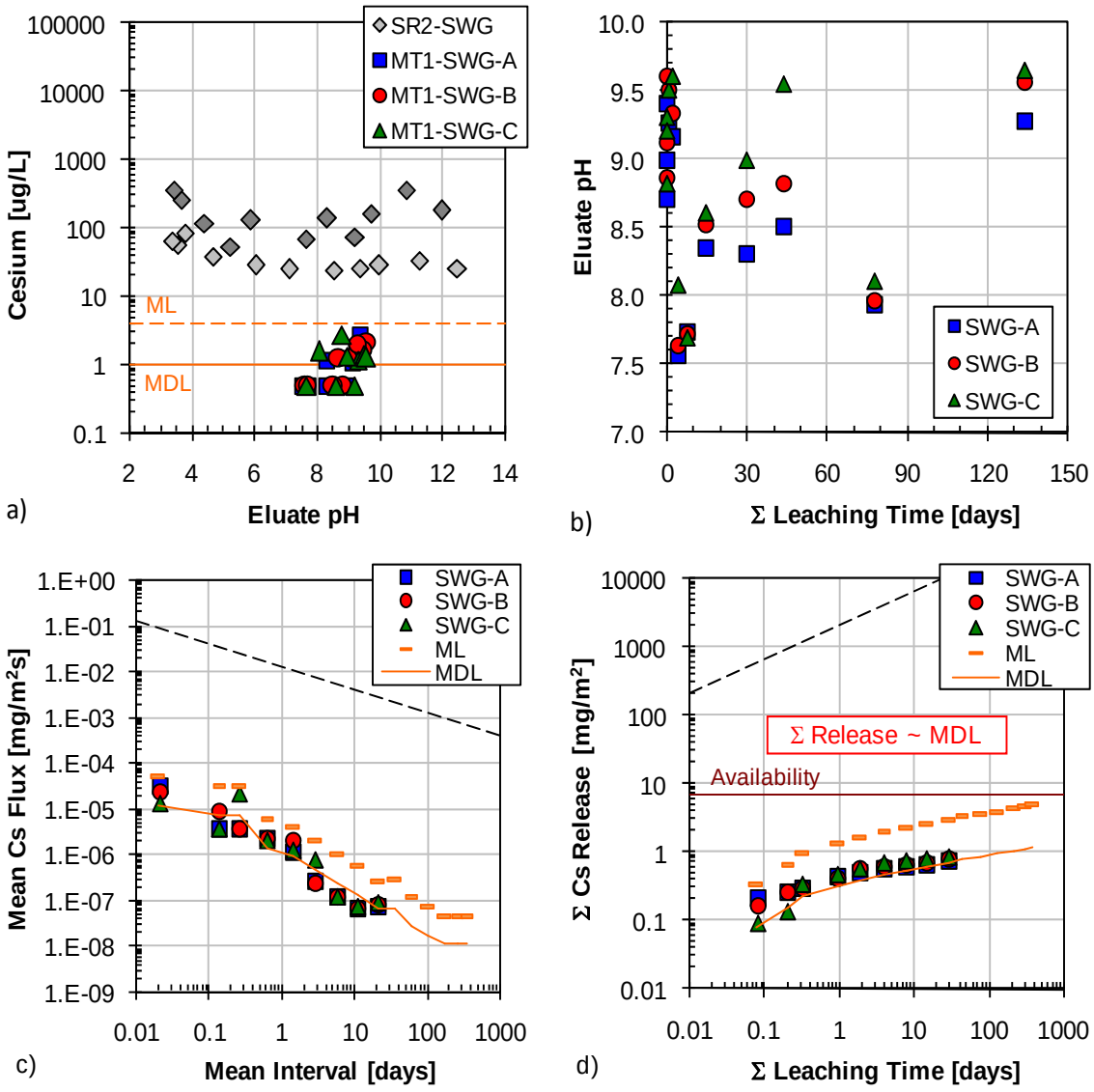

Figure B-33. Cesium leaching test results from SWG: a) comparison of tank leach test eluants to saturation values (SR02 data) and QA/QC parameters, b) pH evolution in tank leach eluants, c) interval flux from tank leach test in comparison to flux values at the method limit ($t^{-1/2}$ model for AMG shown as dashed line), and d) cumulative mass release ($t^{1/2}$ model for AMG shown as dashed line).

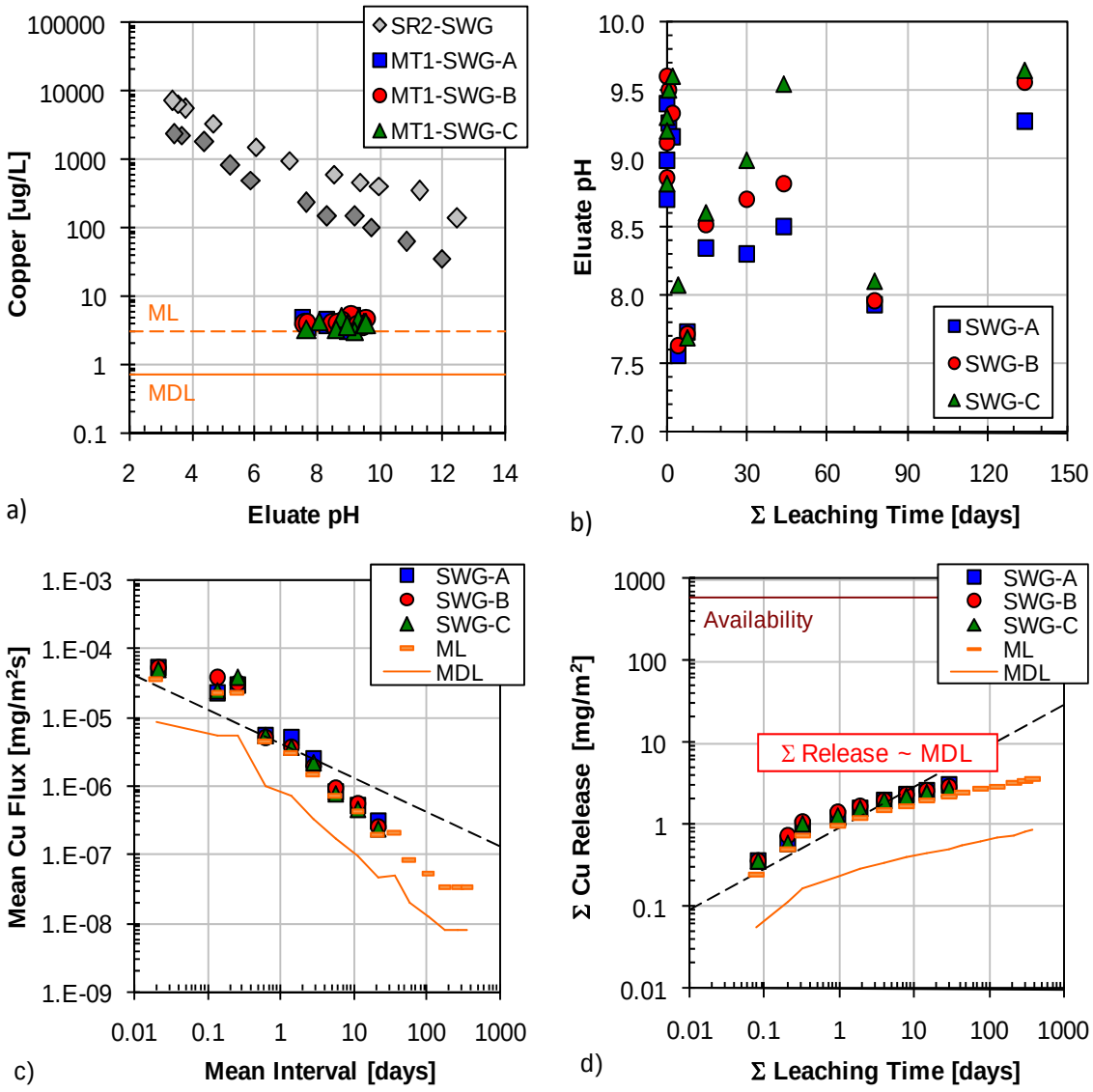

Figure B-34. Copper leaching test results from SWG: a) comparison of tank leach test eluants to saturation values (SR02 data) and QA/QC parameters, b) pH evolution in tank leach eluants, c) interval flux from tank leach test in comparison to flux values at the method limit ($t^{-1/2}$ model for AMG shown as dashed line), and d) cumulative mass release ($t^{1/2}$ model for AMG shown as dashed line).

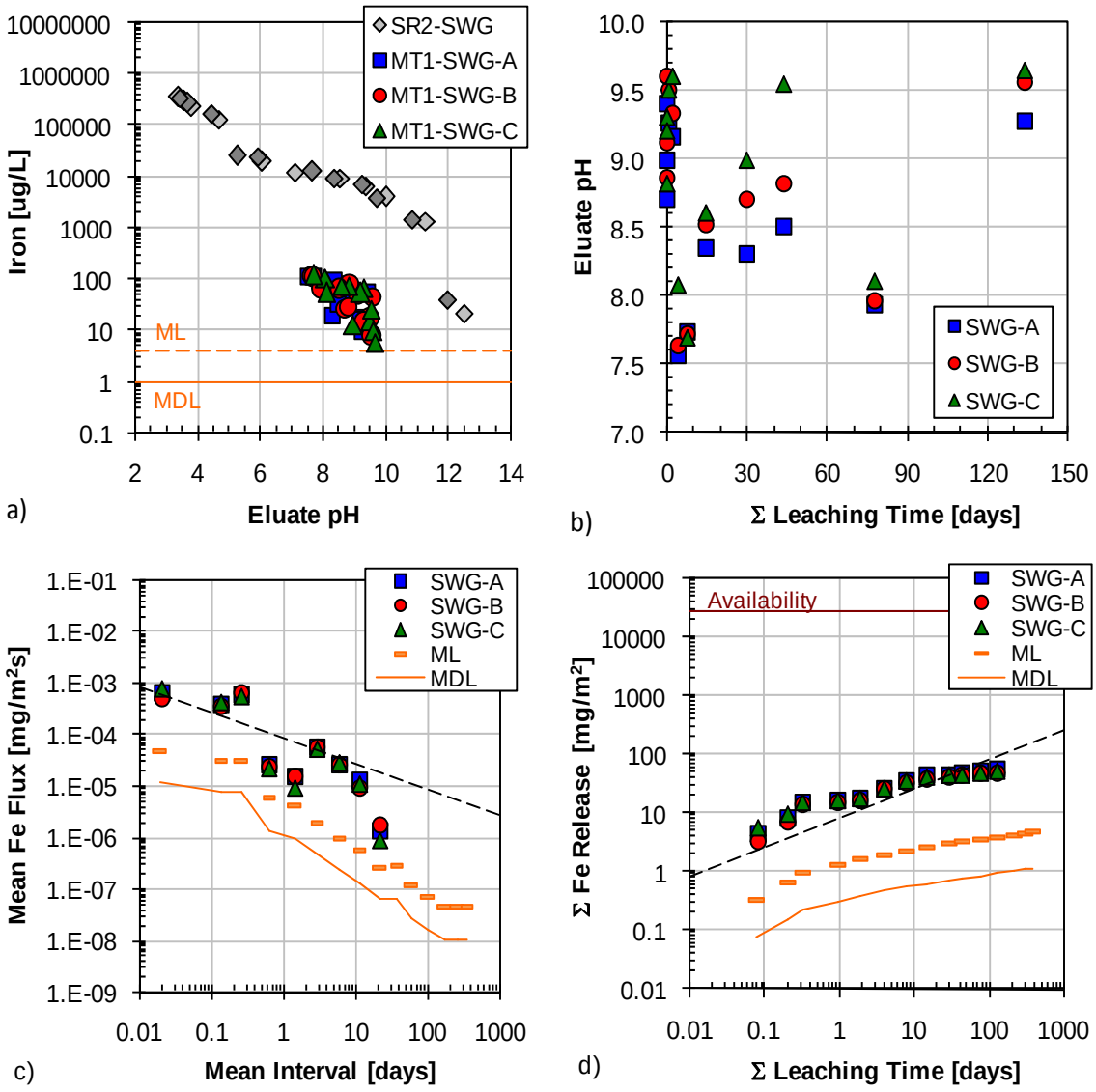

Figure B-35. Iron leaching test results from SWG: a) comparison of tank leach test eluants to saturation values (SR02 data) and QA/QC parameters, b) pH evolution in tank leach eluants, c) interval flux from tank leach test in comparison to flux values at the method limit ($t^{-1/2}$ model for AMG shown as dashed line), and d) cumulative mass release ($t^{1/2}$ model for AMG shown as dashed line).

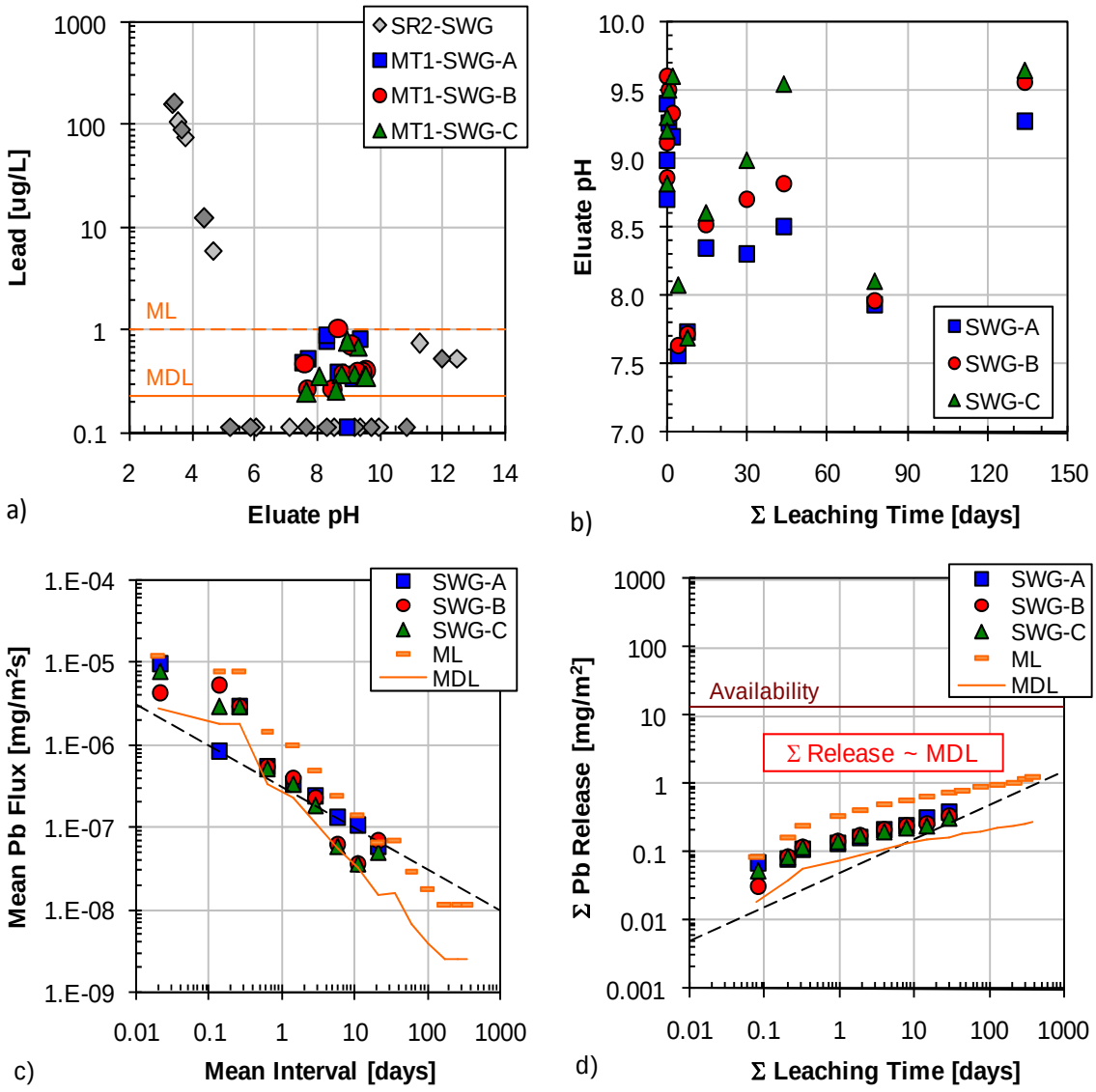

Figure B-36. Lead leaching test results from SWG: a) comparison of tank leach test eluants to saturation values (SR02 data) and QA/QC parameters, b) pH evolution in tank leach eluants, c) interval flux from tank leach test in comparison to flux values at the method limit ($t^{-1/2}$ model for AMG shown as dashed line), and d) cumulative mass release ($t^{1/2}$ model for AMG shown as dashed line).

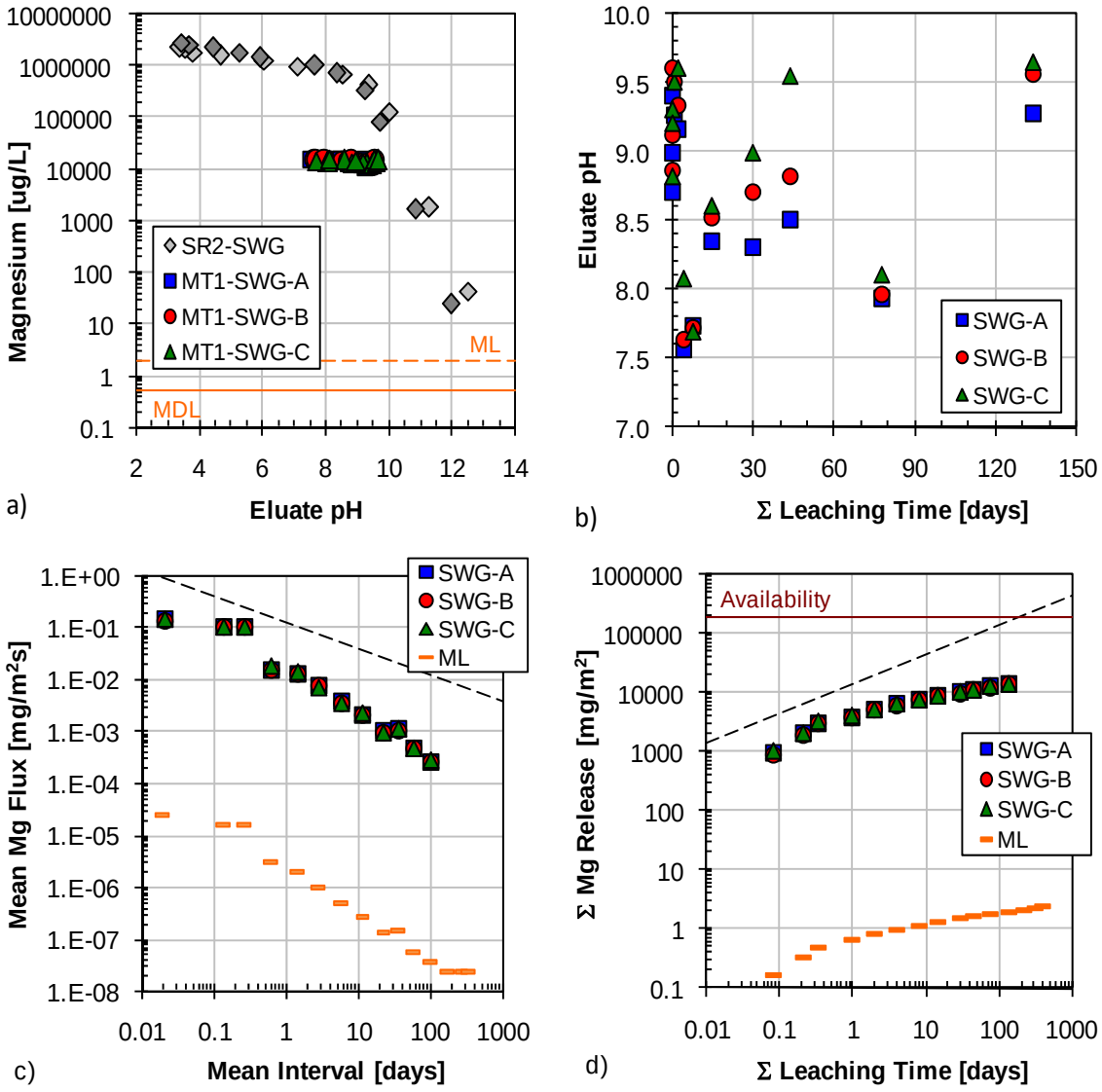

Figure B-37. Magnesium leaching test results from SWG matrix: a) comparison of tank leach test eluants to saturation values (SR02 data) and QA/QC parameters, b) pH evolution in tank leach eluants, c) interval flux from tank leach test in comparison to flux values at the method limit ($t^{-1/2}$ model for AMG shown as dashed line), and d) cumulative mass release ($t^{1/2}$ model for AMG shown as dashed line).

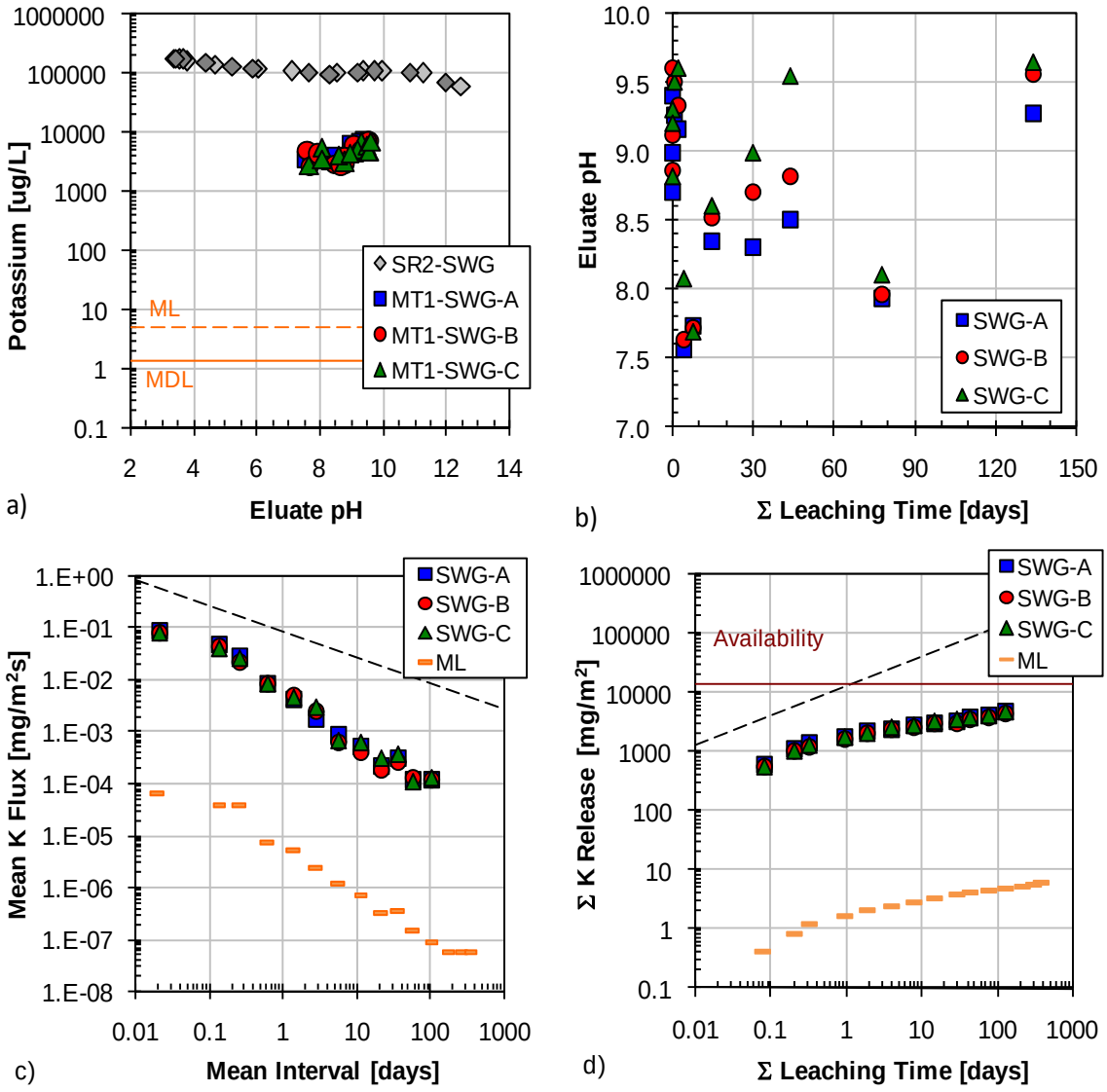

Figure B-38. Potassium leaching test results from SWG matrix: a) comparison of tank leach test eluants to saturation values (SR02 data) and QA/QC parameters, b) pH evolution in tank leach eluants, c) interval flux from tank leach test in comparison to flux values at the method limit ($t^{-1/2}$ model for AMG shown as dashed line), and d) cumulative mass release ($t^{1/2}$ model for AMG shown as dashed line).

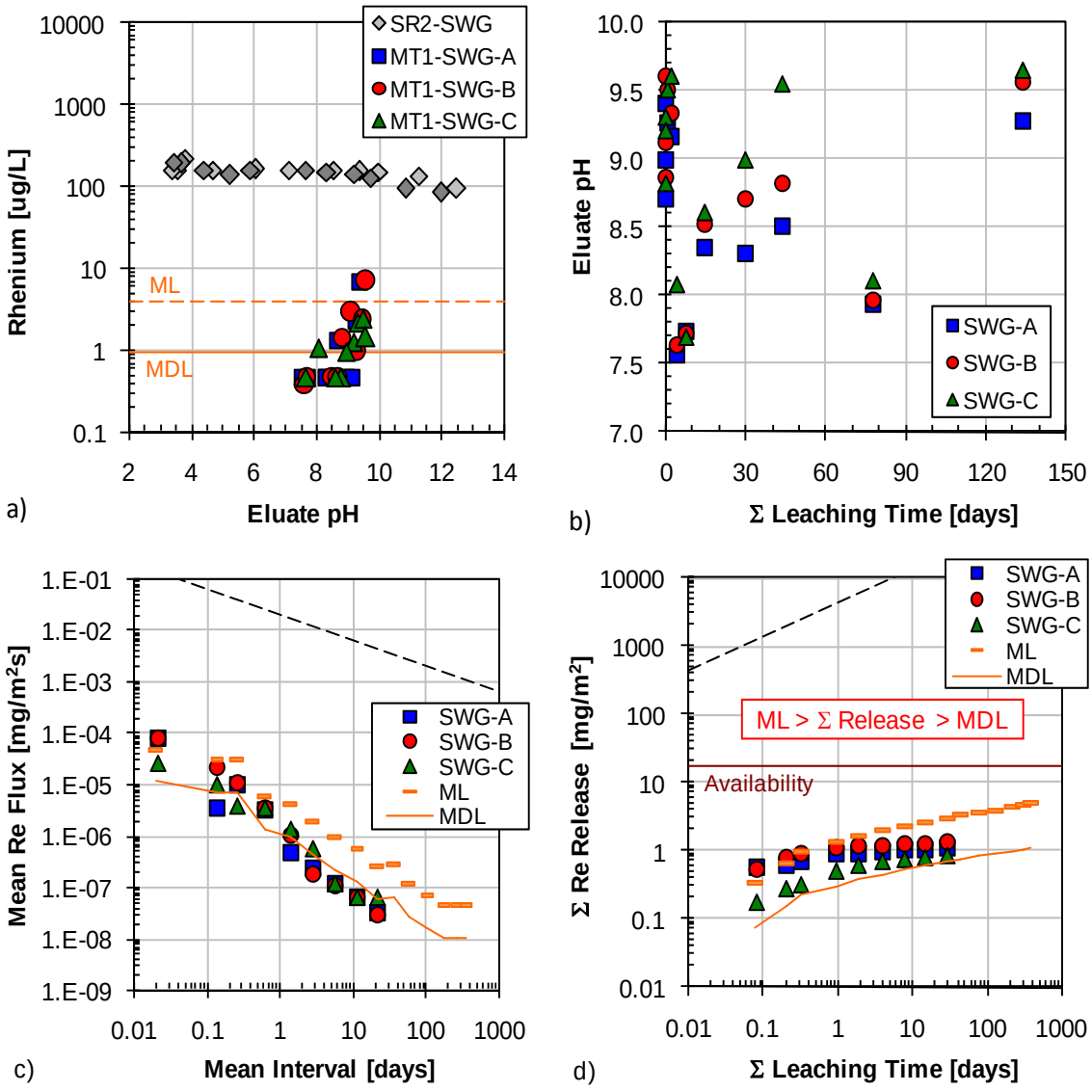

Figure B-39. Rhenium leaching test results from SWG matrix: a) comparison of tank leach test eluants to saturation values (SR02 data) and QA/QC parameters, b) pH evolution in tank leach eluants, c) interval flux from tank leach test in comparison to flux values at the method limit ($t^{-1/2}$ model for AMG shown as dashed line), and d) cumulative mass release ($t^{1/2}$ model for AMG shown as dashed line).

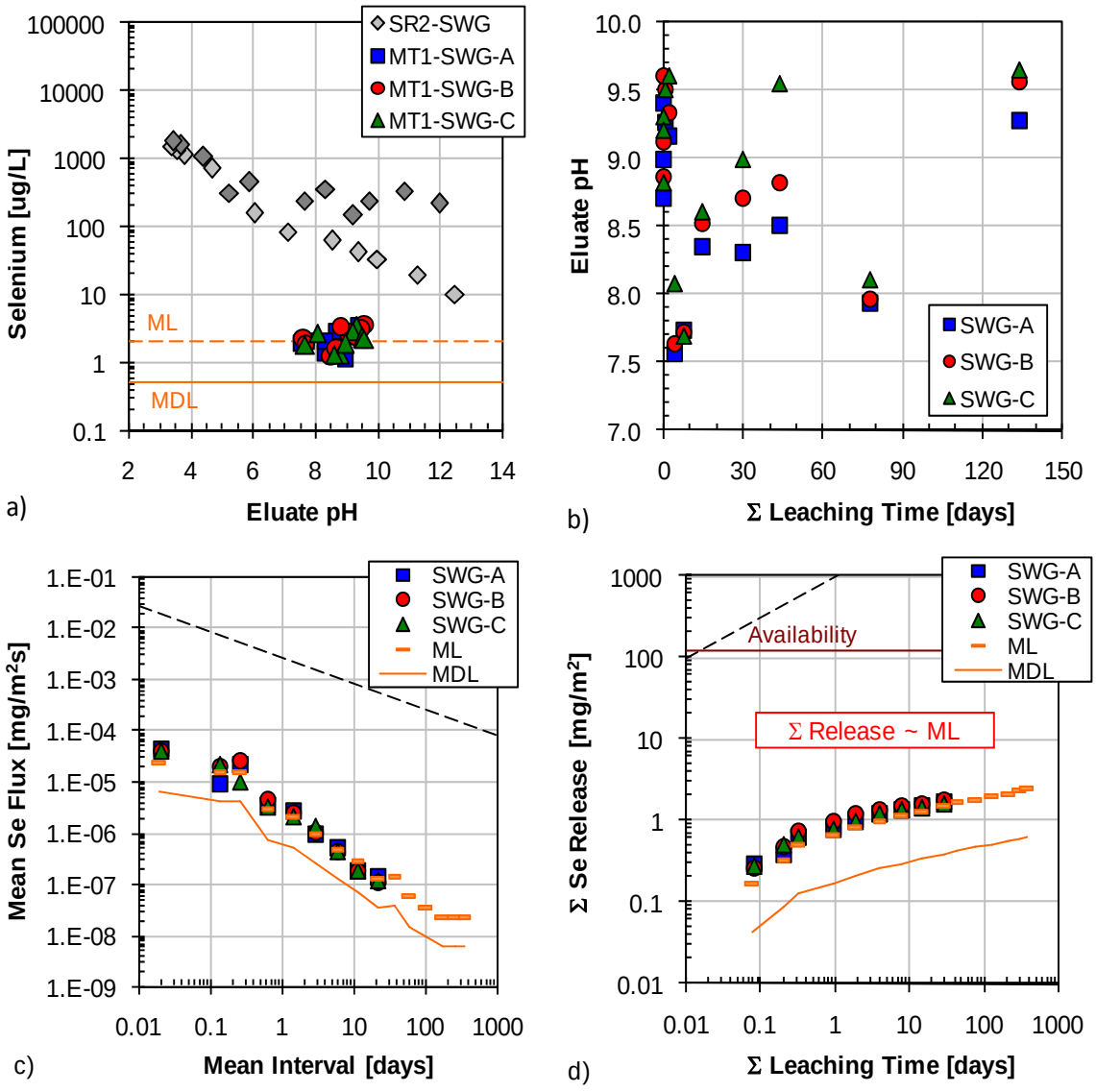

Figure B-40. Selenium leaching test results from SWG matrix: a) comparison of tank leach test eluants to saturation values (SR02 data) and QA/QC parameters, b) pH evolution in tank leach eluants, c) interval flux from tank leach test in comparison to flux values at the method limit ($t^{-1/2}$ model for AMG shown as dashed line), and d) cumulative mass release ($t^{1/2}$ model for AMG shown as dashed line).

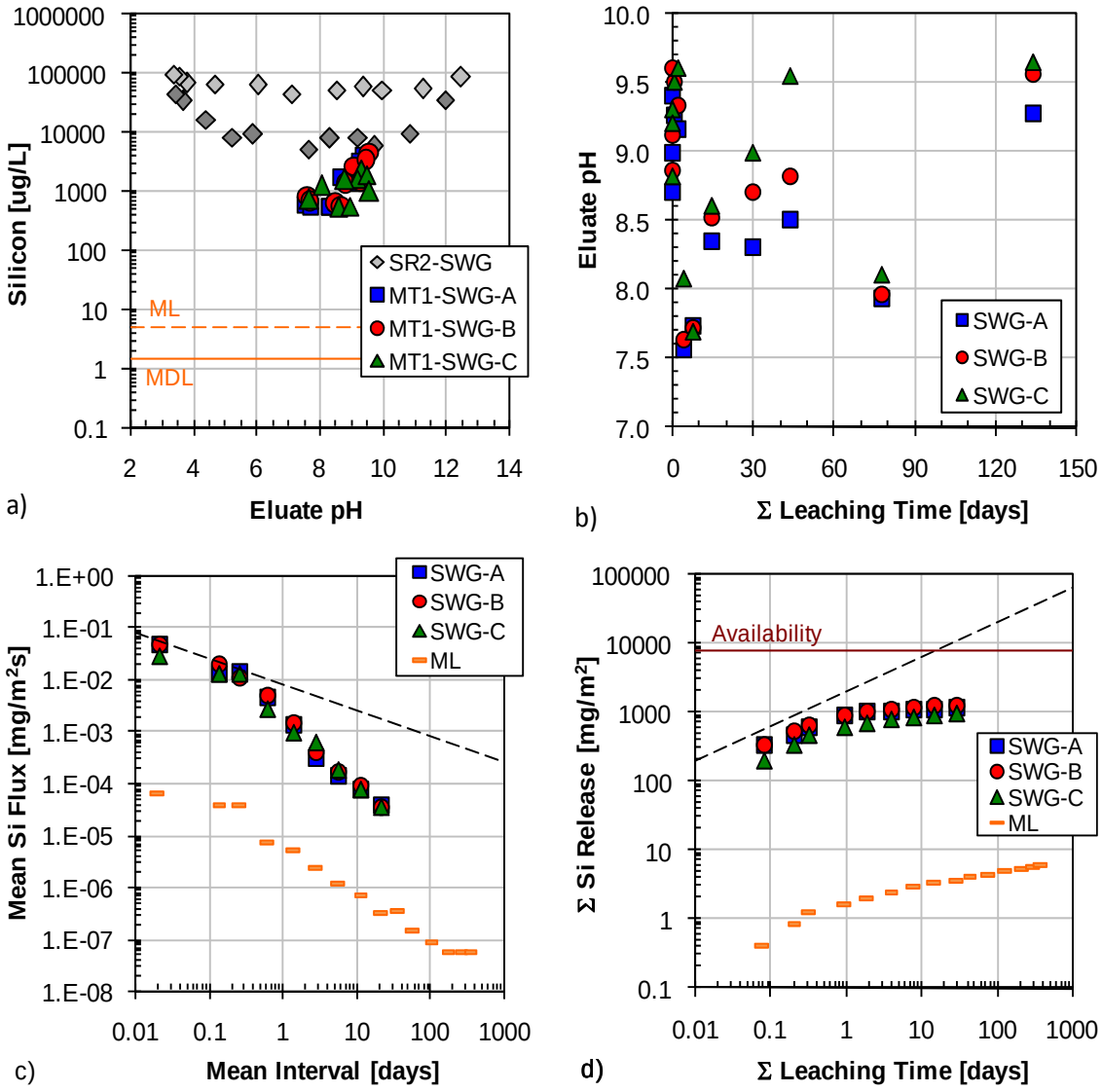

Figure B-41. Silicon leaching test results from SWG matrix: a) comparison of tank leach test eluants to saturation values (SR02 data) and QA/QC parameters, b) pH evolution in tank leach eluants, c) interval flux from tank leach test in comparison to flux values at the method limit ($t^{-1/2}$ model for AMG shown as dashed line), and d) cumulative mass release ($t^{1/2}$ model for AMG shown as dashed line).

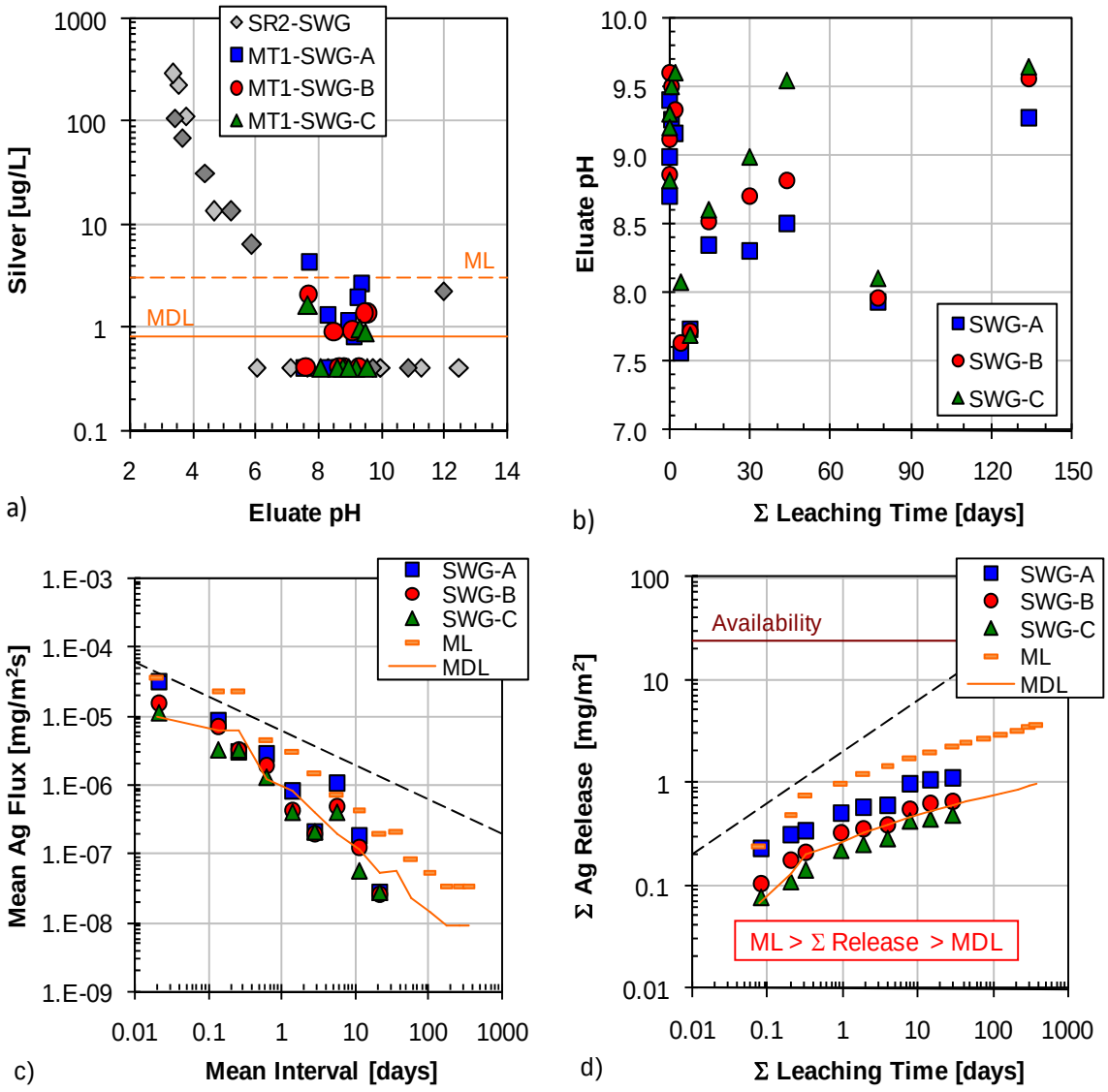

Figure B-42. Silver leaching test results from SWG matrix: a) comparison of tank leach test eluants to saturation values (SR02 data) and QA/QC parameters, b) pH evolution in tank leach eluants, c) interval flux from tank leach test in comparison to flux values at the method limit ($t^{-1/2}$ model for AMG shown as dashed line), and d) cumulative mass release ($t^{1/2}$ model for AMG shown as dashed line).

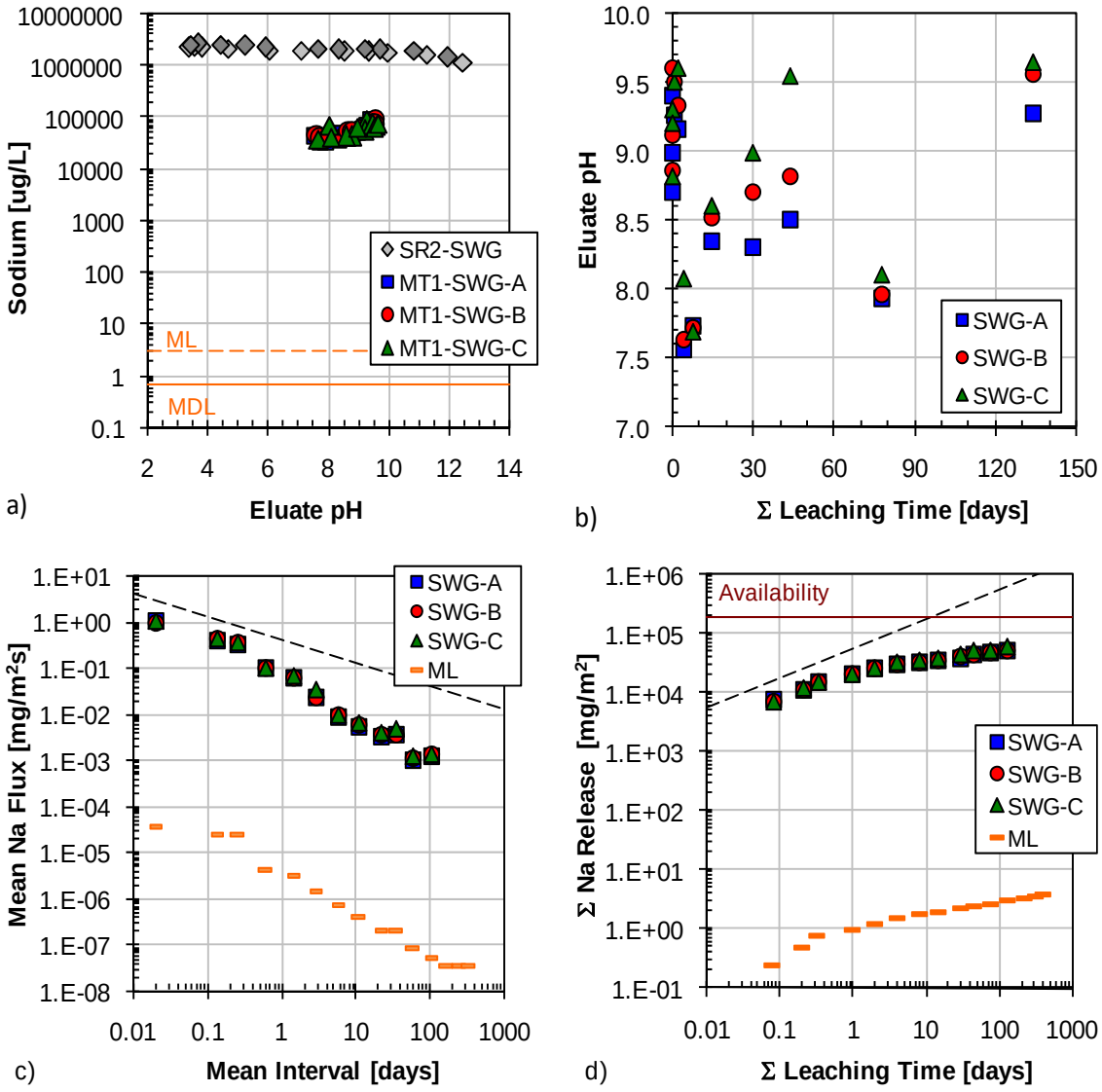

Figure B-43. Sodium leaching test results from SWG matrix: a) comparison of tank leach test eluants to saturation values (SR02 data) and QA/QC parameters, b) pH evolution in tank leach eluants, c) interval flux from tank leach test in comparison to flux values at the method limit ($t^{-1/2}$ model for AMG shown as dashed line), and d) cumulative mass release ($t^{1/2}$ model for AMG shown as dashed line).

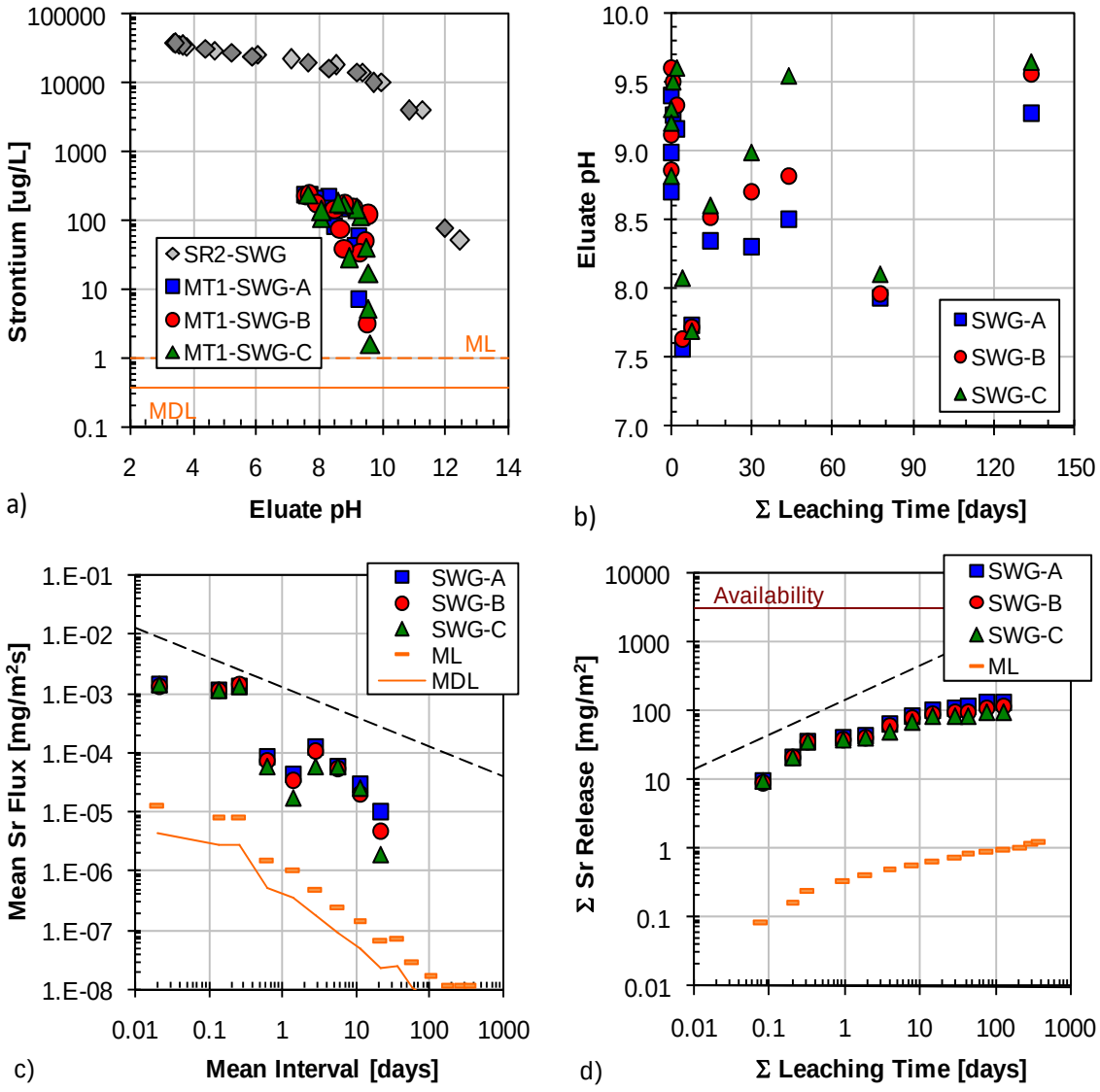

Figure B-44. Strontium leaching test results from SWG matrix: a) comparison of tank leach test eluants to saturation values (SR02 data) and QA/QC parameters, b) pH evolution in tank leach eluants, c) interval flux from tank leach test in comparison to flux values at the method limit ($t^{-1/2}$ model for AMG shown as dashed line), and d) cumulative mass release ($t^{1/2}$ model for AMG shown as dashed line).

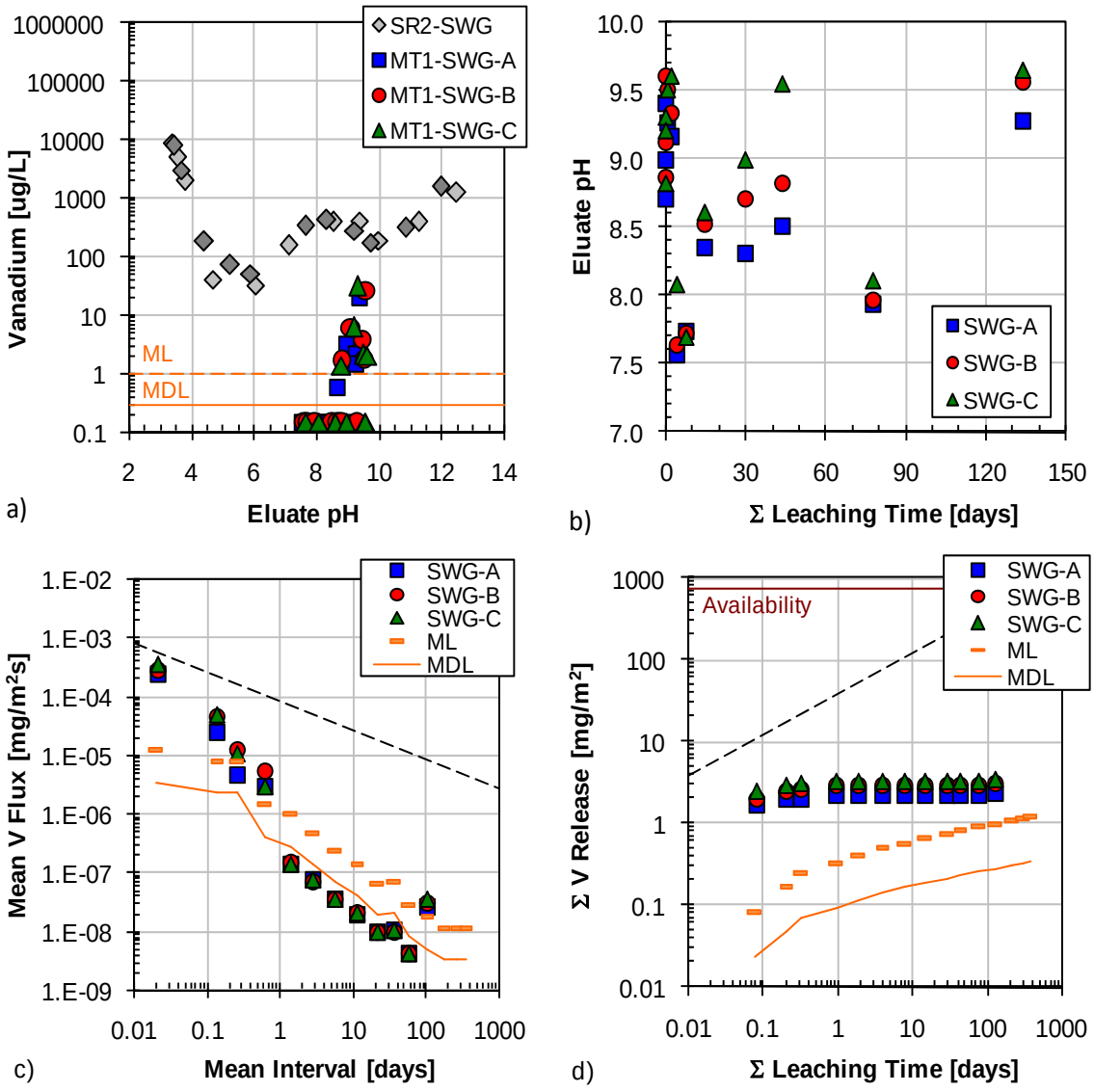

Figure B-45. Vanadium leaching test results from SWG matrix: a) comparison of tank leach test eluants to saturation values (SR02 data) and QA/QC parameters, b) pH evolution in tank leach eluants, c) interval flux from tank leach test in comparison to flux values at the method limit ($t^{-1/2}$ model for AMG shown as dashed line), and d) cumulative mass release ($t^{1/2}$ model for AMG shown as dashed line).

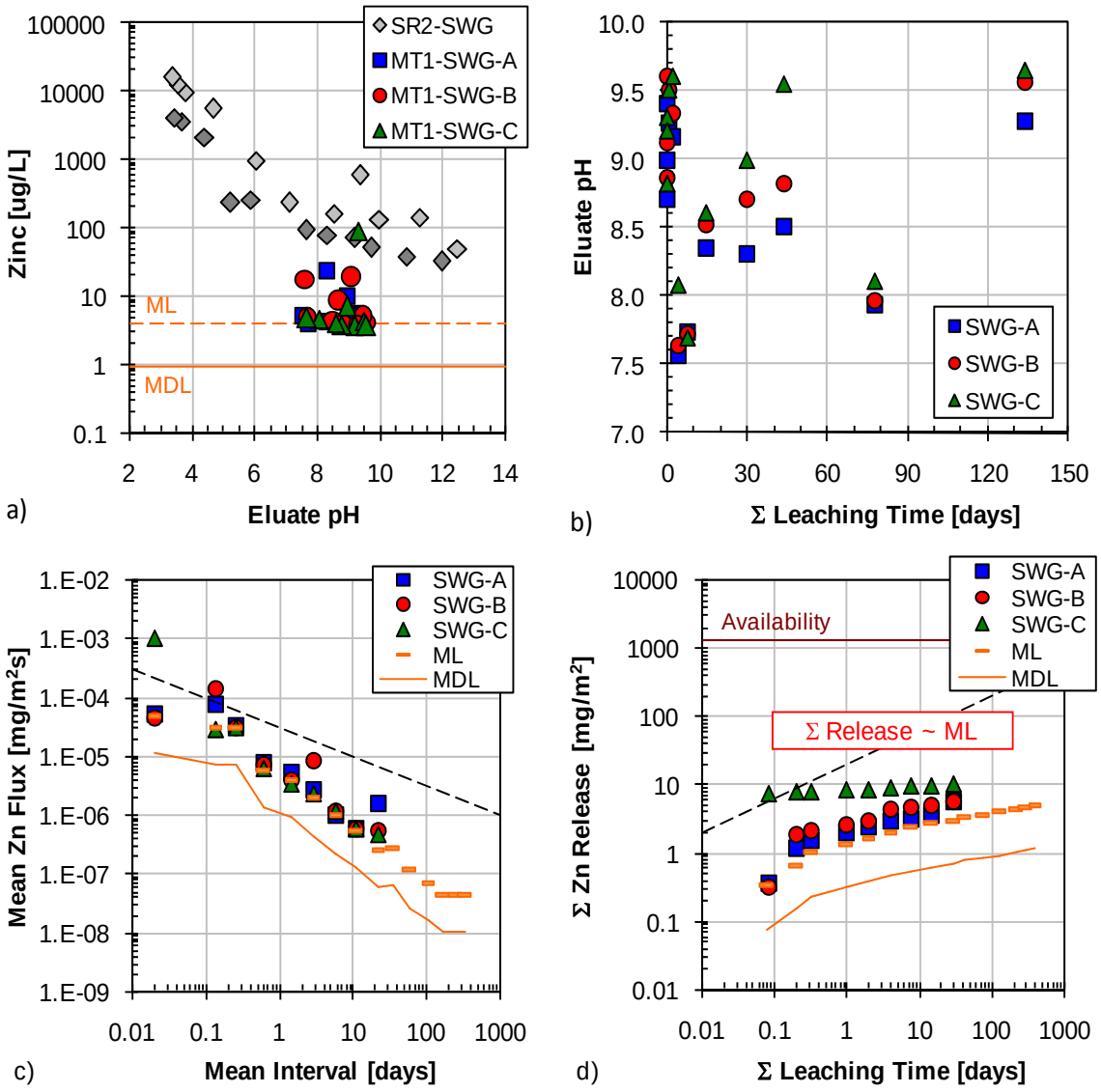

Figure B-46. Zinc leaching test results from SWG matrix: a) comparison of tank leach test eluants to saturation values (SR02 data) and QA/QC parameters, b) pH evolution in tank leach eluants, c) interval flux from tank leach test in comparison to flux values at the method limit ($t^{-1/2}$ model for AMG shown as dashed line), and d) cumulative mass release ($t^{1/2}$ model for AMG shown as dashed line).

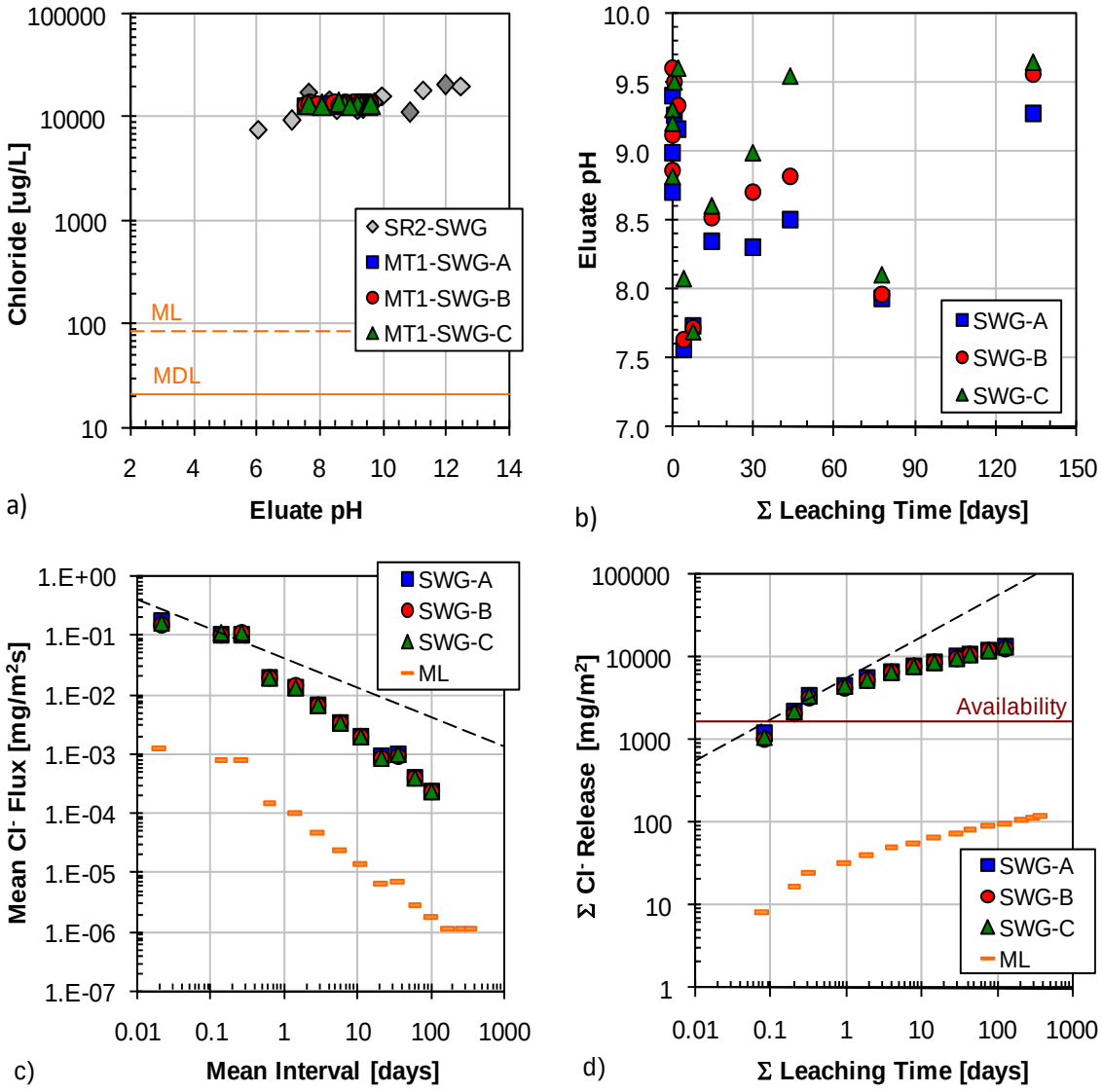

Figure B-47. Chloride leaching test results from SWG matrix: a) comparison of tank leach test eluants to saturation values (SR02 data) and QA/QC parameters, b) pH evolution in tank leach eluants, c) interval flux from tank leach test in comparison to flux values at the method limit ($t^{-1/2}$ model for AMG shown as dashed line), and d) cumulative mass release ($t^{1/2}$ model for AMG shown as dashed line).

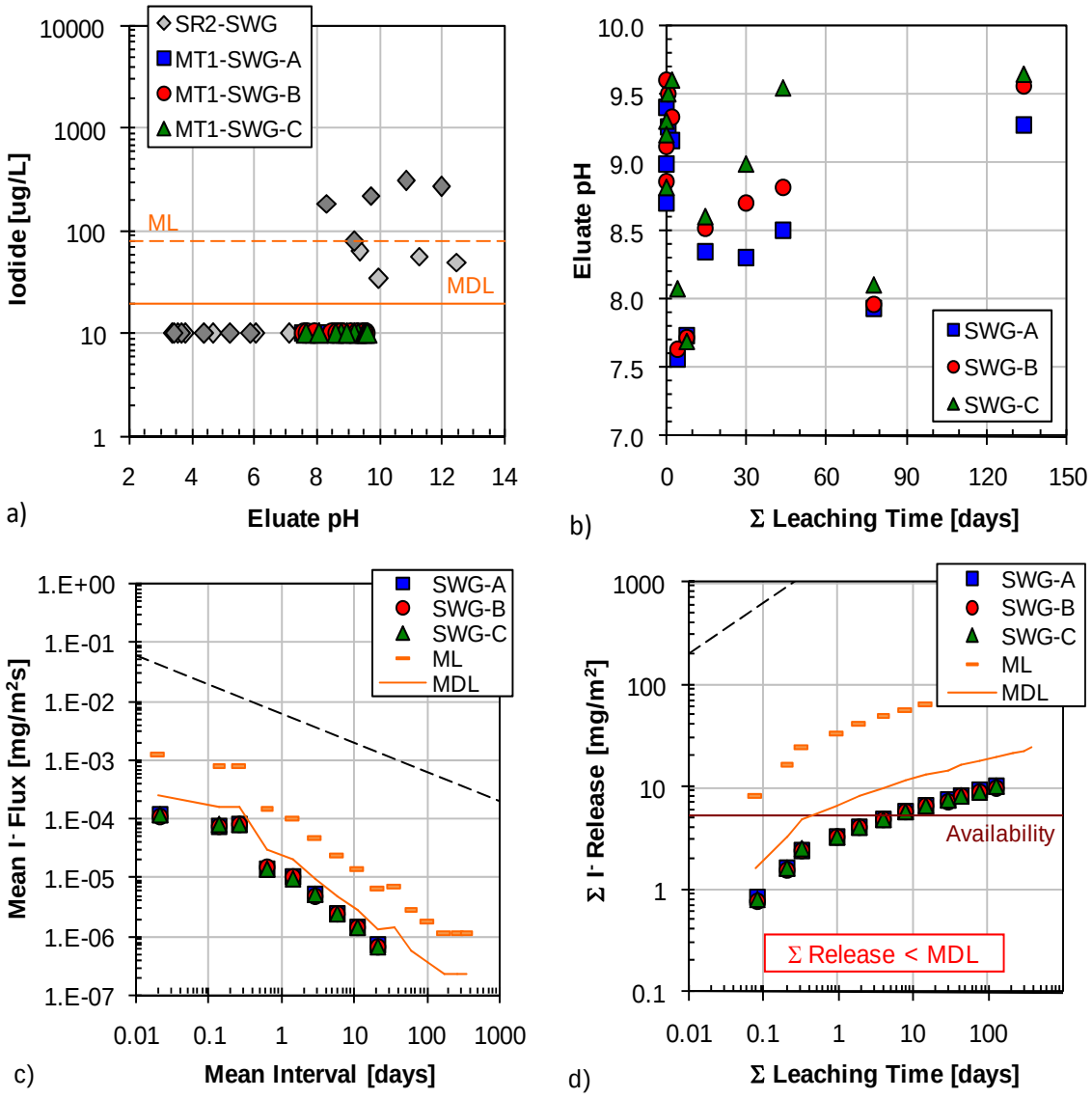

Figure B-48. Iodide leaching test results from SWG matrix: a) comparison of tank leach test eluants to saturation values (SR02 data) and QA/QC parameters, b) pH evolution in tank leach eluants, c) interval flux from tank leach test in comparison to flux values at the method limit ($t^{-1/2}$ model for AMG shown as dashed line), and d) cumulative mass release ($t^{1/2}$ model for AMG shown as dashed line).

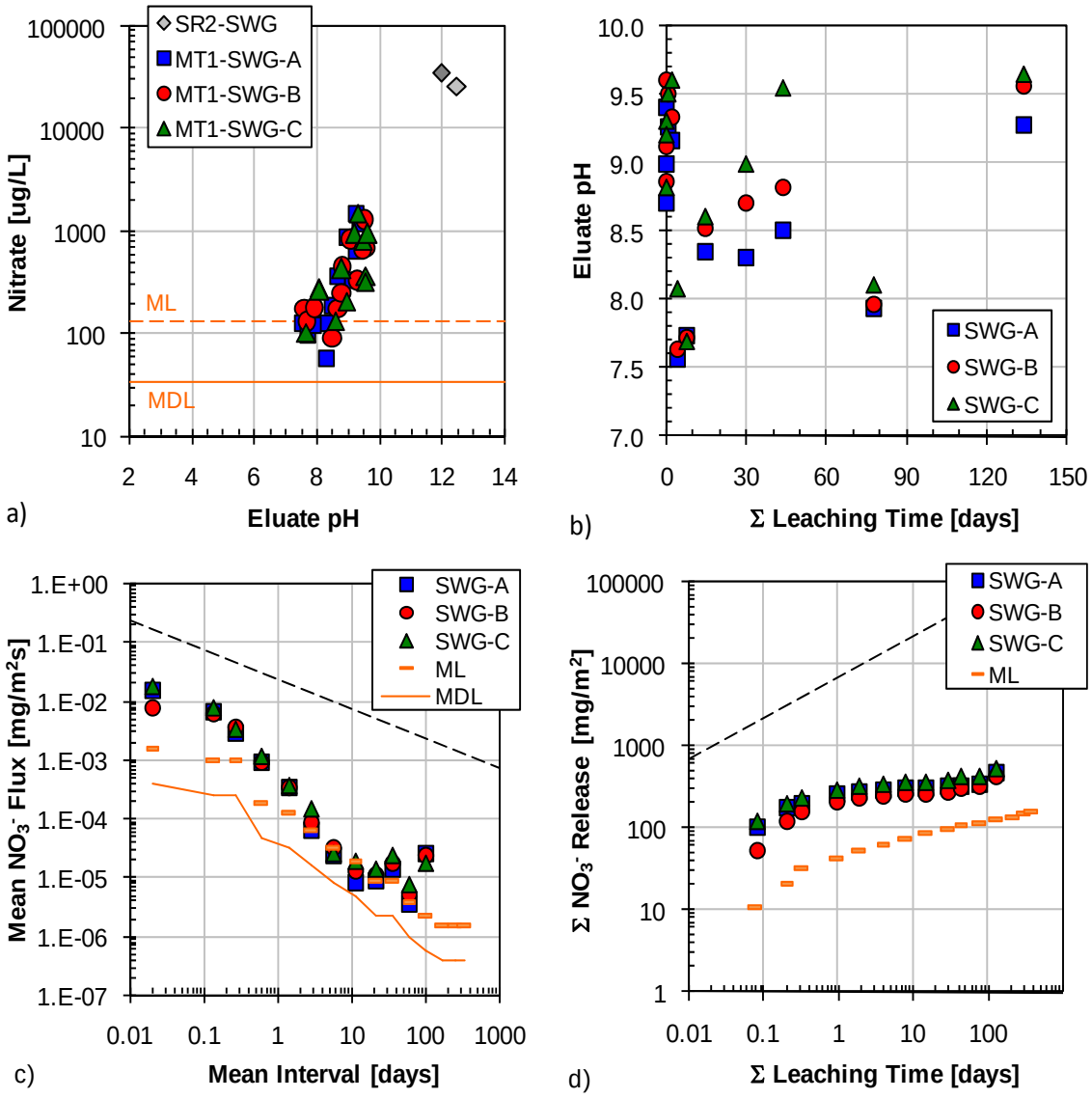

Figure B-49. Nitrate leaching test results from SWG matrix: a) comparison of tank leach test eluants to saturation values (SR02 data) and QA/QC parameters, b) pH evolution in tank leach eluants, c) interval flux from tank leach test in comparison to flux values at the method limit ($t^{-1/2}$ model for AMG shown as dashed line), and d) cumulative mass release ($t^{1/2}$ model for AMG shown as dashed line).

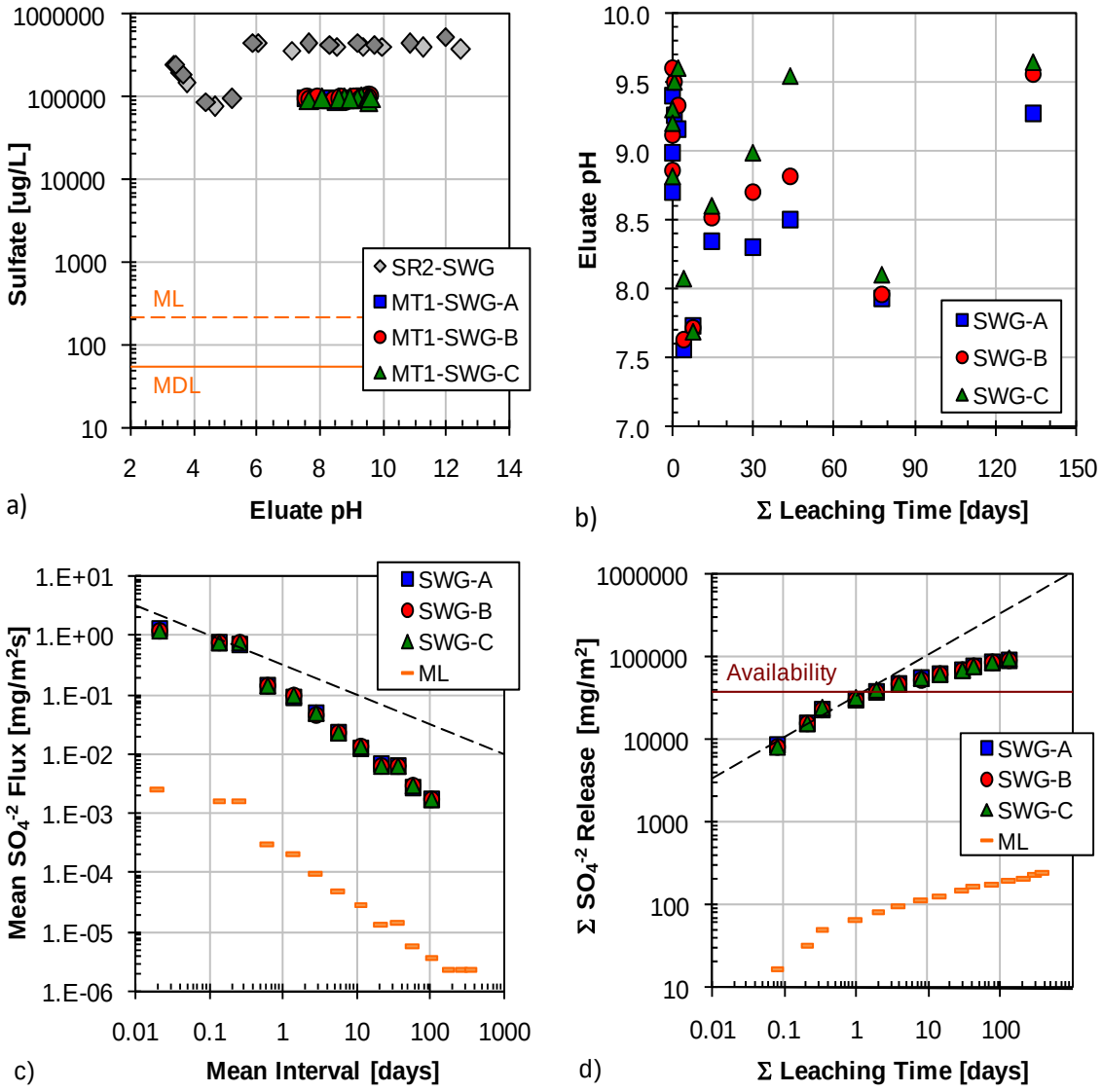

Figure B-50. Sulfate leaching test results from SWG matrix: a) comparison of tank leach test eluants to saturation values (SR02 data) and QA/QC parameters, b) pH evolution in tank leach eluants, c) interval flux from tank leach test in comparison to flux values at the method limit ($t^{-1/2}$ model for AMG shown as dashed line), and d) cumulative mass release ($t^{1/2}$ model for AMG shown as dashed line).

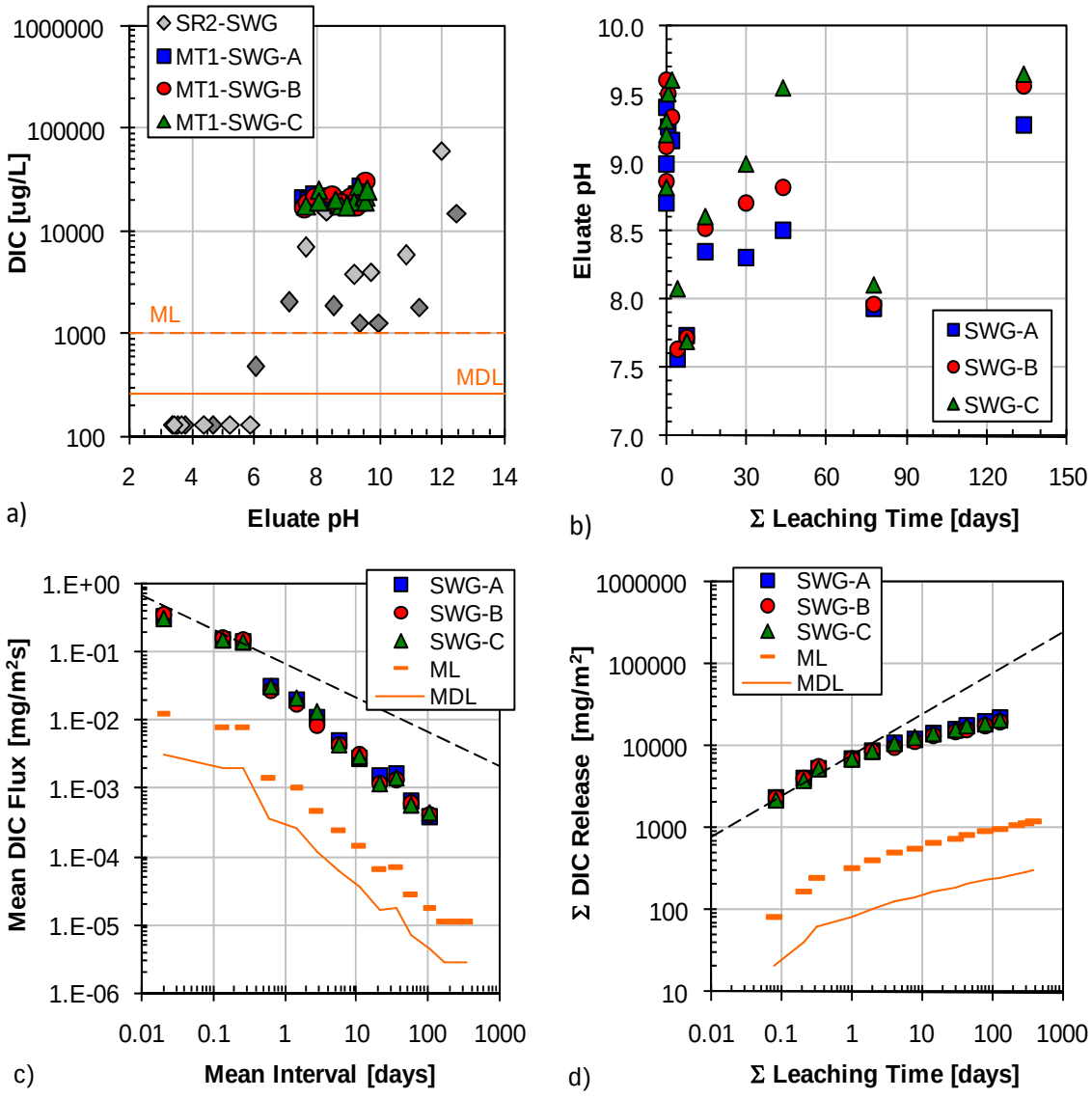

Figure B-51. Dissolved inorganic carbon test results from SWG matrix: a) comparison of tank leach test eluants to saturation values (SR02 data) and QA/QC parameters, b) pH evolution in tank leach eluants, c) interval flux from tank leach test in comparison to flux values at the method limit ($t^{-1/2}$ model for AMG shown as dashed line), and d) cumulative mass release ($t^{1/2}$ model for AMG shown as dashed line).

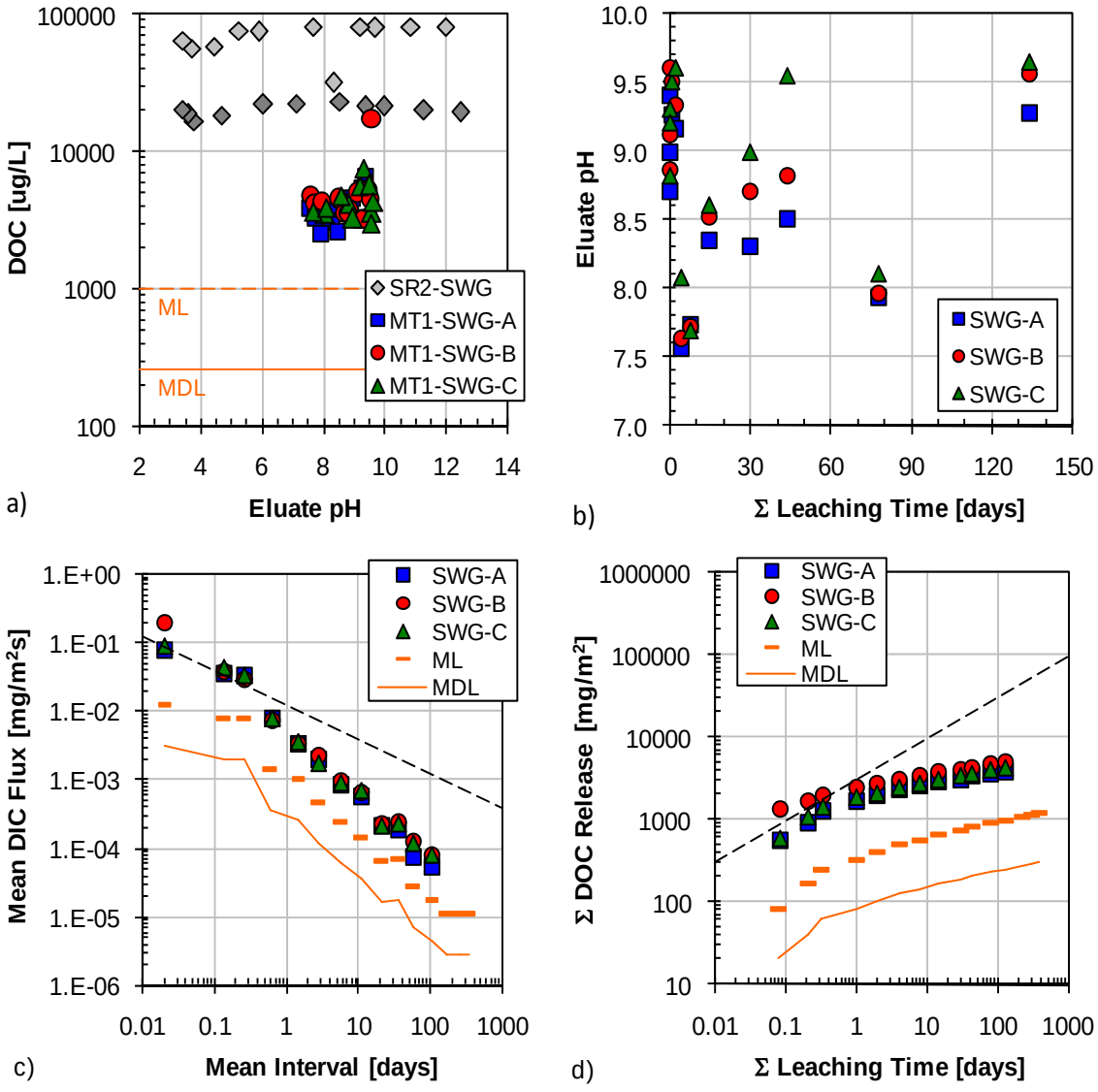

Figure B-52. Dissolved organic carbon leaching test results from SWG matrix: a) comparison of tank leach test eluants to saturation values (SR02 data) and QA/QC parameters, b) pH evolution in tank leach eluants, c) interval flux from tank leach test in comparison to flux values at the method limit ($t^{-1/2}$ model for AMG shown as dashed line), and d) cumulative mass release ($t^{1/2}$ model for AMG shown as dashed line).

Matrix Blank in SHG (MBG)

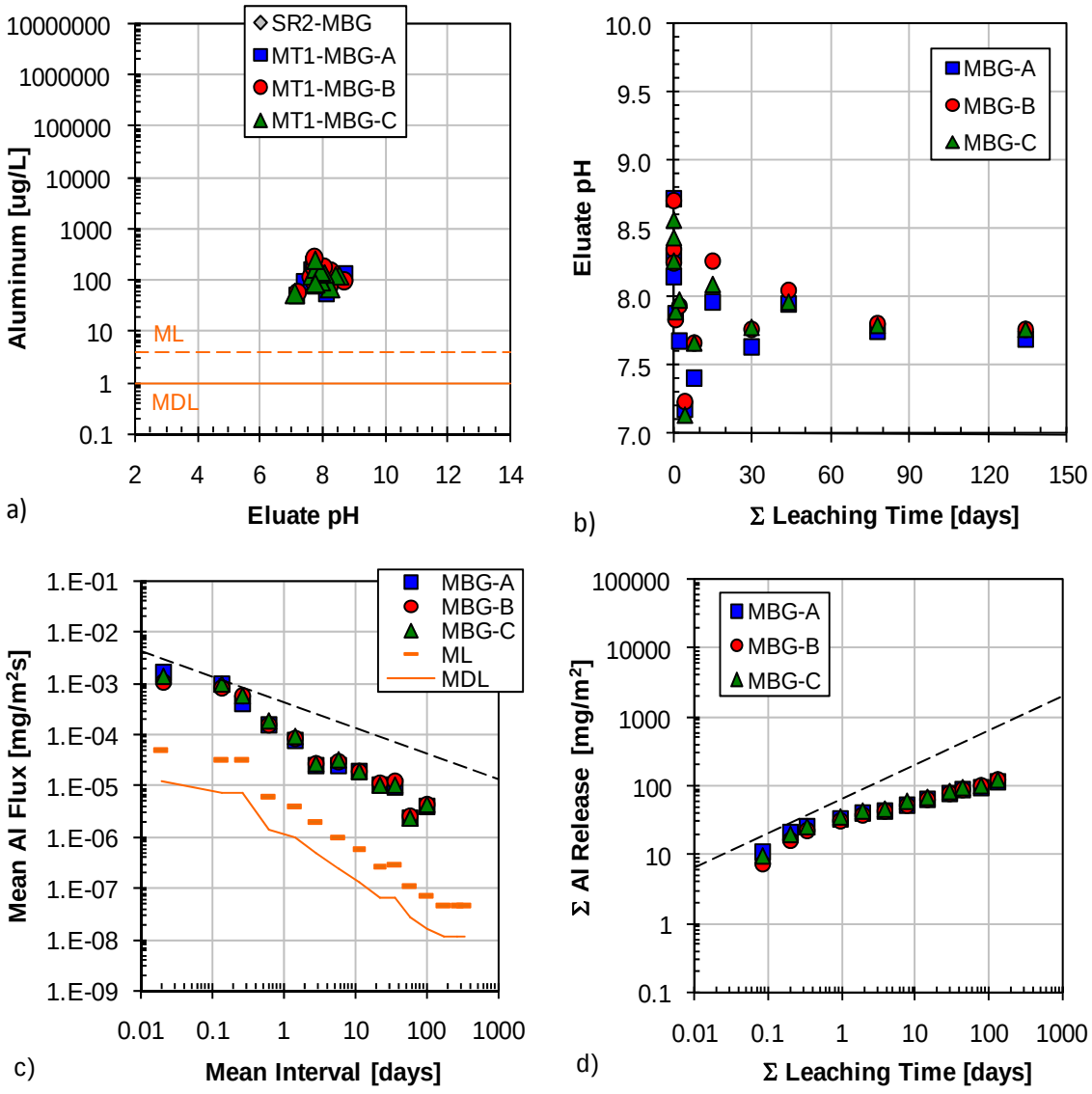

Figure B-53. Aluminum leaching test results from MBG matrix: a) comparison of tank leach test eluants to QA/QC parameters (SR02 not conducted), b) pH evolution in tank leach eluants, c) interval flux from tank leach test in comparison to flux values at the method limit ($t^{-1/2}$ model for AMG shown as dashed line), and d) cumulative mass release ($t^{1/2}$ model for AMG shown as dashed line).

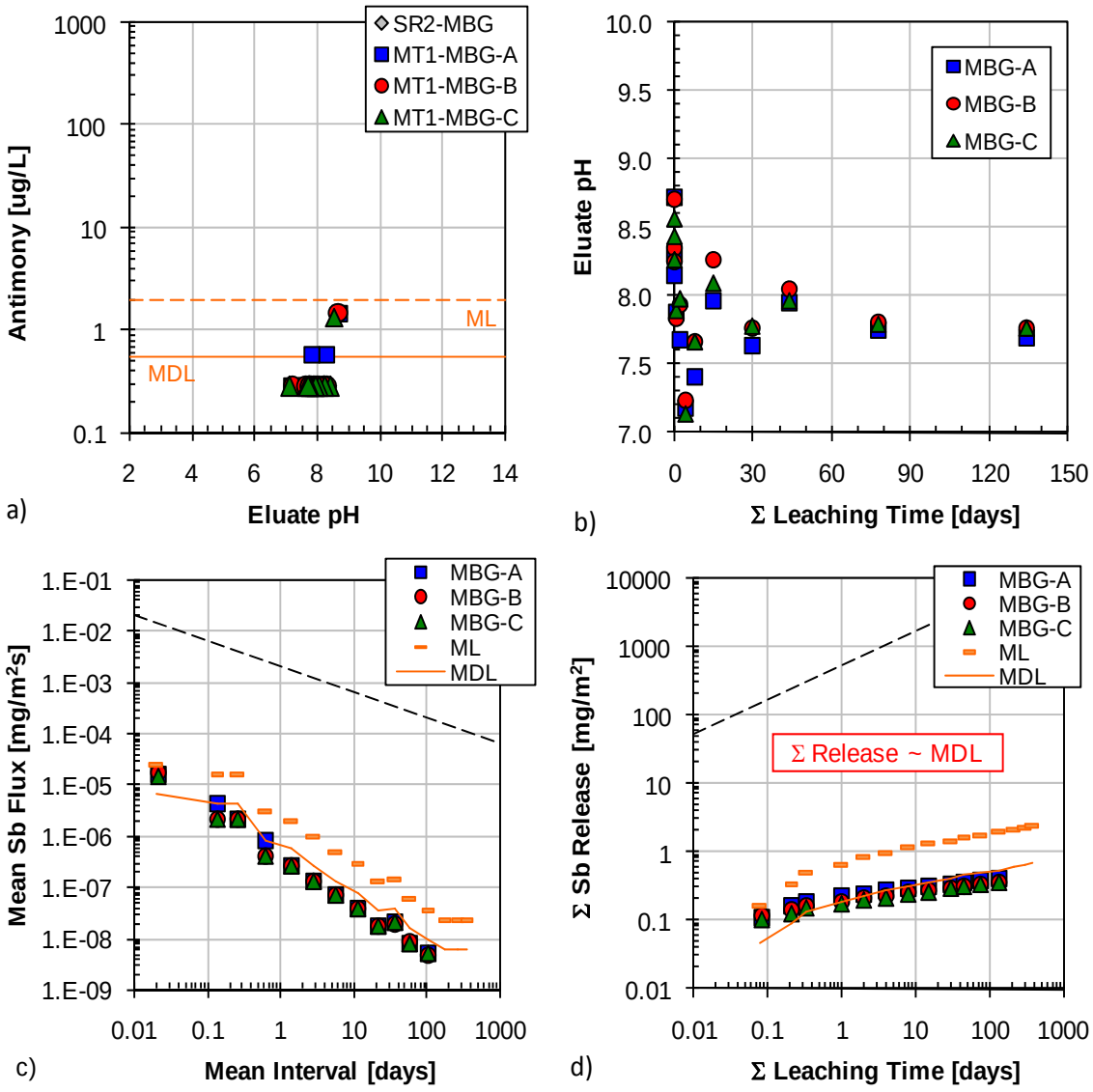

Figure B-54. Antimony leaching test results from MBG matrix: a) comparison of tank leach test eluants to QA/QC parameters (SR02 not conducted), b) pH evolution in tank leach eluants, c) interval flux from tank leach test in comparison to flux values at the method limit ($t^{-1/2}$ model for AMG shown as dashed line), and d) cumulative mass release ($t^{1/2}$ model for AMG shown as dashed line).

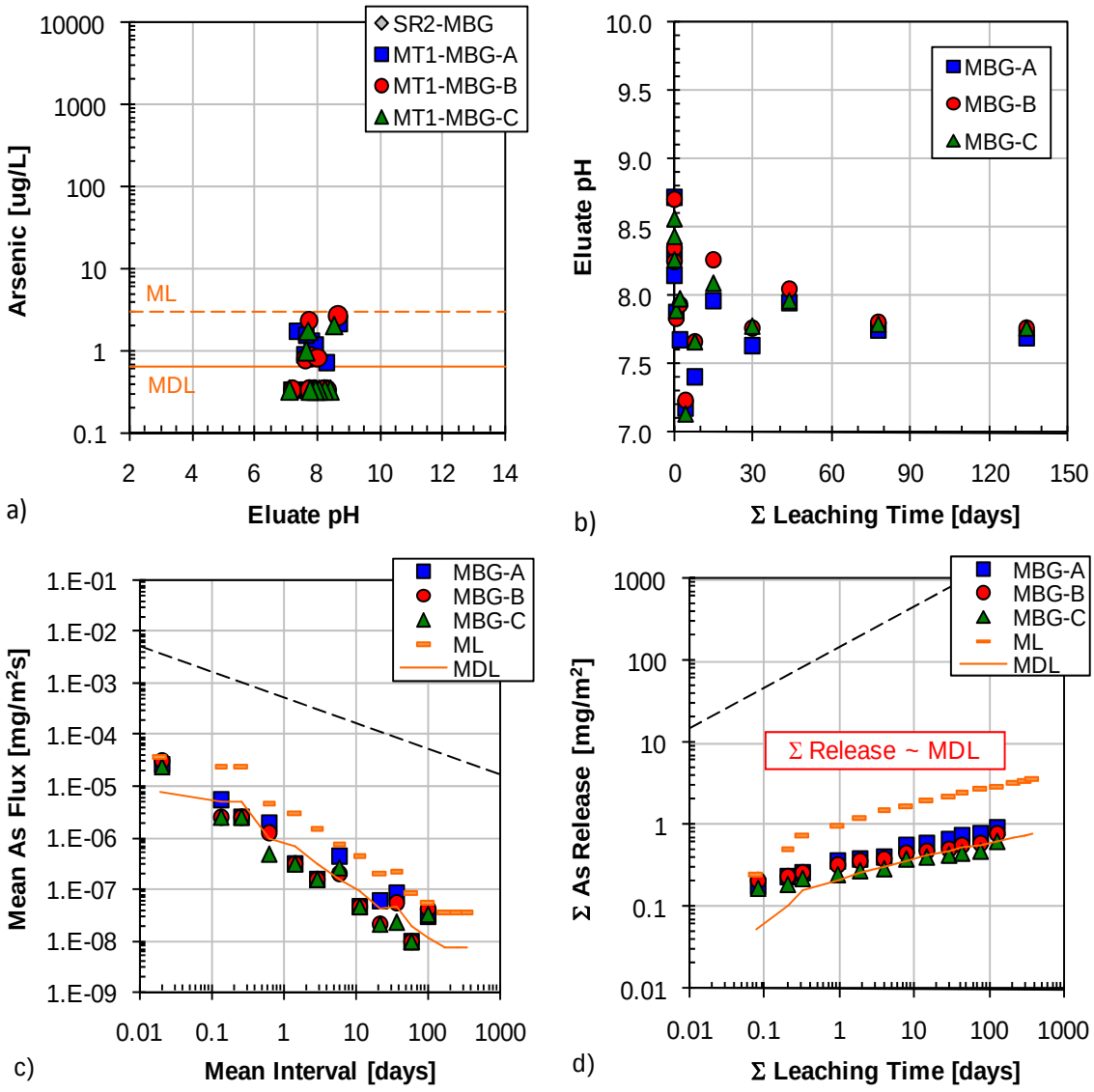

Figure B-55. Arsenic leaching test results from MBG matrix: a) comparison of tank leach test eluants to QA/QC parameters (SR02 not conducted), b) pH evolution in tank leach eluants, c) interval flux from tank leach test in comparison to flux values at the method limit ($t^{-1/2}$ model for AMG shown as dashed line), and d) cumulative mass release ($t^{1/2}$ model for AMG shown as dashed line).

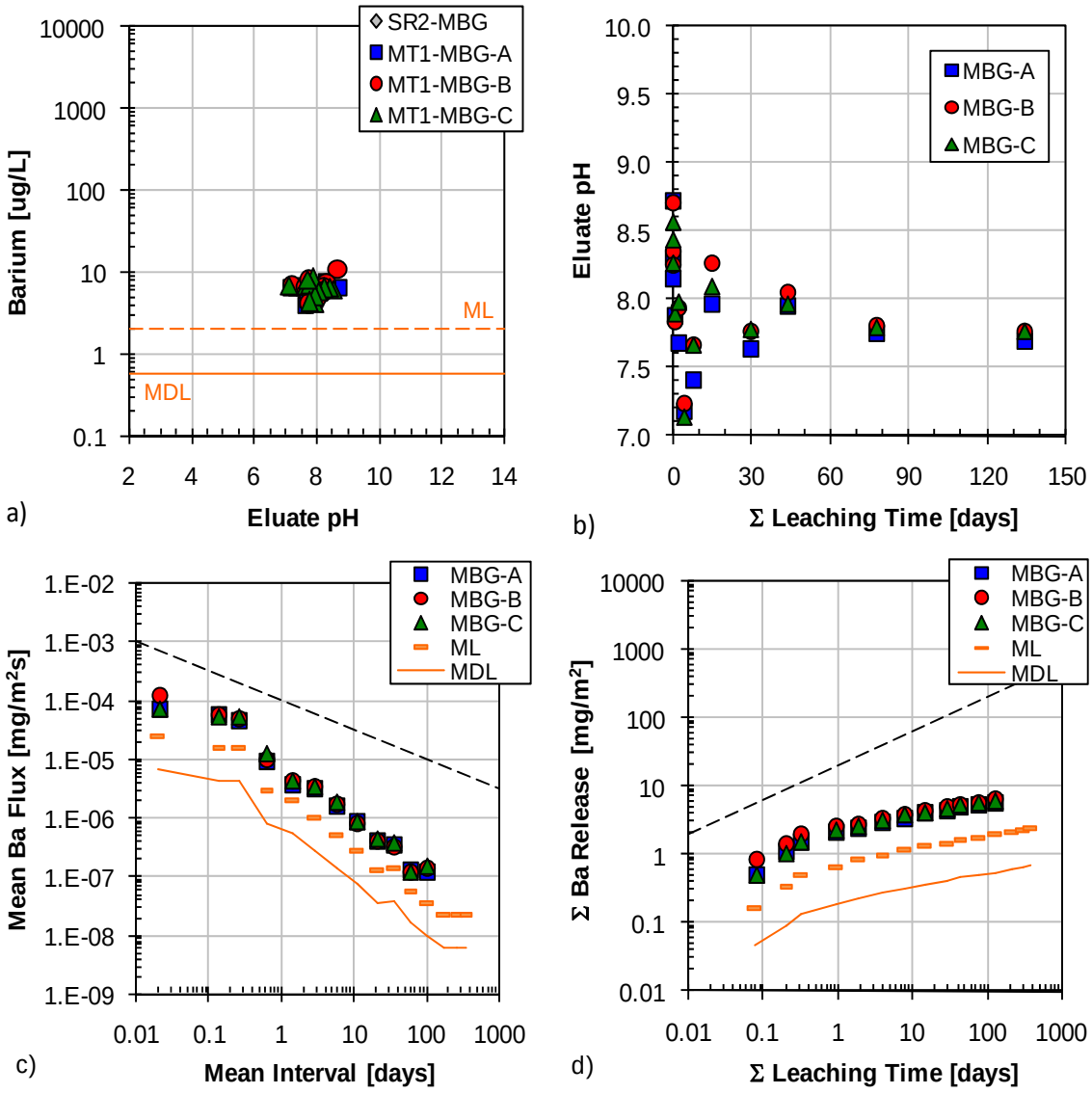

Figure B-56. Barium leaching test results from MBG matrix: a) comparison of tank leach test eluants to QA/QC parameters (SR02 not conducted), b) pH evolution in tank leach eluants, c) interval flux from tank leach test in comparison to flux values at the method limit ($t^{-1/2}$ model for AMG shown as dashed line), and d) cumulative mass release ($t^{1/2}$ model for AMG shown as dashed line).

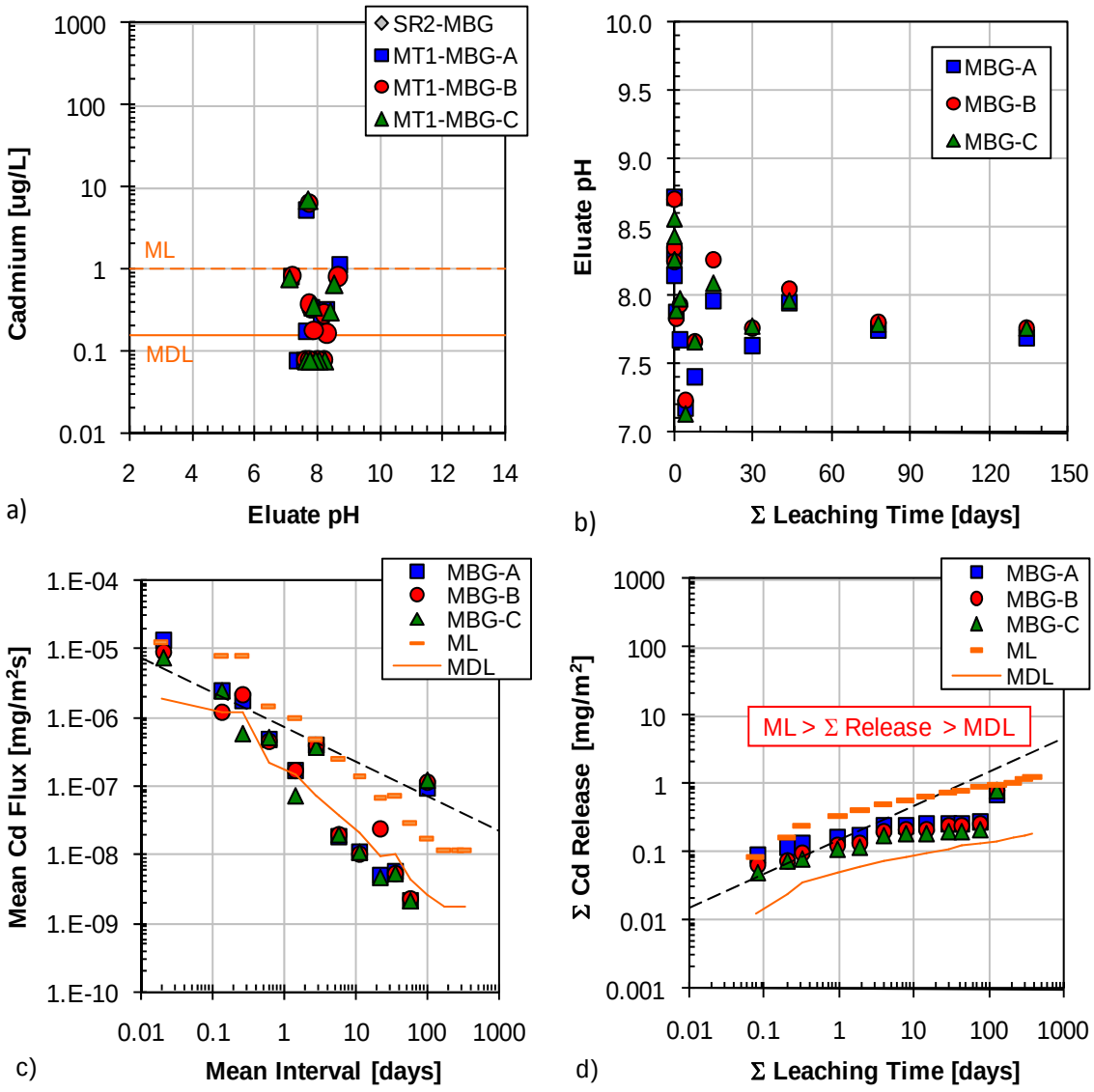

Figure B-57. Cadmium leaching test results from MBG matrix: a) comparison of tank leach test eluants to QA/QC parameters (SR02 not conducted), b) pH evolution in tank leach eluants, c) interval flux from tank leach test in comparison to flux values at the method limit ($t^{-1/2}$ model for AMG shown as dashed line), and d) cumulative mass release ($t^{1/2}$ model for AMG shown as dashed line).

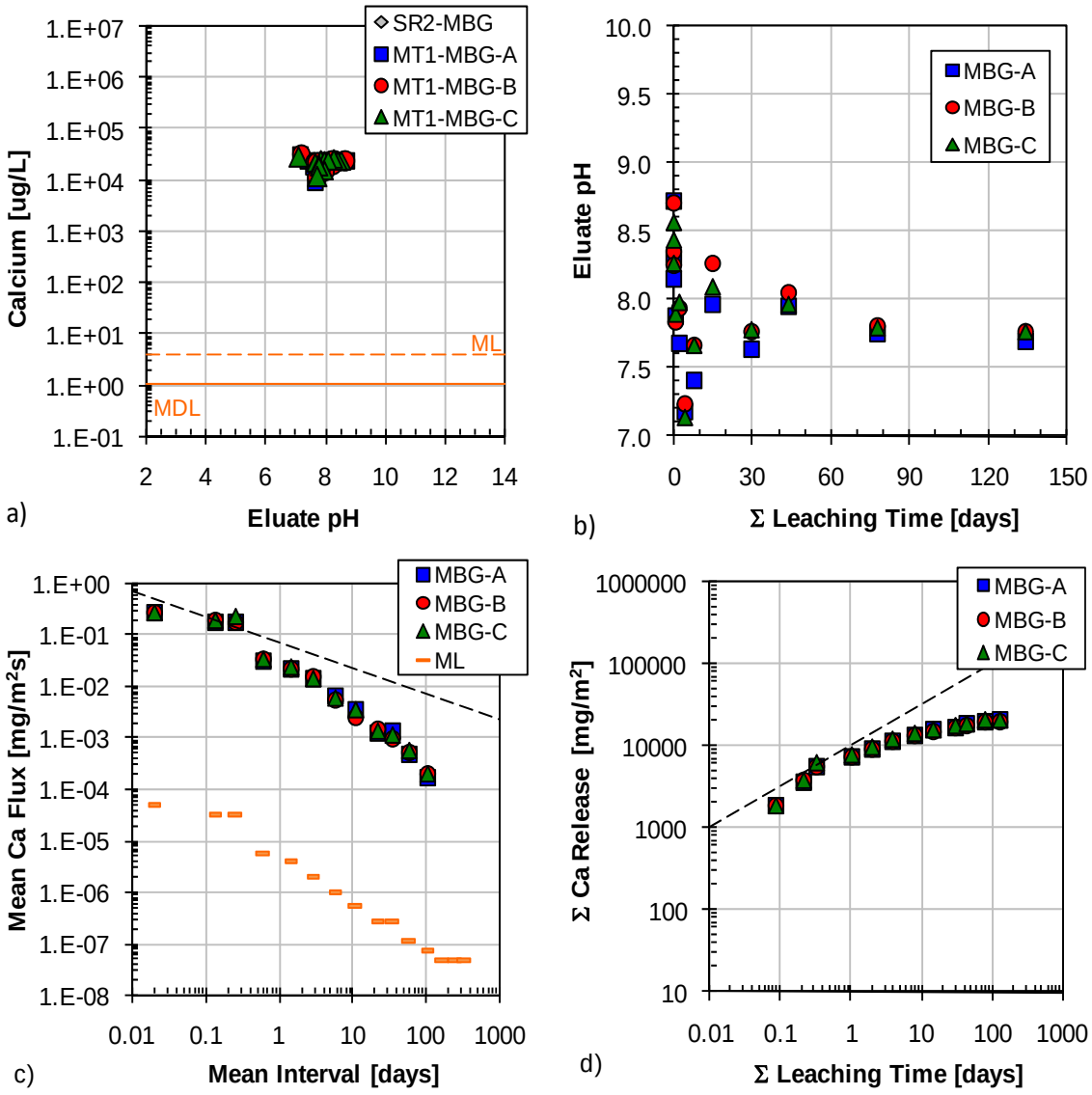

Figure B-58. Calcium leaching test results from MBG matrix: a) comparison of tank leach test eluants to QA/QC parameters (SR02 not conducted), b) pH evolution in tank leach eluants, c) interval flux from tank leach test in comparison to flux values at the method limit ($t^{-1/2}$ model for AMG shown as dashed line), and d) cumulative mass release ($t^{1/2}$ model for AMG shown as dashed line).

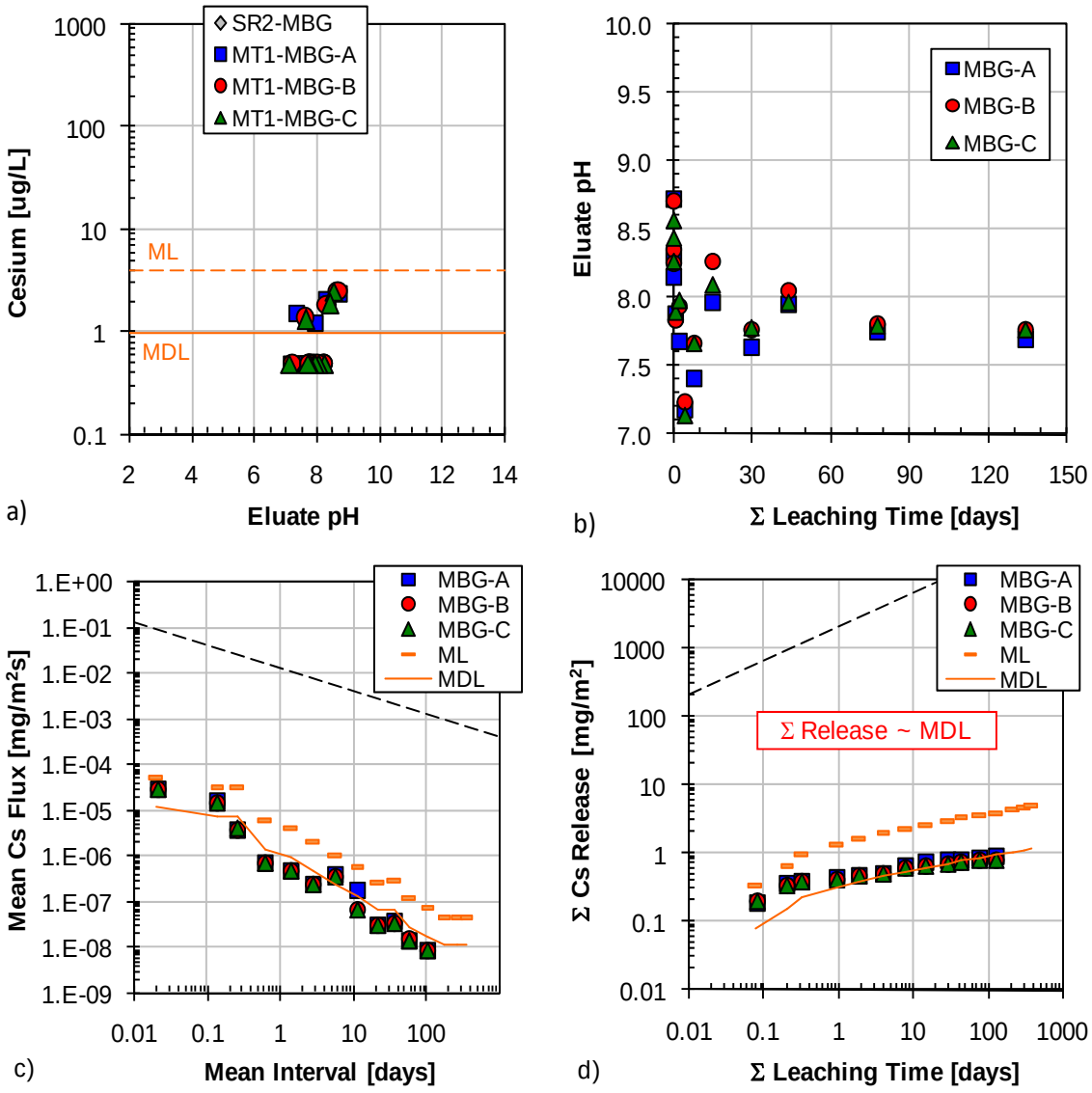

Figure B-59. Cesium leaching test results from MBG matrix: a) comparison of tank leach test eluants to QA/QC parameters (SR02 not conducted), b) pH evolution in tank leach eluants, c) interval flux from tank leach test in comparison to flux values at the method limit ($t^{-1/2}$ model for AMG shown as dashed line), and d) cumulative mass release ($t^{1/2}$ model for AMG shown as dashed line).

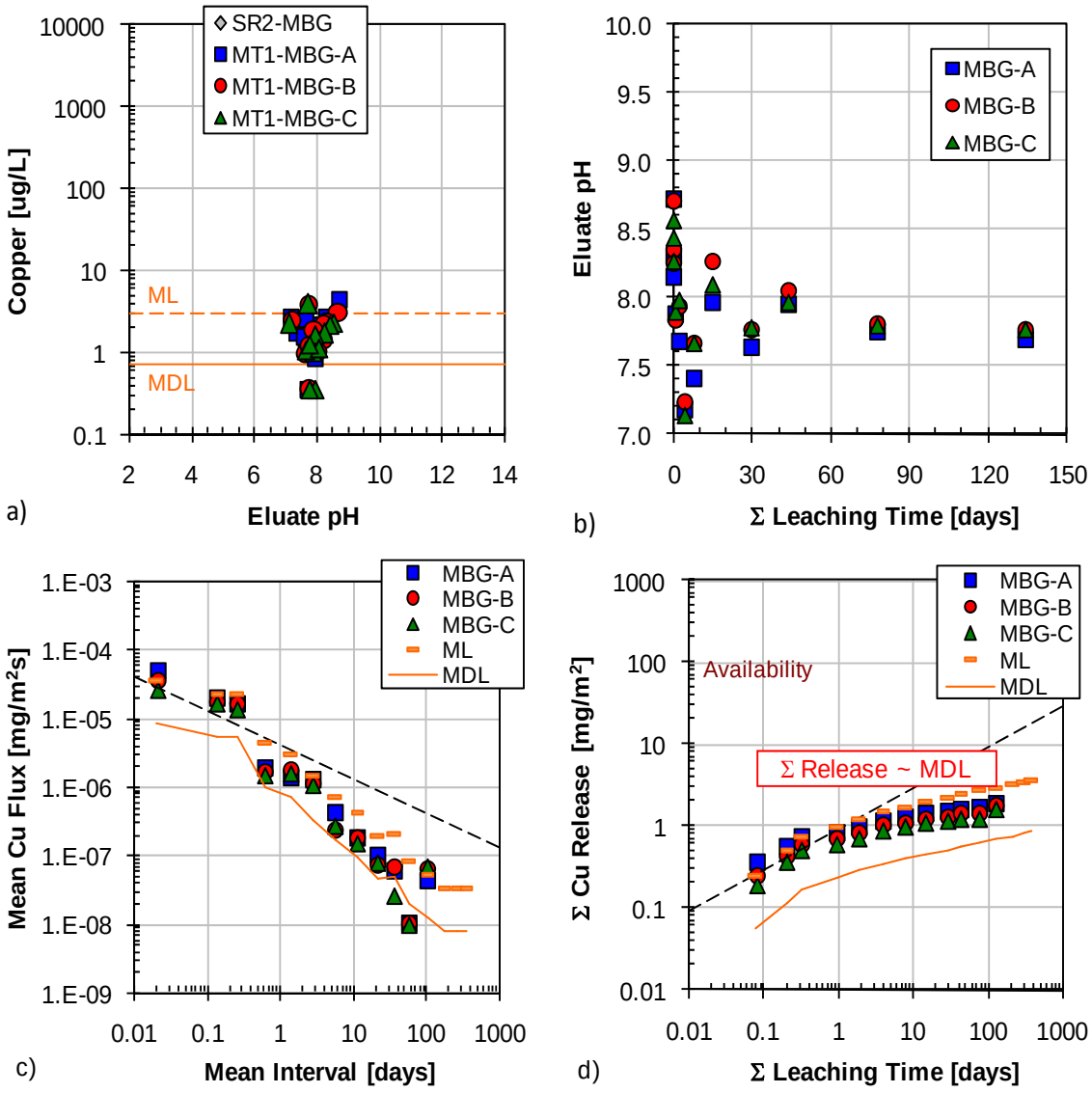

Figure B-60. Copper leaching test results from MBG matrix: a) comparison of tank leach test eluants to QA/QC parameters (SR02 not conducted), b) pH evolution in tank leach eluants, c) interval flux from tank leach test in comparison to flux values at the method limit ($t^{-1/2}$ model for AMG shown as dashed line), and d) cumulative mass release ($t^{1/2}$ model for AMG shown as dashed line).

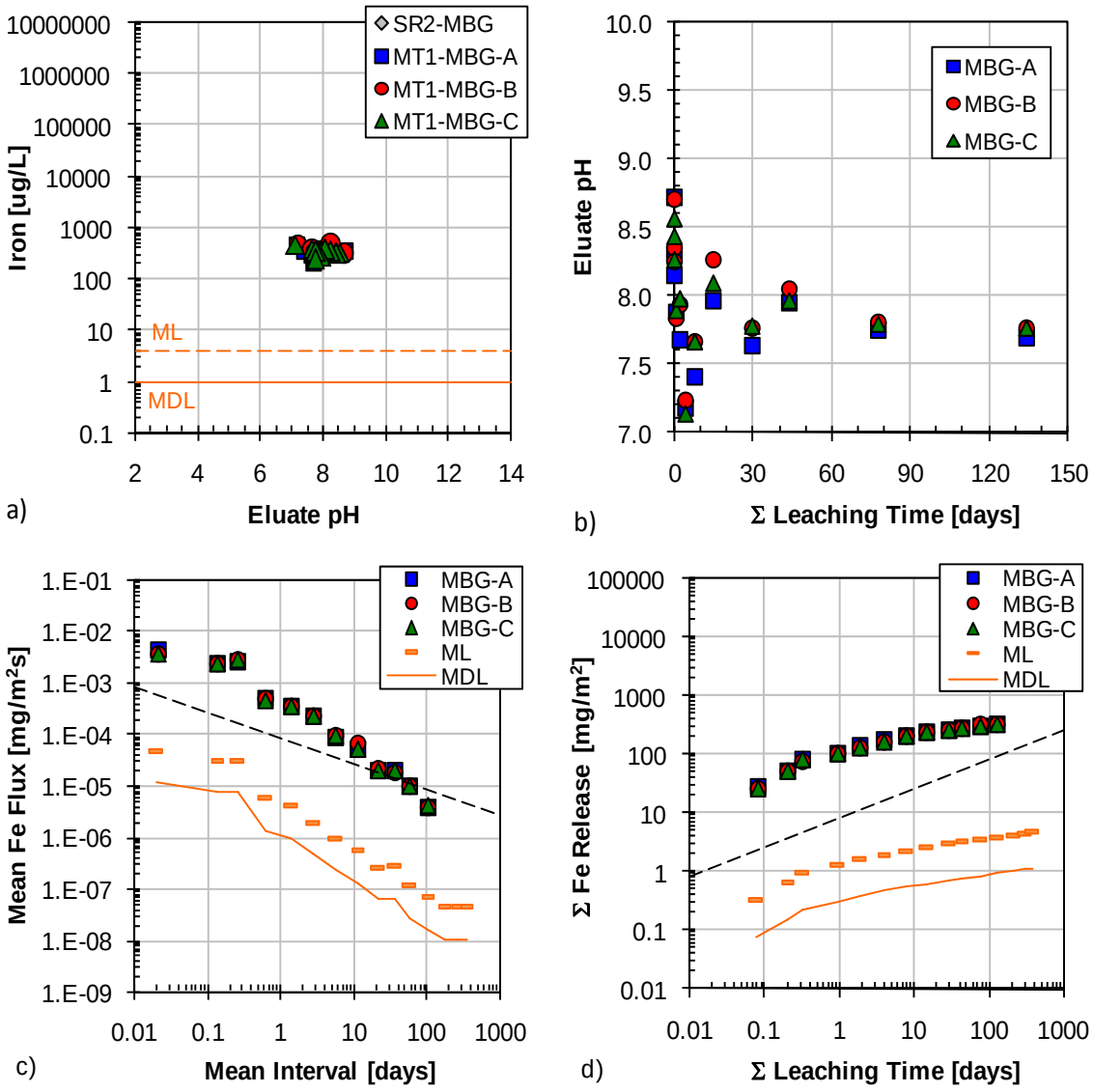

Figure B-61. Iron leaching test results from MBG matrix: a) comparison of tank leach test eluants to QA/QC parameters (SR02 not conducted), b) pH evolution in tank leach eluants, c) interval flux from tank leach test in comparison to flux values at the method limit ($t^{-1/2}$ model for AMG shown as dashed line), and d) cumulative mass release ($t^{1/2}$ model for AMG shown as dashed line).

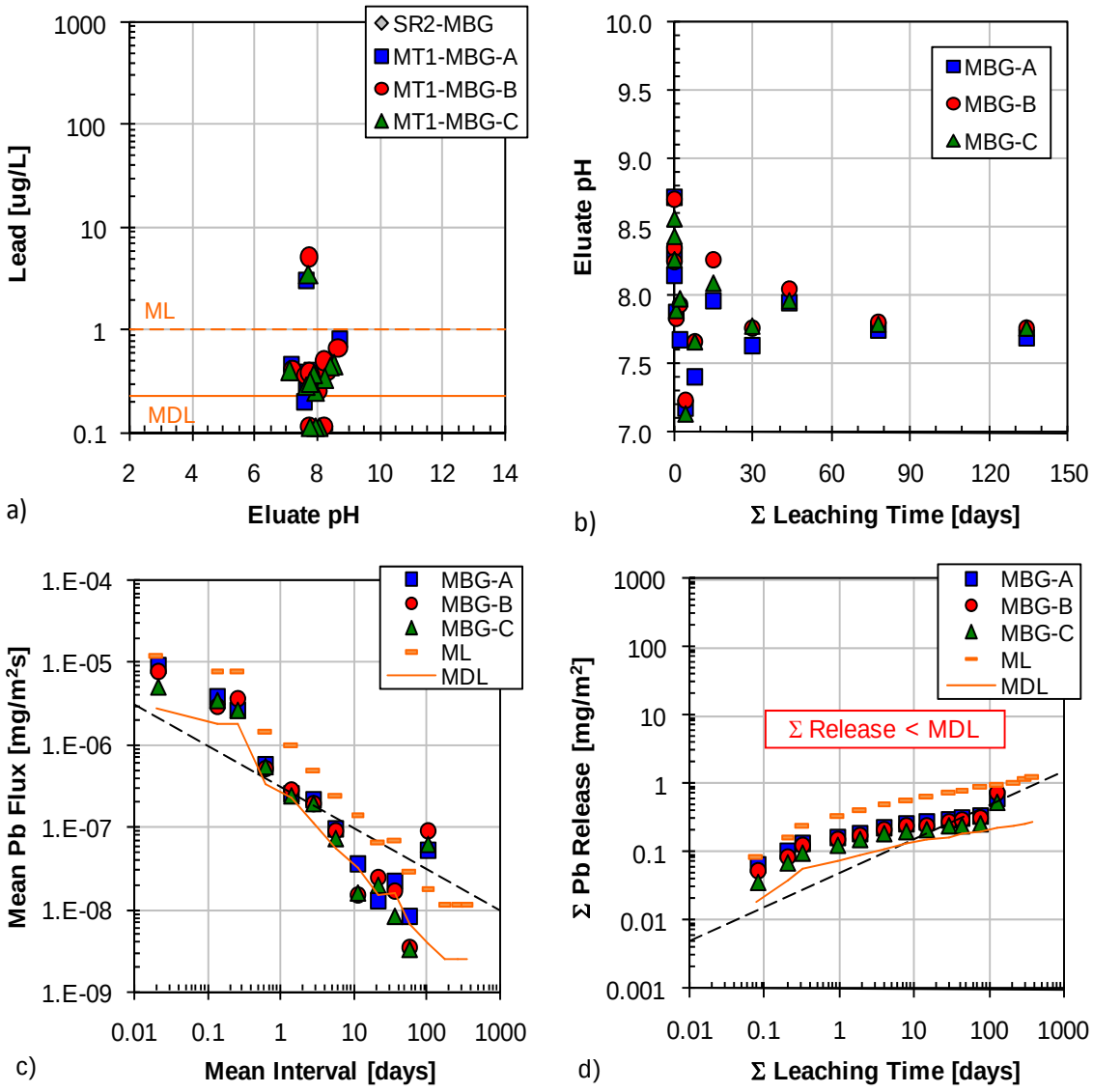

Figure B-62. Lead leaching test results from MBG matrix: a) comparison of tank leach test eluants to QA/QC parameters (SR02 not conducted), b) pH evolution in tank leach eluants, c) interval flux from tank leach test in comparison to flux values at the method limit ($t^{-1/2}$ model for AMG shown as dashed line), and d) cumulative mass release ($t^{1/2}$ model for AMG shown as dashed line).

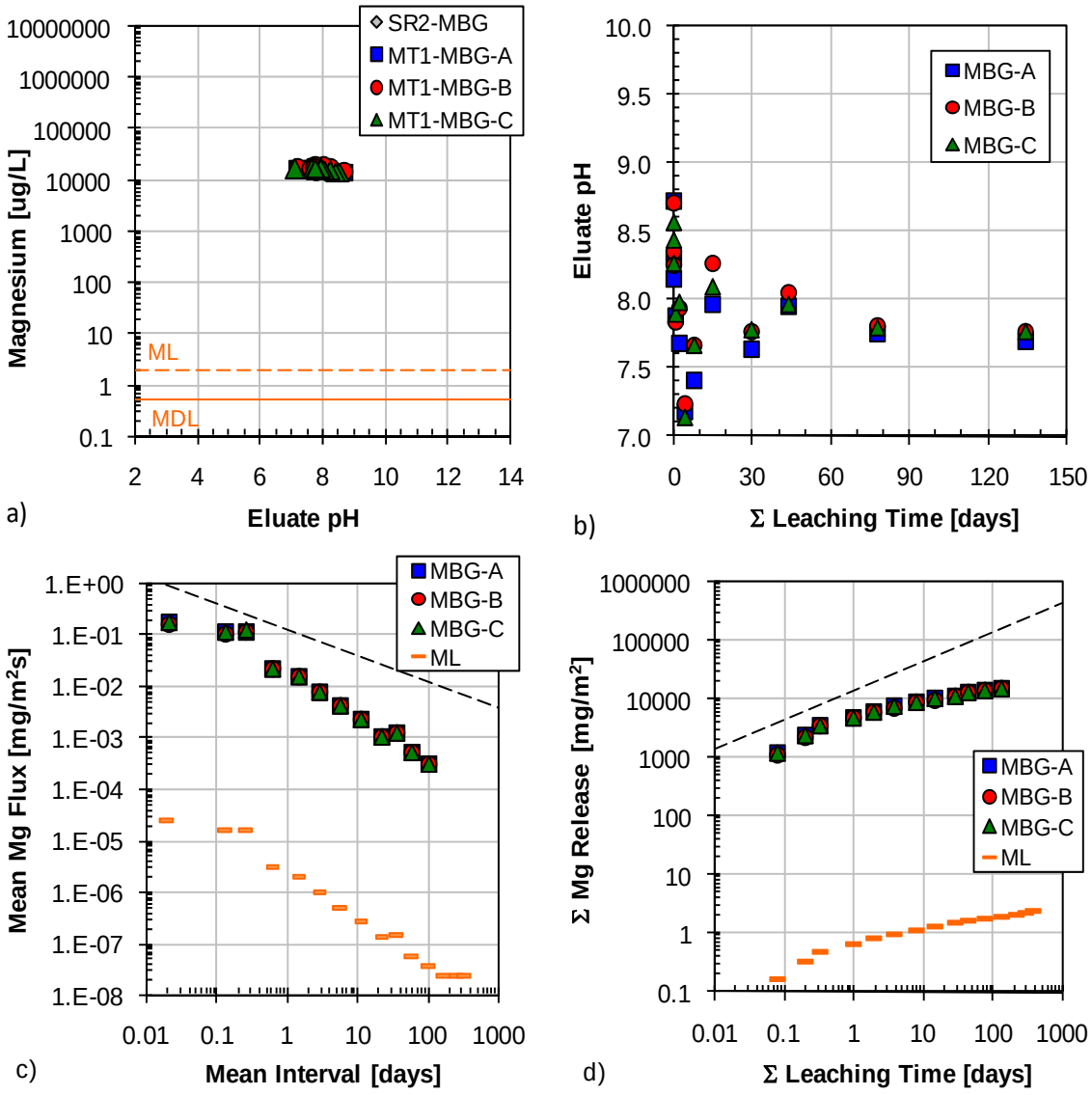

Figure B-63. Magnesium leaching test results from MBG matrix: a) comparison of tank leach test eluants to QA/QC parameters (SR02 not conducted), b) pH evolution in tank leach eluants, c) interval flux from tank leach test in comparison to flux values at the method limit ($t^{-1/2}$ model for AMG shown as dashed line), and d) cumulative mass release ($t^{1/2}$ model for AMG shown as dashed line).

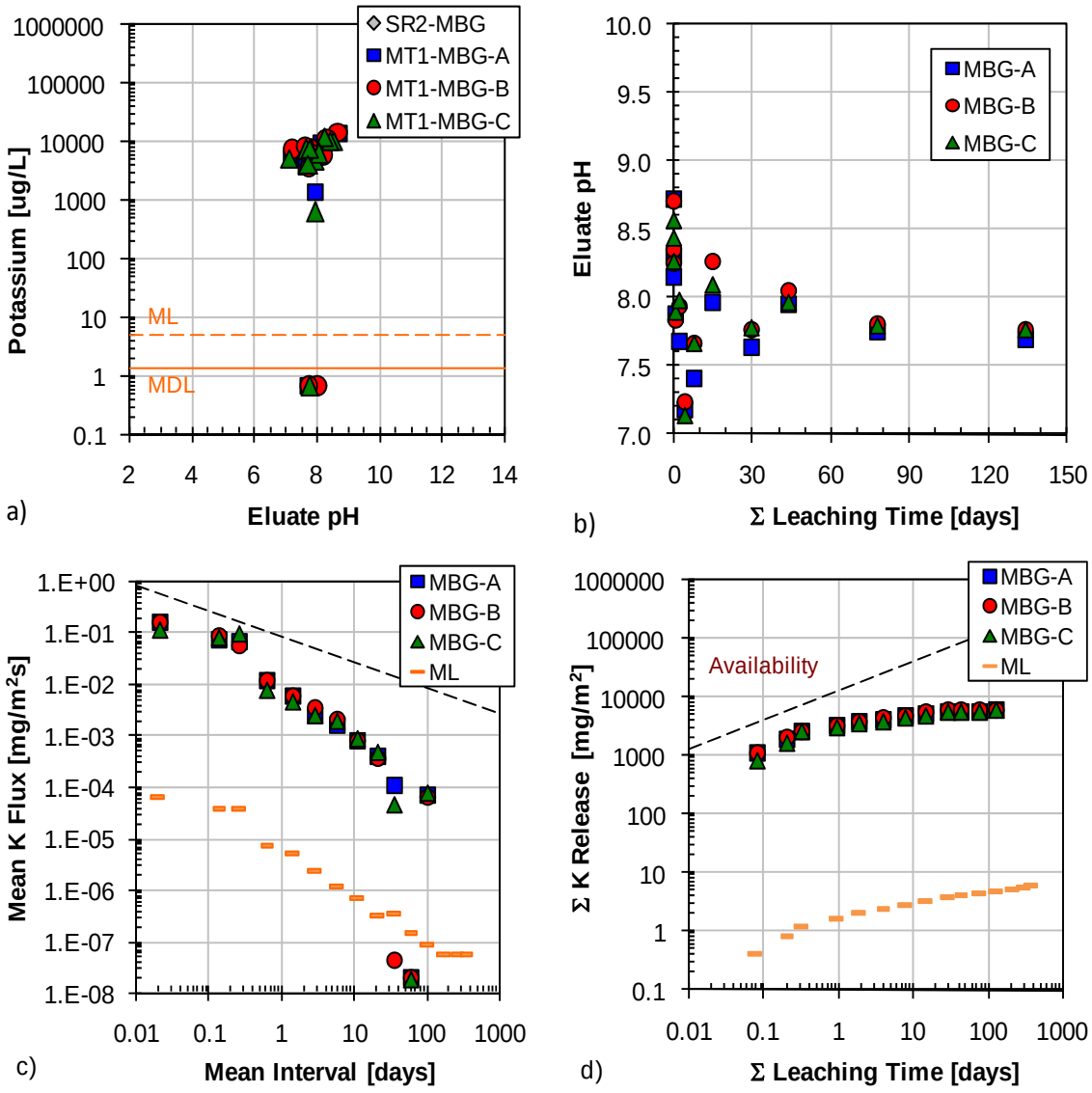

Figure B-64. Potassium leaching test results from MBG matrix: a) comparison of tank leach test eluants to QA/QC parameters (SR02 not conducted), b) pH evolution in tank leach eluants, c) interval flux from tank leach test in comparison to flux values at the method limit ($t^{-1/2}$ model for AMG shown as dashed line), and d) cumulative mass release ($t^{1/2}$ model for AMG shown as dashed line).

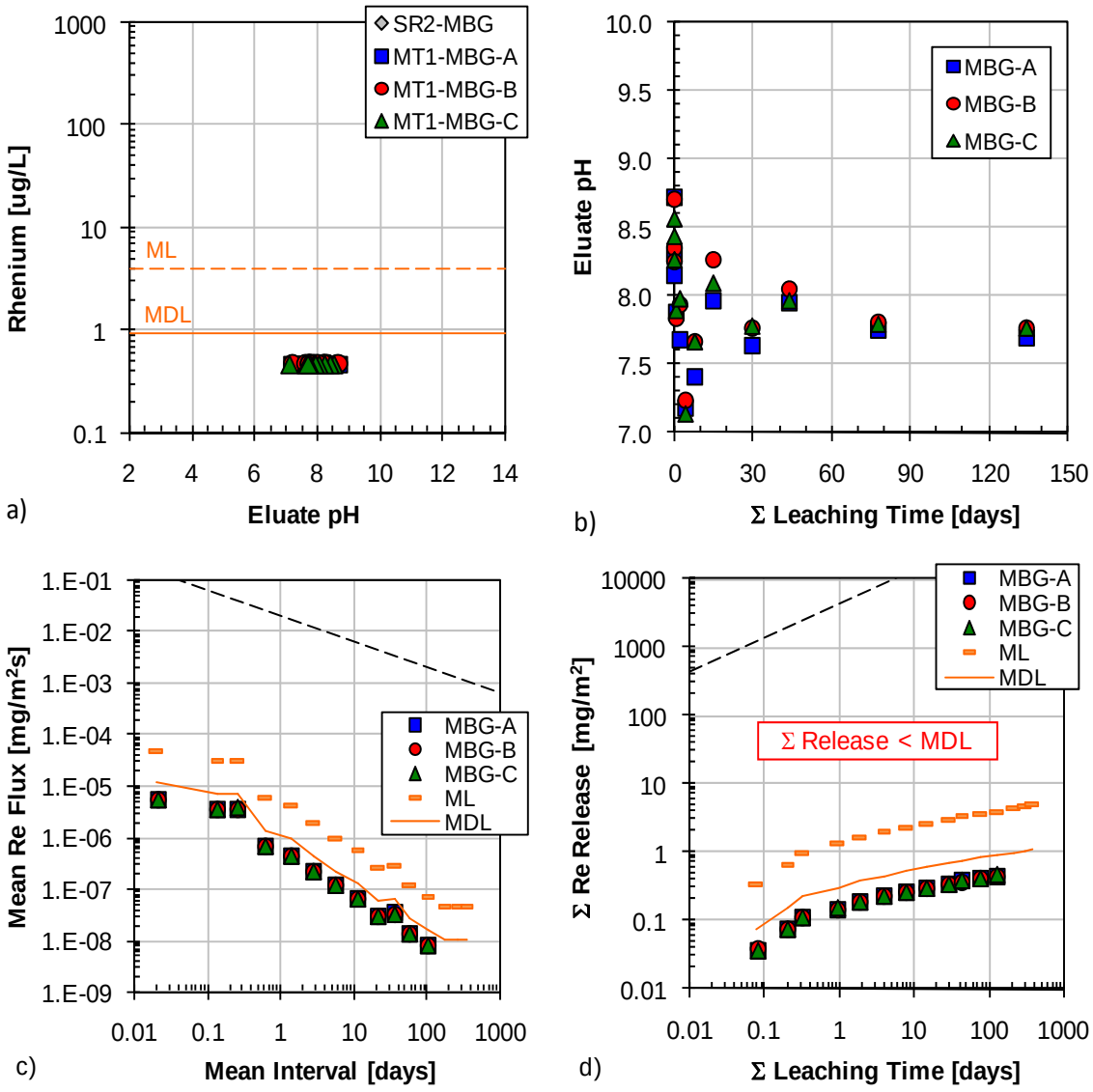

Figure B-65. Rhenium leaching test results from MBG matrix: a) comparison of tank leach test eluants to QA/QC parameters (SR02 not conducted), b) pH evolution in tank leach eluants, c) interval flux from tank leach test in comparison to flux values at the method limit ($t^{-1/2}$ model for AMG shown as dashed line), and d) cumulative mass release ($t^{1/2}$ model for AMG shown as dashed line).

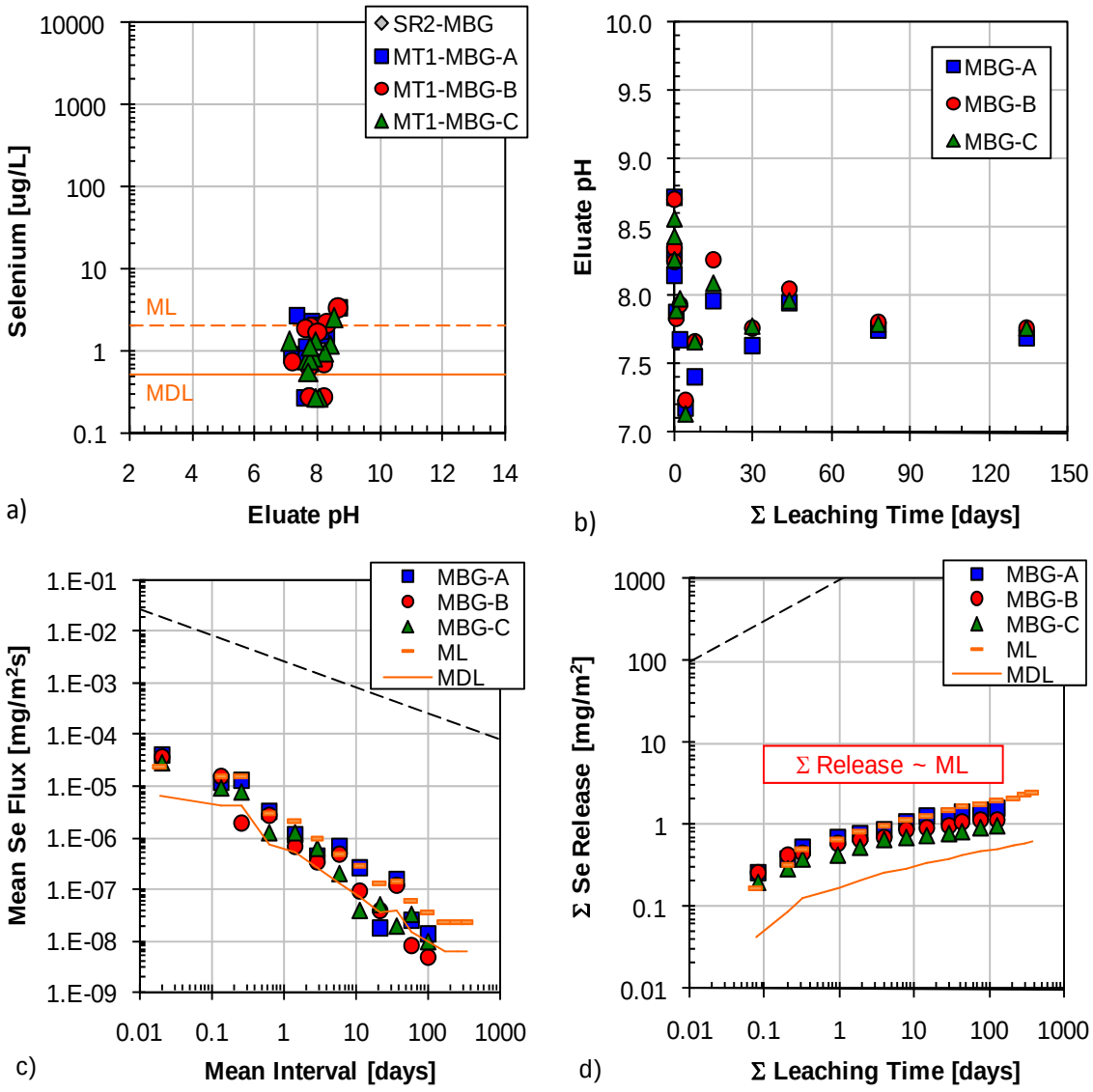

Figure B-66. Selenium leaching test results from MBG matrix: a) comparison of tank leach test eluants to QA/QC parameters (SR02 not conducted), b) pH evolution in tank leach eluants, c) interval flux from tank leach test in comparison to flux values at the method limit ($t^{-1/2}$ model for AMG shown as dashed line), and d) cumulative mass release ($t^{1/2}$ model for AMG shown as dashed line).

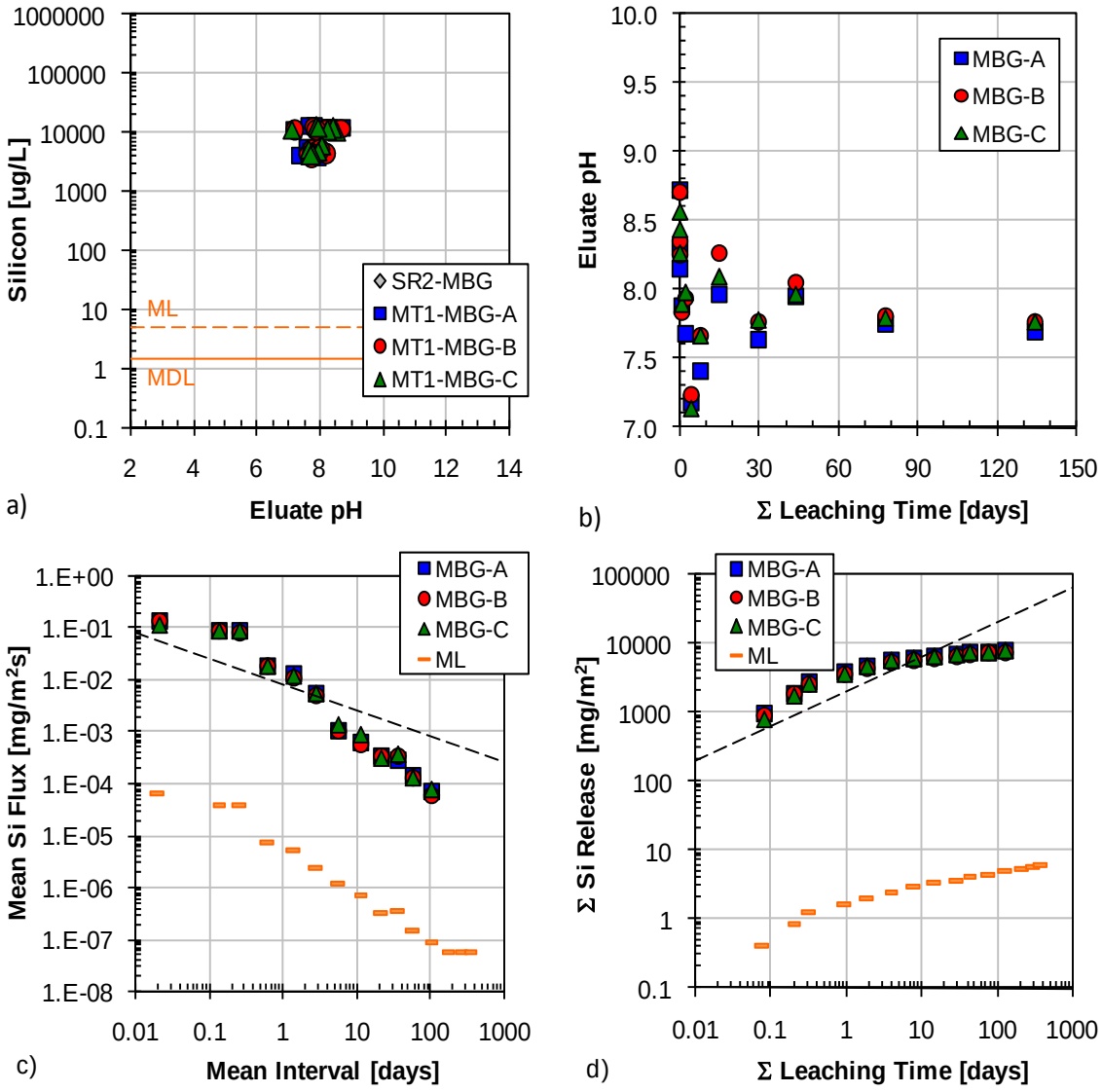

Figure B-67. Silicon leaching test results from MBG matrix: a) comparison of tank leach test eluants to QA/QC parameters (SR02 not conducted), b) pH evolution in tank leach eluants, c) interval flux from tank leach test in comparison to flux values at the method limit ($t^{-1/2}$ model for AMG shown as dashed line), and d) cumulative mass release ($t^{1/2}$ model for AMG shown as dashed line).

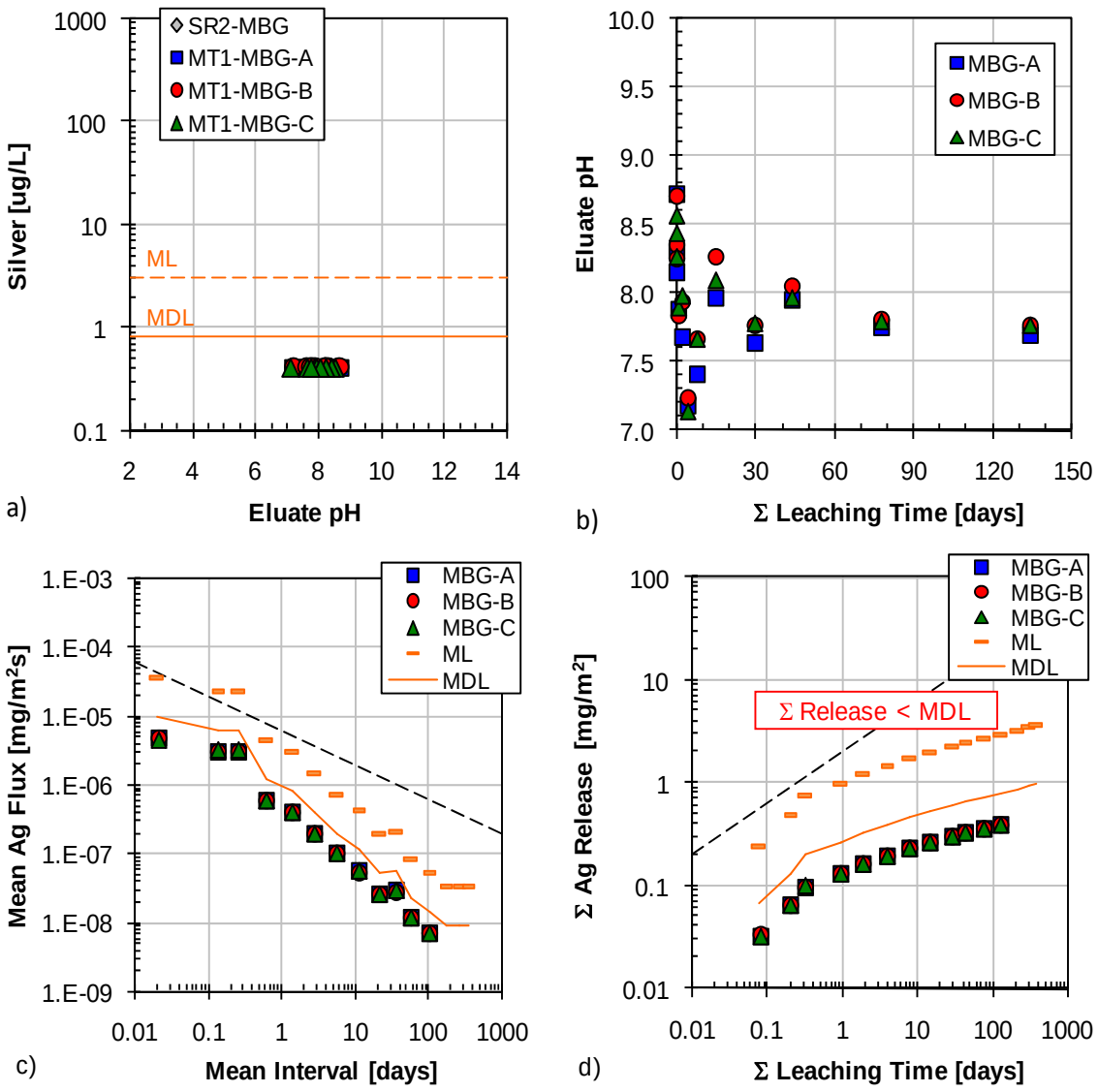

Figure B-68. Silver leaching test results from MBG matrix: a) comparison of tank leach test eluants to QA/QC parameters (SR02 not conducted), b) pH evolution in tank leach eluants, c) interval flux from tank leach test in comparison to flux values at the method limit ($t^{-1/2}$ model for AMG shown as dashed line), and d) cumulative mass release ($t^{1/2}$ model for AMG shown as dashed line).

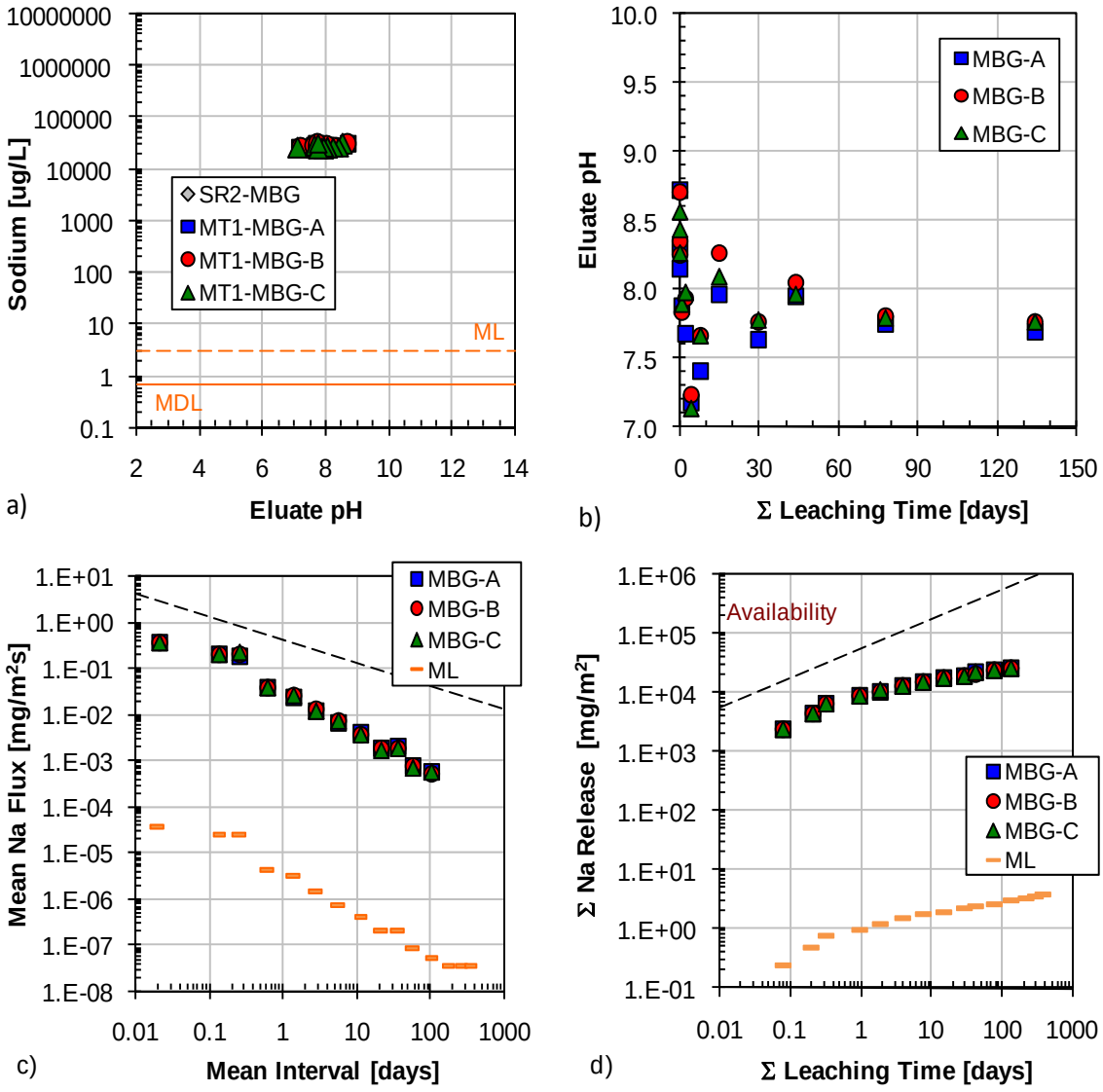

Figure B-69. Sodium leaching test results from MBG matrix: a) comparison of tank leach test eluants to QA/QC parameters (SR02 not conducted), b) pH evolution in tank leach eluants, c) interval flux from tank leach test in comparison to flux values at the method limit ($t^{-1/2}$ model for AMG shown as dashed line), and d) cumulative mass release ($t^{1/2}$ model for AMG shown as dashed line).

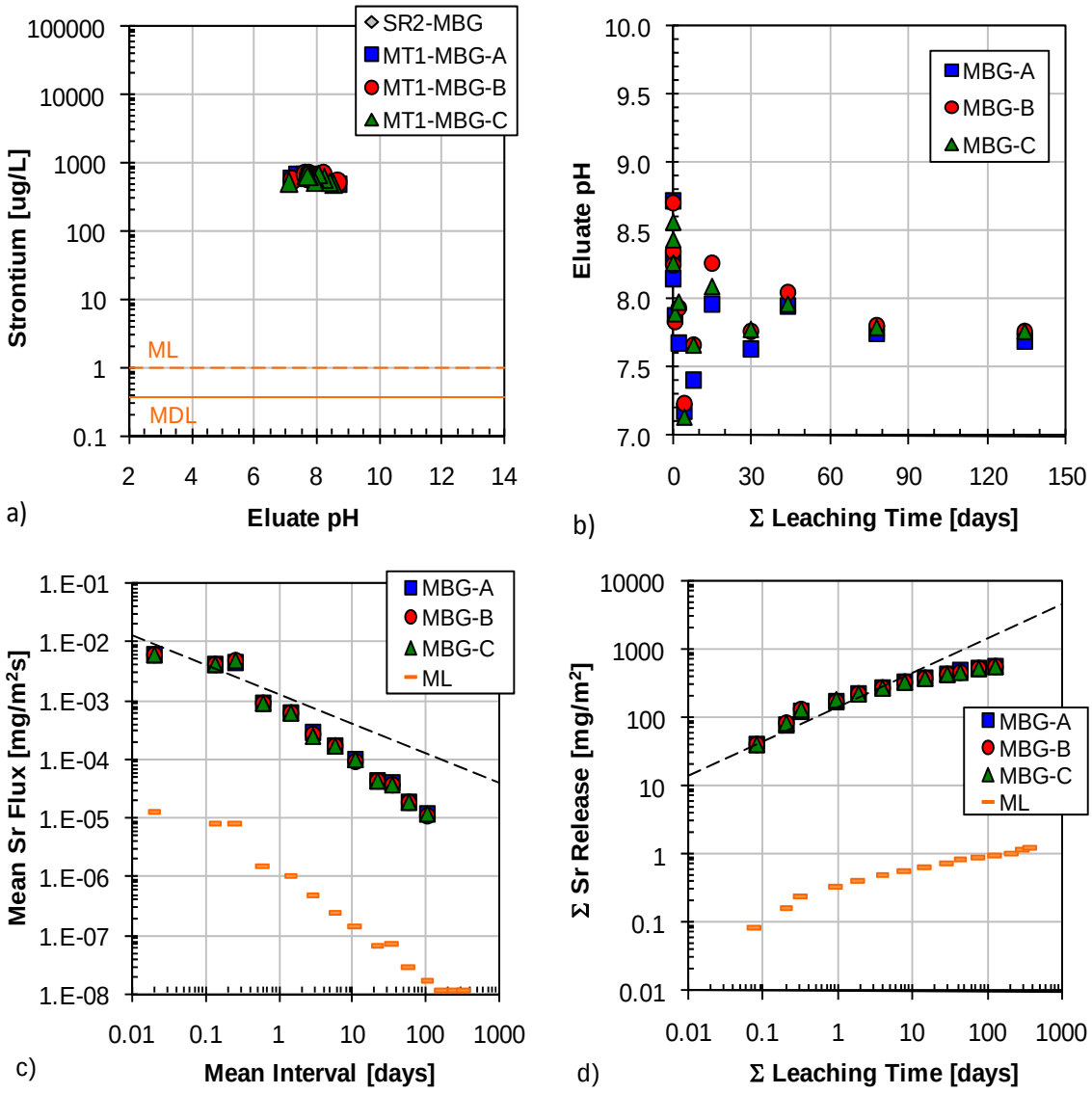

Figure B-70. Strontium leaching test results from MBG matrix: a) comparison of tank leach test eluants to QA/QC parameters (SR02 not conducted), b) pH evolution in tank leach eluants, c) interval flux from tank leach test in comparison to flux values at the method limit ($t^{-1/2}$ model for AMG shown as dashed line), and d) cumulative mass release ($t^{1/2}$ model for AMG shown as dashed line).

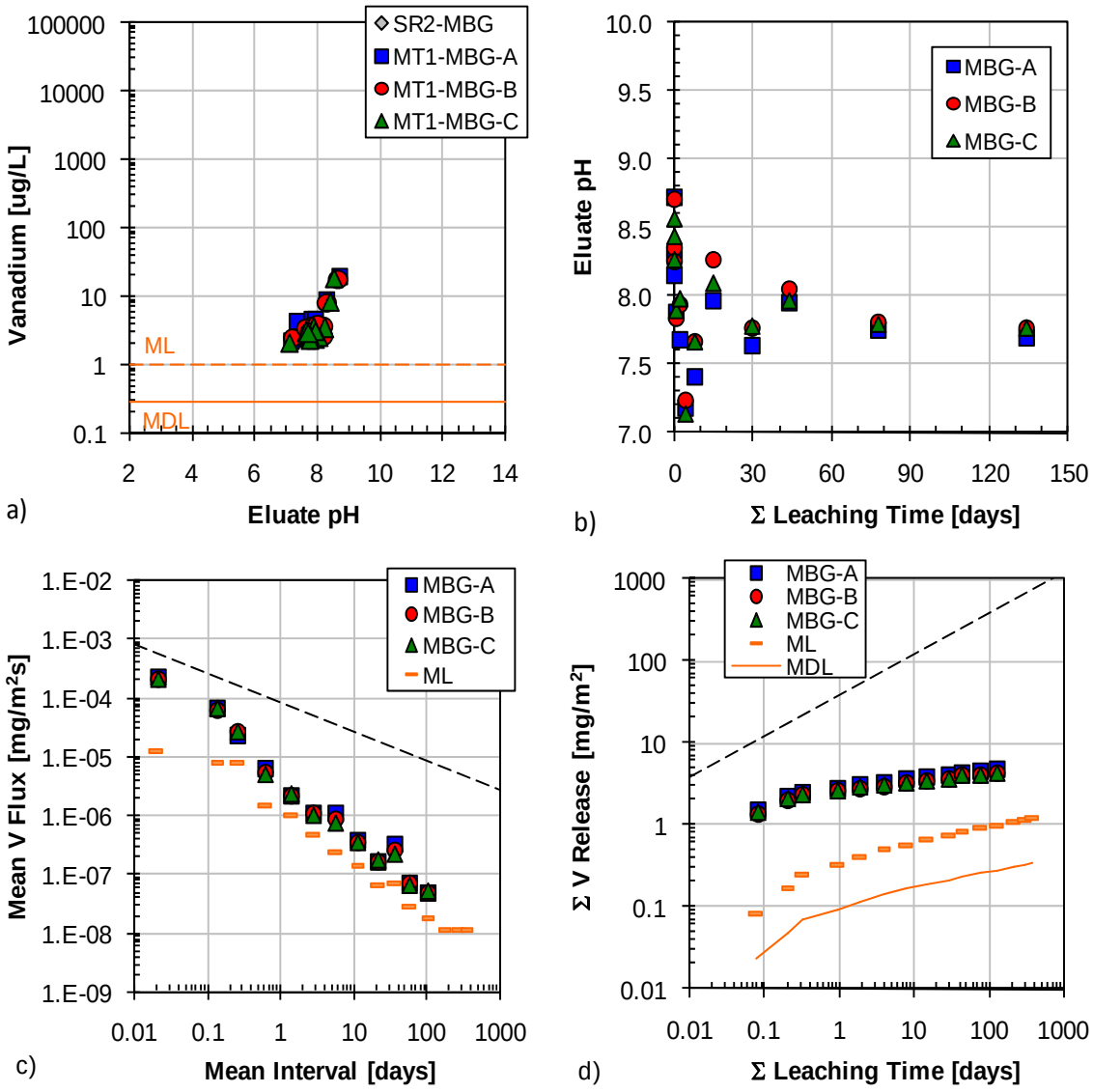

Figure B-71. Vanadium leaching test results from MBG matrix: a) comparison of tank leach test eluants to QA/QC parameters (SR02 not conducted), b) pH evolution in tank leach eluants, c) interval flux from tank leach test in comparison to flux values at the method limit ($t^{-1/2}$ model for AMG shown as dashed line), and d) cumulative mass release ($t^{1/2}$ model for AMG shown as dashed line).

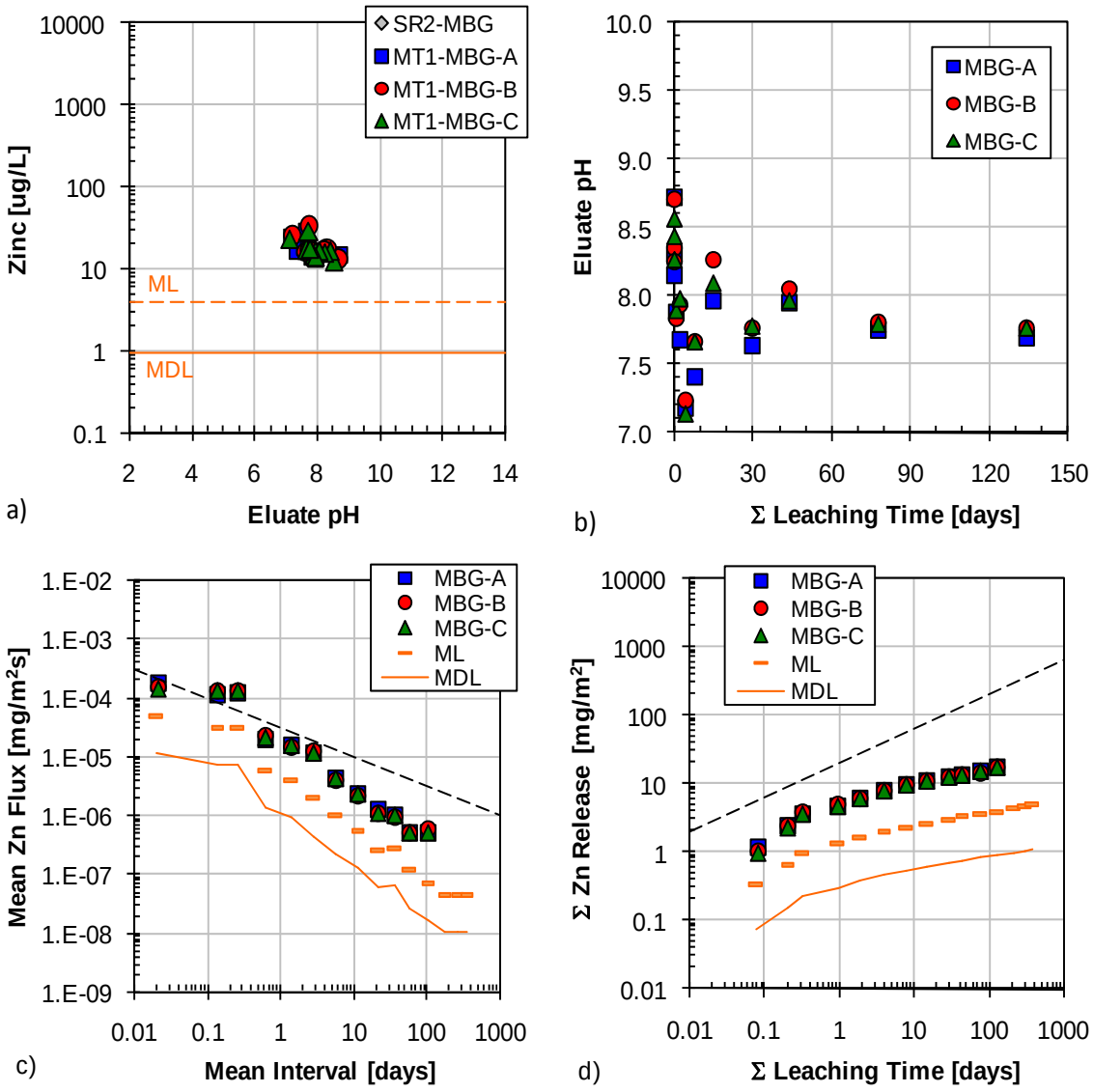

Figure B-72. Zinc leaching test results from MBG matrix: a) comparison of tank leach test eluants to QA/QC parameters (SR02 not conducted), b) pH evolution in tank leach eluants, c) interval flux from tank leach test in comparison to flux values at the method limit ($t^{-1/2}$ model for AMG shown as dashed line), and d) cumulative mass release ($t^{1/2}$ model for AMG shown as dashed line).

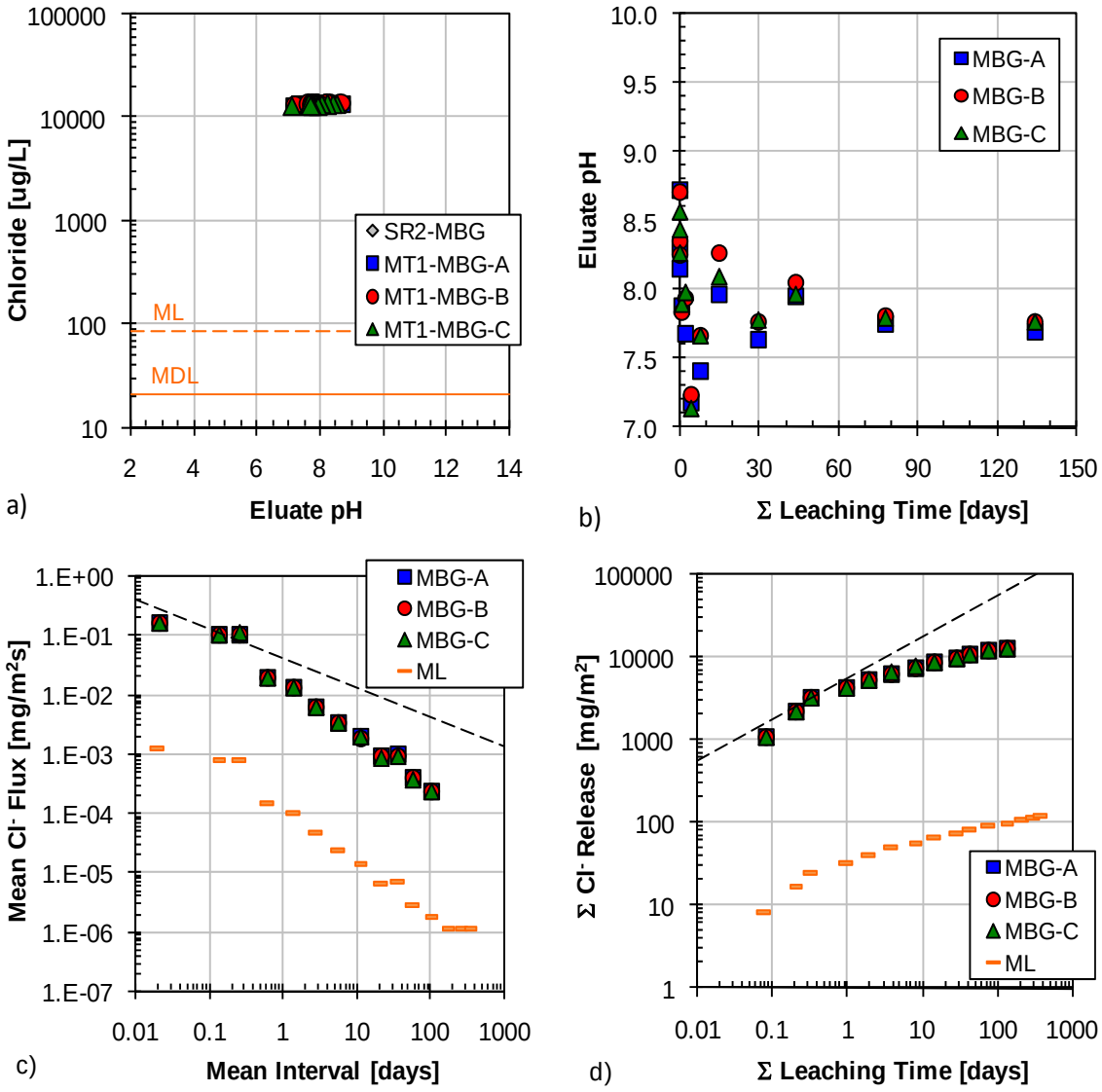

Figure B-73. Chloride leaching test results from MBG matrix: a) comparison of tank leach test eluants to QA/QC parameters (SR02 not conducted), b) pH evolution in tank leach eluants, c) interval flux from tank leach test in comparison to flux values at the method limit ($t^{-1/2}$ model for AMG shown as dashed line), and d) cumulative mass release ($t^{1/2}$ model for AMG shown as dashed line).

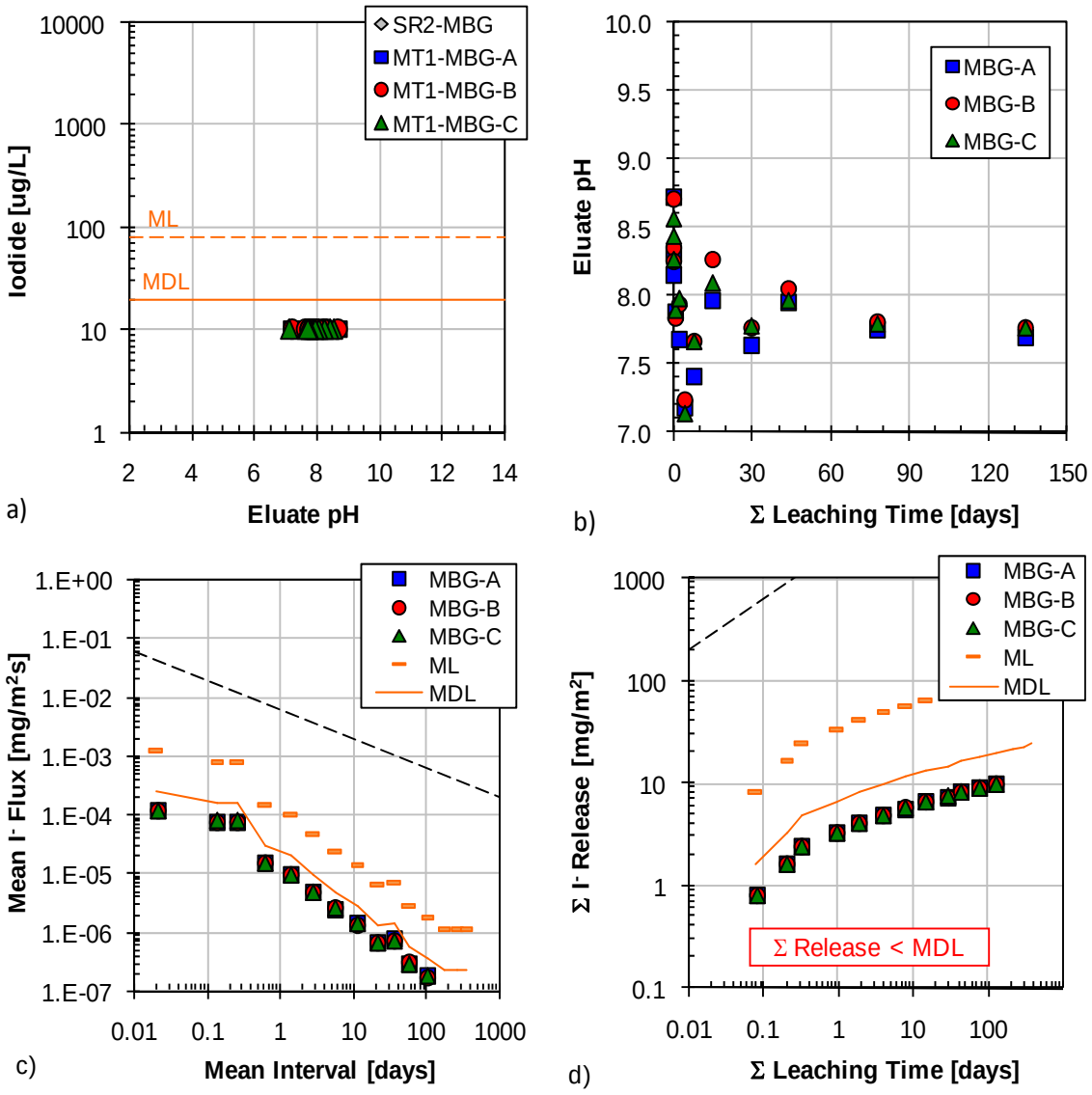

Figure B-74. Iodide leaching test results from MBG matrix: a) comparison of tank leach test eluants to QA/QC parameters (SR02 not conducted), b) pH evolution in tank leach eluants, c) interval flux from tank leach test in comparison to flux values at the method limit ($t^{-1/2}$ model for AMG shown as dashed line), and d) cumulative mass release ($t^{1/2}$ model for AMG shown as dashed line).

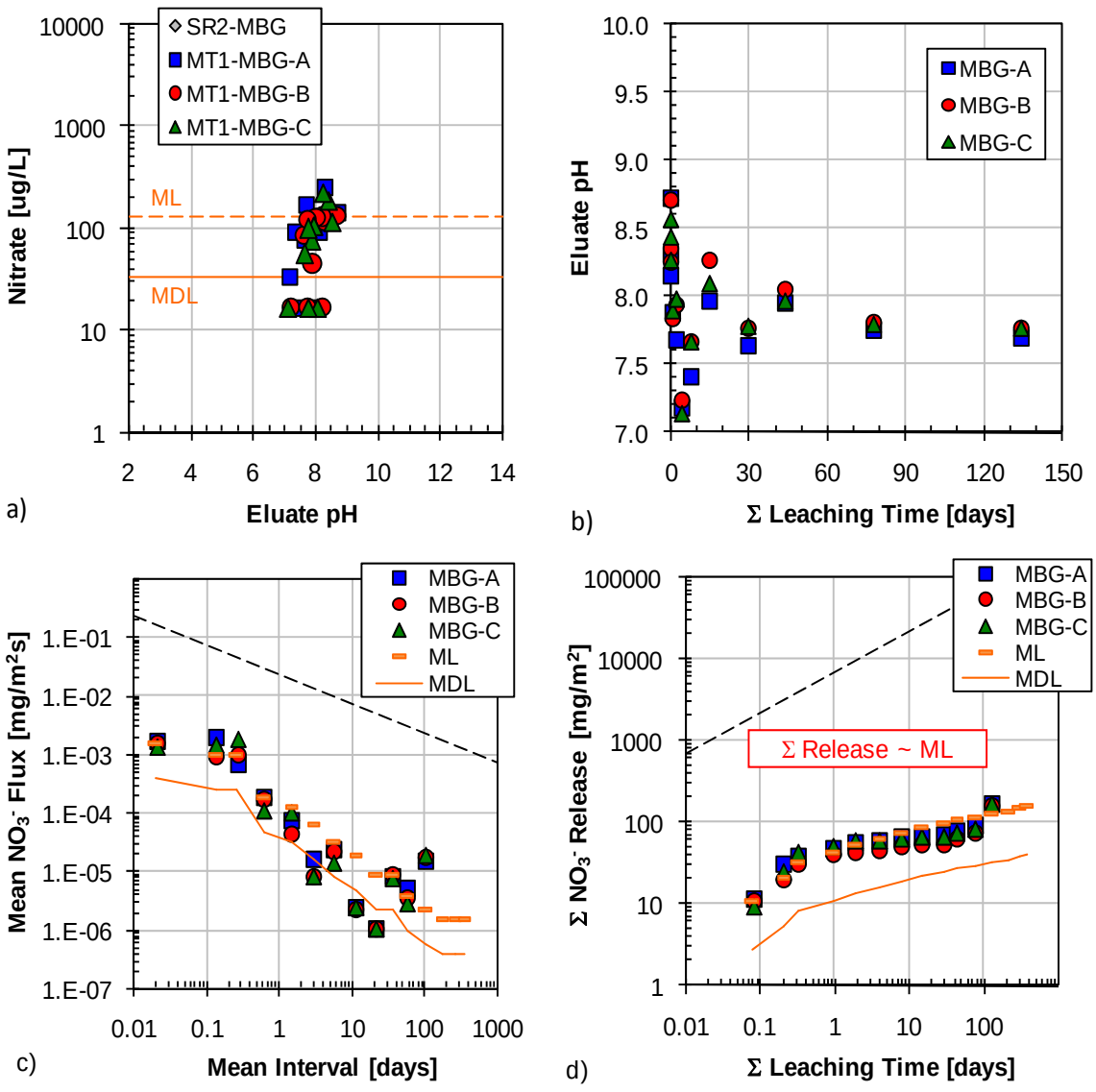

Figure B-75. Nitrate leaching test results from MBG matrix: a) comparison of tank leach test eluants to QA/QC parameters (SR02 not conducted), b) pH evolution in tank leach eluants, c) interval flux from tank leach test in comparison to flux values at the method limit ($t^{-1/2}$ model for AMG shown as dashed line), and d) cumulative mass release ($t^{1/2}$ model for AMG shown as dashed line).

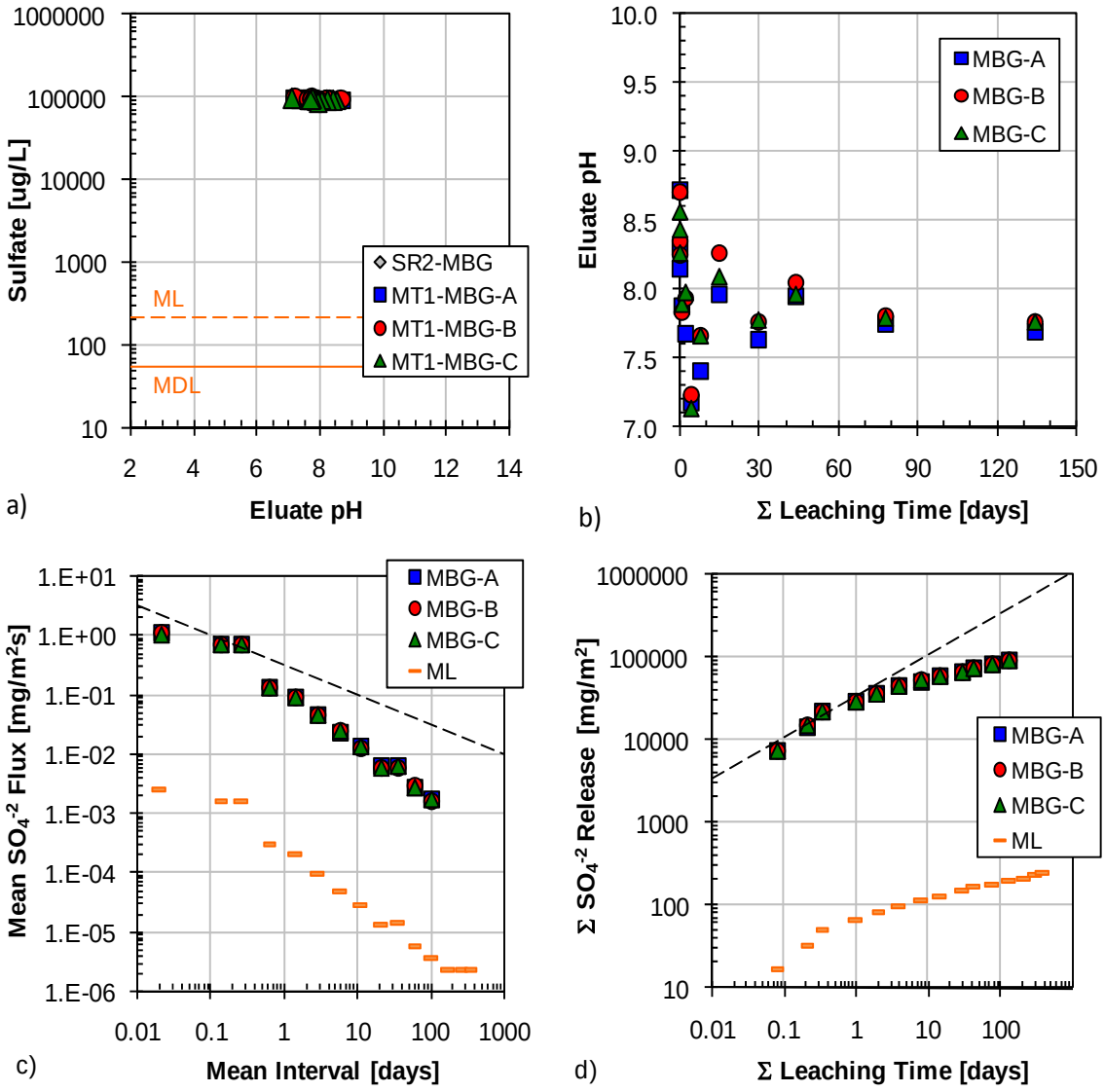

Figure B-76. Sulfate leaching test results from MBG matrix: a) comparison of tank leach test eluants to QA/QC parameters (SR02 not conducted), b) pH evolution in tank leach eluants, c) interval flux from tank leach test in comparison to flux values at the method limit ($t^{-1/2}$ model for AMG shown as dashed line), and d) cumulative mass release ($t^{1/2}$ model for AMG shown as dashed line).

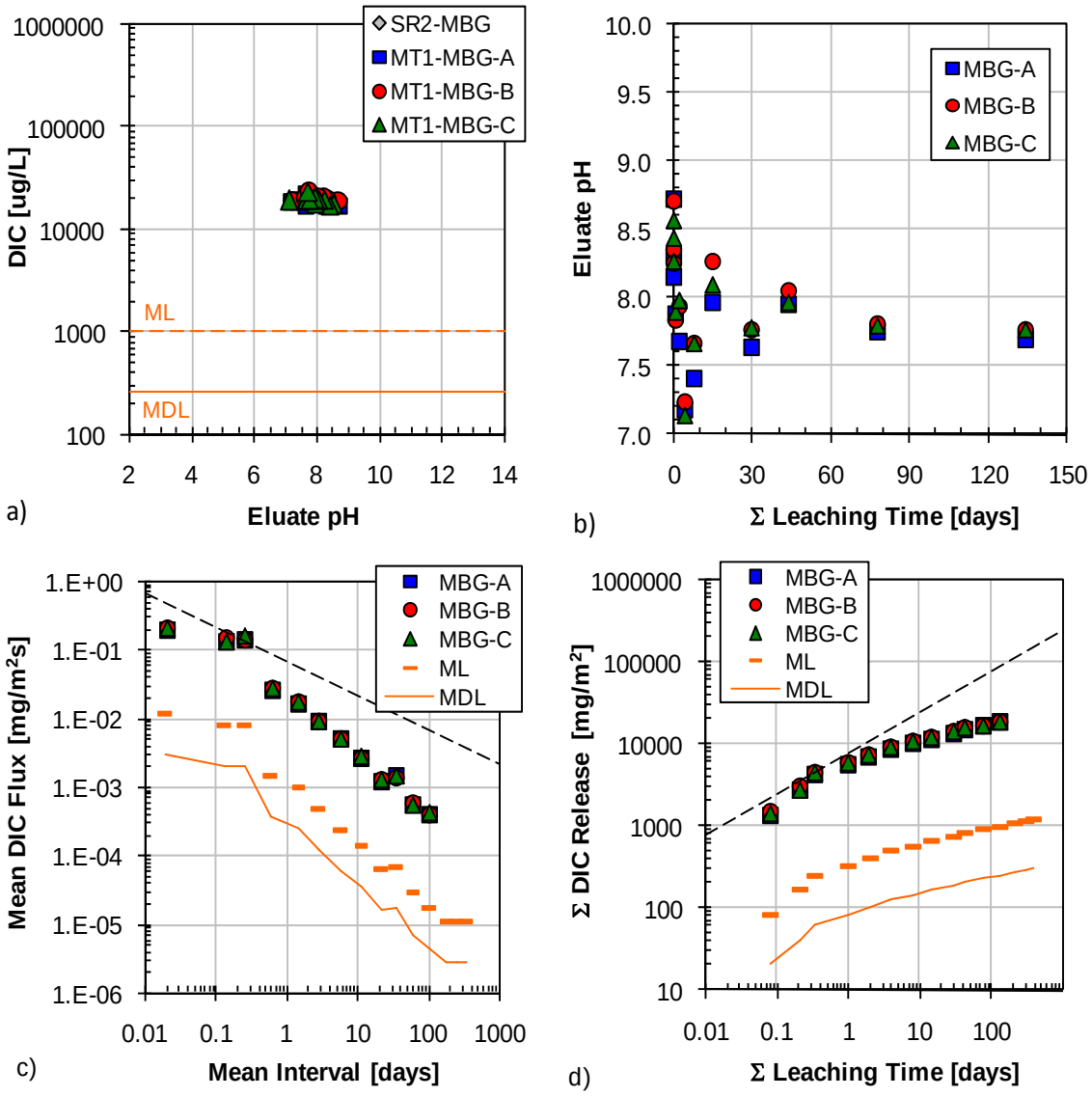

Figure B-77. Dissolved inorganic carbon (DIC) leaching test results from MBG matrix: a) comparison of tank leach test eluants to QA/QC parameters (SR02 not conducted), b) pH evolution in tank leach eluants, c) interval flux from tank leach test in comparison to flux values at the method limit ($t^{-1/2}$ model for AMG shown as dashed line), and d) cumulative mass release ($t^{1/2}$ model for AMG shown as dashed line).

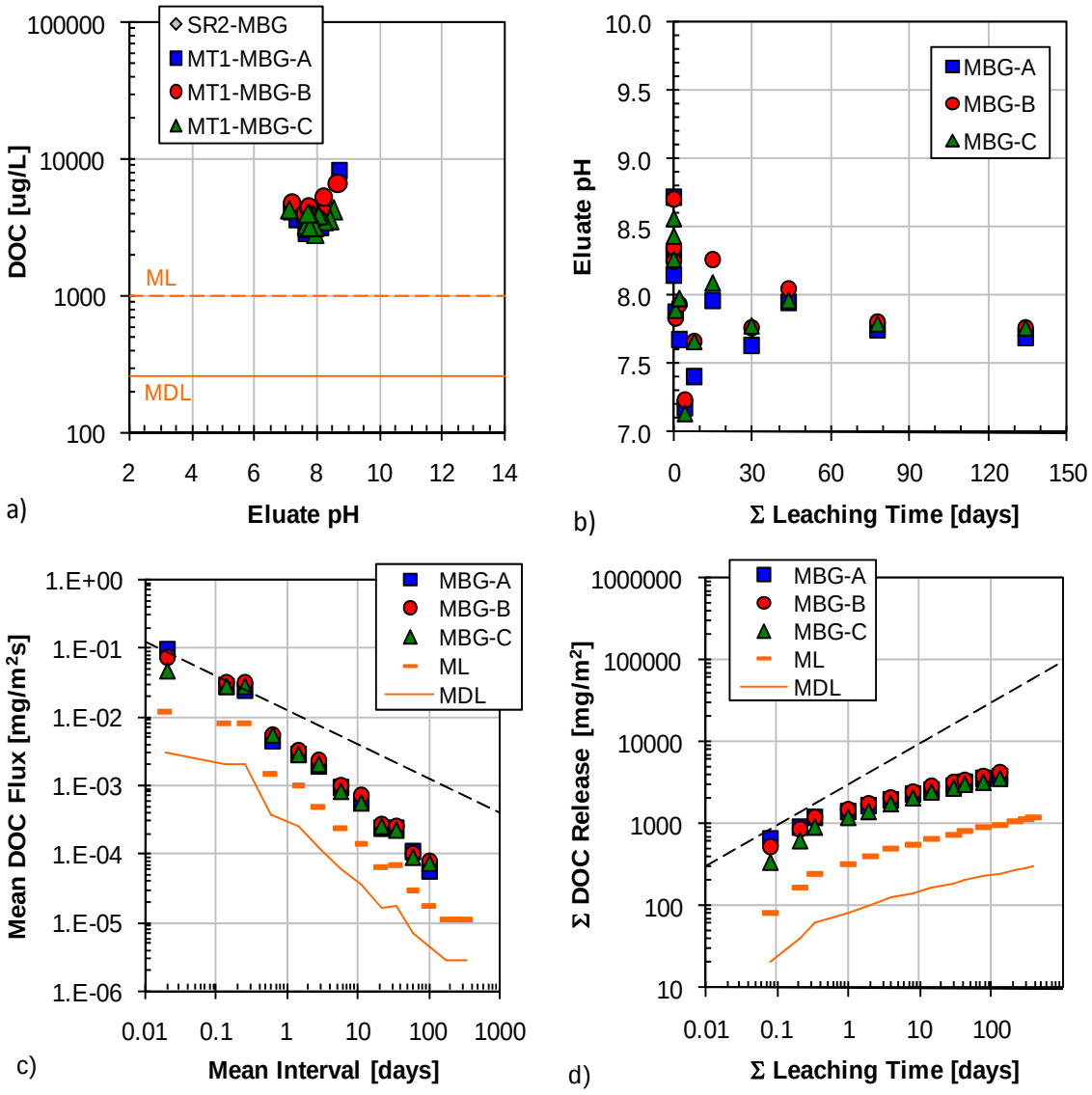

Figure B-78. Dissolved organic carbon (DOC) leaching test results from MBG matrix: a) comparison of tank leach test eluants to QA/QC parameters (SR02 not conducted), b) pH evolution in tank leach eluants, c) interval flux from tank leach test in comparison to flux values at the method limit ($t^{-1/2}$ model for AMG shown as dashed line), and d) cumulative mass release ($t^{1/2}$ model for AMG shown as dashed line).

APPENDIX C: SAMPLE AND PROCEDURE PICTURES

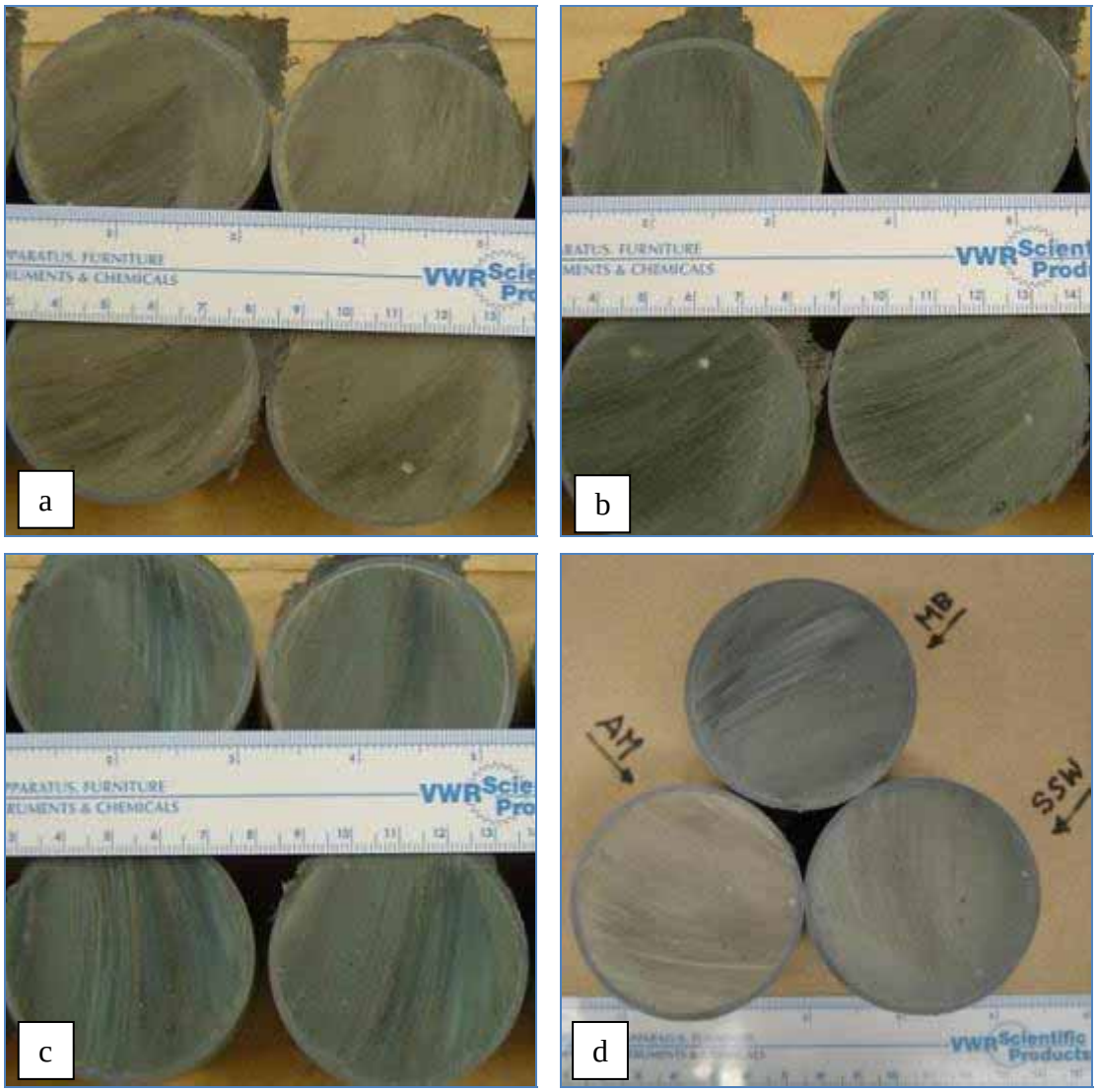

Figure C1. Specimens for tank leaching cut from molds: a) AM samples, b) SW samples, c) MB samples, and d) comparison of three subject materials.

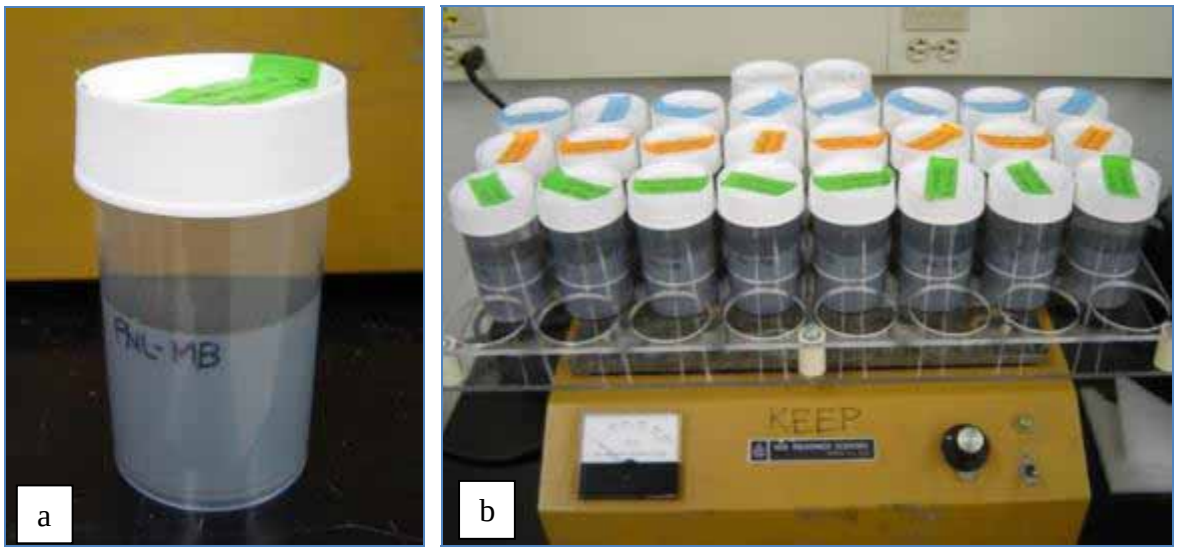

Figure C2. Tank leach test: a) specimen in leaching vessel and b) samples on orbital shaker during tank leach test.

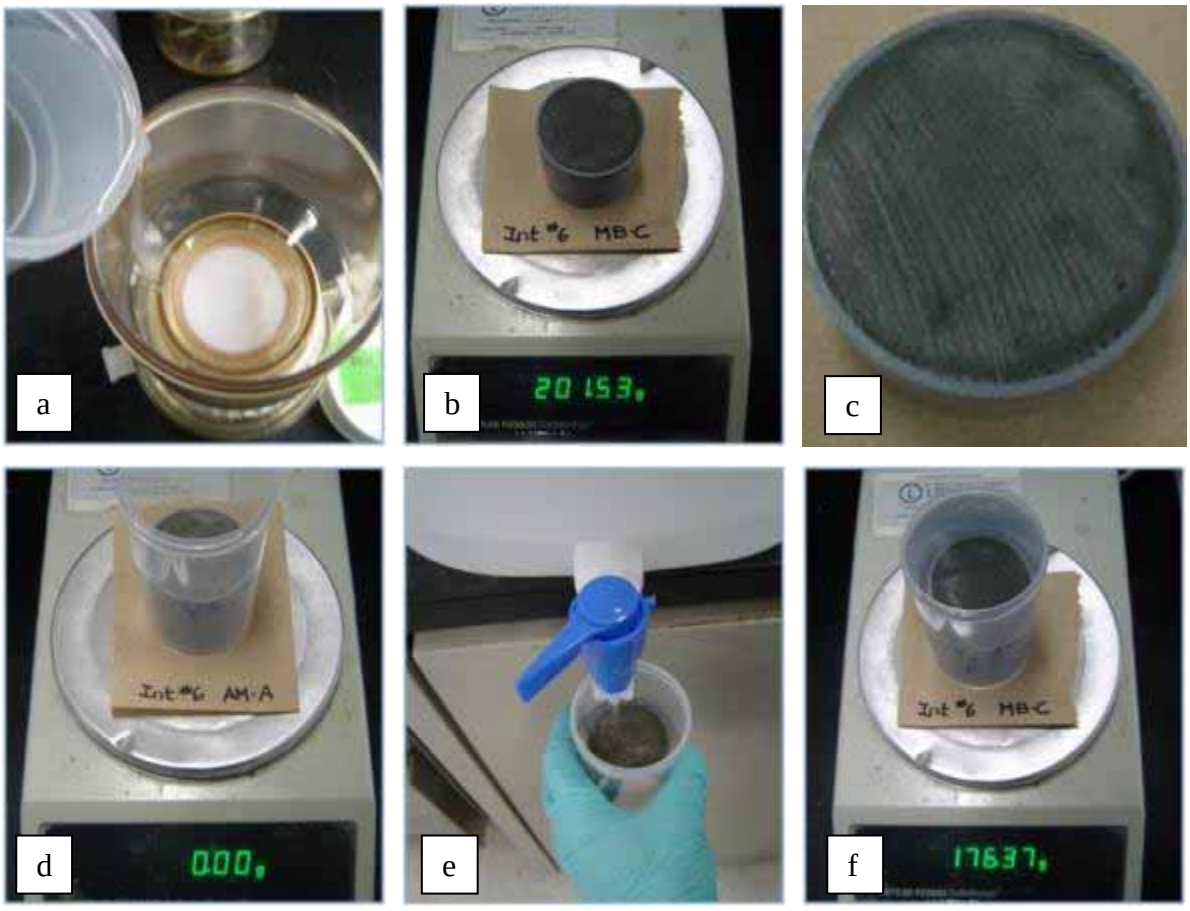

Figure C3. Tank leaching exchange procedure: a) decanting leachate for filtration, b) recording mass of sample and mold, c) close up examination of surface, d) setting tare mass of sample in new leaching vessel, e) filling leaching vessel with leachant, and e) recording mass on leachant.

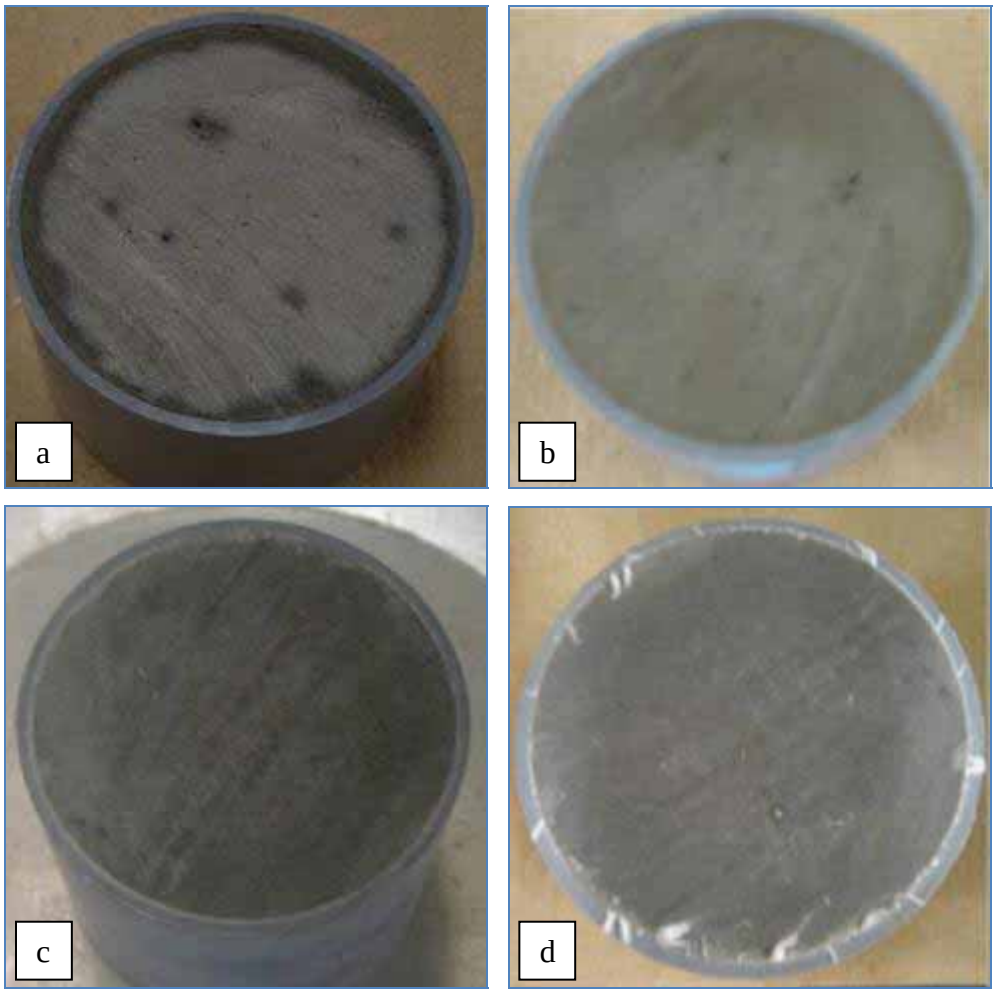

Figure C4. Time comparison of AM samples for tank leaching in deionized water (AMD) and for tank leaching in simulated Hanford groundwater (AMG): a) AMD-B at interval #6, b) AMD-B at interval #12, c) AMG-B at Interval #6, and d) AMG-B at Interval #12.

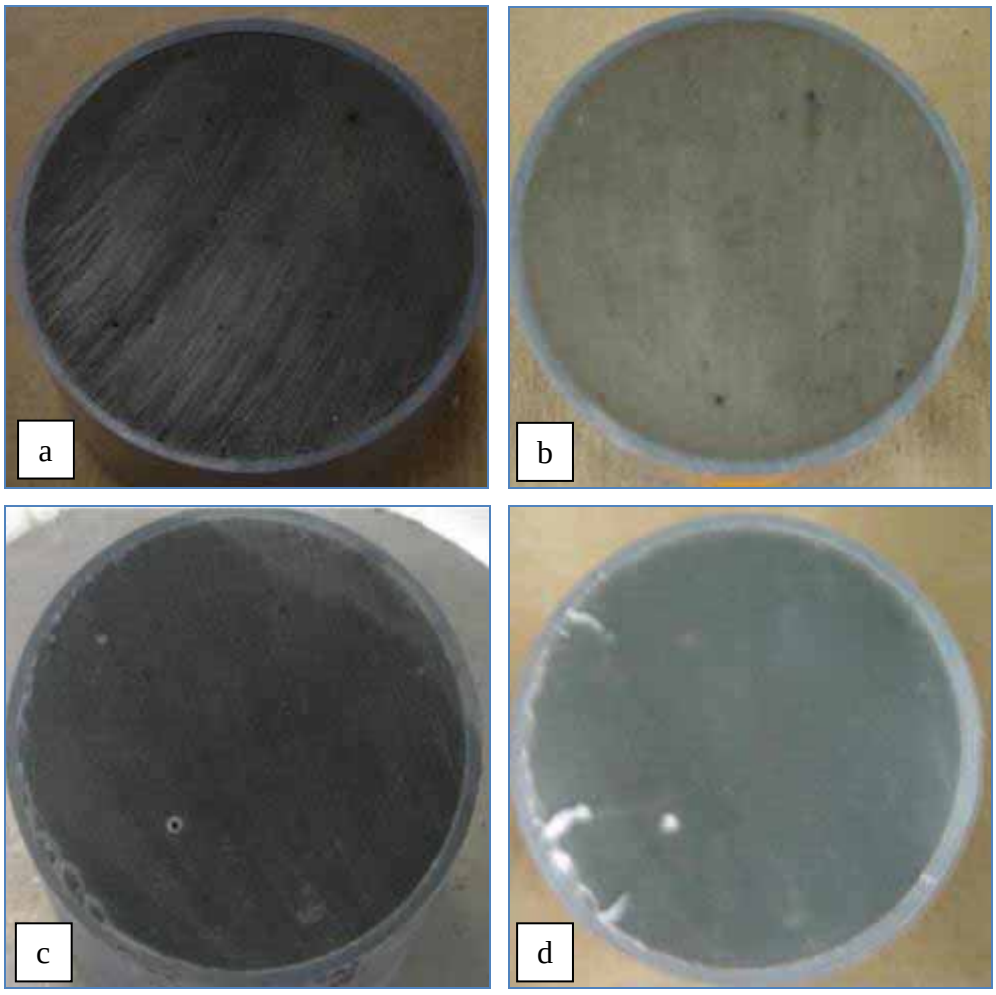

Figure C5. Time comparison of SW samples for tank leaching in deionized water (SWD) and for tank leaching in simulated Hanford groundwater (SWG): a) SWD-B at interval #6, b) SWD-B at interval #12, c) SWG-B at Interval #6, and d) SWG-B at Interval #12.

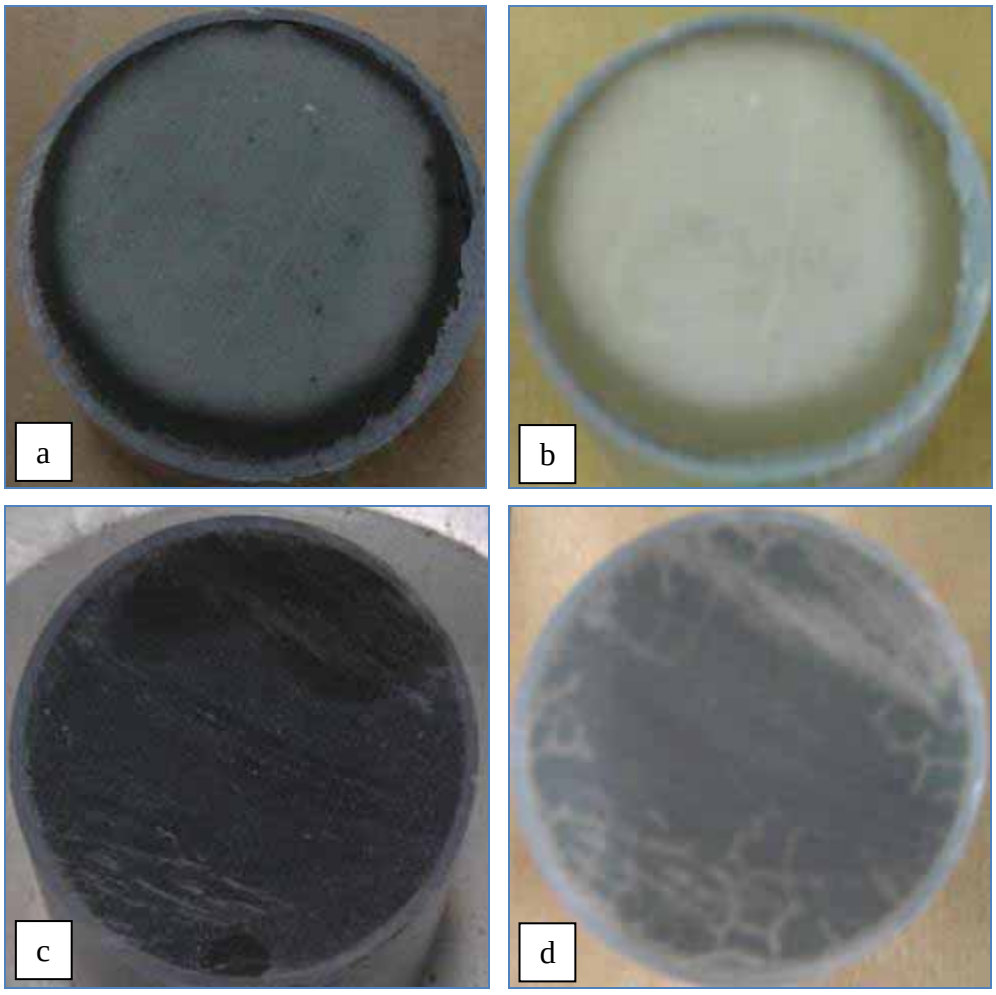

Figure C6. Time comparison of MB samples for tank leaching in deionized water (MBD) and for tank leaching in simulated Hanford groundwater (MBG): a) MBD-B at interval #6, b) MBD-B at interval #12, c) MBG-B at Interval #6, and d) MBG-B at Interval #12.